

Neuromodulation in Depression

Mechanisms, Practice, and Innovation

Emilė Radytė

Christ Church

Supervised by

Dr Beata R. Godlewska

Prof Timothy Denison



This thesis is submitted to the Department of Psychiatry, University of Oxford, in partial fulfilment of the requirements for the degree of Doctor of Philosophy.

Abstract

This thesis explores the mechanisms, clinical applications, and innovations in the use of transcranial magnetic stimulation (TMS) for treating major depressive disorder (MDD).

In the first data chapter, we investigated differences in resting-state functional connectivity between drug-naïve and drug-experienced MDD patients. We found enhanced connectivity between the mediodorsal thalamus and the default mode network in drug-naïve patients, when compared to those who were drug-experienced. These findings align with theories around thalamocortical dysrhythmia and highlight the long-lasting impact of medication exposure on brain networks.

In the second data chapter, we evaluated the real-world use of TMS for MDD treatment in clinical settings across clinics in the United States. We found no significant effects of resting motor thresholds, treatment timing, or patient age on clinical outcomes. However, high inter-clinic variability in data collection and measurement showed inconsistencies that appear to have an impact on TMS treatment efficacy.

In the third data chapter, we piloted personalised targeting of the dorsolateral prefrontal cortex combined with monophasic intermittent theta burst stimulation (iTBS) to see whether a single stimulation session could lead to changes in cognition in patients experiencing low mood. We found no signal that monophasic iTBS, which is unfeasible with conventional TMS machines, leads to significant improvements in positive bias after a single session compared to the standard biphasic iTBS in the small pilot sample. However, the analysis was severely limited, and further investigations are necessary.

This thesis provides actionable considerations to optimise TMS for MDD, emphasising the importance of accounting for medication history, standardising clinical practices, and leveraging emerging technologies such as monophasic iTBS, networked devices and

personalised targeting in future work. We hope this work will contribute to advancing TMS as an accessible and effective treatment for the growing burden of MDD.

Acknowledgments

I have always found it ironic that PhD thesis acknowledgments are rarely read by people to whom the authors feel most grateful. However, they have always been my favourite part of any academic work because they emphasise that no (good) work is ever completed alone. This thesis is dedicated to the many people who made this journey possible.

Firstly, I would never be here if it wasn't for my parents Rasa and Dalius, who grew up in a country under iron curtains, and yet were not afraid to dream and work hard so that I could grow up in a free and democratic country, and even able to write in the language of this thesis. It is only because of them that I know that important things are worth fighting -and working hard- for. I am grateful to my brothers; Tadas - who has never stopped asking 'why' and was probably responsible for me ending up as a scientist, and Aleksas - whose mind I will never understand, which is probably why I find brains the most interesting and fascinating thing there is.

Secondly, I certainly would not be here if it wasn't for Tim, Beata and Jacinta. Tim, I am beyond grateful for your mentorship and belief; thank you for your support in the hardest moments of this journey, and for inspiring me for the journey ahead. I never thought hanging around engineers and starting to think like them (risk management? feedback systems? Arnold tongues?) would transform my perspectives as a neuroscientist, and am so grateful that you took me under your wing with no formal engineering training. Beata, I am deeply grateful for your unwavering support, joining me in the trenches, and your trust in my ability to meet sometimes impossible deadlines. Most importantly, thank you for every clinical and scientific insight you have shared over the last year - your consideration

of clinical and patient needs above all else has been an inspiration to continue conducting research that matters to many patients who may not always be heard. To all of PERL - thank you for welcoming me with open arms, and for their special support I'll be in debt to Dr Amy Gillespie and Dr Marieke Martens.

I have been incredibly lucky to be mentored, supported, challenged, trained, and otherwise welcomed by my wonderful labmates, to whom I am so grateful, and proud to call many my friends. Karen, thank you for your patience with me from day one; Verena, thank you for being there when I needed you most; Majid, thank you for always reminding me of the first principles; Joram, thank you for sharing your wisdom with me when I had run out. Ali, Raveen, Beatriz, Tory, JJ, John, Tory, Rachel - thank you for always bringing a good time. Bronwyn, Ioana - I could not have overcome 2024 without you.

My Oxford experience has in large part been a covid experience, which has brought me so close to my GCR community at Christ Church. Thank you to Linnea, Del, Emily, Charbel, Dawn, Noah, Casey, Kate, Sarah, Lucas and so many others, who made me smile every day.

Finally, none of these words would be on paper if it weren't for the unconditional support of my partner Alex. Thank you for not losing faith in me when I had, thank you for never questioning my commitments even when times were incredibly hard on us both, and thank you for making me coffee (mornings) and tea (evenings) when I (and this thesis) needed you the most.

Table of Contents

List of Abbreviations	10
List of Figures	12
List of Tables	14
1 Introduction	15
1.1 Major depressive disorder (MDD)	15
1.1.1 The evolution of cognitive theories of MDD	16
1.1.2 Neurobiology	18
1.1.2.1 Grey matter changes in MDD	18
1.1.2.2 White matter changes in MDD	20
1.1.3 Neurocircuitry	20
1.1.3.1 The DLPFC-sgACC functional relationship in MDD	21
1.1.4 Current treatments	22
1.1.4.1 Pharmacotherapy	22
1.1.4.2 Psychotherapy	23
1.1.4.3 Non-invasive brain stimulation (NIBS)	24
1.2 Transcranial magnetic stimulation (TMS)	25
1.2.0.1 Targeting the DLPFC with TMS in MDD	25
1.2.0.2 Intermittent theta burst stimulation (iTBS)	26
1.3 Optimisation of TMS protocols for MDD treatment	27
1.3.1 Stimulation pattern	28
1.3.2 Stimulation dose	28
1.3.3 Precision targeting	29
1.3.3.1 5-cm rule	29
1.3.3.2 Beam F3	30

1.3.3.3	MRI-guided neuronavigation	31
1.3.3.4	rsFC-based (sgACC-DLPFC) neuronavigation	32
1.3.4	Pulse shape	33
1.3.4.1	Limitation of traditional TMS electronics	35
1.4	Research objectives	35
2	Mechanisms: Characterising differences in resting state connectivity across drug-experienced and drug-naïve depressed participants	37
2.1	Introduction	37
2.1.1	Resting state functional connectivity (rsFC)	37
2.1.2	7T MRI	38
2.1.3	Key resting state network changes in MDD	38
2.1.3.1	Default mode network (DMN)	39
2.1.3.2	Saliency network (SN)	39
2.1.3.3	Executive control network (CEN)	39
2.1.4	Pharmacological impacts on rsFC in MDD	40
2.1.4.1	SSRIs: fluoxetine and escitalopram	40
2.1.4.2	SNRIs: venlafaxine	40
2.1.4.3	Atypical antidepressants: bupropion	41
2.1.4.4	Ketamine	41
2.1.5	rsFC in TMS treatment for MDD	41
2.2	Research questions	42
2.3	Methods	43
2.3.1	Participants	43
2.3.2	Data acquisition	44
2.3.3	Preprocessing	45
2.3.4	Data quality assessment	46

2.3.5	Functional connectivity analysis	46
2.4	Results	47
2.4.1	Demographic and clinical characteristics	47
2.4.2	Resting state network analysis	52
2.4.3	Independent component analysis - drug-naïve vs drug-experienced	53
2.4.4	Independent component analysis - medicated vs unmedicated	55
2.5	Discussion	56
2.5.1	Summary of findings	56
2.5.2	Interpretation of rsFC findings	56
2.5.3	Clinical relevance	57
2.5.4	Limitations	58
2.5.5	Future directions	60
2.5.5.1	Absence of healthy control group:	60
2.5.5.2	Considering medication-matched cohorts:	60
2.5.5.3	Clinician-reported measures:	60
2.5.5.4	Alternative rsFC analysis approaches:	61
2.6	Conclusions and contributions	61
3	Practice: Implications of TMS precision targeting in real-world, large scale clinical practice	63
3.1	Introduction	63
3.1.1	TMS in clinical practice	63
3.1.2	Resting motor threshold (RMT) measurement and significance	64
3.1.3	Influence of real-world clinical practice on clinical outcomes .	65
3.2	Research Questions	66
3.3	Methods	67
3.3.1	Dataset acquisition	67
3.3.2	Data Quality Assessment	68

3.3.3	Statistical Analysis	68
3.3.3.1	RMTs	69
3.3.3.2	PHQ-9 Distributions and Change Scores	69
3.3.3.3	Diurnal Variation Analyses	70
3.3.3.4	Age	70
3.3.3.5	Early Changes in PHQ-9 as Predictors of Ultimate Response	71
3.4	Results	71
3.4.1	Does individual RMT impact MDD treatment outcomes? . .	71
3.4.1.1	Understanding RMTs across the dataset	73
3.4.1.2	Understanding clinical outcomes across the dataset	75
3.4.2	Does the time of day of when treatment is administered im- pact treatment outcomes?	78
3.4.3	Does the age of the patient at the start of treatment impact treatment outcomes?	80
3.4.4	Does early change in the course of TMS treatment for MDD predict ultimate treatment outcomes?	82
3.5	Discussion	86
3.5.1	Summary of findings	86
3.5.2	Clinical relevance	86
3.5.3	Methodological limitations	88
3.5.3.1	Data heterogeneity	88
3.5.3.2	Selection bias and missing data	89
3.5.3.3	Time of RMT measurement	89
3.5.3.4	Observational data	89
3.5.3.5	Result generalisability	90
3.5.3.6	Predictive modelling methods	90

3.5.4	Recommendations for future research	90
3.6	Conclusions and contributions	92
4	Innovation: Single-session effects of using monophasic vs biphasic iTBS on cognition	93
4.1	Introduction	93
4.1.1	Modelling of monophasic and biphasic pulse shapes	93
4.1.2	xTMS	95
4.1.3	Impact of monophasic vs biphasic stimulation on MEPs	95
4.1.4	Cognitive changes as predictors of treatment outcomes	97
4.1.4.1	Negative bias	99
4.1.4.2	Limitations of the CNT	100
4.1.4.3	Negative bias in pharmacological MDD research	101
4.2	Research questions	102
4.3	Methods	103
4.3.1	Ethical data collection and analysis:	103
4.3.2	Participants	103
4.3.3	Experimental design and treatment	104
4.3.4	Facial Expression Recognition Task (FERT)	110
4.3.5	Statistical Analysis	113
4.3.5.1	Sample demographics, clinical and physiological char- acteristics	113
4.3.5.2	rsMRI-derived target locations	113
4.3.5.3	Single-session changes in emotion recognition bias	114
4.3.5.4	Single-session changes relative to sham stimulation	114
4.3.5.5	Single-session changes in recognition of specific emo- tions	114

4.3.5.6	Single-session changes in recognition of ambiguous (50% intensity) emotions	115
4.4	Results	115
4.4.1	Sample demographics, clinical and physiological characteristics	115
4.4.2	rsMRI-derived target locations	116
4.4.3	Single-session changes in negative bias after monophasic vs biphasic iTBS	116
4.4.4	Single-session changes relative to sham stimulation	117
4.4.5	Single-session changes in individual emotion recognition after monophasic vs biphasic iTBS	118
4.4.6	Single-session changes in the recognition of ambiguous (50% intensity) emotions in monophasic vs biphasic iTBS	120
4.5	Discussion	120
4.5.1	Summary of findings	120
4.5.2	Interpretation of findings	122
4.5.3	Clinical relevance	122
4.5.4	Limitations	124
4.5.4.1	Sources of error	124
4.5.5	Recommendations for future research	128
4.5.5.1	Larger sample sizes	128
4.5.5.2	Different sub-populations	128
4.5.5.3	Longitudinal designs	129
4.5.5.4	Further investigation of stimulation parameters	129
4.5.5.5	Neural mechanisms of emotional processing changes	129
4.5.5.6	Clinical applicability of personalised targeting	130
4.5.5.7	Alternative cognitive and emotional measures	130
4.6	Conclusions and contributions	130

5	General Discussion	132
5.1	Summary	132
5.2	Clinical implications and future directions	134
5.3	Concluding remarks	135
6	Literature	137
	Appendix A xTMS Study Documents	170
A.1	Step-by-step study procedures	171
A.2	MRI Safety Screening Form	182
A.3	TMS Safety Screening Form	185
A.4	SCID Scoresheet	188
A.5	Beck Depression Inventory (BDI)	198
A.6	CUREC 2 Approval	202
A.7	MRI Scanning Protocol	204
A.8	Participant Information Sheet (PIS)	209
A.9	Follow-up Letter for participants not included in the study	216
A.10	AP21 CUREC procedure appendix for TMS parameters	218
A.11	sgACC Localisation Raw Code	221
	Appendix B 7T MRI Study Documents	235
B.1	Ethics (NHS) Approval	236
B.2	Participant Information Sheet (PIS)	241
B.3	7T MRI Scanning Protocol	247

List of Abbreviations

ANOVA Analysis of Variance	FWHM Full-Width Half-Maximum
BBR Boundary-Based Registration	GM Grey Matter
CEN Central Executive Network	HIPAA Health Insurance Portability and Accountability Act
CNT Control Network	IGBTs Insulated Gate Bipolar Transistors
cTMS Continuous Transcranial Magnetic Stimulation	iTBS Intermittent Theta-Burst Stimula- tion
DMN Default Mode Network	iTMS Interleaved Transcranial Magnetic Stimulation
DLPFC Dorsolateral Prefrontal Cortex	IQR Interquartile Range
ECT Electroconvulsive Therapy	KDE Kernel Density Estimation
EMG Surface Electromyography	KIT Ketamine Infusion Therapy
EPI Echo Planar Imaging	li-TMS Low-Intensity Transcranial Mag- netic Stimulation
ES Efficiency Score	MELODIC Multivariate Exploratory Linear Optimized Decomposition into Independent Components
FAST FMRIB's Automated Segmenta- tion Tool	MEPs Motor Evoked Potentials
FDA Food and Drug Administration	M1 Primary Motor Cortex
FIX FMRIB's ICA-based Xnoiseifier	MDD Major Depressive Disorder
FERT Facial Emotion Recognition Task	MSO Maximum Stimulator Output
FMRIB Oxford Centre for Functional MRI of the Brain	
FSL FMRIB Software Library	

MRI Magnetic Resonance Imaging	sgACC Subgenual Anterior Cingulate Cortex
NIBS Non-Invasive Brain Stimulation	SN Salience Network
PANAS Positive and Negative Affect Schedule	SNRI Serotonin-Norepinephrine Reuptake Inhibitor
PCC Posterior Cingulate Cortex	SSRI Selective Serotonin Reuptake Inhibitor
PHI Personal Health Information	STAI State-Trait Anxiety Inventory
PHQ-9 Patient Health Questionnaire-9	SNT Stanford Neuromodulation Therapy
PFC Prefrontal Cortex	tACS Transcranial Alternating Current Stimulation
PWM Pulse Width Modulation	tDCS Transcranial Direct Current Stimulation
QPS Quadripulse Stimulation	TFCE Threshold-Free Cluster Enhancement
RCT Randomised Controlled Trial	TMS Transcranial Magnetic Stimulation
ROI Region of Interest	TOD Time of Day
RMT Resting Motor Threshold	TRD Treatment Resistant Depression
rsFC Resting-State Functional Connectivity	UnHR Unbiased Hit Rate
RSN Resting State Network	UTC Universal Time Coordinate
RT Reaction Time	
rTMS Repetitive Transcranial Magnetic Stimulation	

List of Figures

1.1	Hierarchical relationship between cognition, mood, and behaviour.	17
1.2	Intermittent theta burst stimulation (iTBS) pattern.	26
1.3	Individualised functional connectivity MRI-guided target locations for Stanford neuromodulation therapy in relation to an average F3 coordinate. . .	33
2.1	Resting-state networks identified in the study.	53
2.2	Increased functional connectivity in drug-naïve patients compared with medicated patients between the left mediodorsal thalamus and the default mode network (DMN).	55
3.1	Relationship between initial motor threshold (RMT) levels and PHQ-9 change scores in TMS treatment.	72
3.2	Relationship between initial motor threshold (RMT) levels and PHQ-9 change scores in TMS treatment after correcting for inter-clinic variability.	73
3.3	Distribution of resting motor thresholds (RMTs) of all patients.	74
3.4	Distribution of RMT levels for each of the 25 clinics included in the analysis.	75
3.5	Kernel density estimation plots comparing PHQ-9 scores at treatment initiation and completion	76
3.6	Box plots depicting the distribution of PHQ-9 change scores across all 25 clinics.	77
3.7	The moving average of raw mean RMT (%MSO) plotted across the adjusted time of day (hh:mm).	78
3.8	The moving average of z-scored RMT (%MSO) plotted across the adjusted time of day (hh:mm).	79
3.9	Box plots illustrating the distribution of changes in PHQ-9 scores for participants in the morning and afternoon groups.	80
3.10	Box plots showing the distribution of participant ages across clinics, with variance explained by clinic ID reported as 15.55%.	81

3.11 Scatterplot showing the relationship between PHQ-9 change and age at first assessment.	82
3.12 Moving average of PHQ-9 scores over time of treatment.	83
3.13 Scatterplot showing the relationship between PHQ-9 change from baseline to Week 1 and PHQ-9 change from Week 1 to the end of treatment. . . .	85
4.1 Modelling of monophasic and biphasic stimulation in motor cortex neurons.	94
4.2 Overview of the xTMS device.	96
4.3 Group mean MEP amplitude for the monophasic and biphasic M1 iTBS conditions and the control condition are shown for the baseline and across the post-iTBS time points.	97
4.4 Cognitive Neuropsychological Theory of Antidepressant Action.	98
4.5 Schematic illustration of the study design, treatment, and evaluation schedule.	104
4.6 Illustration of the testing setup for the TMS familiarisation and experimental iTBS sessions.	106
4.7 Change in positive bias after a single iTBS stimulation session does not differ between monophasic and biphasic stimulation.	117
4.8 No significant differences in change in positive bias between real and sham stimulation across monophasic and biphasic conditions.	118
4.9 No statistically significant shifts in ambiguous emotion recognition. . . .	121

List of Tables

2.1	Demographics summary of all study participants.	48
2.2	Demographic comparison between drug-naïve and drug-experienced participants.	49
2.3	Demographic comparison between drug-free and medicated participants.	50
2.4	Counts of participants in the sample by clinical history category.	51
2.5	Counts of medications used, grouped by pharmacological category, with total and per-medication counts.	52
2.6	Summary of clusters with increased functional connectivity in drug-naïve patients compared to drug-experienced patients.	54
4.1	Demographics summary of all study participants.	115
4.2	Individualised functional connectivity MRI-guided DLPFC target coordinates in MNI and Subject Space across participants.	116
4.3	No difference in recognising key emotions between biphasic and monophasic stimulation.	119

1 | Introduction

The burden of mental health disorders, as measured by the proportion of global disability-adjusted life-years attributed to mental health concerns, is continuing to increase. In fact, the WHO estimates that 15% of working-age adults have a mental disorder at any one point in time (World Health Organisation, 2022). This has many negative consequences, including tremendous costs to society due to lost lives and lives lived with disability, reduced productivity and unemployment, as well as caretaking needs, and secondary mental health impact, among others (Greenberg et al., 2023). Depression, clinically known as major depressive disorder or MDD, and anxiety alone are estimated to account for at least 12 billion lost workdays every year, costing the global economy about 1 trillion USD every year (Malik et al., 2023).

1.1 Major depressive disorder (MDD)

Major depressive disorder (MDD) remains one of the most prevalent and commonly diagnosed psychiatric conditions. It is a mood disorder characterised by persistent feelings of sadness and hopelessness and loss of interest in activities one used to enjoy. In order to receive such a diagnosis based on DSM-V criteria, symptoms must persist for a period of at least two weeks and need to include at least five symptoms, such as feelings of worthlessness, fatigue, weight loss or gain, and even suicidal ideation, in addition to experiencing either low mood or anhedonia (American Psychiatric Association, 2015). The lifetime prevalence of the disorder averages 12%, with the prevalence being double among women when compared to men (Pedersen et al., 2014). Furthermore, these numbers appear to have doubled since the 2019 Covid-19 pandemic (Bueno-Notivol et al., 2021), and MDD is expected to rank first as the leading cause of burden of disease worldwide by 2030 (Malhi & Mann, 2018). Understanding the mechanisms of this psychiatric condition, as well as improving its treatments, is therefore urgently important.

1.1.1 The evolution of cognitive theories of MDD

The current understanding of the mechanisms involved in the symptomatology of MDD focuses on the inter-dependence of hierarchical cognitive networks in the brain, and has evolved from theories around the hierarchical organisation of emotion and cognition.

The cognitive theory of depression, proposed by Aaron Beck (1967, 2nd ed. 2009), first suggested that psychopathological states represent extreme or excessive forms of normal cognitive, emotional, and behavioural functioning. At its core, the key proposition is that there is a strong hierarchical relationship between one's thinking and beliefs (cognitions) and one's emotional state. When these beliefs are based on habitual yet maladaptive thinking, this can lead to a self-reinforcing cycle (shown in Fig. 1.1). In this cycle, a biased interpretation of personal experiences can justify inaccurate beliefs, and interpret those experiences based on pre-existing cognitive schema (Southam-Gerow et al., 2011). This implies the existence of an underlying cognitive hierarchy, where the inability of higher-level processes (cognitions) to effectively regulate the activity of lower-level processes (emotions) results in a functional inability to regulate emotional and cognitive states. This inability, when exacerbated in a melancholic or low mood direction, can lead to major depressive disorder. To date, this remains one of the most significant theories informing cognitive behavioural therapy, one of the most common treatments, for depression (Salkovskis et al., 2024).

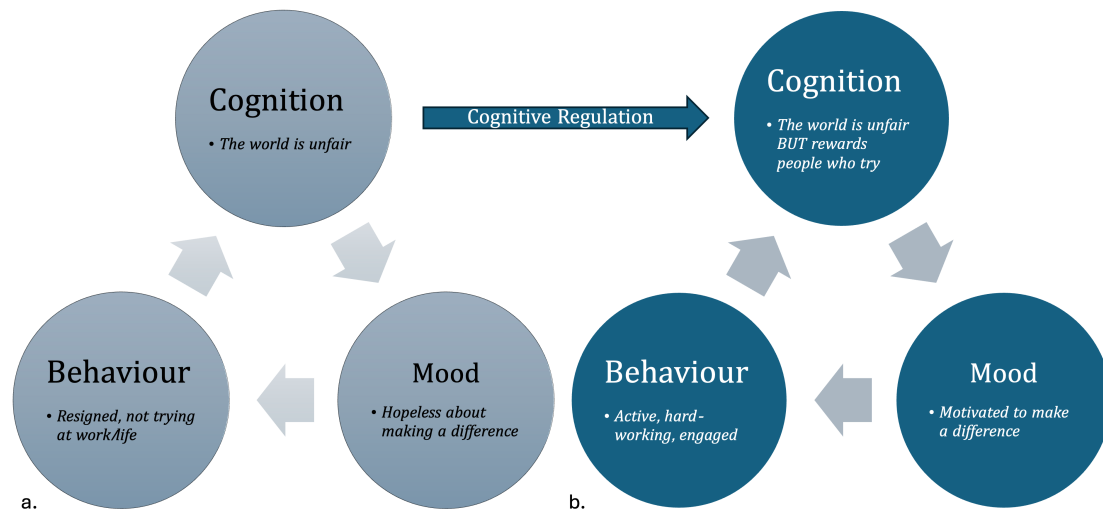


Figure 1.1: **Hierarchical relationship between cognition, mood, and behaviour highlights how maladaptive cognitive patterns can perpetuate depressive states through a self-reinforcing cycle.** (a) shows the maladaptive cycle that arises from habitual negative thinking. The cognition serves as a biased interpretation of personal experiences, informed by pre-existing cognitive schemas. This cognition influences mood and behaviour, interacting recursively and reinforcing the underlying maladaptive belief system and emotional state. (b) illustrates the role of cognitive regulation in disrupting this maladaptive cycle. Through a reframed cognition, higher-level cognitive processes exert regulatory control over lower-level emotional and behavioural processes, demonstrating how cognitive regulation can restore functional emotional and behavioural patterns.

Recently, this theoretical view has been updated with emerging neurobiological findings in depression research, giving rise to the integrated cognitive neurobiological model of depression (Disner et al., 2011; Beck, 2008; Roiser et al., 2012). According to this theory, negative stimuli lead to biased attention, biased processing, and biased memory and rumination pathways in underlying brain activity. Specifically, this theory suggests that in patients with MDD, the hierarchical top-down dysregulation can be linked to the relationship between regions in the prefrontal cortex (PFC) and structures in the limbic system. This is evidenced by the observed hypoactivity of the dorsolateral prefrontal cortex (DLPFC), and increased and sustained amygdala reactivity to negative stimuli, increased thalamic activity, and blunted nucleus accumbens and caudate nucleus responses

to positive stimuli (positive blockade) (Disner et al., 2011) in patients with MDD. This is not surprising as emotionally salient information is normally processed in the amygdala (Zheng et al., 2017), first and foremost, as well as the ventral striatum and the insula (Klepzig et al., 2024), which are controlled in a top-down manner by cortical structures, such as the DLPFC (Berboth & Morawetz, 2021). Based on existing research, the relay of this top-down control is understood to occur via the anterior cingulate cortex (ACC) and the dorsomedial thalamus (Parneadeau et al., 2018; Li et al., 2022; Nejati et al., 2021), which enables the controlled weighting of emotionally salient information between cortical and limbic structures. In depressed patients, this balance is disturbed (Yang et al., 2023), which leads to the inappropriate processing of emotional information, namely the hyperactivity of limbic structures and the hypoactivity of prefrontal structures, also discussed later, which has downstream behavioural as well as clinical impacts.

1.1.2 Neurobiology

As mentioned above, since 1990, advances in neuroimaging have enabled researchers to study the structural and functional differences in the brains of depressed and healthy adults to better understand the neuro-anatomical substrates of MDD. It is now known that MDD is related to structural changes in both grey and white matter.

1.1.2.1 Grey matter changes in MDD

MDD has been linked to a reduction in the grey matter volume (GMV) of key brain regions involved in cognition and emotion regulation, particularly the prefrontal cortex, the hippocampus, and the amygdala (Grieve et al., 2013; Ancelin et al., 2018).

Prefrontal cortex volumes, broadly responsible for the integration and the interpretation of cognitive and emotional interpretation, have reliably shown GMV reduction in MDD patients (Ketter et al., 1996; Shad et al., 2012; Chang et al., 2012). One of the largest global studies, the ENIGMA, found that depressed individuals had thinner cortical gray matter in the orbitofrontal (OFC), anterior and posterior cingulate cortices, as well as

in the insula and the temporal lobes (Schmaal et al., 2017). Other studies have shown reductions in the dorsolateral (right superior frontal gyrus) and medial (left superior frontal gyrus) regions of the prefrontal cortex (Bludeau et al., 2017). This shows not only prefrontal-specific but also broader impacts on GMV in MDD patients that likely impact both the cognitive processing of emotional inputs in the prefrontal cortex, as well as the quality of the input itself.

The hippocampus is a key structure involved in memory, spatial and emotional processing in the brain, and the reduction of hippocampal volume in patients with MDD is arguably one of the best replicated findings in the field. In the last 7 years, as more refined MRI segmentation methods have emerged, studies have shown that while patients with MDD will have bilateral reductions in overall grey matter volume of the hippocampus, these reductions primarily impact the hippocampal substructures (in order) of the dentate gyrus, the cornu ammonis (CA3 -> CA1), and the subiculum (Roddy et al., 2019). Most importantly, the dentate gyrus (DG) is part of the hippocampal trisynaptic circuit, directly interacting with both the amygdala and the cingulate cortex, relationships that both show abnormal disruptions in MDD patients (Jacob et al., 2022; Hao et al., 2020).

Finally, reductions in amygdala volume have also been consistently observed in MDD patients (Liang et al., 2023; Zheng et al., 2021), though some recent studies have suggested that overall reductions in GMV in the amygdala should be further analysed in order to understand how the volumes of individual amygdalar nuclei are impacted by MDD and disease severity (Roddy et al., 2021).

It is critical to note that multiple studies have shown that the proportion of GMV lost is directly correlated with the length and severity of MDD (Wise et al., 2017; Ancelin et al., 2019), suggesting that these structural changes are dynamic and progressive. It is also worth noting that recent studies suggest that accounting for age and suicidality in analyses of MDD patients is critical, as GMV changes seem to impact distinct cognitive regions in relation to the age of disease onset (Chen et al., 2024), which may have an impact on treatment protocols.

1.1.2.2 White matter changes in MDD

In addition to the grey matter reductions discussed above, white matter abnormalities have also been observed in MDD patients. Studies conducted with diffusion tensor imaging (DTI), an MRI modality focused on understanding the patterns of white matter in the brain, have shown significant reductions in white matter integrity (via fractional anisotropy (FA) reductions) in key regions associated with signal transmission. These regions included the corpus callosum (Lee et al., 2020; van Velzen et al., 2020) and the superior longitudinal fasciculus (Lai et al., 2014). This reduction in white matter integrity is likely to contribute to the inefficient signal transmission between different brain regions, leading to cognitive dysfunction, impaired executive function, and memory deficits seen in MDD. These observations emphasise the importance of white matter connectivity in maintaining normal cognitive and emotional functioning.

While structural changes in the brains of MDD patients continue to be investigated, it is increasingly clear that these structural pathophysiological changes become apparent at the functional level much earlier in the course of disease, and contribute to the emergence of structural changes as the disease progresses.

1.1.3 Neurocircuitry

Given that MDD manifests with a wide range of symptoms characteristic of altered cognitive and emotional function, such as low mood, anxiety, irritability, lack of or excessive hunger and sleep cues, among others, changes in functional connectivity must be part of the explanation underlying depressive mechanisms of action. Disruptions in three major resting state networks (RSNs), namely the default mode network (DMN), the salience network (SN), and the central executive network (CEN), have been found in MDD, as described in more depth in **Chapter 2**.

1.1.3.1 The DLPFC-sgACC functional relationship in MDD

The theme of disrupted top-down control in depression is central to understanding MDD as well as approaches to innovate its treatment. The left dorsolateral prefrontal cortex (DLPFC) and the subgenual anterior cingulate cortex (sgACC) are two crucial brain regions implicated in MDD, and the relationship between the two has been an emerging focus among researchers keen to improve treatment outcomes for patients.

The left DLPFC is a brain region involved in numerous cognitive and affective processes that are disrupted in depression, especially those associated with low mood (Xiong et al., 2023). It is a core component of the central executive network (CEN), responsible for functions such as working memory, attention, decision-making, and emotional regulation. In individuals with MDD, studies consistently show reduced activation and connectivity in the left DLPFC (Lee et al., 2023), particularly during tasks that require cognitive control and emotion regulation. This hypoactivity of the left DLPFC is consistent with the overall reduced activity of the CEN, further discussed in **Chapter 2**. Neuroimaging studies suggest that the reason for the specific role of the left DLPFC in MDD emerges from the asymmetry of the PFC in modulating emotions. Specifically, neural activity in the left DLPFC has been associated with approach-related emotions, such as motivation and positive affect, at least one of which must be reduced in MDD patients (see required diagnostic criteria for anhedonia and low mood in the DSM-V, which are the opposites of motivation and positive affect), while the right DLPFC is generally linked to withdrawal-related emotions, such as anxiety and rumination (Palmiero & Piccardi, 2017).

The relationship between the sgACC and the left DLPFC in the context of depressive symptomatology is of particular interest. Resting-state functional MRI studies have shown aberrant patterns of resting-state functional connectivity between the sgACC and the left DLPFC, specifically that they tend to be anti-correlated (Vasic et al., 2009; Connolly et al., 2013; Benschop et al., 2022). This means that while the DLPFC tends to be hypoactive in MDD, the sgACC tends to be hyperactive, as has been consistently

shown in other prefrontal and limbic regions. Hyperactivity of the sgACC has been associated with negative mood states (Martins et al., 2021), so interventions that lead to increased activity of the left DLPFC are likely to inhibit the sgACC leading to a reduction in low mood symptomatology, and are explored further in **Chapter 4**.

1.1.4 Current treatments

Current state-of-the-art, standard treatments for MDD are pharmacological, psychological, and neurostimulatory.

1.1.4.1 Pharmacotherapy

Traditional pharmacological treatments cover a range of antidepressant medications, including but not limited to selective serotonin reuptake inhibitors (SSRIs), such as sertraline, fluoxetine and citalopram (Chu & Wadhwa, 2023), and serotonin norepinephrine reuptake inhibitors (SNRIs), such as venlafaxine and duloxetine (Sansone & Sansone, 2014), among others. Some other pharmacological treatments have recently become approved (for example, esketamine (Vasiliu, 2023)) or are under active research investigation (for example, psilocybin (Goodwin et al., 2022)).

Remission rates of antidepressant medication treatment depend on the medication used, treatment regimen and individual factors. Generally, the response to an individual medication varies significantly across patients, and most patients will need to try multiple options before a good therapeutic fit is found, as achieving remission with an initial antidepressant treatment is reported in fewer than 40% of patients (Avari et al., 2020; Rush et al., 2008). With multiple medication changes and monitoring, remission with antidepressants can be achieved in 30.3-70.4% of cases (Alemi et al., 2021; Kim et al., 2021). This is because inter-individual variability, including depressive biotypes (Drysdale et al., 2017), is not understood well enough to be able to identify more effective treatments for particular patients a priori (Williams, 2016; Hack et al., 2023), and the mechanisms of action of antidepressant treatments in the context of the symptomatology

and neurobiology of the disorder (Harmer et al., 2017) remain to be understood.

It has been suggested that pharmacological antidepressants and behavioural therapies (like cognitive behavioural therapy, CBT; below) act by inhibiting the hyperactivity in the limbic structures and strengthening top-down control with increased activity of the prefrontal cortex (Godlewska & Harmer, 2021). Notably, however, these structures and networks are interlinked, and changes through entire circuits are observed across all antidepressant treatments (Dunlop et al., 2023).

1.1.4.2 Psychotherapy

Among psychotherapeutic treatment options, which are often used in combination with pharmacological treatment, cognitive behavioural therapy (CBT) is understood to be the most evidence-based and standardised method (Gautam et al., 2020), though other approaches (such as interpersonal psychotherapy, nondirective supportive treatment and others) are common. Newer, often psychotherapy-inspired forms of treatment, have also emerged, such as virtual reality-based interventions (Baghaei et al., 2021; Lindner et al., 2019) that enable more control over experiential and exposure learning. When used alone, the efficacy of psychotherapy (especially CBT) is rather limited (remission rate of 36.8%), though it is significantly boosted when therapy is pursued jointly with antidepressant medication treatment (remission rates of 50.0%) (Renner et al., 2014). In practice, the two are almost always prescribed jointly (Saul et al., 2020).

Generally, about a third of patients will not respond to multiple adequate treatment trials (antidepressant medication or psychotherapy), and will be classified as patients with treatment-resistant depression, or TRD (Gaynes et al., 2020). It is for those patients that non-invasive brain stimulation (NIBS) methods will generally be recommended, as the failure of first line treatments is generally necessary in order to access NIBS treatment under the NHS (NICE, 2015).

1.1.4.3 Non-invasive brain stimulation (NIBS)

Non-invasive brain stimulation (NIBS) refers to methods that use electric or magnetic fields to engage neural networks across the skull, without surgery or other intervention. Transcranial magnetic stimulation (TMS) and transcranial direct/alternating current stimulation (tDCS/tACS) are the most common types of NIBS approved and commonly used in the treatment of MDD.

Mechanistically, the use of NIBS relies on the understanding of MDD as a disorder of balance between top-down control in the prefrontal cortex and bottom-up emotional inputs from the limbic system, with the suggestion that if top-down cortical control were to be restored, i.e., the hypoactivity of the DLPFC eliminated, in patients with MDD, this would in turn reduce the hyperactivity of the associated limbic regions, leading to the remission of MDD symptoms. This is why stimulation of the DLPFC was historically chosen as the target for excitatory NIBS treatments, persisting to this day (Zheng et al., 2024; Brunoni et al., 2017).

The deeper mechanisms underlying the efficacy of NIBS in the treatment of MDD, however, remain to be understood. It is of note that while NIBS methods, unlike antidepressant pharmacological or psychotherapeutic treatment, are able to target brain regions and associated circuits quite precisely even if superficially (need to rely on connectivity networks to impact regions deeper in the brain), the associated treatment has delayed response times of 4-6 weeks. After 4-6 weeks, about 50% of patients will go on to respond to NIBS treatment (Perera et al., 2016). A similar length of delay in clinical efficacy has been observed with pharmacological treatment using antidepressant medications (Machado-Vieira et al., 2010). Given that hormonal and neurotransmitter-focused pharmacological theories do not fully explain this effect (Stahl, 1998; Golyszny & Obuchowicz, 2019), a theory was put forth by Harmer & Godlewska at the cognitive and behavioural level of explanation, in the form of the cognitive neuropsychological theory (CNT) of antidepressant action, discussed further in **Chapter 4**.

1.2 Transcranial magnetic stimulation (TMS)

The most studied NIBS method in the context of MDD is transcranial magnetic stimulation (TMS). TMS uses brief, rapidly changing magnetic field pulses to induce targeted electrical currents in cortical tissue underlying the scalp and skull under the coil, which is used to administer them (Hallett, 2007). These currents, in turn, lead to the depolarisation of neurons that trigger action potentials in the region. TMS pulses can be administered in different patterns, doses and frequencies, and different combinations have been studied for their therapeutic impact and clinical benefit. While modelling studies show that the focal point of stimulation is the cortical tissue directly underneath and perpendicular to the centre of the stimulating coil, i.e. at the cortical surface (Dannhauer et al., 2023), indirect effects in other, functionally and structurally connected cortical and subcortical regions are expected to account for much of the observed therapeutically relevant change (Benschop et al., 2022) as a result of engaging disease-relevant networks in the brain. Since 2008 in the US (Yan, 2008), and 2015 (NICE, 2015) in the UK, TMS has been an approved option for the treatment of MDD using the 10-Hz rTMS protocol. Under this protocol a daily stimulation is delivered over 20 to 30 days, during which a patient receives repetitive magnetic pulses at a 10 Hz frequency for 37.5 minutes, for a total of 3,000 pulses per session, over their left dorsolateral prefrontal cortex (DLPFC) (McClintock et al., 2018).

1.2.0.1 Targeting the DLPFC with TMS in MDD

Given its role as a node of the central executive network (CEN), the DLPFC became a primary target for therapeutic interventions in MDD, particularly with NIBS techniques such as TMS and tDCS. As discussed above, the therapeutic effects of stimulating the DLPFC are understood to be mediated by its ability to enhance cognitive control over negative emotions and restore the balance between the CEN and the DMN, likely through the modulation of other brain regions, such as the subgenual anterior cingulate cortex (sgACC) and the amygdala. Critically, the subregion of the sgACC most strongly anti-

correlated with the DLPFC at rest in depressed individuals has been shown to be the most effective for the clinical efficacy of TMS in targeting the DLPFC for the treatment of MDD (Cole et al., 2021; Fox et al., 2012), and is now viewed as the most advanced way to target the DLPFC for MDD treatment, as discussed later in the **Introduction**.

1.2.0.2 Intermittent theta burst stimulation (iTBS)

In 2018, the application of TMS in the context of depression treatment underwent a major transformation, when the classic rTMS protocol of administering TMS was found to be non-inferior to the novel intermittent theta burst stimulation (iTBS) protocol (Blumberger et al., 2018). iTBS, a patterned form of TMS, was found to be a much more efficient protocol, where 600 pulses are delivered in 'bursts' of three 50-Hz pulses, repeated at 5 Hz for 2 seconds (a 'train' of 10 bursts), for a total of 20 trains delivered over the DLPFC during a single iTBS session, lasting around 3 minutes. This protocol is not only tenfold quicker to administer than its predecessor, but is also based on a more mechanistic understanding of the brain.

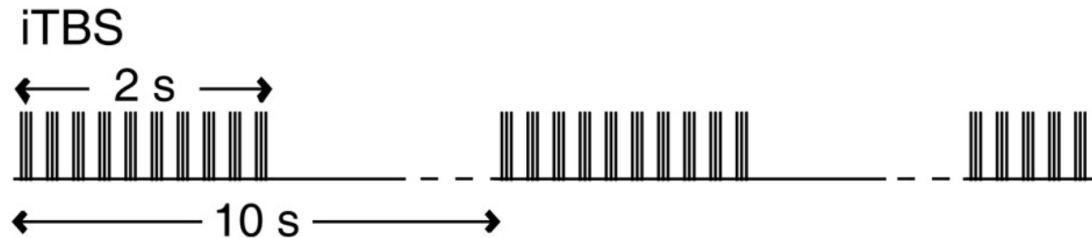


Figure 1.2: **Intermittent theta burst stimulation (iTBS) pattern.** Reproduced from Huang et al., 2005.

Specifically, theta burst patterns have become commonly used to induce plasticity in animal brain slices, after discovering a burst discharge in the theta (4-7 Hz) range in the hippocampus of rats during exploratory behaviour (Diamond et al., 1988). Typically, brain slices are stimulated using four bursts at a frequency of 100 Hz (Hernandez et al., 2005).

The TMS machines at the time, however, had technical limitations when administering iTBS. Consequently, to adapt these protocols for human trials, three pulses at a frequency of 50 Hz were selected based on feasibility to deliver the power from the electronics. Initially, these protocols were administered in a continuous manner (known as cTBS), which led to the observation that in humans, administering TBS initially leads to long-term potentiation (LTP) effects on neurons but, if given continuously (for as little as 20s), will lead to long-term depression (LTD) effects (Dhuna et al., 1991; Kearney-Ramos et al. 2018). The initial protocols were then adjusted to deliver short, repeated trains of pulses, in order to take advantage of the immediate LTP effects and lead to an overall excitatory rather than inhibitory effect on the targeted region (Suppa et al., 2016), see Fig. 1.2.

Given that iTBS protocols have been shown to be non-inferior to standard rTMS treatment protocols for MDD, iTBS has become popular in clinics, where shorter treatment protocols mean that more patients can benefit from treatment, while reducing operational costs. It remains a second-line treatment, most prescribed when multiple antidepressants and psychotherapy has failed.

1.3 Optimisation of TMS protocols for MDD treatment

Clinical practice is increasingly moving to specialised protocols of TMS to enhance the efficacy and reduce the clinical burden of treatment. Several parameters, including stimulation pattern and dose, pulse shape and targeting, are believed to be key in achieving the best clinical results.

1.3.1 Stimulation pattern

As discussed above, while high-frequency repetitive TMS (rTMS) targeting the left dorsolateral prefrontal cortex (DLPFC) remains the most used protocol in MDD treatment, iTBS is increasingly used by clinics as well due to its shorter administration. Other patterns are used in specific cases, such as continuous TMS (cTMS), deep TMS (dTMS), quadripulse stimulation (QPS), interleaved TMS (iTMS) and low-intensity TMS (li-TMS), but are much less common than rTMS and iTBS.

1.3.2 Stimulation dose

TMS stimulation dose depends on the duration, frequency, intensity and total number of sessions delivered during treatment.

Standard MDD protocols typically involve daily sessions over four to six weeks (20 to 30 sessions), with some studies suggesting that extending the treatment duration or increasing the number of pulses per session can enhance clinical outcomes (Berlim et al., 2014). Furthermore, maintenance TMS sessions have been explored as a means to prevent relapse, with preliminary evidence supporting their utility in sustaining remission (Hovington et al., 2013), and are commonly administered in once-monthly frequencies following successful TMS treatment.

When it comes to the intensity of the stimulation, the resting motor threshold (RMT) is often used as a reference point to determine the appropriate intensity for a particular patient undergoing treatment. Most therapeutic protocols use intensities ranging from 70% to 120% of RMT. Individual differences in skull thickness, cortical excitability, and neuroanatomy are believed to underlie the inter-individual variation in RMT, though increasing evidence supports additional variables impacting RMT such as gender and time of day, as explored further in **Chapter 3**.

New, hyper-intensive TMS delivery protocols have recently picked up and been cleared by the US FDA, such as the Stanford Neuromodulation Therapy (Cole et al., 2020; Cole et

al., 2022). These protocols administer 10 daily sessions, at triple the dose of a usual iTBS protocol (18,000 instead of 600 pulses per session), without showing increased prevalence of side effects, and demonstrating that following 5 days of treatment, 79% of participants in the active group achieved remission from their depressive episodes at some point during the 4-week follow-up. All of these results have been tested in comparison with placebo (or sham) stimulation, in double-blinded clinical setups, to account for the potential of heavy clinician presence and high levels of patient-clinician interaction impacting clinical outcomes.

Such protocols have challenged the notion that TMS treatment needs to maintain a similar treatment horizon as that seen in pharmacological interventions of 4-6 weeks, and could be safely intensified for quicker symptom relief and MDD remission.

1.3.3 Precision targeting

In addition to significantly increasing the dose and frequency of stimulation in the SNT, the protocol also used personalised targeting of the DLPFC based on resting state functional connectivity, rather than the standard targeting methods currently deployed in clinics, such as the 5-cm rule and MRI-guided neuronavigation.

1.3.3.1 5-cm rule

The oldest method of targeting the DLPFC for MDD treatment is the 5-cm rule. This method is a straightforward, non-neuronavigated approach to positioning the TMS coil over the DLPFC, based on scalp measurements, and is therefore the most accessible option in clinics that do not have access to neuronavigation equipment (Shao et al., 2024; Hsu et al., 2024; Brunoni et al., 2018). With this method, the 'motor hotspot' is identified by finding the area on the scalp where TMS stimulation elicits a motor response, typically causing movement (a 'twitch') of the contralateral hand or fingers. Then, the TMS coil is moved 5 cm anterior (towards the forehead) along a parasagittal line on the scalp, which is generally thought to position the coil over the DLPFC, where

stimulation is administered. It is, of course, a highly constrained method, as it does not account for differences in head size, brain anatomy, or individual variability in the precise location of the DLPFC, and can therefore result in suboptimal targeting for some patients, potentially affecting the efficacy of TMS treatment. The impact of such, potentially imprecise targeting, remains to be understood as studies have not reached consensus (Trapp et al., 2023; Fitzgerald et al., 2009; Fitzgerald, 2021).

Given this, more advanced techniques like the Beam F3 method and MRI-guided neuronavigation are now recommended as the standard targeting method in clinics.

1.3.3.2 Beam F3

An intermediate method between the simplicity of the 5-cm rule and the precision of MRI-guided neuronavigation is the Beam F3 targeting method. Developed to offer enhanced accuracy without requiring imaging equipment, the Beam F3 method is based on standardised EEG electrode positioning (the international 10â20 EEG system) to identify the DLPFC.

Using three simple scalp measurements, the distance from the nasion to the inion, and between the left and right preauricular points, the Beam F3 algorithm calculates a tailored coordinate for placing the TMS coil over the left DLPFC. These measurements are then input into a validated calculation (often implemented via accessible smartphone or online applications) that identifies the F3 electrode site, corresponding closely to the underlying cortical area of the DLPFC targeted for depression treatment.

Compared to the traditional 5-cm rule, Beam F3 significantly reduces variability and improves accuracy by accounting for individual head size and shape, making it especially useful in clinical settings without access to MRI or neuronavigation technology (Mir-Moghtadaei et al., 2015; Beam et al., 2009). However, while Beam F3 enhances precision over the 5-cm rule, it still lacks the fine anatomical specificity achievable with MRI-guided neuronavigation or functional connectivity-based approaches. Despite this limitation, Beam F3 remains a widely recommended alternative when MRI-based methods are not

feasible.

1.3.3.3 MRI-guided neuronavigation

Unlike the 5-cm rule and the Beam F3 method, which rely on general scalp measurements, MRI-guided neuronavigation uses individual brain imaging data, or a standardised template, to more accurately locate the DLPFC for an individual patient.

In an ideal scenario, before the TMS session, each patient undergoes structural magnetic resonance imaging (MRI) scanning, showing both the cortical anatomy and specific brain structures, including the DLPFC. Then, the patient's MRI data is integrated into a neuronavigation system, which uses specialised software to recreate a 3D model of the patient's brain. When the patient comes in for a stimulation session, with the neuronavigation system tracking the position of the TMS coil in real time, and with the reference of the 3D model in the system, the clinician can guide the coil to the exact coordinates of the patient's DLPFC as identified in the MRI scan. This allows for consistent and accurate stimulation of the targeted brain region, tailored to the individual's unique anatomy.

Alternatively, when the patient's own MRI scan cannot be acquired (for financial or access reasons), a modified protocol can be used, where the patient's anatomical landmarks during the session are aligned to a standard 3D model template, most commonly that of the Montreal Neurological Institute (MNI), to best approximate the position of the DLPFC. This modification leads to a method that is less precise than when the 3D model is built upon the patient's brain but is still thought to be much more precise than the 5-cm rule. As discussed later, and especially in **Chapter 4**, the accessibility of MRI, as well as technicians and clinicians needed to implement the use of scans in clinical practice, remains an important consideration when balancing precision over treatment accessibility and scalability.

1.3.3.4 rsFC-based (sgACC-DLPFC) neuronavigation

Ultimately, while both methods aim to target a consistent location within the DLPFC, the research on the functional connectivity underlying MDD discussed above clearly suggests that it is a dynamic and heterogeneous condition. This implies that a fixed anatomical target may not account for individual variability in network dysfunction. Recent advances in understanding functional connectivity now enable us to move beyond static targeting approaches, such as MNI coordinates or anatomical landmarks and structures, and allow for more precise and personalised targeting methods to potentially improve therapeutic outcomes.

One of such methods, becoming increasingly popular since its use in the SNT protocol as above, is target identification based on the anti-correlated connectivity between the sgACC and the DLPFC. This method is based on the observed close relationship between the DLPFC and the sgACC, and suggests that when the target used in TMS is the sub-region of the DLPFC that is most anti-correlated with the sgACC (see section **The DLPFC-sgACC functional relationship in MDD**), antidepressant responses may be enhanced (Cole et al., 2020). As shown in Fig. 1.3, most personalised coordinates will fall more laterally and deeper in the brain than standard scalp-based DLPFC coordinates.

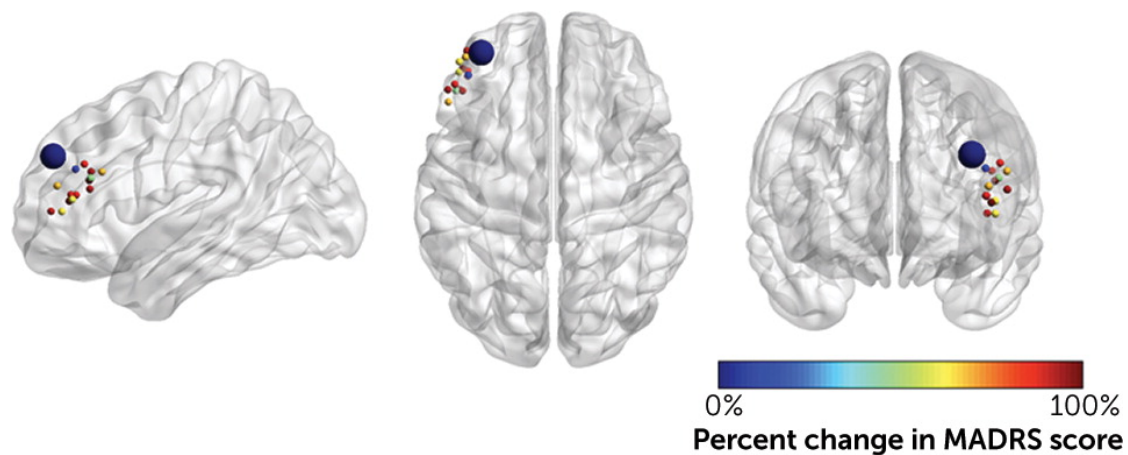


Figure 1.3: **Individualised functional connectivity MRI-guided target locations for Stanford neuromodulation therapy in relation to an average F3 coordinate.** The location of the standard F3 coordinate is shown in dark blue. The colors of the targets represent the maximum percentage change from baseline in Montgomery-Asberg Depression Rating Scale (MADRS) score following the SNT treatment protocol. Reproduced from Cole et al., 2020.

There is still no standardised pipeline for applying this method, but the general workflow consists of participants undergoing both structural and resting state MRI scans. The structural scans are used to create a 3D model of the patient's brain in the neuronavigation software, as in standard neuronavigation, while the resting state scans are analysed to find the anti-correlated relationship between the sgACC and the DLPFC. The peak anti-correlation coordinates in the DLPFC are then loaded onto the neuroimaging software to guide the coil to the exact coordinates of the patient's DLPFC as identified in the MRI scan. This method was used by the author to optimise TMS treatment in the study in **Chapter 4**, and the pipeline is documented in the **Methods** section of the chapter.

1.3.4 Pulse shape

Two main pulse shapes are relevant when discussing TMS - biphasic and monophasic. When applying iTBS and rTMS, as well as most other patterns of NIBS, biphasic pulses

are the standard pulse shape. Biphasic pulses involve a rapid reversal of the magnetic field direction mid-pulse and are more energy-efficient (allow for energy recovery back into the electronics) compared to monophasic pulses, allowing for lower energy usage and reduced coil heating, making them more suitable for extended, or intensive, treatment sessions (Wassermann, 1998; Rossi et al., 2012).

Monophasic pulses consist of a single, unidirectional magnetic field pulse, which leads to a rapid change in electric field strength. This pulse type is known for its ability to produce more focused stimulation, which can be advantageous in targeting specific brain regions with greater precision (Peterchev et al., 2011). However, monophasic pulses generally require higher energy levels to achieve the same level of neuronal activation as biphasic pulses, potentially leading to increased coil heating and patient discomfort during prolonged sessions (Ilmoniemi et al., 2024).

Most importantly, monophasic pulses are hypothesised to recruit cortical neurons more selectively than biphasic pulses, predicting stronger plasticity effects. This is because while biphasic pulses are widely used due to their efficiency and reduced power consumption, they may not fully align with the intrinsic properties of neuronal excitability (Sommer et al., 2018). Monophasic pulses, on the other hand, are theorised to be more efficient as they produce a more focused and unidirectional current flow, which is thought to better mimic natural physiological neuronal activity and enhance synaptic efficacy (Wendt et al., 2023; Radyte et al., 2022).

Given that monophasic pulses are understood to be better aligned with physiological neural activity, it has been hypothesised that their use could lead to improved therapeutic outcomes in clinical applications of TMS (Wendt et al., 2023; Wang et al., 2024). This approach would offer a more physiologically congruent stimulation method, potentially optimising the activation of cortical circuits relevant to treatment outcomes.

1.3.4.1 Limitation of traditional TMS electronics

As alluded to above, conventional TMS devices have hardware constraints that mean that they have limited pulse shape control, such as efficiently using monophasic pulses for more intensive protocols, and may not be able to optimally target specific neural circuits, limiting the potential to achieve desired therapeutic effects.

In conventional TMS devices, carrier-based pulse-width modulation (PWM) is limited by the switching frequency of commercial Insulated Gate Bipolar Transistors (IGBTs), which can lead to deviations from the desired pulse shapes and reduce stimulation accuracy (Sorkhabi et al., 2022). These devices often have fixed hardware configurations, making them difficult to adapt or upgrade for different research or clinical applications, which has led to limited clinical testing of alternative (non-biphasic) pulse shapes. Additionally, conventional TMS devices can generate excess heat and consume significant power, which limits their use for extended or repeated sessions and intensive protocols, such as iTBS and the SNT.

1.4 Research objectives

The focus of this thesis is on investigating important considerations when personalising TMS treatment for MDD based on magnetic resonance imaging, understanding the sensitivity to demographic and clinical variables in the real-world application of TMS in the treatment of MDD, and how treatment outcomes could be improved with emerging technology and corresponding protocols.

The overarching motivation guiding this work is: how can TMS treatment for MDD be made most effective, and how can we best consider individual differences when optimising treatment? It is broken down into the following research questions, corresponding to data chapters:

1. **Chapter 2: Mechanisms** How do patterns of high-resolution resting state activ-

ity differ across depressed patients?

2. **Chapter 3: Practice** How do real-world TMS treatment circumstances impact clinical outcomes?
3. **Chapter 4: Innovation** Can a single session of optimised TMS treatment in depressed patients lead to cognitive change?

2 | Mechanisms: Characterising differences in resting state connectivity across drug-experienced and drug-naïve depressed participants

2.1 Introduction

2.1.1 Resting state functional connectivity (rsFC)

Resting state functional connectivity (rsFC) measures spontaneous brain activity by analysing the temporal correlations between spatially distinct brain regions when the subject is not engaged in any specific task, i.e. the subject's "resting state". This form of connectivity is assessed using functional magnetic resonance imaging (fMRI), which detects fluctuations in blood oxygen level-dependent (BOLD) signals that are believed to reflect underlying neuronal activity (Biswal et al., 1995), though this view of a direct link has been challenged by multimodal studies (Ekstrom, 2009; Zhang et al., 2020).

The temporal correlation of BOLD signals between various brain regions can be used to calculate functional connectivity measures, which show intrinsic networks, known as resting state networks (RSNs) that remain active even when task-specific stimuli are not present (Fox and Raichle, 2007). Previous research has linked these variations in rsFC to a number of neurological and psychiatric disorders, making them a useful tool for both investigating the underlying mechanisms of these conditions (Greicius et al., 2003), as well as for examining minute variations in brain connectivity in response to therapeutics (Tura et al., 2023). Most studies investigating brain connectivity use 3T MRI neuroimaging, but there is increasing interest in higher resolution methods of neuroimaging, such as 7T MRI.

2.1.2 7T MRI

When compared to standard 3T neuroimaging, ultra-high-field MRI, or 7T, neuroimaging has a higher signal-to-noise ratio (SNR), higher spatial and temporal resolution, and therefore higher sensitivity to connectivity patterns.

Higher magnetic field strength enhances the SNR, a core metric of imaging quality, which is notably greater at 7T compared to 3T (Triantafyllou et al., 2005). This increase in SNR allows for shorter scan times or improved image quality for the same duration, facilitating more reliable detection of subtle resting-state connectivity patterns.

7T scans have significantly higher spatial resolution than 3T scans because the higher field strengths allow for a reduction in voxel size while maintaining the SNR, which makes it easier to visualise finer anatomical details on resulting scans (Maruyama et al., 2019; Lecler et al., 2022). Many neuropsychiatric conditions, including MDD, involve changes in the connectivity of small, deep and critical brain structures, such as the amygdala and the habenula, so improved spatial resolution can help detect previously missed changes. 7T scans also have higher temporal resolution than 3T scans, as 7T MRI allows for faster acquisition without a loss in data quality, enhancing the temporal fidelity of resting-state connectivity measures (Lawrence et al., 2018). This can be especially useful in studying the rapid dynamics of brain networks involved in emotional processing and cognitive control, which may show disrupted or altered patterns in individuals with depression.

It is therefore generally believed that the high spatial and temporal resolution of 7T MRI can provide a more comprehensive view of network-level interactions underlying psychiatric disorders and the mechanisms of action underlying their response to treatment.

2.1.3 Key resting state network changes in MDD

rsFC research consistently points to disruptions in three primary networks in MDD: the default mode network (DMN), the salience network (SN), and the central executive network (CEN). These networks, central to cognitive and emotional regulation, exhibit

distinctive connectivity alterations in MDD that correlate with key depressive symptoms and cognitive dysfunctions. Impaired task-dependent network switching, resulting from reduced CEN-DMN connectivity (Vidal-Pineiro et al., 2014; Tozzi et al., 2021; Yan et al., 2019), is one of the best replicated findings in MDD rsFC and is understood to be responsible for maladaptive cognitive and emotional patterns sustaining MDD symptomatology over time.

2.1.3.1 Default mode network (DMN)

The DMN, typically active during rest and self-referential thought, includes the medial prefrontal cortex (mPFC), posterior cingulate cortex (PCC), precuneus, angular gyrus, and hippocampus (Raichle, 2015). In MDD, studies report increased connectivity within the DMN, which aligns with ruminative and negative thought patterns prevalent in depression (Hamilton et al., 2015). This hyperconnectivity likely underlies the persistent negative bias observed in MDD patients.

2.1.3.2 Salience network (SN)

The SN, which includes the hubs of the anterior cingulate cortex and anterior insula, preferentially processes emotionally salient stimuli, and is primarily responsible for switching between the DMN and the CEN (Seeley, 2019). SN shows dysregulation in MDD, which is linked to impairments in emotional processing and symptoms like anhedonia, the decreased ability to experience pleasure (Liu et al., 2018; Lynch et al., 2024).

2.1.3.3 Executive control network (CEN)

Unlike the DMN and the SN, the CEN, which supports higher-order cognitive functions such as working memory and decision-making, is often underactive in MDD (Chakrabarty et al., 2016). Key regions within the CEN include the dorsal anterior cingulate cortex, amygdala, anterior insula, ventral striatum, and thalamus. Reduced CEN activity correlates with the cognitive deficits commonly reported in MDD (Sarpal et al., 2022). As

mentioned above, effective connectivity between the DMN and CEN is diminished in MDD, interfering with the dynamic switching required for attentional focus on goal-directed tasks, thereby reinforcing ruminative states (Li et al., 2021).

2.1.4 Pharmacological impacts on rsFC in MDD

We now know that specific medications will impact rsFC networks central to cognitive and emotional processing. These changes are increasingly recognised as potential markers for treatment response and symptom improvement.

2.1.4.1 SSRIs: fluoxetine and escitalopram

SSRIs, including fluoxetine and escitalopram, are widely used in MDD and have been shown to reduce hyperconnectivity within the DMN, particularly in areas like the medial prefrontal cortex (mPFC) and posterior cingulate cortex (PCC) (Gudayol-Ferre et al., 2015; Cui et al., 2021). This reduction in DMN connectivity correlates with decreases in ruminative thought and self-referential processing, core symptoms in MDD (Posner et al., 2013). Additionally, fluoxetine & escitalopram have been associated with enhanced connectivity within the CEN, involving the dorsolateral prefrontal cortex (DLPFC), which supports improvements in cognitive function and executive control (Martens et al., 2022; Capitao et al., 2020; Liu et al., 2023). Escitalopram has also demonstrated effects on inter-network connectivity, aiding in dynamic switching between the DMN and task-positive networks (namely the CEN), which may alleviate the cognitive rigidity often observed in MDD (Ionescu et al., 2015).

2.1.4.2 SNRIs: venlafaxine

Studies have shown that venlafaxine increases connectivity between the anterior insula and the ACC within the SN, which supports improvements in emotional processing and mood stability (Gerlach et al., 2022). In addition, venlafaxine's effect on CEN connectivity seems to help improve task-related attentional control and working memory in MDD

patients, which is linked to improvements in cognitive symptoms (Tian et al., 2016).

2.1.4.3 Atypical antidepressants: bupropion

Bupropion, an atypical antidepressant that primarily affects dopaminergic and norenergic pathways, has been shown to enhance CEN connectivity, particularly in areas linked to cognitive control and motivation, such as the DLPFC and thalamus. This enhancement supports improved executive function and a reduction in cognitive symptoms of depression (Patel et al., 2016; Rzepa et al., 2017). Bupropion has also been found to reduce hyperconnectivity within the DMN, potentially decreasing self-referential and ruminative thinking, thereby contributing to symptomatic relief in MDD (Nam et al., 2017).

2.1.4.4 Ketamine

Ketamine, an NMDA receptor antagonist known for its rapid-acting antidepressant effects, has been shown to produce immediate alterations in rsFC within and between the DMN, CEN, and SN. Studies indicate that ketamine reduces DMN connectivity and increases CEN connectivity, in line with neural activity in healthy adults, associated with the rapid reduction in depressive symptoms (Abdallah et al., 2018). Ketamine also modulates the SN, which may alleviate symptoms like anhedonia (Mueller et al., 2018).

As above, across most pharmacological interventions for MDD, we see an impact on either the DMN itself, or the ability to switch between network-specific states. Studying similar impacts in NIBS, therefore, is an important step to investigate the mechanistic similarities between pharmacological and neurostimulatory antidepressant treatments.

2.1.5 rsFC in TMS treatment for MDD

In line with the hypotheses underlying TMS treatment, recent MRI evidence suggests that there is a causal relationship between DLPFC stimulation and the activation of the ACC (Tik et al., 2023), showing direct influences of the stimulatory treatment over a key

relationship in MDD pathophysiology. This is consistent with other studies that showed that TMS normalised MDD-related subgenual ACC hyperconnectivity in the DMN but did not alter connectivity in the CEN (Liston et al., 2015). This suggests a mechanism of action similar to that observed in SNRIs, where the antidepressant effect appears to rely on the strengthening of the limbic system, though it may be more direct in TMS than it is with pharmacologically-mediated effects.

However, it is important to note that few MDD patients will access TMS (and other NIBS modalities) as a first-line treatment, which poses significant challenges when trying to discern the impacts of TMS as the first treatment versus the combined impacts of prior pharmacotherapy use on the TMS-naïve patients' brains and resting state functional connectivity patterns. It may cause further challenges as methods to optimise TMS treatment emerge that rely on patterns of rsFC which may or may not be influenced by prior antidepressant medication use and can impact the reliability of the underlying methodology, as explored in **Chapter 4**.

2.2 Research questions

As discussed, pharmacological interventions for MDD influence resting state functional connectivity (rsFC), leading to symptom relief for many patients. However, for those failing initial treatment, a challenge emerges as only the initial MDD intervention administered to a brain is being applied to "standard", drug-naïve MDD rsFC patterns, while subsequent interventions, particularly second-line treatments such as TMS, need to contend with pre-existing changes in rsFC resulting from prior medication use. It is therefore critical to understand whether there are any changes, and what changes if so matter if rsFC-based methods are to be used in optimising and/or improving NIBS treatment in MDD as will be explored in **Chapter 4**.

To test how prior and current antidepressant medication influences resting-state functional connectivity (rsFC) in MDD patients, we focused on two primary research ques-

tions:

1. Is there a difference in 7T rsFC connectivity between MDD patients who are fully medication-naïve and those with prior drug exposure?
 - **Hypothesis:** Medication-naïve patients will show distinct patterns of rsFC compared to drug-experienced patients, reflecting medication-related neuro-functional alterations even after symptom relapse.
2. Is there a difference in 7T rsFC connectivity between MDD patients who are currently receiving medication and those who are medication-free on the day of the MRI scan?
 - **Hypothesis:** Patients currently receiving antidepressant medication will exhibit different rsFC patterns compared to medication-free patients, although these effects may be more subtle given the variability in treatment duration and medication type.

These research questions focus on two definitions of antidepressant use experience, common among MDD patients: drug-naïveté as not having ever taken any antidepressant medication, and drug-free, when an MDD patient may have taken antidepressant medication in the past, but is not taking medication at the time of the study/rsMRI scan. We believe that having a more nuanced understanding of both the clinical history, as well as pre-existing brain states, of patients going into NIBS treatment is critical to later understanding variability in treatment outcomes, as explored further in **Chapter 3**.

2.3 Methods

2.3.1 Participants

This study was run at the University of Oxford, under the ethical review of the NRES Committee South Central - Oxford B (REC reference 13/SC/0328, IRAS project ID

128597). Seventy four participants with an active diagnosis of major depressive disorder (aged 18-70) were included in the study. A posteriori power analysis indicated that with our sample size of approximately 74 participants, we were adequately powered (>80%) to detect medium-sized effects (Cohen's $d = 0.6$) in functional connectivity differences between groups at a corrected significance threshold ($\alpha = 0.05$, TFCE corrected for multiple comparisons). All participants underwent screening to confirm their fitness for the study based on identified inclusion and exclusion criteria, and signed an informed consent form. Their diagnosis was confirmed using a Structured Clinical Interview for DSM-IV (American Psychiatric Association, 1999) by a qualified psychiatrist, and there was a minimum period of being medication-free to take part in the study, with participants required to have discontinued antidepressant medication at least 2 weeks prior to the study. However, due to the prolonged half-life of fluoxetine and its active metabolite, norfluoxetine, which remain in the body significantly longer than other antidepressants, a washout period of at least four weeks was required for participants previously taking fluoxetine (Gury & Cousin, 1999). Exclusion criteria included psychosis or substance dependence as defined by DSM-IV, clinically significant risk of suicidal behaviour, contraindications to MR imaging, the use of concurrent medication which could alter MRS neurochemicals (eg. benzodiazepines), patients in need of urgent drug treatment, pregnant or breast feeding patients, participants involved or recently involved (last month) in a research project. It's worth noting that despite being recruited for the study and asked to be drug-free, some participants still took medication the day of the scheduled scan and their data is assessed as 'medicated' in one of the studied sub-populations.

2.3.2 Data acquisition

Resting-state functional MRI (rs-fMRI) data were collected using a Siemens MAGNETOM 7T scanner. A gradient-echo EPI sequence was employed with the following parameters: repetition time (TR) of 3000 ms, echo time (TE) of 25.00 ms, and a flip angle of 90° . The acquisition matrix size was 110x110, with a voxel size of 1.0x1.0x1.0 mm. Fifty-

two axial slices were acquired in an interleaved fashion to provide whole-brain coverage with a slice thickness of 2.0 mm and no gap. Parallel imaging was implemented using GRAPPA (factor 2), with 40 reference lines in the phase-encoding direction. A multi-band acceleration factor of 1 was applied. The field of view (FOV) was 220 mm, and the bandwidth was 1748 Hz/Px. Subjects were instructed to remain still with their eyes open and to focus on a fixation cross during the scan (scanning protocols are provided for completeness in **Appendix B**).

2.3.3 Preprocessing

The preprocessing of rsMRI data was performed using FSL (FMRIB Software Library; Smith et al., 2004; Woolrich et al., 2009; Jenkinson et al., 2012). Firstly, the structural T1 images and fieldmap magnitude images were brain-extracted using an adapted, manually modified and individually corrected BET pipeline to ensure smooth extraction of the brain, then motion correction was carried out using the MCFLIRT tool, aligning each volume to the middle volume of the time series. Fieldmap corrections were made using a prepared phase (rads) image and brain-extracted magnitude fieldmap. Effective EPI (echo planar imaging) spacing and TE (echo time) values were taken from the imaging protocol, and B0 unwarping was performed to correct for distortions (especially important at 7T due to increased susceptibility artifacts). For spatial smoothing, we applied a Gaussian kernel with a 4 mm full-width half-maximum (FWHM), which is on the higher end of usual smoothing for 7T scans, chosen to optimally balance the enhanced signal-to-noise ratio (SNR) at 7T and reduced anatomical variability across participants. High-pass temporal filtering with a 100-second cutoff was applied to remove low-frequency drifts, ensuring appropriate handling of resting-state signals. Functional data were registered to the subject's bias-field corrected T1-weighted structural image using boundary-based registration (BBR). Single-session ICA (independent component analysis) was conducted using automatic dimensionality estimation to identify independent components for noise removal. Spatial maps were thresholded at $z = 0.5$. The FIX (FMRIB's ICA-based

Xnoiseifier) tool was used to clean the data by creating a training dataset by manually labeling components for 20 (of 74) participants, and the classifier was trained and applied to the entire dataset to identify signal and noise; noise components were identified and removed from the data. The cleaned data were then transformed into MNI152 standard space for group-level analysis.

2.3.4 Data quality assessment

Preprocessed images were visually inspected to identify any remaining artifacts or issues with preprocessing. Signal and noise labels from the FIX training dataset were identified by visual inspection, independently by the author, reviewed and consulted with multiple other, MRI-experienced researchers (Dr Godlewska and Dr Martens), and automatically generated signal and noise labels were checked at random to confirm labelling quality.

2.3.5 Functional connectivity analysis

Group ICA: We conducted group ICA using MELODIC (Multivariate Exploratory Linear Optimized Decomposition into Independent Components (Beckmann et al. 2006)) on the cleaned, standard-space data from all subjects. We applied multiple splits, including a 25-fold dimensionality split and a 100-fold dimensionality split, to identify the major resting-state networks. When generated, group-level spatial maps corresponding to each component were visually inspected and compared with reference networks described in previous literature (Smith et al., 2009).

Dual regression: We used dual regression to link subject-specific time series to the group-level spatial maps. Firstly, the group ICA spatial maps were regressed into each subject's 4D rsMRI data to obtain subject-specific time series. Then, these time series were regressed back into the rsMRI data to generate subject-specific spatial maps, representing the functional connectivity of each component for each subject.

Connectivity (randomise) analysis: We applied non-parametric permutation testing using FSL’s *randomise* tool (5,000 permutations) to subject-specific spatial maps to assess group-level differences in functional connectivity. Contrasts of interest were predefined based on hypotheses related to connectivity patterns in specific resting-state networks, as described in **Results**. We applied a cluster-based Z-threshold of 3.1 and p-value threshold of 0.05 to control for multiple comparisons.

Statistical analysis: We applied cluster-based thresholding using the Threshold-Free-Cluster-Enhancement (TFCE) and corrected the cluster significance threshold of $p < 0.05$ for family-wise-error (Nichols and Holmes 2002, Smith and Nichols, 2009). Structural gray matter images were used as additional covariates on a voxel-by-voxel basis for higher robustness of the findings. GM images of each subject were extracted using FMRIB’s Automated Segmentation Tool (FAST), registered to standard space, smoothed to match the intrinsic smoothness of the rsMRI data, voxel-wise demeaned across all subjects in both groups together and added as a confounding regressor (nuisance) to the GLM design matrix used to analyse rs-fMRI data. This was done using an FSL script `feat_GM_prepare`, which estimates the smoothness of the functional data from the MELODIC folder and matches the rsMRI data. Adding GM maps reduces variance in the data due to potentially confounding anatomical differences between subjects (Oakes et al. 2007).

2.4 Results

2.4.1 Demographic and clinical characteristics

Presented below are the demographic and clinical characteristics of the research sample. The average participant in this study has had depression episodes (either continuously, or with remission periods) for over 10 years, is experiencing an episode of moderate (according to HAM-D scores) to severe depression at the time of study participation,

and is slightly overweight.

Variable	Mean	Standard Deviation
Age	31.95	10.67
Age at First MDD Episode	21.00	10.30
Gender (F:M)	39:35	
Beck's Depression Index (BDI)	30.72	8.52
Hamilton Depression Scale (HAM-D)	15.32	7.89
Height (in m)	1.71	0.10
Weight (in kg)	73.60	16.36
BMI (in kg/m ²)	25.24	5.07

Table 2.1: **Demographics summary of all study participants.** Includes mean and standard deviation for each variable.

There were slightly more women than men included in the study, and for most participants this was a recurrent depressive episode, where 50 of the 74 participants have had over two MDD episodes in the past. Most participants (41) had a first degree relative (mother, father, brother or sister) with a history of MDD, and most (57) had no psychiatric comorbidities. Of those with comorbidities, 48 had generalised anxiety disorder (GAD) and 22 had panic attacks. Most relevantly for this study, 58 participants were not taking any antidepressant medication during the study, and 42 had never taken any medication for their MDD, labeled as "drug-naïve".

Variable	drug-naïve		Drug-Experienced		p-value
	Mean	SD	Mean	SD	
Age (years)	30.3	10.3	34.5	11.2	0.11
Gender (F:M)	22:20		16:14		
Beck's Depression Index (BDI)	30.5	8.5	30.3	8.5	0.92
Hamilton Depression Scale (HAM-D)	21.6	5.1	22.4	6.2	0.52
Height (m)	1.7	0.1	1.7	0.1	0.81
Weight (kg)	68.0	13.3	80.0	17.8	0.002*
BMI (kg/m ²)	23.2	2.0	27.7	6.0	0.0001*

Table 2.2: **Demographic comparison between drug-naïve and drug-experienced participants.** Means, standard deviations (SD), and p-values for each demographic variable are presented.

When comparing demographic characteristics between drug-naïve and drug-experienced participants, age and gender distribution were broadly similar between the groups, with no significant difference in mean age ($p = 0.11$) and a comparable female-to-male ratio. Depression severity, as measured by Beck's Depression Index (BDI) and Hamilton Depression Scale (HAM-D), was nearly identical between the groups, indicating a comparable clinical profile in terms of symptom burden. Physical characteristics such as height did not differ significantly ($p = 0.81$); however, drug-experienced participants had significantly higher body weight ($p = 0.002$) and body mass index (BMI; $p = 0.0001$) compared to their drug-naïve counterparts. These differences in weight and BMI may reflect medication-induced metabolic changes associated with previous antidepressant use (Meshkat et al., 2025), underscoring the importance of considering somatic variables in clinical and neuroimaging studies involving pharmacologically treated populations.

Variable	Drug-Free		Medicated		p-value
	Mean	SD	Mean	SD	
Age (years)	31.7	10.6	32.6	11.3	0.78
Gender (F:M)	31:27		8:8		
Beck's Depression Index (BDI)	30.0	8.3	33.2	9.3	0.19
Hamilton Depression Scale (HAM-D)	21.2	5.0	24.9	6.4	0.02*
Height (m)	1.7	0.1	1.7	0.1	0.40
Weight (kg)	72.1	15.9	79.0.0	17.4	0.14
BMI (kg/m ²)	24.8	5.1	27.0	4.7	0.13

Table 2.3: **Demographic comparison between drug-free and medicated participants.** Means, standard deviations (SD), and p-values for each demographic variable are presented.

When it comes to a demographic comparison between drug-free and medicated participants at the time of the MRI scan, however, there were a few notable differences. Age and gender distributions were broadly comparable between groups, with no significant difference in mean age ($p = 0.78$). While depressive symptom severity measured by the Beck's Depression Index (BDI) was slightly higher in the medicated group (mean = 33.2) compared to the drug-free group (mean = 30.0), this difference was not statistically significant ($p = 0.19$). However, the Hamilton Depression Scale (HAM-D) scores were significantly higher in the medicated group ($p = 0.02$), indicating greater clinician-rated depression severity. Physical characteristics such as height, weight, and BMI showed no statistically significant differences between groups, though there was a trend toward higher weight and BMI in the medicated group. These patterns may reflect more severe symptomatology in the medicated cohort, as well as potential metabolic effects associated with antidepressant treatment.

Variable	Category	Count
Gender	F	39
	M	35
Recurrence	Recurrent depression	61
	Current episode is first	13
Psychiatric comorbidities (GAD and/or panic attacks)	None	57
	Yes	17
First degree family history of MDD	Yes	41
	No	23
	N/A	1
Number of past episodes	2+	50
	2	6
	1	4
	0	13
On AD medication at the time of MRI scan	No	58
	Yes	16
drug-naïve	Yes	42
	No	30

Table 2.4: Counts of participants in the sample by clinical history category.

Of the participants who used medications, SSRIs were the most common (with sertraline and fluoxetine being the most prevalent amongst them), with some SNRIs, tricyclics and other medications also represented among participants in the sample.

Category	Medication	Count
SSRIs (Total: 42)	Citalopram	10
	Sertraline	13
	Fluoxetine	13
	Paroxetine	4
	Escitalopram	1
	Fluvoxamine	1
SNRIs (Total: 6)	Venlafaxine	6
Augmenting agents (Total: 14)	Aripiprazole	4
	Quetiapine	6
	Olanzapine	3
	Promethazinum	1
Tricyclics (Total: 6)	Clomipramine	2
	Amitriptyline	2
	Lofepamine	2
Others (Total: 18)	Mirtazapine	8
	Bupropion	2
	Zopiclone	2
	Dormicum	1
	Gabapentin	1
	Trazodone	1
	Xanax	1
	Reboxetine	1
	Agomelatine	1

Table 2.5: Counts of medications used, grouped by pharmacological category, with total and per-medication counts.

None of the participants were scanned when taking benzodiazepines or zopiclone (as per exclusion criteria); they are listed as they were taken between the episodes.

2.4.2 Resting state network analysis

Firstly, we made sure that RSNs of interest were successfully captured in the analyses, as displayed below. This indicates that networks of interest were successfully imaged for the detection of differences between groups, including networks of interest in this study, i.e.

DMN, SN and CEN (frontoparietal networks are largely considered to be overlapping with the CEN), and other expected networks, such as the visual and sensorimotor networks shown as an example in Figure 2.1.

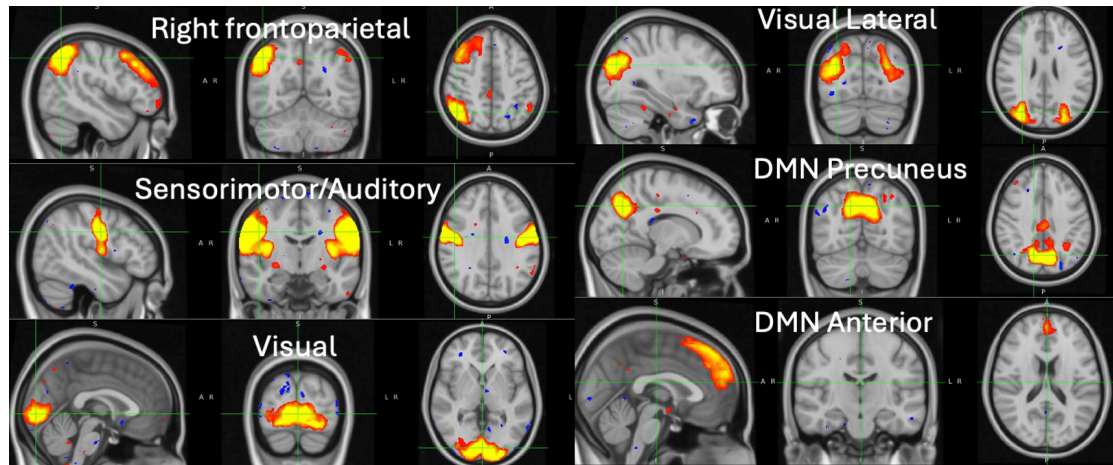


Figure 2.1: **Resting-state networks identified in the study.** Axial, coronal, and sagittal slices for the main resting-state networks detected, overlaid onto the standard MNI brain. All maps are thresholded at $Z = 3.1$.

2.4.3 Independent component analysis - drug-naïve vs drug-experienced

Here, we investigated whether there was a difference in 7T rsFC connectivity between MDD patients who were fully medication-naïve and those with prior drug exposure ('drug-experienced'). Prior drug exposure means having ever taken an antidepressant medication, while not being on antidepressant medication during the scan (and in the 2 weeks prior to the scan (or 4 weeks for those taking fluoxetine prior to the study)). Three statistically significant clusters of increased functional connectivity in drug-naïve patients compared to drug-experienced patients were identified as shown in Table 2.6. The largest one (MNI coordinates 92, 118, 68) is shown in Figure 2.2.

Contrast	Network	Cluster	Cluster size (# of voxels)	Peak voxel	Pmax value
Naive > Exposed	Default mode network (DMN)	Left mediodorsal thalamus	15	92, 118, 68	0.977
Naive > Exposed	Default mode network (DMN)	Left mediodorsal thalamus	4	91, 113, 68	0.981
Naive > Exposed	Parietal network	Frontal medial cortex	1	82, 176, 71	0.974

Table 2.6: Summary of clusters with increased functional connectivity in drug-naïve patients compared to drug-experienced patients.

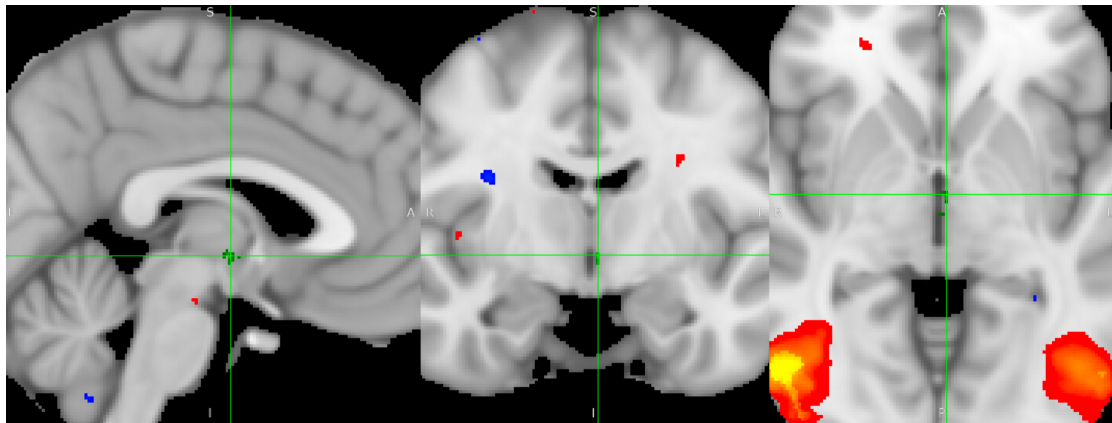


Figure 2.2: **Increased functional connectivity in drug-naïve patients compared with drug-experienced patients between the left mediadorsal thalamus and the default mode network (DMN).** Red-yellow regions indicate areas with a correlated BOLD signal time course; blue regions indicate areas with an anti-correlated BOLD signal time course. Green crosshairs denote the group differences in connectivity between drug-naïve and medicated patients. MNI coordinates of the cursor are (92, 118, 68). Results are shown with threshold-free cluster enhancement (TFCE) correction, achieving family-wise error (FWE) cluster significance at $p < 0.05$.

2.4.4 Independent component analysis - medicated vs unmedicated

Then, we investigated whether there was a difference in 7T rsFC connectivity between MDD patients who are currently receiving medication and those who are not on medication the day of the MRI scan, regardless of their medication history (and naivete). No significant clusters were identified that differentiated between groups based on current medication state, the reasons for which are explored in the Discussion section.

2.5 Discussion

2.5.1 Summary of findings

This chapter examined variations in resting-state functional connectivity (rsFC) among individuals with major depressive disorder (MDD) as a function of medication status. Using group independent component analysis (ICA) with a 100-component split, we compared two sets of patient groups: drug-naïve versus drug-experienced, and currently medicated versus currently unmedicated individuals. The most robust finding was the identification of three clusters showing significantly greater rsFC in drug-naïve individuals compared to drug-experienced patients. The largest of these clusters was located in the left mediodorsal thalamus (MNI coordinates: 92, 118, 68), showing increased connectivity with the default mode network (DMN) in the drug-naïve group (Figure 2.2). No significant differences in rsFC were found between currently medicated and currently unmedicated participants, which may reflect either an absence of short-term effects of current pharmacological treatment or limitations related to sample size imbalance (58 unmedicated vs 16 medicated).

2.5.2 Interpretation of rsFC findings

Our findings add to the increasing evidence that the thalamus is structurally and functionally impacted by medication use in patients with MDD. Prior studies have shown decreased bilateral thalamic volumes in drug-naïve MDD patients, and have even suggested the use of reduced thalamic volumes as a potential biomarker for diagnosing MDD (Choi et al., 2020; Xiong et al., 2021). Other studies have highlighted the hemispheric asymmetry in the pathophysiology of MDD, namely the hypoactivity of the left when compared to the right prefrontal cortex, which could potentially be explained by the significant decrease in left thalamic volume noted in drug-naïve MDD patients that shows lateralised structural vulnerabilities (Cho et al., 2021; Chibaatar et al., 2023). This

improved connectivity in drug-naïve patients is in line with previous research showing that previous medication exposure can have longer-term effects on MDD patients, even if they relapse in their symptom severity post-treatment (Buckman et al., 2018). The study did not differentiate between drug-experienced patients who had or had not experienced symptom relief/treatment response because of their prior antidepressant use.

The rsFC changes found in this chapter between drug-naïve and drug-experienced patients provide more understanding of the effects of antidepressant medication on brain circuitry. The higher connectivity in the left mediodorsal thalamus and its stronger relationship with the default mode network (DMN) in drug-naïve individuals imply that medication exposure may lead to enduring neuronal changes in thalamocortical networks. This observation would correspond with the notion of thalamocortical dysrhythmia (Llinas et al., 1999; Schulman et al., 2011; Kim et al., 2021), where modified thalamic connection impairs cortical networks associated with self-referential processing and emotional regulation, fundamental to the symptomatology of MDD where the thalamus is a key relay centre of signals between cognitive processing in the prefrontal cortex and emotional processing in the limbic system.

2.5.3 Clinical relevance

The dorsomedial thalamic nucleus is a fundamental subcortical relay to the prefrontal cortex, and is known to be highly implicated in the development and modulation of cognitive performance (Ferguson & Gao, 2015; Parnaudeau et al, 2018; Ouhaz et al; 2018) as well as having reciprocal anatomical connections to the subgenual cingulate cortex (sgACC), contributing to its potential relevance to TMS targeting studies. Very recent optogenetic research in mice models has shown that the dorsomedial thalamic nucleus-prefrontal cortex connection could even provide a potential mechanistic explanation for depression, being able to induce depression-like symptoms (Li et al., 2024). Similarly, we show above that there is enhanced rsFC connectivity between the left mediodorsal thalamus and the DMN in drug-naïve patients with MDD.

In this chapter, we demonstrate that while current medication usage could not be associated with clear changes in rsFC, patients' medical history, namely drug-naïvete, appears to be a clear indicator of altered connectivity patterns. This outcome is very relevant for personalising brain stimulation methods, such as transcranial magnetic stimulation (TMS), in MDD. To qualify for reimbursed TMS treatment, most patients in the US and the UK must be treatment-resistant, specifically - they must have failed at least two antidepressant medications. Consequently, in clinical settings, unlike in research, MDD patients receiving TMS are unlikely to be drug-naïve. If their resting-state functional connectivity is used for personalised targeting (elaborated upon in **Chapter 4**), this may result in unaccounted variation if prior medication history is not adequately considered in preprocessing or the analysis and interpretation of results. We suggest that future research on personalised targeting with NIBS should take into consideration the medical history, and specifically past experiences with pharmacological interventions, into consideration, and that the recommendations of NIBS treatment be considered for drug-naïve MDD patients earlier on in the course of their treatment to maximise overall treatment outcomes.

2.5.4 Limitations

Sample generalisability: The study primarily includes individuals with recurrent MDD episodes, many of whom have a family history of depression and no comorbid psychiatric conditions. This sample composition may limit generalisability to MDD patients with different clinical profiles, such as those with first-time episodes or those with more complex psychiatric comorbidities, which are especially common with generalised anxiety disorders and post-traumatic stress disorders. There was also a significantly different split between the number of patients on medication and medication-free during the time of the scan, which limited the potential for splitting data analysis further.

Potential for medication selection bias: Given that a subset of participants has

used multiple antidepressant classes, including SSRIs, atypicals, SNRIs, and tricyclics, there may be confounding factors related to past medication exposure or treatment history. Selection bias may affect results if drug-naïve patients differ systematically from drug-experienced patients in ways not captured by other variables, such as in their attitudes towards Western medicine, comorbid physical disorders or other contraindications. An important consideration here, moreover, is that we could not access information about whether study participants were or were not drug-responders, which could potentially have impacted our findings between the medicated and drug-free groups, if non-responders' rsFC is more similar to that of drug-free patients than responders', between which we could not differentiate.

Adjustment for depression severity: The severity of depression is a critical variable that can influence functional brain changes and should ideally be accounted for in statistical analyses. While measures such as the BDI and HAM-D were collected in this study, adjustments for severity were not implemented across all MRI analyses. This omission may limit the interpretability of certain findings, particularly when comparing drug-free and medicated groups, where baseline differences in symptom burden could confound interpretations of neurofunctional patterns (null findings). Future analyses should aim to incorporate depression severity as a covariate or stratification variable to enhance the robustness and specificity of results.

Cross-sectional study design: This is a cross-sectional study, which cannot capture causality or longitudinal changes in rsFC related to antidepressant medication exposure. If it were available, longitudinal data could provide insight into how rsFC evolves with medication (or other, such as TMS, treatment) initiation, continuation, or cessation.

Focus on RSNs: The analysis in this chapter focuses on RSNs, which, while informative, may not fully capture task-specific or dynamic functional connectivity patterns relevant

to MDD. Task-based fMRI could offer complementary insights into neural processes affected by depression and antidepressant use, and similar studies are ongoing (Pilmeyer et al., 2022).

2.5.5 Future directions

2.5.5.1 Absence of healthy control group:

While the study included the collection of scans for healthy controls, their data was not analysed as in-scope for this chapter, given the focus on differences among MDD who may choose to undergo TMS (or other NIBS) treatment in the future. In the future, it could be helpful to compare healthy controls with drug-naïve and drug-experienced cohorts of MDD patients to best understand the proximity and/or distance between these clinical groups on rsFC measures.

2.5.5.2 Considering medication-matched cohorts:

To mitigate medication selection bias, future research could use stratified sampling techniques or matched cohorts to ensure that drug-naïve and drug-experienced groups, and currently medicated and unmedicated groups, are more comparable. In addition, detailed tracking of specific medication history, duration, and dosage could help parse out the differential impact of various antidepressant classes on rsFC.

2.5.5.3 Clinician-reported measures:

While this dataset is incredibly rich in clinical, neuroimaging and other data, most clinically reported measures (other than HAM-D) were taken via self-reports from patients, including both present and past medical history. This is known to lead to some patient-based bias, so future studies should consider including some more benchmarked clinician-administered questionnaires and/or otherwise validated evaluation and patient history metrics, which tends to be easier to implement in real-world clinic-embedded research

studies.

2.5.5.4 Alternative rsFC analysis approaches:

This analysis used ICA to understand the differences in rsFC between groups based on established analysis protocols, but future directions should explore using more dynamic measures of FC, more network-based statistics methods to identify subnetworks with altered connectivity rather than individual clusters, or machine learning techniques, such as support vector machines or deep learning models, which should be further validated and considered for the classification of MDD patients based on rsFC patterns.

2.6 Conclusions and contributions

This chapter investigates resting-state functional connectivity (rsFC) differences resulting from different past or present medication history using 7T MRI. Here, we were interested specifically in differences between rsFC patterns in depressed participants based on their medication history, to better understand whether it is fair to consider interventions on depressed participants, especially ones that depend on rsFC patterns, to be homogeneous, or whether a more nuanced analysis of MDD patients's rsFC is necessary to best refine treatment strategies.

The results suggest specific connectivity patterns linked to previous antidepressant use, particularly increased connectivity in the left mediodorsal thalamus with the default mode network (DMN) in individuals who have never been exposed to antidepressant medication, when compared to those who have. This indicates that antidepressant medication may induce enduring neuronal alterations in thalamocortical networks, reinforcing the theory of thalamocortical dysrhythmia in MDD. These findings add to our understanding of how previous medication exposure may affect brain network functionality, which could complicate the interpretation of current resting-state functional connectivity in clinical populations with varied treatment histories.

The contributions of the chapter are threefold. It demonstrates that rsFC patterns significantly vary according to antidepressant exposure, highlighting the importance of incorporating medication history in clinical practice and research. Secondly, it emphasises the effectiveness of ultra-high-field 7T MRI in identifying subtle connectivity alterations, especially in subcortical areas such as the thalamus, which are essential to depressive symptomatology. Given the high specificity of our findings, it is unclear whether our findings could be replicated with lower field strengths, such as 3T MRI, routinely used in research settings, and is therefore worth considering further. Finally, the chapter highlights the importance of considering prior drug exposure when designing and targeting non-pharmacological interventions, such as transcranial magnetic stimulation (TMS), as treatment resistance criteria frequently exclude drug-naïve patients from eligibility for these types of clinical treatments.

These contributions suggest that further investigations into the effects of antidepressant use on resting-state functional connectivity (rsFC) are critical if rsFC is to be used for future treatment personalisation methods.

3 | Practice: Implications of TMS precision targeting in real-world, large scale clinical practice

3.1 Introduction

3.1.1 TMS in clinical practice

While transcranial magnetic stimulation (TMS) as a treatment for MDD has been around for a while and has been approved as a medical treatment for MDD for at least 6 years at the time of writing, the clinical prevalence of TMS is still limited, even though the prevalence of MDD has continued to increase and the efficacy of pharmacological solutions has not changed. Data about the availability and access to TMS remains scarce, but a recent study estimated that as of 2020, the US had less than one mental health facility offering at least one of electroconvulsive therapy (ECT), ketamine infusion therapy (KIT), and TMS per 100,000 US adults (Basiru et al., 2024). This suggests that not only TMS is still not as widespread as the prevalence of MDD would require, but also that there is still much to learn about how best to integrate basic TMS applications for MDD into clinical practice, and what factors in real-life practice can lead to the most significant differences in treatment outcomes.

The present study benefited from access to a unique and valuable dataset obtained through an industry collaboration. This dataset included detailed TMS stimulation parameters as well as clinician-reported outcome measures for a large and heterogeneous cohort of individuals receiving TMS for MDD in naturalistic treatment settings in the United States. The availability of such real-world data is rare and represents an important opportunity to investigate the clinical utility and mechanistic underpinnings of TMS treatment under routine conditions.

Nonetheless, the dataset was affected by considerable omissions of data points across several variables, including critical demographic details, treatment history, stimulation targeting and protocols, among others. Due to variable data quality and completeness, only a subset of factors could be included in the analyses presented in this chapter. These included time of day of stimulation, individual differences in motor threshold, patient age, and validated clinical outcome measures. While this limited the breadth of the investigation, it allowed for a focused analysis of the most complete and methodologically sound variables, providing preliminary insights into how such factors may influence TMS efficacy in real-world clinical practice.

3.1.2 Resting motor threshold (RMT) measurement and significance

Resting motor threshold (RMT) is a fundamental parameter in TMS, and represents the minimum stimulation intensity required to elicit a motor response in a target muscle, typically the first dorsal interosseous (FDI) muscle, while at rest. In clinical settings, RMT is usually determined by applying single TMS pulses over the motor cortex until a visible 'twitch' can be seen in 50% of trials (usually out of 10 trials). Better equipped clinical settings with more highly trained staff may use a more accurate and precise measurement setup, where they detect motor evoked potentials (MEPs) using surface electromyography (EMG) connected directly to the first dorsal interosseous (FDI) muscle, and define the RMT as the lowest stimulation intensity that produces an MEP of at least 50 μV .

RMT calibration is supposed to ensure individualised and safe TMS delivery, accounting for variations in cortical excitability influenced by factors such as age, medication use, and previous stimulation experience, among many others (Karabanov et al., 2015; Wendt et al., 2023; Cotovio et al., 2021). Standard TMS protocols typically deliver stimulation as a percentage of the RMT (e.g., 120% of RMT for rTMS therapeutic sessions). This approach optimises efficacy while reducing discomfort and adverse effects, such as

overstimulation or seizure risk (Miron et al., 2021).

In most patients, RMT ranges from 40% to 70% of the device's maximum stimulator output (MSO) (Temesi et al., 2014), with lower thresholds indicating higher cortical excitability, often because of lower skull thickness. Understanding these standard ranges helps to tailor treatment protocols and ensure the reproducibility of findings across clinical and research applications. Measuring RMTs precisely is therefore incredibly important to control TMS (and other NIBS) treatment doses to ensure consistency, efficacy and safety of TMS interventions for MDD and other neuropsychiatric disorders.

3.1.3 Influence of real-world clinical practice on clinical outcomes

RMTs are supposed to be the ground-truth of an individually adjusted dose, and while previous work has shown variability between days (Cotovio et al., 2021), based on preceding activity levels (Ma et al., 2023), and across differently experienced clinicians taking the measurement (Kotonen et al., 2022; Wang et al., 2022), prior work in our lab did not find significant effects of time of day itself on RMTs (Wendt et al., 2023). RMTs are also the standard of determining TMS stimulation doses for individual patients, even though the relationship between motor thresholds, the minimum stimulation dose needed to elicit a motor response, and cognitive thresholds, the minimum stimulation dose needed to elicit a cognitive response, such as those required in MDD treatment, remains unclear (Kaminski et al., 2011; Schiktanz et al., 2013).

It is therefore not clear whether there is a link between RMT, time of day of stimulation, and the patient's age on the clinical efficacy of TMS treatments for MDD. If such links exist, they could shed light on not only the mechanisms underlying the variability of treatment response among patients, but also on how real-world clinical practice of TMS could be updated to ensure the best outcomes for those undergoing treatment.

3.2 Research Questions

In order to better understand how TMS treatments for MDD have been applied in real-world clinical practice over the last 3 years, we raised three exploratory and one predictive research questions based on data available in the dataset.

Exploratory questions:

1. Does individual RMT impact MDD treatment outcomes?
 - **Hypothesis:** There is no impact of RMTs on clinical responsiveness to TMS treatment in patients with MDD, as RMTs are supposed to reflect individually-adjusted stimulation dosing.
2. Does the time of day when treatment is administered impact MDD treatment outcomes?
 - **Hypothesis:** TMS treatment administered at any point in the day leads to equal clinical improvement, as prior data from our group demonstrated no impact of time of day on RMTs.
3. Does the age of the patient at the start of treatment impact MDD treatment outcomes?
 - **Hypothesis:** Younger patients demonstrate greater clinical improvement following TMS treatment for MDD compared to older patients.

Predictive research question: Do early clinical changes in the course of TMS treatment predict further changes over the course of MDD treatment?

- **Hypothesis:** Greater improvement in depressive symptoms during the initial sessions of TMS treatment will predict more substantial overall clinical improvement by the end of the treatment course.

The exploratory research questions aim to lay the foundation to understanding how basic variables of RMT measurement, time of day and age may impact clinical outcomes in real-world settings, and the predictive research question aims to ask whether there is sufficient data to suggest that early treatment response patterns would be predictive of future treatment response and MDD remission, which would ultimately lead to more efficient treatment, if non-responders could be identified early on and offered alternative treatment. For the purposes of this study, early clinical changes were changes after one week of treatment within a six-week treatment course, as previous studies have shown that ultimate treatment response could be predicted as early as one week following the start of antidepressant treatment with antidepressant pharmaceutical medication (Godlewska et al., 2016).

3.3 Methods

3.3.1 Dataset acquisition

This chapter uses Magstim Horizon 3.0 TMS data from real-world clinics treating neuropsychiatric diseases. The register began collecting data on October 11, 2021, and this report covers data acquired until March 10, 2024 across clinics in the United States of America. Local site personnel recorded patient demographics and site identifiers; some clinics also recorded primary and co-morbid mental diagnoses, and clinical scores for each clinical site. Some treatment parameters were recorded automatically, such as session date, stimulation location (DLPFC), RMT, number of pulses per session, treatment level (% MSO output relative to RMT), pulse frequency, duration, intertrain interval (ITI), and number of sessions completed. All data was collected using Magstim Ltd's Horizon 3.0 system (Wales) in compliance with HIPAA requirements and clinic agreements, and all personal health information (PHI) was removed by the dataset owner (Welcony, Inc) prior to access being granted to researchers from the University of Oxford. All stimulators had a biphasic pulse design and a figure-of-8 coil. The dataset includes data from

4,469 individual patients across 130 individual clinics. All patients were receiving TMS for major depressive disorder.

3.3.2 Data Quality Assessment

Since this is among the first opportunities to understand the predictors of clinical outcomes with TMS in real-life clinical use, at scale, we only considered data from patients who had clinical outcome scores reported alongside the automated session reporting. Across the dataset, only 18.2% of patients had clinical outcomes reported in the form of the PHQ-9 questionnaire, reflective of depressive symptom severity, and they all came from only 25 clinics (only 19.2% clinics had reported at least one clinical outcome associated with treatment). Gender was only recorded in 9.67% of cases (432 individuals), with 2/3 of participants where gender was recorded being female. Full diagnoses (including secondary diagnoses and comorbidities), ethnicity and handedness were recorded in fewer than 1% of the cases in the dataset, and could therefore not be used for further analysis. All patients' date of birth was replaced by their year of birth to preserve anonymity, so all age estimates are based on the patient's year of birth. All the analyses were conducted only on patients that had at least 2 PHQ-9 scores available, at the beginning and end of treatment (740 individuals), except for predictive analyses, which could only be conducted on patients that had at least 3 PHQ-9 scores available, at the beginning, after one week, and at the end of treatment (678 individuals).

3.3.3 Statistical Analysis

All statistical analyses were conducted in Python 3 (via Jupyter Notebook) using a connector thread to a SQL database. Access to the SQL database was provided by Welcony, Inc. Statistical significance was determined at $p < 0.05$ across all analyses.

3.3.3.1 RMTs

For most patients, a single resting motor threshold (RMT) measurement was taken at the beginning of the treatment course to determine the % maximum stimulator output (%MSO) settings. In cases where participants returned for subsequent treatment courses after an extended period (3â24 months), a new RMT was measured. For this analysis, only the first RMT per participant was used. Device time recorded in UTC was converted to local clinic time zones based on provided UTC adjustments.

Linear regression was used to evaluate the relationship between initial RMT levels and changes in PHQ-9 scores, where the dependent variable was PHQ-9 change (final score minus baseline score) and the independent variable was RMT (%MSO). Model parameters (R^2 , F-statistic, p-values, slope, and intercept) were reported, with 95% confidence intervals where appropriate. To account for inter-clinic variability, a secondary regression analysis was performed including clinic membership as a random effect. The proportion of variance explained by clinic was also computed.

While we considered a mediation analysis to examine whether the relationship between RMT and clinical outcomes was influenced by the time of day of TMS administration, we ultimately did not pursue it due to several methodological constraints. First, the dataset lacked the temporal granularity and longitudinal structure necessary to establish a clear temporal ordering among the variablesâa critical assumption for valid mediation analysis (there was only one RMT measure per participant, at the beginning of their treatment). Additionally, the observational nature of the data introduced the potential for unmeasured confounding variables affecting both the mediator (TOD) and the outcome (PHQ-9), which would violate key assumptions required for causal inference.

3.3.3.2 PHQ-9 Distributions and Change Scores

Kernel density estimation (KDE) was used to model the distribution of PHQ-9 scores at treatment initiation and completion across the cohort. KDE provided a non-parametric

estimate of the score distributions without binning artifacts, allowing for a smooth visualisation of symptom severity changes over time. To formally test whether the distributions of PHQ-9 scores differed significantly between the initiation and completion timepoints, a two-sample Kolmogorov-Smirnov (KS) test was performed. To assess variability in PHQ-9 change scores across clinics, we used a linear mixed-effects model, with clinic membership included as a random effect. ANOVA tests were conducted to evaluate whether between-clinic differences in PHQ-9 change scores were statistically significant.

3.3.3.3 Diurnal Variation Analyses

The relationship between RMT (%MSO) and time of day (TOD) was assessed using 6-minute moving average plots. Raw mean RMT values were plotted against adjusted local time, with shaded areas representing the standard error. To assess statistical significance relative to random temporal fluctuations, temporal shuffling (10,000 iterations) was used to generate null distributions. Dashed lines representing the 5th and 95th percentiles of the shuffled data were plotted for comparison.

To test whether the time of day of stimulation (morning vs afternoon) impacted clinical outcomes, patients were stratified into morning-only and afternoon-only groups based on their treatment start times. Patients who received treatment in both periods were excluded. Change in PHQ-9 scores was compared between the morning and afternoon groups using a two-sample t-test.

3.3.3.4 Age

Linear regression was used to test whether patient age at treatment initiation predicted PHQ-9 change scores. The dependent variable was PHQ-9 change (final minus baseline score), and the independent variable was patient age (estimated from year of birth for PHI protection). A linear mixed-effects model was also used to quantify the proportion of variance attributable to clinic membership.

3.3.3.5 Early Changes in PHQ-9 as Predictors of Ultimate Response

A moving average of PHQ-9 scores was computed across the six-week treatment period, with initial assessments aligned at $x = 0$ to visualize symptom trajectories over time. Subsequently, we used linear regression to test whether early changes in PHQ-9 scores (baseline to Week 1) predicted subsequent symptom changes (Week 1 to end of treatment). Model outputs included slope, intercept, R^2 , and statistical significance, and we used the proportion of variance explained by early changes in PHQ-9 scores ($R^2 = 0.042$) to quantify the predictive value of the model.

3.4 Results

3.4.1 Does individual RMT impact MDD treatment outcomes?

There was no meaningful relationship between initial resting motor threshold (RMT) levels and PHQ-9 change scores ($R^2 = 0.001$, $F(1,738) = 0.5115$, $p = 0.475$), as shown in Figure 3.1.

$$\text{PHQ-9 Change} = -7.91 + 0.01 \times \text{RMT} \quad (3.1)$$

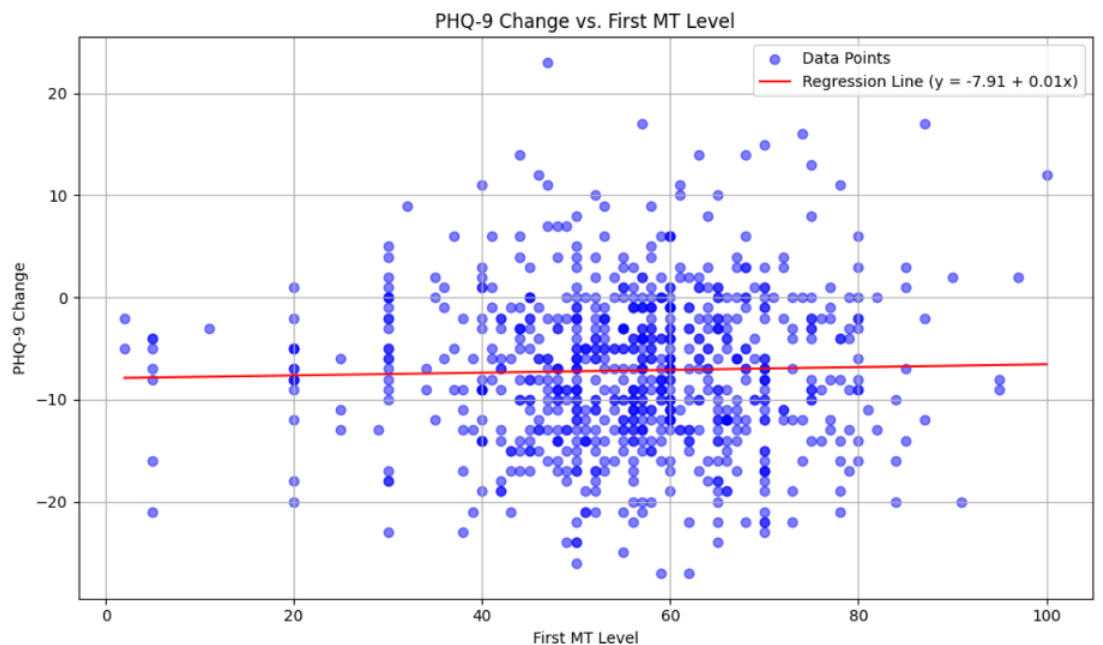


Figure 3.1: **Relationship between initial motor threshold (RMT) levels and PHQ-9 change scores in TMS treatment.** Scatter plot displays individual patient data points ($n=740$) showing PHQ-9 score changes (last minus first assessment) as a function of initial RMT levels (%MSO). Red line represents the fitted linear regression ($y = -7.91 + 0.01x$, $R^2 = 0.001$, $F(1,738) = 0.5115$, $p = 0.475$). Negative values on y-axis indicate symptom improvement. Model diagnostics revealed non-normal residuals (Jarque-Bera = 12.160, $p = 0.00229$), with kurtosis of 3.377 and skewness of 0.251.

When adjusted for inter-clinic variability, there was still no significant relationship between initial motor threshold (RMT) levels and PHQ-9 change scores ($R^2 = 0.001$), as shown in Figure 3.2.

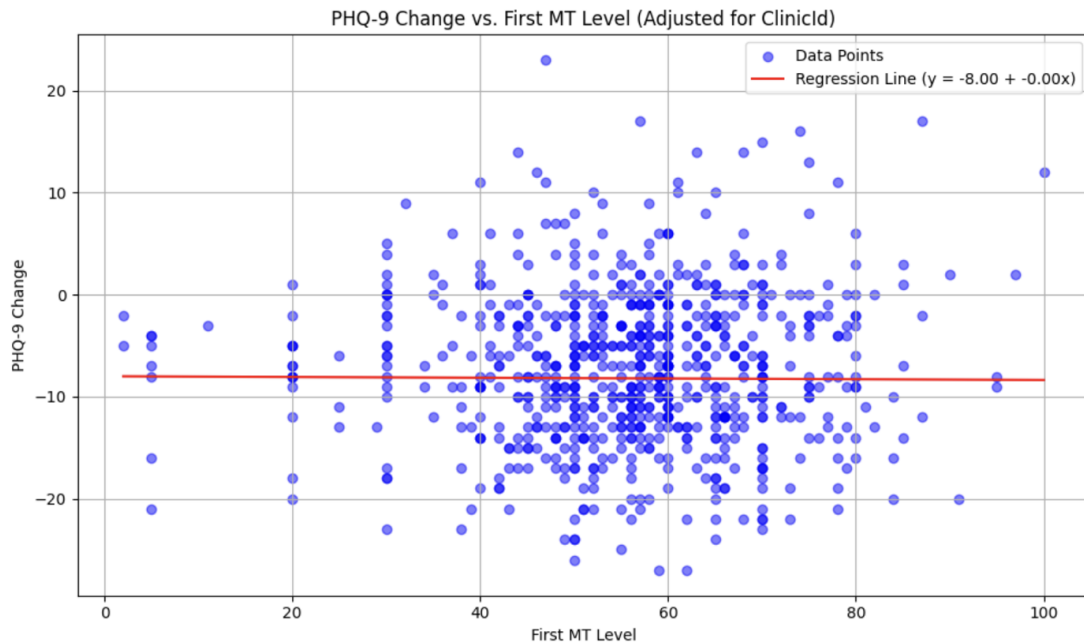


Figure 3.2: **Relationship between initial motor threshold (RMT) levels and PHQ-9 change scores in TMS treatment after correcting for inter-clinic variability.** Scatter plot displays individual patient data points ($n=740$) showing PHQ-9 score changes (last minus first assessment) as a function of initial RMT levels (%MSO), after correcting for inter-clinic variability. Red line represents the fitted linear regression ($y = -8.00 + 0.00x$, $R^2 = 0.001$). Negative values on y-axis indicate symptom improvement. Data points represent individual patients. Darker points demonstrate the overlap of multiple data points. Model diagnostics revealed non-normal residuals (Jarque-Bera = 12.160, $p = 0.00229$), with kurtosis of 3.377 and skewness of 0.251.

3.4.1.1 Understanding RMTs across the dataset

To understand the above, we looked into each of the variables underlying the outcomes separately. Analysis of the RMT distribution across our patient cohort (Figure ??) showed a predominantly unimodal pattern with a clear peak at approximately 60% of maximum stimulator output (MSO), where we observed the highest frequency of approximately 155 patients. The data demonstrated a right-skewed distribution, with RMT values ranging from 0% to 100% MSO, though the majority of measurements clustered

between 40% and 80% MSO. A small subset of patients displayed extremely low RMTs (<30% MSO) or very high RMTs (>80% MSO), which could reflect measurement inconsistencies or true physiological variability, so we conducted sub-analyses to understand the variability of RMTs between individual clinics.

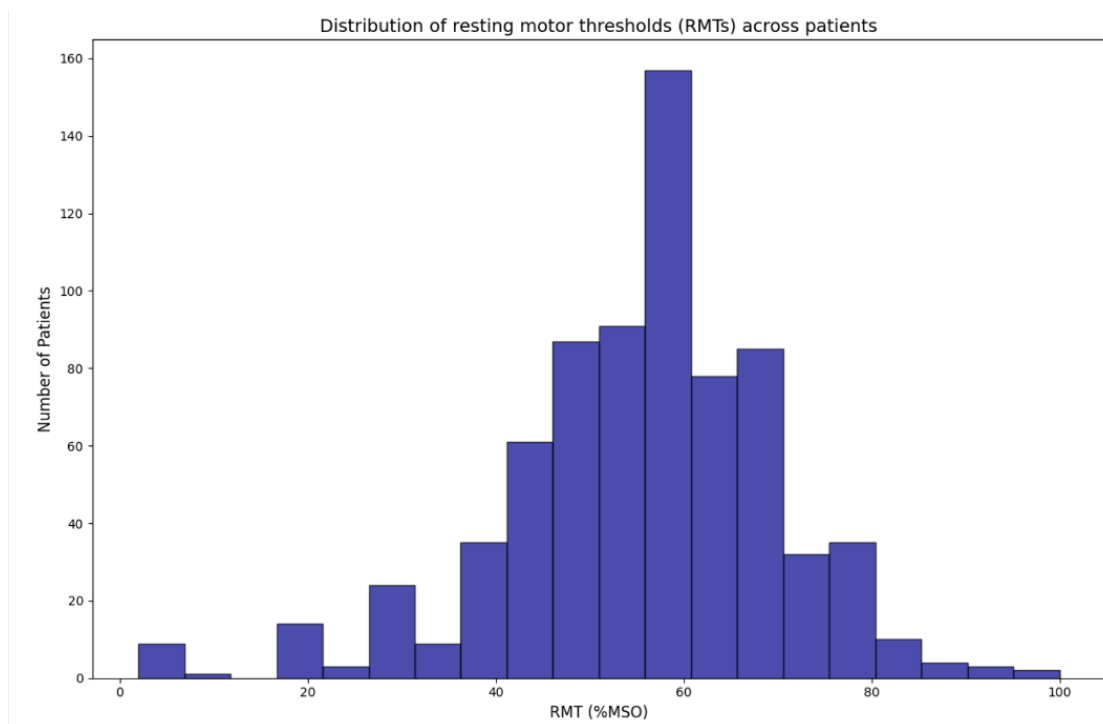


Figure 3.3: Distribution of resting motor thresholds (RMTs) of all patients. The x-axis shows RMT expressed in % maximum system output (MSO).

Variability between individual clinics (clinic ID in Figure 3.4) explained 36.40% of RMT measurement variance among the 25 participating centres. Most clinics had median RMT levels of 50-70% MSO, however clinics 71 and 72 had much lower median values at 30-40% MSO. The violin plots below show that certain clinics (85, 92) had tight, concentrated distributions, indicating consistent measuring techniques, whereas others (49, 71) had broad, bimodal patterns, suggesting methodological errors. The sample size ranged from n=1 to n=159, with clinic 85 having the most robust distribution (n=159) and clinics 46, 72, and 74 giving minimum data (n=1). These findings suggest

that systematic differences between clinics, such as protocols, equipment calibration, or operator expertise, may explain the previously observed variability in RMT values, emphasising the need to standardise measurement procedures across sites in order to best capture true, underlying physiological RMTs.

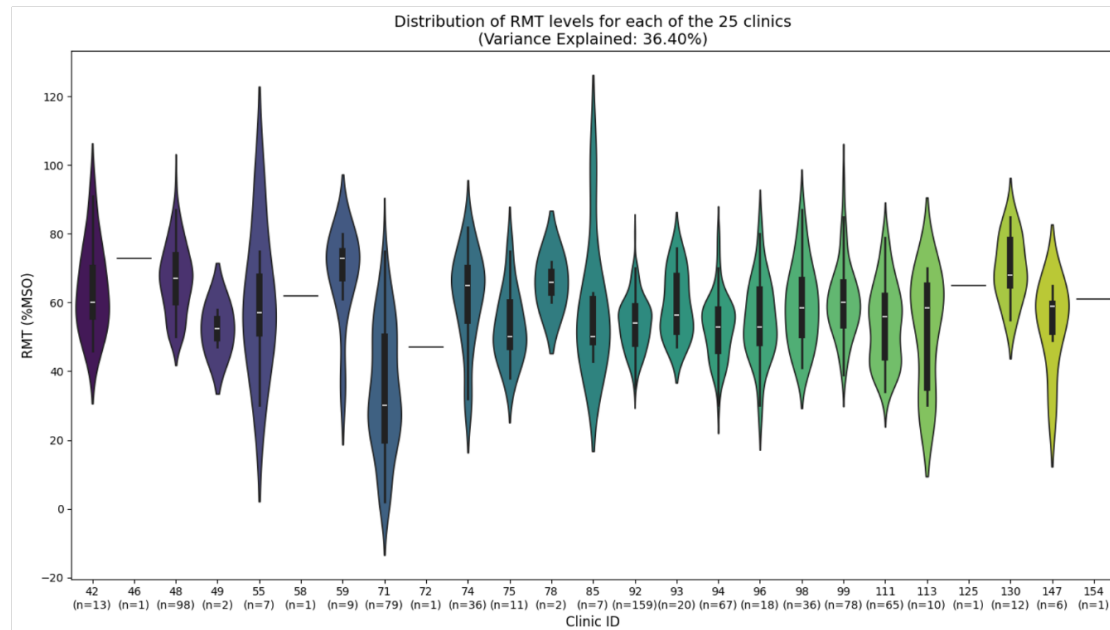


Figure 3.4: The distribution of RMT levels is shown for each of the 25 clinics (anonymised by ID) included in the analysis. The number of patients included in the analysis for each of the clinics is shown under the clinic ID on the x-axis. The y-axis shows RMT expressed in % maximum system output (MSO).

3.4.1.2 Understanding clinical outcomes across the dataset

When looking at clinical outcomes as measured via the PHQ-9 questionnaire, KDE analysis of PHQ-9 scores revealed a significant therapeutic response to TMS treatment, characterised by a substantial shift in distribution patterns between initial and final assessments. The initial PHQ-9 distribution demonstrated a single prominent peak in the severe range (scores 20-22), with most patients presenting with moderately severe to severe depressive symptoms. Following treatment, the distribution exhibited a marked leftward shift, with a bimodal pattern emerging: a primary peak in the minimal-to-mild

range (scores 5-7) and a secondary peak in the moderate range (approximately score 10). This bimodal pattern in final scores suggests two distinct response groups: those achieving near-complete remission and those showing partial improvement while maintaining moderate symptomatology. The broader, more platykurtic shape of the final distribution, compared to the initial concentrated peak, indicates substantial variability in treatment response, with a clear trend toward symptom reduction across the patient population, consistent with previous data and validating of the use of TMS in the treatment of MDD.



Figure 3.5: **Kernel density estimation plots comparing PHQ-9 scores at treatment initiation (purple) and completion (pink)**, illustrating a marked shift from predominantly severe depression scores (peak at 20-22) to a bimodal distribution with peaks in the minimal-to-mild (5-7) and moderate (10) ranges. Severity categories are indicated on the x-axis for clinical reference. A Kolmogorov-Smirnov (KS) test confirmed a statistically significant difference between the two distributions, with a KS statistic of 0.431 and a p-value of $5.24e^{-68}$.

Analysis of PHQ-9 change scores demonstrated relatively modest inter-clinic variabil-

ity, with clinic membership explaining only 6.07% of the total variance in treatment outcomes. The box plots revealed consistent therapeutic benefits across most clinics, with median improvements typically ranging from -5 to -10 points on the PHQ-9 scale. Within-clinic variability was substantial, with most clinics showing interquartile ranges of 5-10 points and occasional outliers, particularly in the positive direction indicating symptom worsening. Several clinics, such as clinic 48 (n=98) and 99 (n=78), exhibited notably larger outcome variability, while smaller clinics (clinic 49 (n=2), clinic 78 (n=2)), tended to have outliers due to limited sample sizes. The relatively low proportion of variance explained by clinic membership suggests that individual patient factors, rather than clinic-specific practices, may be the primary determinants of treatment outcomes.

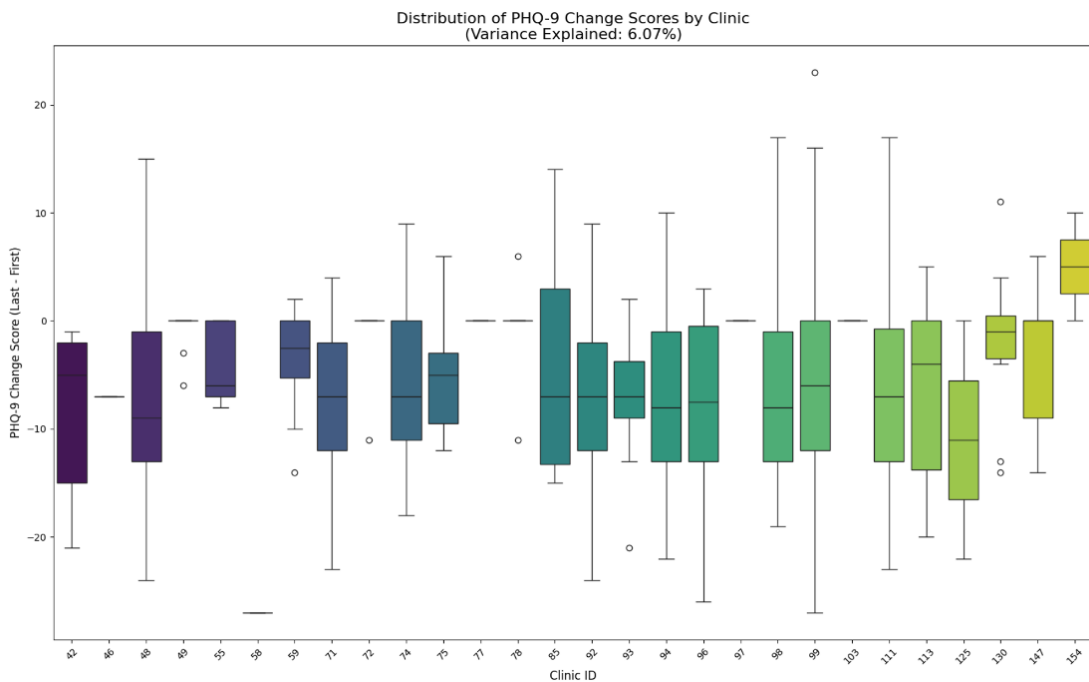


Figure 3.6: **Box plots depicting the distribution of PHQ-9 change scores (last minus first assessment) across all 25 clinics**, with clinic membership accounting for 6.07% of total outcome variance. Negative values indicate symptom improvement. Box boundaries represent first and third quartiles, whiskers extend to 1.5 times the interquartile range, and points indicate outliers. Note clinics 46, 58, 72, 125 and 154 only had a single patient whose data could be included, but are included for comprehensiveness.

3.4.2 Does the time of day of when treatment is administered impact treatment outcomes?

The moving average of raw resting motor threshold (RMT) values (%MSO) across the adjusted time of day (Figure 3.7) shows a general increase in RMT levels from morning to afternoon, peaking around midday but, when normalised using Z-scores (by clinic, Figure 3.8), it is clear that there is no clear diurnally patterned variance in mean RMT in this patient population. This is because z-scoring allows to standardise RMT data when accounting for inter-clinic variability, and is consistent with previous research (Wendt et al., 2023).

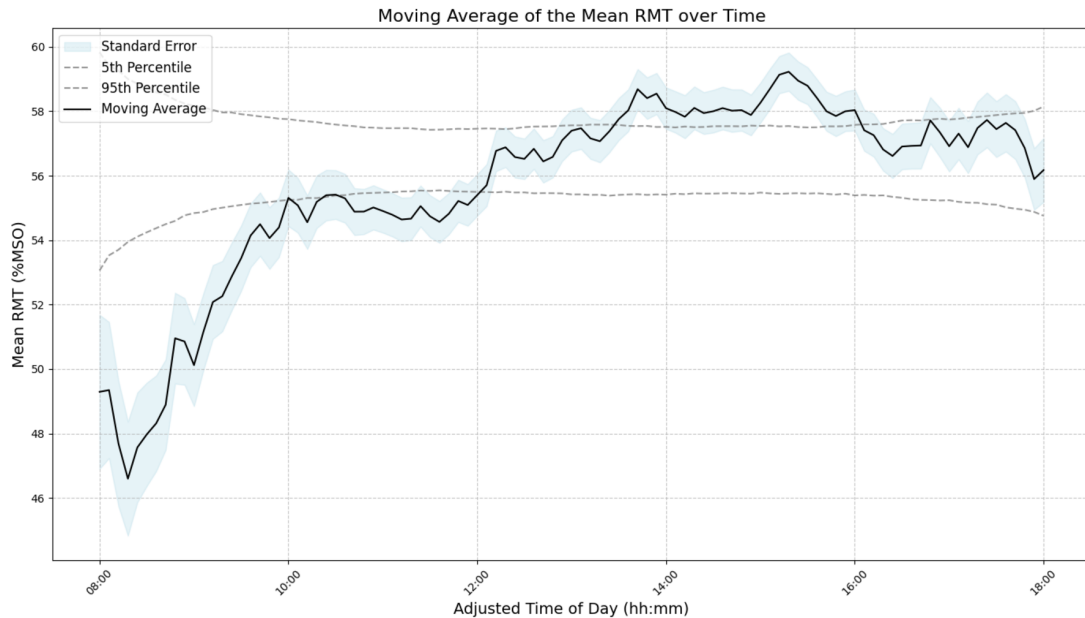


Figure 3.7: **The moving average of raw mean RMT (%MSO) plotted across the adjusted time of day (hh:mm).** The solid black line represents the z-scored moving average RMT, calculated using a 6-minute moving average window, while the shaded region indicates the standard error of the mean. Dashed grey lines represent the 5th and 95th percentiles derived from temporally shuffled data, serving as a null distribution for comparison.

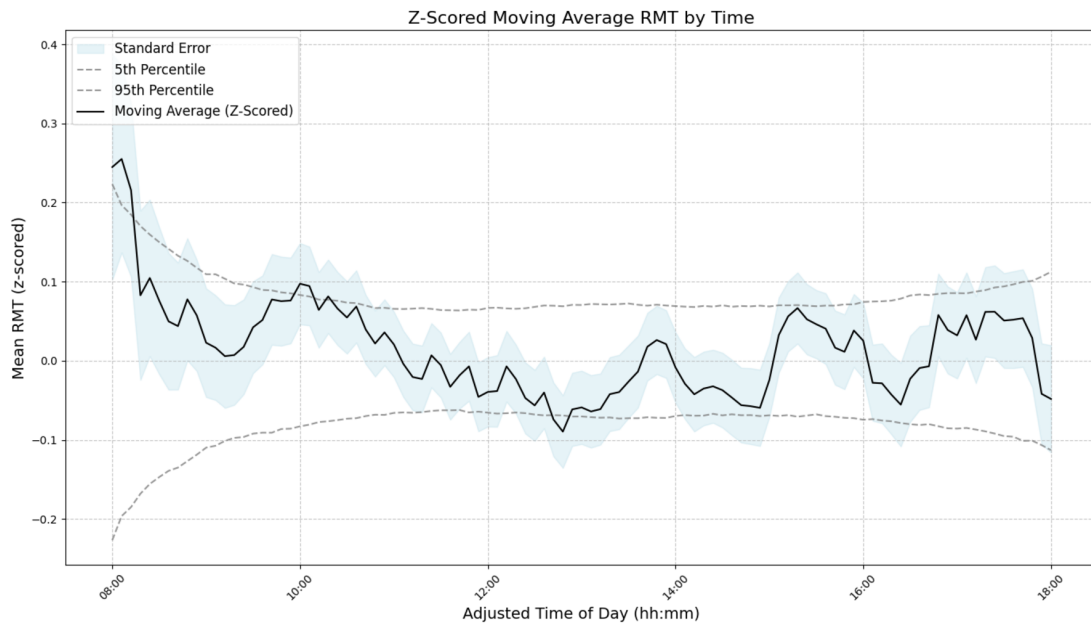


Figure 3.8: **The moving average of z-scored RMT (%MSO) plotted across the adjusted time of day (hh:mm).** The solid black line represents the z-scored moving average RMT, calculated using a 6-minute moving average window, while the shaded region indicates the standard error of the mean. Dashed grey lines represent the 5th and 95th percentiles derived from temporally shuffled data, serving as a null distribution for comparison.

To create a more objective test and study the difference in clinical outcomes when applying TMS treatment in the morning vs afternoon in real-world clinical settings, Figure 3.9 shows the distribution of PHQ-9 change scores for the morning and afternoon cohorts. However, both groups demonstrate a comparable range of changes, characterised by overlapping interquartile ranges and similar medians, and there were no significant statistical differences between groups ($t(739) = -0.38$, $p = 0.701$), suggesting that there is no difference in treatment outcomes resulting specifically from the time of day of when stimulation was applied.

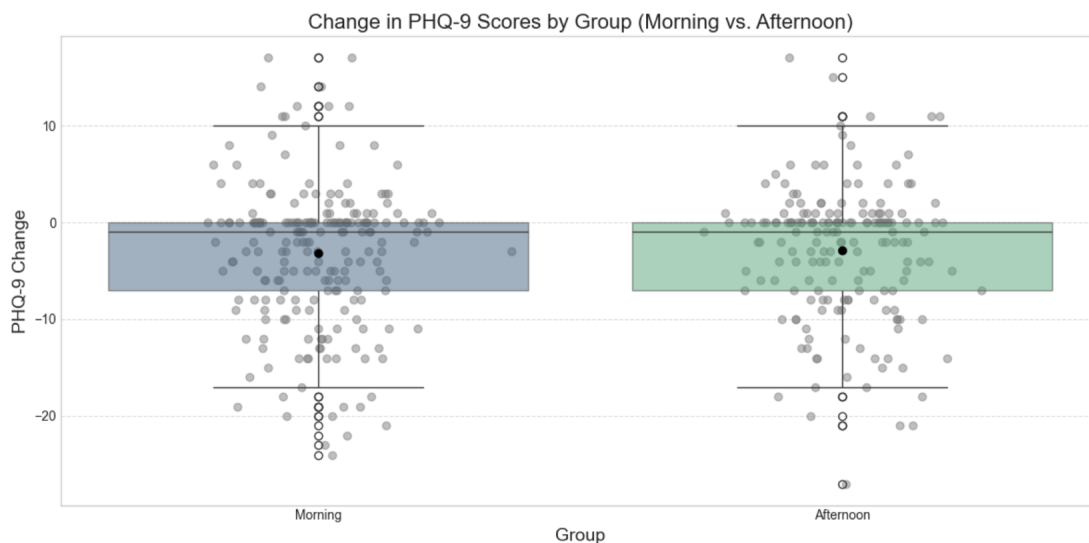


Figure 3.9: **Box plots illustrating the distribution of changes in PHQ-9 scores for participants in the morning and afternoon groups.** A two-sample t-test revealed no significant difference between the groups, $t(739) = -0.38, p = 0.701$. Individual data points are overlaid as scatterplots, showing variability within each group. The dark horizontal lines indicate group medians, and the shaded boxes represent the interquartile range. Whiskers extend to 1.5 times the interquartile range, and outliers are shown as individual points beyond the whiskers.

3.4.3 Does the age of the patient at the start of treatment impact treatment outcomes?

The age distribution of participants across clinics shows substantial variability, as illustrated by the box plots in Figure 3.10, and variance explained by clinic ID was 15.55%. Median ages ranged from approximately 30 to 70 years, with interquartile ranges (IQR) reflecting clinic-specific distributions. Clinics exhibit varying age ranges, with some clinics displaying narrower distributions and others showing broader spreads, likely related to their urban vs rural locations and reflective of the local population, variations in recruitment strategies and demographic characteristics.

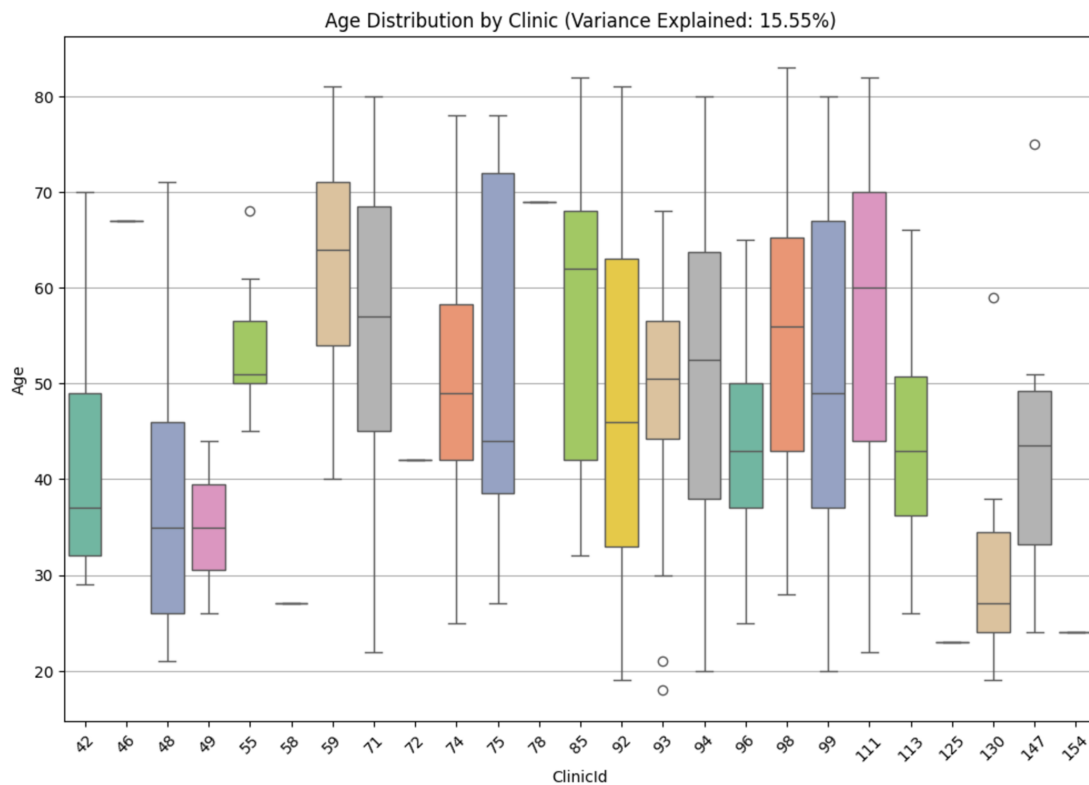


Figure 3.10: **Box plots showing the distribution of participant ages across clinics, with variance explained by clinic ID reported as 15.55%.** Each box plot represents the age distribution within a specific clinic, where the box denotes the interquartile range (IQR), the horizontal line indicates the median age, and whiskers extend to 1.5 times the IQR. Outliers are represented as individual points beyond the whiskers. The figure highlights variability in age distribution between clinics, with some clinics showing narrower age ranges and others displaying broader distributions. This suggests moderate heterogeneity in participant ages by clinic.

As shown in Figure 3.11, the relationship between PHQ-9 change (last score minus first score) and age at first assessment was not significant ($\beta = 0.0057, t(740) = 0.35, p = 0.729$). The R^2 value of 0.000 indicates that age at first assessment accounted for none of the variance in PHQ-9 change. These results suggest that patient age at the beginning of treatment does not influence the degree of symptom improvement as measured by PHQ-9 scores.

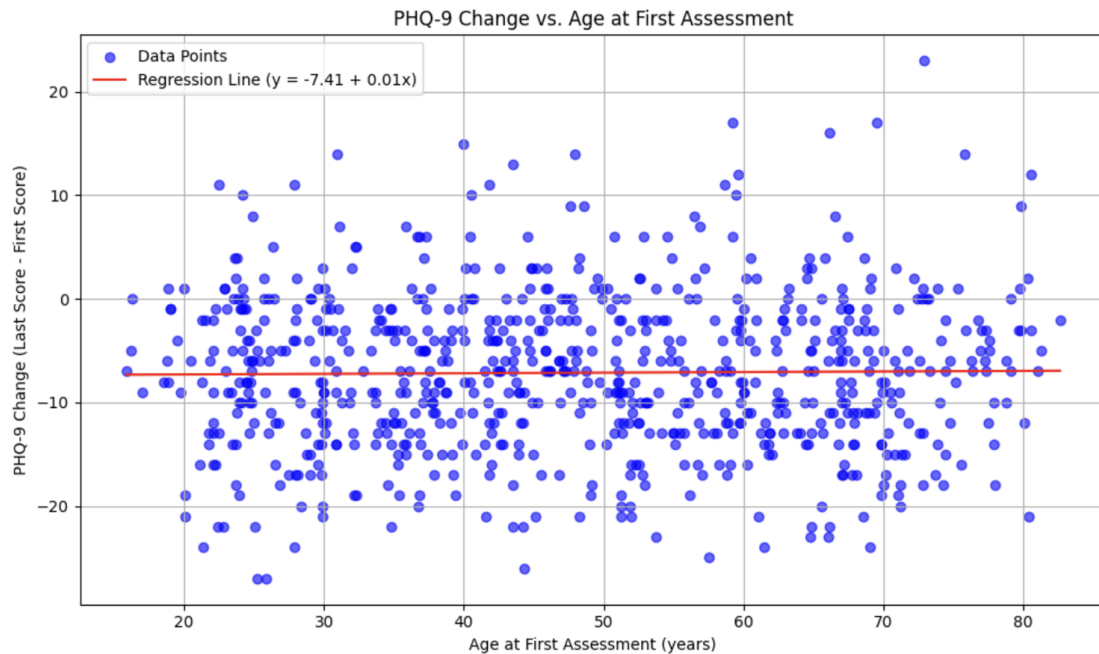


Figure 3.11: Scatterplot showing the relationship between PHQ-9 change (last score minus first score) and age at first assessment. Each blue point represents an individual participant, and the red line indicates the linear regression fit ($y = -7.41 + 0.01x$). The regression analysis revealed no significant association between age at first assessment and PHQ-9 change ($\beta = 0.0057$, $t(740) = 0.35$, $p = 0.729$). The R^2 value was 0.000, indicating that age at first assessment explained none of the variance in PHQ-9 change.

3.4.4 Does early change in the course of TMS treatment for MDD predict ultimate treatment outcomes?

Figure 3.12 illustrates the moving average of PHQ-9 scores over a six-week treatment period, with the first assessment aligned at $x = 0$. A gradual decline in PHQ-9 scores was observed, indicating overall symptom improvement across the patient cohort over the first 6 weeks of treatment. Fluctuations in the scores are evident throughout the time window, as shown by the shaded standard error region, highlighting inter-patient variability.

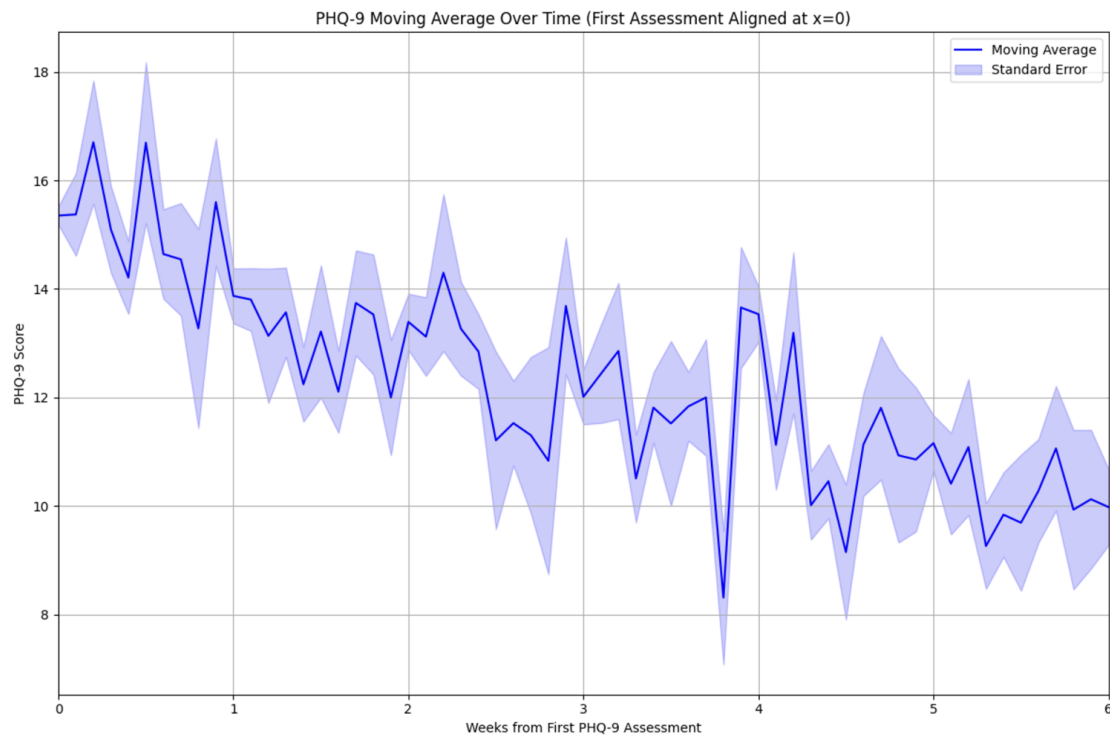


Figure 3.12: **Moving average of PHQ-9 scores over time, with the first assessment aligned at $x = 0$.** The solid blue line represents the moving average PHQ-9 score across weeks from the initial assessment, while the shaded region indicates the standard error. The graph shows a general decrease in PHQ-9 scores over the six-week period, with fluctuations observed at various time points. The decline suggests a potential trend of symptom improvement following the initial assessment, though variability remains notable throughout the time window.

As shown in Figure 3.13, we investigated the relationship between change in PHQ-9 score from baseline to Week 1 (x-axis) and change from Week 1 to the end of treatment (y-axis). A significant negative slope ($\beta = -0.210$, $p < 0.001$) indicates that greater early symptom improvement is associated with a smaller reduction in symptoms during the remainder of the treatment course. This pattern is likely driven, at least in part, by floor effects in PHQ-9 scoring, as scores falling below a threshold of 10 are generally considered subclinical for MDD and may constrain the extent of further measurable improvement. However, the relatively low coefficient of determination ($R^2 = 0.042$) suggests that early

response accounts for only 4.2% of the variability in subsequent symptom change, underscoring that the observed relationship, though statistically significant, has limited predictive value.

It is also important to acknowledge the limitations of interpreting week-by-week change scores in the presence of potential floor effects. Patients who respond strongly in the first week may reach low PHQ-9 values early on, leaving limited room for further improvement and thus compressing variability in subsequent scores. This nonlinearity in symptom reduction may obscure more complex trajectories of response and recovery, and caution should be taken in using early change as a standalone predictor of long-term outcome. Future models may benefit from nonlinear approaches or ordinal frameworks to better accommodate bounded scoring instruments like the PHQ-9.

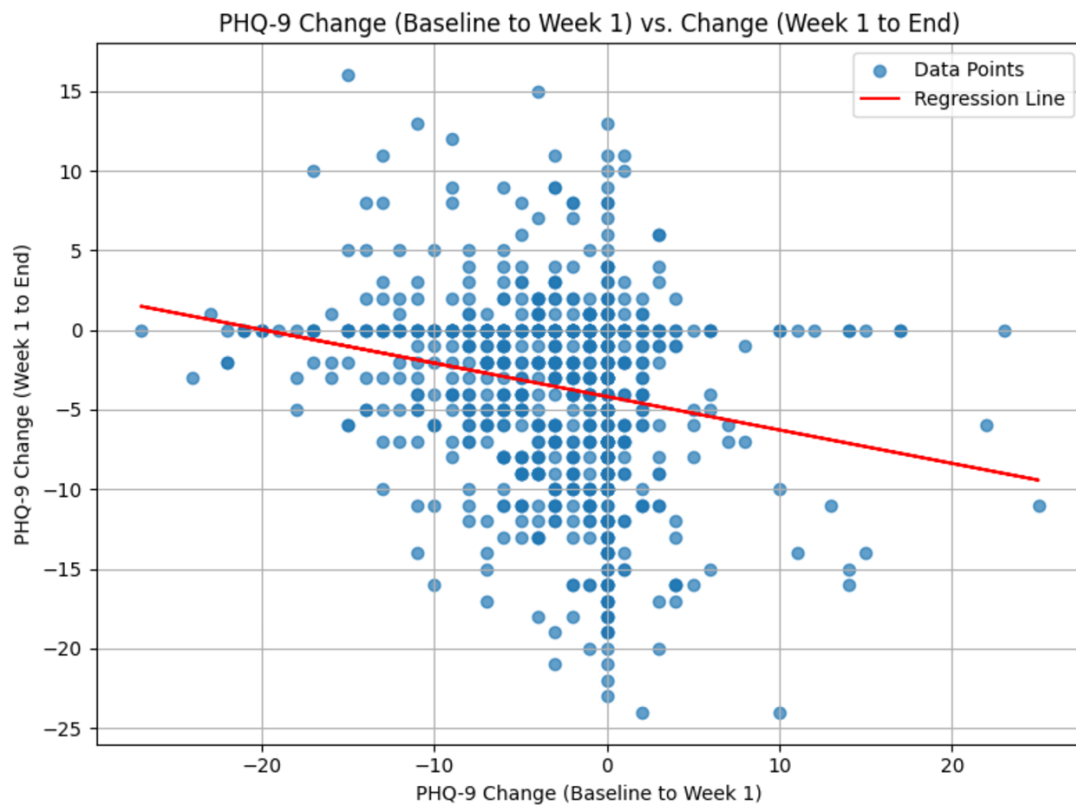


Figure 3.13: Scatterplot showing the relationship between PHQ-9 change from baseline to Week 1 (x-axis) and PHQ-9 change from Week 1 to the end of treatment (y-axis). Each blue point represents a participant, and the red line indicates the linear regression fit. Regression analysis revealed a slope of -0.210 , suggesting that for every one-unit improvement in PHQ-9 during the first week, there is a corresponding decrease of 0.21 units in the subsequent change. The intercept was -4.175 , and the R^2 value was 0.042, indicating that 4.2% of the variability in Week 1 to end-of-treatment change is explained by the baseline-to-Week 1 change. The relationship was statistically significant ($p < 0.001$), but the small effect size suggests that most of the variability is accounted for by factors beyond the early Week 1 response.

3.5 Discussion

3.5.1 Summary of findings

This chapter investigated the clinical utility of transcranial magnetic stimulation (TMS) in real-world settings by examining whether resting motor threshold (RMT), time of day (TOD) of stimulation, patient age, and early symptom change were associated with treatment outcomes in individuals with major depressive disorder (MDD). Across the dataset, no significant associations were found between individual RMT values and changes in PHQ-9 scores. Likewise, time of day of treatment and patient age at treatment onset were not significantly associated with treatment response. However, early clinical improvement, measured as the change in PHQ-9 score from baseline to Week 1, was significantly associated with subsequent symptom change, although the effect size was small ($R^2 = 0.042$) and likely challenged by floor effects.

Further analysis suggested that variation in RMT may be influenced by methodological differences across clinics, such as differences in measurement protocols or equipment calibration, which could obscure any potential relationship with treatment outcomes. The absence of a TOD effect persisted after controlling for inter-clinic variability, and the null finding related to age was consistent across the sample. Although early improvement was statistically significant, the limited variance explained restricts its practical predictive value in clinical decision-making.

3.5.2 Clinical relevance

These findings provide early critical insights into the application of TMS in large-scale, real-world clinical settings, highlighting the complexities and limitations of current practices. It also aims to demonstrate the opportunity to use data science infrastructure to better understand treatments, run experiments as scale, and perform quality control on existing and commonly deployed treatments.

The high inter-clinic variance between resting motor thresholds (RMT) and treatment outcomes raises questions about the consistency and accuracy of RMT measurement across clinics, likely stemming from differences in methodology, equipment calibration, and clinician training. This suggests an urgent need for standardised protocols in clinical settings to make sure that research generated to improve TMS treatment in laboratories actually translates into effective treatment outcomes for MDD patients. Ensuring consistency in RMT determination is one of the easiest and most observable changes that, if implemented, could enhance the reliability of TMS dosing and potentially improve outcomes in MDD treatment across larger patient groups.

The absence of significant differences in treatment efficacy based on the time of day (TOD) further supports the flexibility of TMS scheduling in clinical practice, as seen in Wendt et al. (2023), which could improve accessibility and convenience for patients and clinics alike. However, this study could not account for other circadian factors or patient-specific variations, such as sleep debt, individual chronotypes, cognitive loads etc, which could play a significant role in both cortical excitability and treatment responsiveness, but are not currently collected as part of standard clinical practice. It is worth noting, however, that individual chronotyping as suggested here can be clinically burdensome, so may be more worth considering once treatment protocols have been optimised for the shared features of the treatment sample, such as that of patients with MDD.

Similarly, our finding that patient age at the start of treatment does not significantly impact PHQ-9 outcomes suggests that TMS can be broadly effective across diverse age groups, which has also been shown before (Cappon et al., 2022; Croarkin et al., 2020). However, the observed demographic variability across clinics highlights the importance of accounting for clinic-specific factors when designing and interpreting treatment protocols, which may be particularly relevant in tailoring interventions to meet the needs of local populations.

Finally, while early changes in PHQ-9 scores show some association with treatment outcomes, these changes would need to be strongly predictive of treatment response (or

lack thereof) to have clinical utility for decision-making, which is not possible at the moment given the small effect size observed in our analyses. It is also important to note that it appears that symptom worsening early on in the course of treatment may still result in positive treatment outcomes at the end of 6 weeks, which will be an important paradoxical observation to consider when building predictive tools informing clinical decisions. Regardless, our findings highlight the potential for early monitoring to provide preliminary indicators of response, which, combined with other predictive markers, could eventually guide treatment adjustments or alternative interventions, and are worth exploring further.

3.5.3 Methodological limitations

Several methodological elements should be considered when interpreting the findings of this study, which highlight potential limitations in data collection, analysis, and the broader generalisability of the results and conclusions.

3.5.3.1 Data heterogeneity

While this is a very unique dataset that allows for some of the first large-scale explorations of variables impacting clinical response to TMS treatment for MDD, a major challenge in analysing large datasets that are compiled from multiple sources, like clinics in this case, lies in the heterogeneity of TMS administration and data collection practices across clinics. Resting motor thresholds (RMTs), for instance, are a key parameter in TMS treatment but are subject to significant variability depending on the methodologies employed at individual sites, clinician experience and thoroughness, the calibration of other relevant equipment (such as neuronavigation and/or EMG). This variability in measurement methodology could have obscured true physiological differences in cortical excitability across patients and diminish the ability to detect clinically meaningful relationships between RMT and treatment outcomes.

3.5.3.2 Selection bias and missing data

Although the dataset encompasses a large number of clinics and patients, only 18.2% of patients had clinical outcome data (PHQ-9 scores) reported, and were therefore included in the analyses presented in this chapter. This limited subset raises concerns about potential selection bias, as patients with complete data may differ systematically from those without reported outcomes, most simply because of the clinic in which they pursued their treatment. It is again worth emphasising that fewer than 1 in 5 clinicians reported clinical measures for their patients, meaning that we don't know how the data presented here would compare if full data were available, accounting for the actual diversity in treatment -and therefore outcomes- of patients. Furthermore, key demographic variables such as gender, ethnicity, and handedness were missing for the majority of cases, limiting the ability to account for these factors in our analyses, which may have helped eliminated confounding variables in our sample.

3.5.3.3 Time of RMT measurement

RMTs were typically measured only at the beginning of treatment, assuming a stable value throughout the course of TMS therapy. However, given that RMTs can fluctuate based on factors such as time of day, prior activity levels, and intersession intervals, a single measurement may fail to account for more nuanced relationships between RMT and treatment efficacy.

3.5.3.4 Observational data

As an observational study, this analysis cannot establish causal relationships between treatment parameters and clinical outcomes. While we used statistical models in our analyses to account for inter-clinic variability and controlled for several confounds, unmeasured variables such as co-morbid conditions, medication use, and socioeconomic factors may still have influenced the observed results. Randomised controlled trials (RCTs) would be necessary to validate these findings and establish causal links, especially for the

predictive elements of this study.

3.5.3.5 Result generalisability

The study population we had access to consisted of patients receiving TMS for MDD in real-world clinical settings using a specific TMS machine (Horizon 3.0). However, variability in clinic resources, including training and methodology, geographic distribution, and population demographics may limit the generalisability of these results to other healthcare systems or populations, and the exclusive use of Magstim's Horizon 3.0 systems may not fully reflect outcomes associated with other TMS devices or coil designs, even if it does reduce one variable across all patients in this study.

3.5.3.6 Predictive modelling methods

While early changes in PHQ-9 scores showed statistical significance in predicting later treatment outcomes, the small effect size ($R^2 = 0.042$) suggests that additional factors are likely influencing treatment response that could be explored further. More sophisticated predictive modelling approaches, such as generalised additive models that allow for non-linear relationships, machine learning methods that account for more complex data structures underlying the final prediction, or clustering methods for different response patterns as transition states, may improve predictive accuracy and are therefore worth exploring further.

3.5.4 Recommendations for future research

Future research should focus on addressing key methodological challenges highlighted above to improve the robustness and generalisability of findings related to real-world clinical TMS treatment for MDD. Standardising TMS administration and data collection is critical, as heterogeneity in practices across clinics likely influenced the observed variability in outcomes and led to the lack of conclusive findings in understanding the relationship between cortical excitability and clinical outcomes. Consistent protocols

for RMT measurement, such as the use of EMG-based detection, should be prioritised alongside comprehensive clinician training and centralised quality control mechanisms to ensure reliability across sites, especially when all clinics use the same equipment, such as the Horizon 3.0 machine. This study also highlights the tremendous opportunity to use networked systems, such as the Horizon 3.0, to push out 'community-wide', or centralised/standardised, protocols to test different implementation methods across clinical sites to see which are clinically most significant and optimise both treatment outcomes as well as easier adoption of novel treatment protocols and tools.

Additionally, standardising outcome reporting, including routine collection of PHQ-9 scores and key demographic variables, would help mitigate selection bias and enable better control for confounding factors and more representative samples in future analyses. This would likely lead to the inclusion of data from more diverse populations, healthcare systems, and geographic regions. If it would be possible to expand the scope of the dataset to evaluate outcomes with other TMS devices and coil designs, this could further help determine device-specific effects, as we are aware of other companies with similar large datasets (Sackeim et al., 2024), the combination of which could lead to more informative results.

Another recommendation is that future studies should incorporate repeated RMT measurements throughout the treatment course to capture changes in cortical excitability, and refine dosing protocols accordingly to maintain their relevance and applicability over time and optimise treatment outcomes for patients.

Further analyses should explore more predictive modelling approaches that move beyond linear regression, and leverage more advanced predictive techniques and models, hopefully helping to identify novel predictors of treatment response and improve the ability to stratify patients into responder (and non-responder) subgroups.

Multimodal data integration, finally, such as including neuroimaging measures, genetic markers, and patient-reported outcomes, could also be a fruitful future avenue to provide

a more comprehensive understanding of TMS mechanisms and efficacy in MDD.

3.6 Conclusions and contributions

In this chapter, we explored and highlighted the complexities and challenges of implementing TMS for MDD in real-world clinical practice. Through the analysis of a large, unique, multi-site dataset, we demonstrated that key variables such as resting motor threshold (RMT), time of day, and patient age had limited explanatory power for clinical outcomes, emphasising the need for more precise and consistent measurement practices. In our predictive analyses, we found that while early improvements in depressive symptoms showed a statistically significant association with ultimate treatment response, the effect size was small, suggesting that other factors contribute substantially to variability in outcomes, even if early predictors are a good early indicator.

Our findings contribute to the growing body of evidence supporting the importance of standardised protocols, both for RMT calibration and clinical outcome reporting, to reduce inter-clinic variability and enhance the generalisability of results across clinical treatments. We further propose that advanced predictive modelling techniques and longitudinal tracking of treatment parameters, such as RMT, may provide valuable insights for improving the precision of TMS delivery over time, and therefore improving treatment outcomes.

4 | Innovation: Single-session effects of using monophasic vs biphasic iTBS on cognition

4.1 Introduction

It is clear that there is still much to be understood and optimised in the way NIBS treatments work in the treatment of MDD. In the **Introduction** of this thesis, we discussed that conventional TMS devices have hardware constraints that mean that they have limited pulse shape control to experiment with novel clinical protocols. At the same time, we discussed that recent modelling work suggests that the pulse shapes used in TMS treatment for MDD now may not be optimised based on our understanding of underlying scientific mechanisms, but rather technical limitations of the tools, such as TMS machines, available to us. Innovation in the hardware underlying treatment delivery is therefore necessary for clinical research to be able to develop more evidence-based and personalised stimulation protocols for treatment.

4.1.1 Modelling of monophasic and biphasic pulse shapes

Modelling work conducted in our research lab (Wendt et al., 2021) and elsewhere (Sommer et al., 2006; Arai et al., 2007) suggested that monophasic pulses may require higher stimulation thresholds, but are likely to be more focal and efficient when engaging targeted neuronal populations than biphasic ones. In this study, modelling was conducted only in the motor cortex, using individual neuronal models (Aberra et al., 2020) and as expected, given the unidirectional nature of monophasic pulses, monophasic pulses showed direction-dependent sensitivity in terms of their activation thresholds, where posterior-anterior (PA) directed monophasic pulses had lower activation thresholds compared to anterior-posterior (AP) directed pulses; the opposite was observed for biphasic pulses. This suggests that monophasic stimulation may engage neuronal populations in

a more targeted and specialised manner, as shown in Figure 4.1, and this targeting may have beneficial downstream implications for clinical interventions.

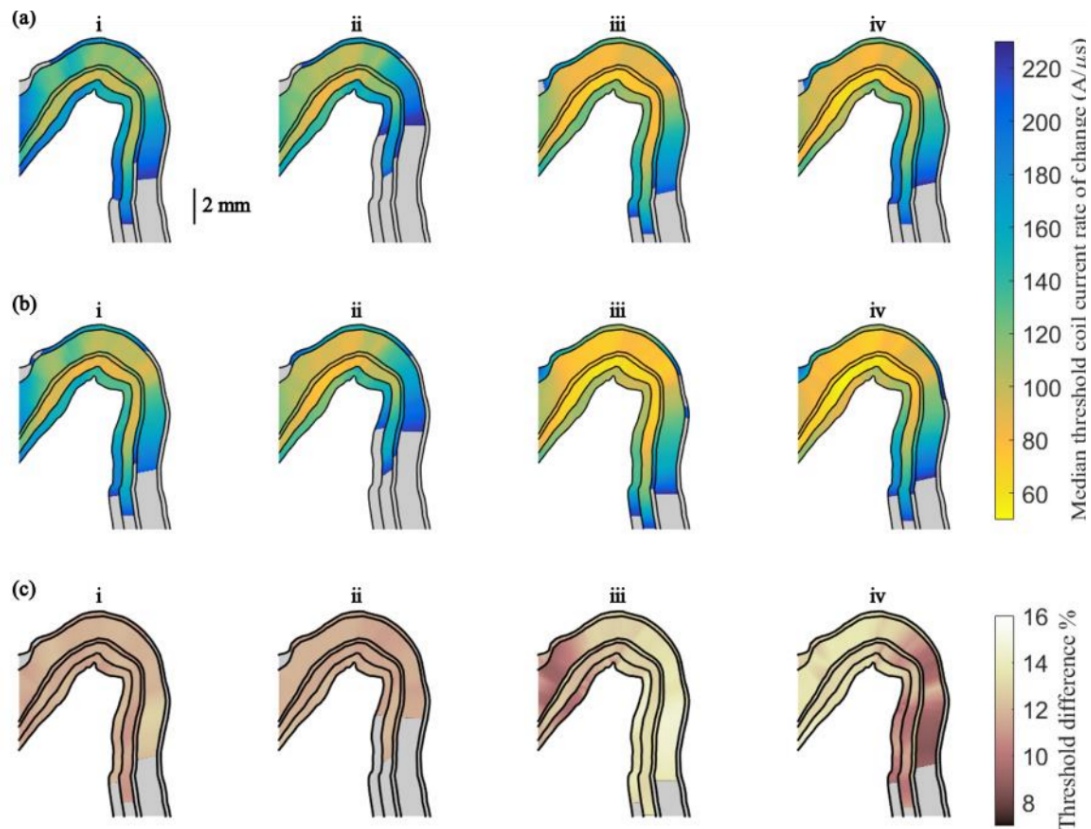


Figure 4.1: **Modelling of monophasic and biphasic stimulation in motor cortex neurons.** The median thresholds of the change in coil current for the six cortical layers are shown on a 2D cross section of the crown of the pre-central gyrus on a plane parallel to the stimulation coil orientation. (a) shows the thresholds for the pulse waveforms from the Magstim devices for i. monophasic stimulation in the PA direction, ii. monophasic stimulation in the AP direction, iii. biphasic stimulation in the AP direction and iv. biphasic stimulation in the PA direction. (b) shows the thresholds for 5-level pulse-width modulated approximations of each of the pulses in (a). The thresholds are given in $A/\mu s$, and thresholds above $230 A/\mu s$ are displayed in grey. (c) shows the percent difference in median thresholds between the conventional and pulse-width modulated pulses. Reproduced from Wendt et al., 2021.

4.1.2 xTMS

Our research group (led by Prof. Denison at the MRC Brain Network Dynamics Unit) has developed a version of a TMS machine, the xTMS, that allows control over pulse duration, generation of multiple voltage levels, and variable pulse widths and interpulse intervals (Ali et al., 2023). This is achieved by a new-generation, modular design TMS machine not operating at the resonant frequency but being controlled by a technique called pulse-width modulation (PWM) in which the IGBTs are rapidly switched on and off to create pulses with varying widths (Sorkhabi, 2021; Sorkhabi, 2022). Most importantly, the xTMS is able to produce monophasic iTBS, which can be tested for early clinical applications. The xTMS machine, shown in Fig. 4.2, was used in the data collection for this Chapter as it can generate monophasic iTBS protocols, which haven't yet been tested in clinical settings.

It is important to note that previous work in our group was able to demonstrate that monophasic and biphasic waveforms generated through PWM showed strong correlations with conventional TMS pulses, indicating that programmable TMS devices can reproduce both types of pulses with high accuracy, and tend to require slightly less energy to achieve equivalent neuronal activation compared to conventional TMS pulses (Wendt et al., 2021). This means that the programmable TMS architecture on which xTMS is built is capable of replicating both monophasic and biphasic pulses effectively, offering flexibility for different clinical and research applications.

4.1.3 Impact of monophasic vs biphasic stimulation on MEPs

Following this modelling work, biphasic and monophasic pulses generated with the xTMS were tested in human participants. The study (Wendt et al., 2023) investigated the strength of motor evoked potentials (MEPs), an indication of motor corticospinal excitability, induced by the stimulation of the motor cortex by biphasic and monophasic, individual pulses and iTBS protocols, respectively. The study hypothesised that

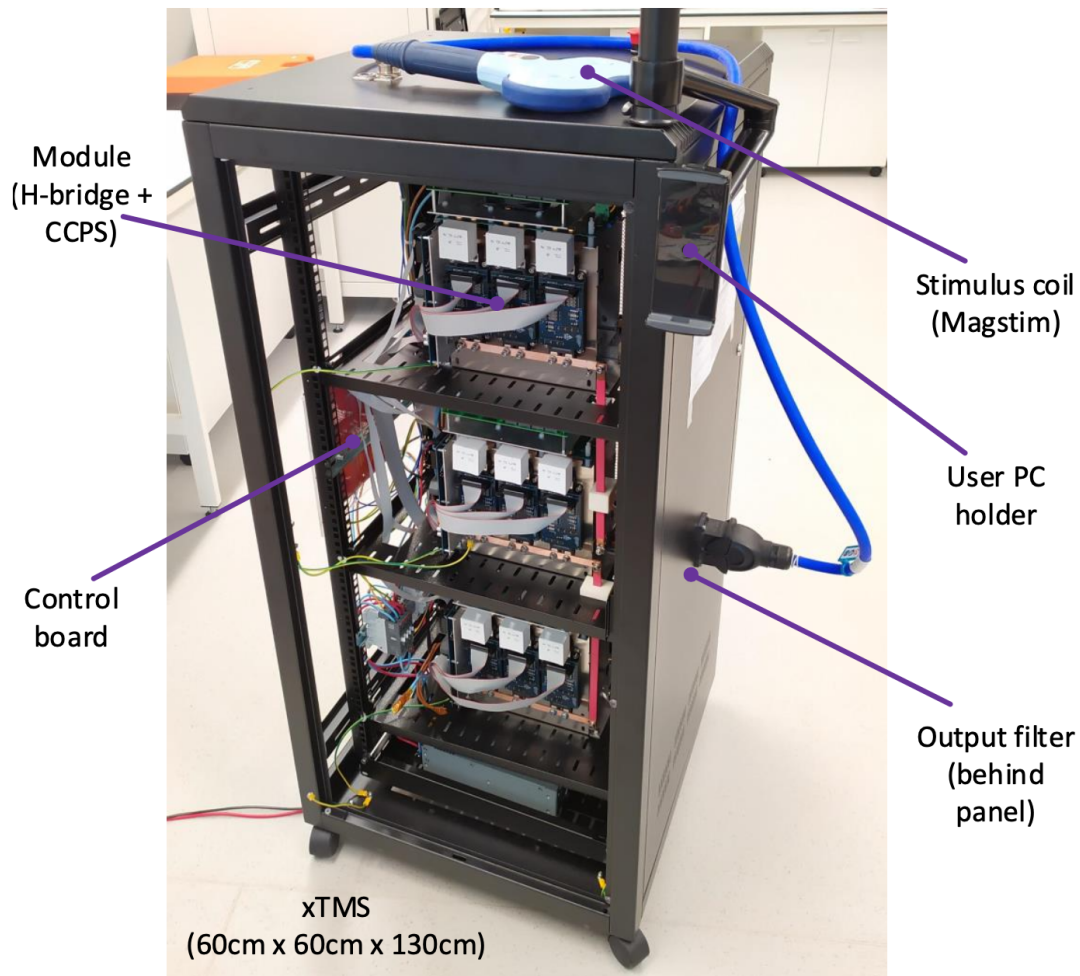


Figure 4.2: **Overview of the xTMS device.** Reproduced from Ali et al., 2023.

monophasic pulses would lead to stronger plasticity effects in the motor cortex than biphasic pulses. In line with this hypothesis, experimental data showed indeed that monophasic iTBS induced a stronger MEP response than biphasic, as shown in Fig. 4.3. Based on this data, the authors proposed that monophasic iTBS may have potential for greater functional impact when compared to standard biphasic iTBS, which could lead to improvements in further clinical applications of iTBS.

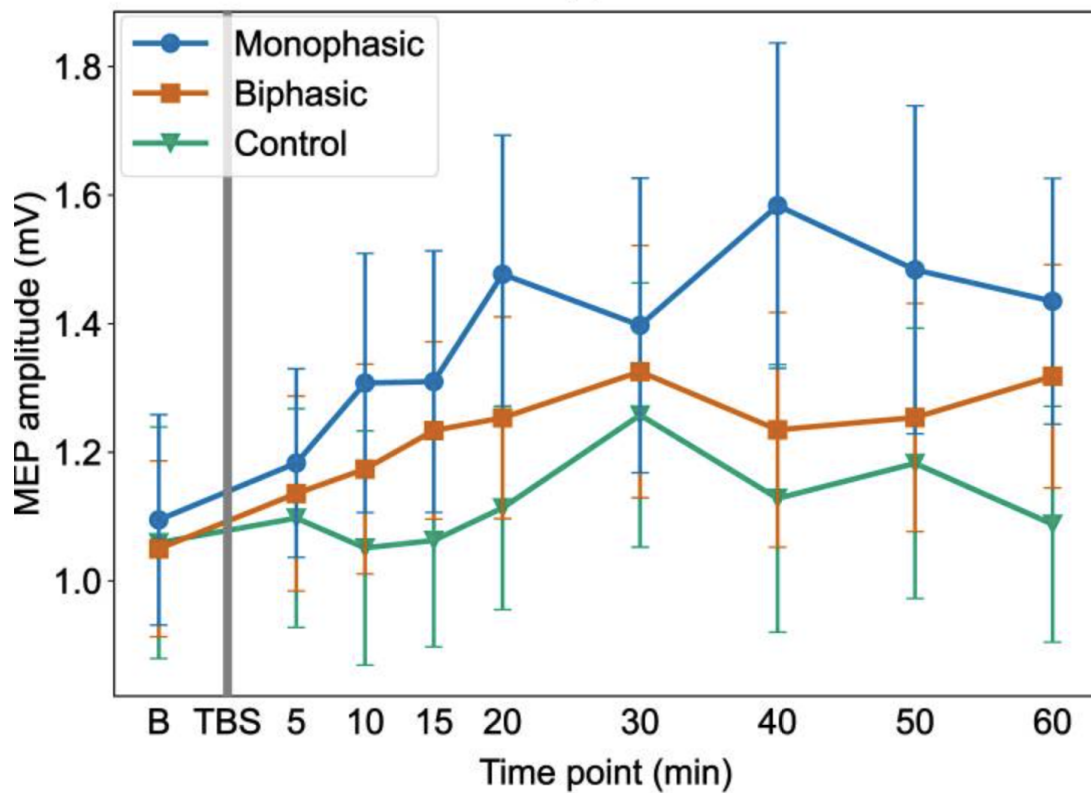


Figure 4.3: Group mean MEP amplitude for the monophasic and biphasic M1 iTBS conditions and the control condition are shown for the baseline and across the post-iTBS time points. Absolute MEP values are shown in mV for ease of interpretation. Reproduced from Wendt et al., 2023.

4.1.4 Cognitive changes as predictors of treatment outcomes

As discussed in the **Introduction**, individuals with major depressive disorder (MDD) exhibit altered processing of emotionally salient information, particularly a heightened sensitivity to negative stimuli. Notably, changes in this cognitive-affective processing often emerge early in the course of antidepressant treatment (Martens et al., 2021). Recent evidence suggests that such early shifts in emotional bias may serve as predictors of longer-term clinical outcomes and treatment response (Godlewska et al., 2016).

The Cognitive Neuropsychological Theory (CNT) of antidepressant action provides a framework for understanding the temporal gap between the onset of biological effects

of antidepressants and the observable clinical improvements in mood. According to this model, although neurochemical changes, such as those induced by selective serotonin reuptake inhibitors (SSRIs), can occur within hours of treatment initiation, these early biological effects are not sufficient on their own to produce mood improvements. Rather, CNT posits that antidepressants exert their therapeutic effects by modifying negative cognitive biases, thereby facilitating the formation of new, more positive emotional associations. These altered biases must then be reinforced through engagement with the environment, particularly through social interactions, to yield clinically meaningful improvements in mood (Godlewska & Harmer, 2021).

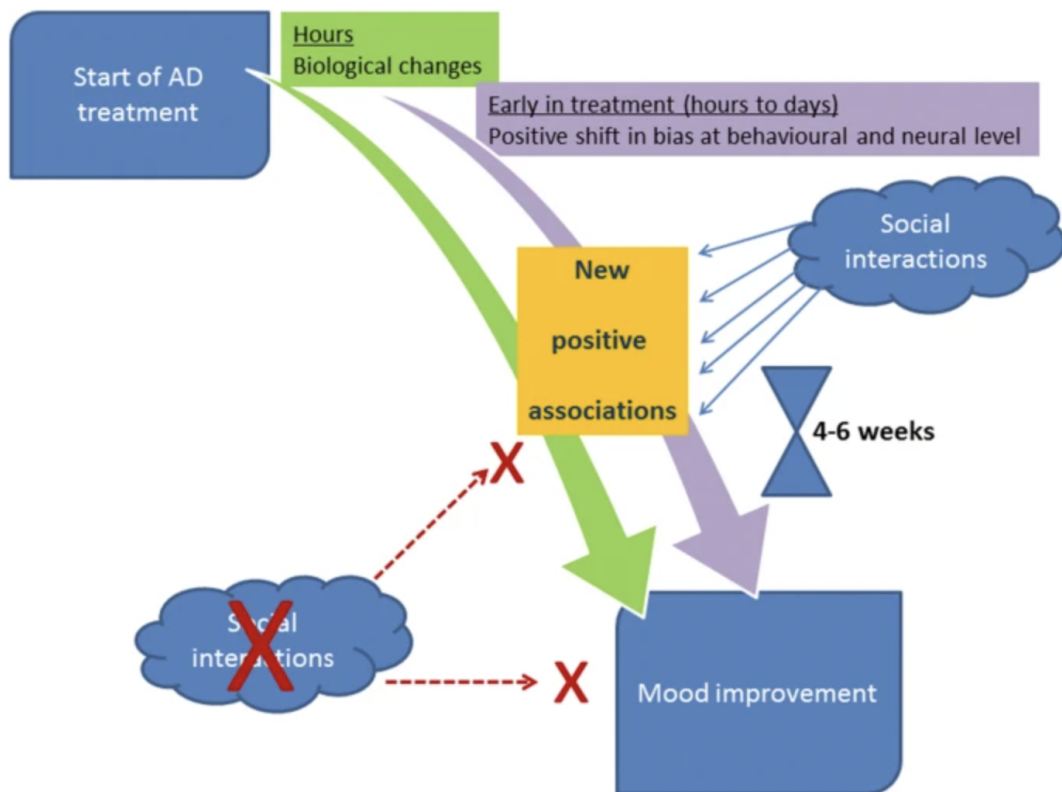


Figure 4.4: **Cognitive Neuropsychological Theory of Antidepressant Action.** Reproduced from Godlewska and Harmer, 2021.

This process is illustrated in Figure 4.4, which outlines the multi-step pathway from antidepressant initiation to eventual mood improvement. As depicted, biological changes

begin within hours (green arrow), leading to an early positive shift in emotional bias at both behavioral and neural levels (purple arrow). This bias shift enables the development of new positive associations (yellow box), which, when activated through real-world experiences—particularly social interactions (blue cloud)—contribute to mood improvement over a period of 4–6 weeks. Notably, the figure also highlights that in the absence of environmental reinforcement (i.e., lack of social engagement), the formation of new positive associations may not be sufficient to drive mood improvement, emphasising the role of behavioral activation in the treatment process.

Support for this model has been demonstrated in both behavioral and neuroimaging research. Early changes in performance on cognitive tasks assessing emotional bias (Harmer et al., 2003; Harmer et al., 2009; Tranter et al., 2009), as well as changes in neural activity during emotion processing tasks (Godlewska et al., 2016), have been shown to predict treatment response at later stages, typically 4–6 weeks after initiation.

4.1.4.1 Negative bias

A central construct within the CNT is negative bias - the tendency to more readily attend to, interpret, and remember negative emotional information. This bias is considered a key cognitive marker in predicting treatment response early in the course of treatment (Anderson et al., 2011). It has been defined as the tendency to interpret ambiguous emotional stimuli in a negative manner (Berna et al., 2011; Everaert et al., 2017), to preferentially recall negative emotional material, and to show slower responses to positive emotional cues across a variety of cognitive tasks (Roiser et al., 2012).

This bias extends across multiple cognitive domains and is frequently observed using the Facial Expression Recognition Task (FERT), in which individuals with MDD are more likely to misinterpret neutral or ambiguous facial expressions as negative, and show reduced accuracy in recognising positive emotions such as happiness or surprise (Harmer et al., 2004; Ruhe et al., 2019; Harmer et al., 2022). These cognitive-affective distortions contribute to the maintenance of depressive symptoms by reinforcing negative mood

states and maladaptive thought patterns. At the neurobiological level, this is aligned with evidence of increased rumination-related activity in the default mode network (DMN), alongside reduced activation in the central executive network (CEN), reflecting diminished top-down control of emotion through disrupted cortico-limbic connectivity (Luking et al., 2011).

Targeting this negative bias, primarily through antidepressant pharmacotherapy, as outlined by the CNT, is consistent with prevailing mechanistic hypotheses regarding the pathophysiology of depression. However, it remains an open question whether the CNT also applies to non-invasive brain stimulation (NIBS) approaches, such as transcranial magnetic stimulation (TMS), which may exert antidepressant effects via different or complementary mechanisms.

4.1.4.2 Limitations of the CNT

One critique of the CNT is that it may overemphasise negative bias while overlooking the possibility of broader deficits in emotional processing. Specifically, some evidence suggests that individuals with MDD may experience a more generalized impairment in emotion recognition, not limited to negative cues. A recent meta-analytic review reported a global facial emotion recognition deficit in MDD, with participants exhibiting lower accuracy across emotional categories. Furthermore, greater symptom severity was associated with poorer performance, regardless of emotion valence (Dalili et al., 2014; Krause et al., 2021).

This aligns with additional findings indicating that improvements in emotional processing post-treatment are not confined to negative emotions. For example, Tranter et al. (2009) observed treatment-related improvements in recognising both positive (happy, surprised) and negative (disgusted) facial expressions. Similarly, Harmer et al. (2003) found early improvements in the recognition of happy faces, while Brennan et al. (2017) noted enhanced recognition of angry, disgusted, and happy expressions following treatment. These findings support alternative accounts, such as emotion context insensitivity

(ECI) (Rottenberg et al., 2005) and emotional blunting (Ma et al., 2021), which describe reduced responsiveness to both positive and negative stimuli as characteristic of MDD.

Together, these observations suggest that while CNT provides a useful framework, it may require expansion to fully capture the breadth of affective impairments in MDD and how these are modulated by treatment.

4.1.4.3 Negative bias in pharmacological MDD research

Emotion recognition tasks, particularly the FERT, provide valuable insights into how negative bias manifests in individuals with MDD. These individuals are more likely to interpret neutral or ambiguous facial expressions as sad or negative, rather than positive. For example, Leppanen et al. (2004) found that depressed individuals exhibited both increased negative bias and reduced positive bias in facial emotion recognition, often misclassifying neutral faces as sad. Similarly, Gotlib et al. (2004) demonstrated that adolescents at high risk for depression displayed heightened negative bias compared to low-risk peers, suggesting its potential as an early vulnerability marker.

Treatment studies have also shown that antidepressants can reduce negative bias. Harmer et al. (2009) reported that antidepressants may enhance positive emotional processing even before observable improvements in mood. Complementary findings by Godlewska et al. (2012) demonstrated that serotonin reuptake inhibitors normalize prefrontal and amygdala activity in a manner consistent with reduced negative bias during emotion recognition tasks.

By understanding these specific patterns of cognitive-affective bias, and their neural correlates, we can improve our ability to predict treatment response and develop more targeted therapeutic strategies for individuals with depression.

4.2 Research questions

This chapter presents the results and analysis of a pilot study investigating the effects of a single session of optimised monophasic vs. biphasic intermittent theta burst stimulation (iTBS) delivered via a novel TMS device, xTMS, on negative bias in low mood individuals. To our knowledge, this is the first study to test and compare monophasic to biphasic iTBS in a clinically relevant population to understand single-session effects that may be predictive of future treatment response.

This chapter focuses on three main research questions:

1. Is there a difference in negative bias change after a single session of monophasic vs. biphasic iTBS?
 - **Hypothesis:** Monophasic iTBS will lead to a greater reduction in negative bias compared to biphasic iTBS, reflecting improved positive emotional processing.
2. Can the changes in the recognition of individual emotions explain the changes, if any, observed at the negative bias level?
 - **Hypothesis:** Improvements in negative bias will be driven primarily by enhanced recognition of positive emotions (e.g., happiness) rather than changes across all emotion categories.
3. Can the changes in the recognition of ambiguous (50% intensity) faces explain the changes, if any, observed at the negative bias (or individual emotion) level?
 - **Hypothesis:** Increased positive interpretation of ambiguous (50% intensity) emotional faces will be associated with reductions in negative bias, serving as a key mediator of overall emotional bias shifts.

4.3 Methods

4.3.1 Ethical data collection and analysis:

This dataset was collected at the Oxford Centre for Human Brain Activity in the Department of Psychiatry at the University of Oxford, under the supervision of PI Dr Jacinta O’Shea, Prof Timothy Denison and Dr Verena Sarrazin. The study was approved by the Central University Research Ethics Committee (CUREC) at the University of Oxford under the identification of R87506/RE003. All participants gave in-person informed, written consent.

4.3.2 Participants

Eleven healthy volunteers (mean age: 23.9 ± 3.4 years; 7 females) with a Beck Depression Inventory (BDI) score of 30.8 ± 8.3 completed the study, which consisted of an online screening session followed by four data collection sessions in a single-blind, within-participants crossover study. All 11 datasets are included in this analysis.

All participants included in the study were (1) willing and able to give informed consent, (2) otherwise healthy adults, either male or female, (3) aged between 18 and 45 years, (4) fluent in English, (5) right-handed, (6) scoring 10 or higher on the BDI (Beck Depression Inventory) questionnaire, (7) able to adhere to the intervention schedule. Participants were excluded if they: (1) were currently taking any medications, excluding the contraceptive pill (e.g., antiepileptics, antipsychotics, psychostimulants, SSRIs, SNRIs), (2) had a current significant medical condition, (3) had significant suicidal ideation, determined as a score of 2 or above on the suicide item in the BDI (Beck Depression Inventory), (4) had participated in any other psychological or medical study involving the intake of any kind of drugs within the last 3 months, (5) had been diagnosed with bipolar disorder, (6) had a family history of extreme mood fluctuations, such as elated mood states, (7) had safety contraindications to TMS, such as a family history of epilepsy, (8) had safety con-

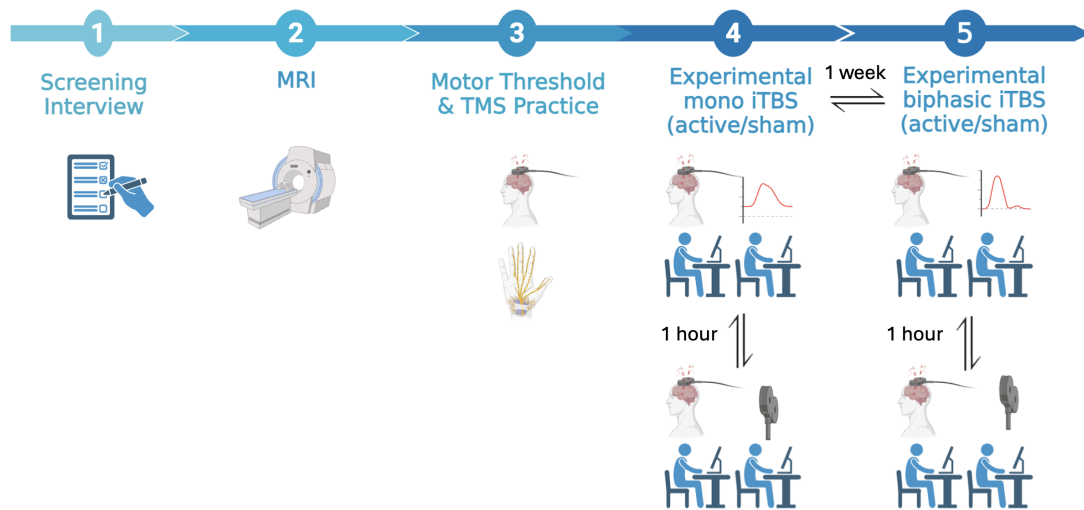


Figure 4.5: **Schematic illustration of the study design, treatment, and evaluation schedule.** Bidirectional arrows indicate counter-balanced order.

traindications to MRI, such as having a pacemaker, (9) were pregnant or breastfeeding, (10) had previously participated in a brain stimulation study, where the type, location, and number of sessions of stimulation received were considered by the PI to potentially interfere with the results of the present study. If a participant was not included in the study, but still showed a BDI score above 10 and/or indicated a score of 2 or above on the BDI and/or indicated suicidal ideation during screening, they were sent the follow-up letter provided in **Appendix A**.

4.3.3 Experimental design and treatment

The study consisted of three main stages: screening, MRI, and experimental iTBS (active & sham) sessions, as shown in the study schedule in Figure 4.5.

Screening: After expressing interest in the study, participants received the participant information sheet and, after consenting to take part in screening procedures, completed pre-screening questions, including a depression questionnaire (BDI) screening of potential contraindications for TMS or MRI, and handedness. Participants with a BDI score

above 10 were then invited to a 1-hour screening session conducted via video call on Microsoft Teams, except if they scored 2 or above on the suicide item. During this session, the researcher conducted a clinical interview (SCID) and confirmed TMS and MRI screening forms to ensure no contraindications to brain stimulation and neuroimaging applied. Participants showing signs of bipolar disorder based on the SCID results, or if any additional contraindications were identified, were excluded. Otherwise, participants were invited to a TMS familiarisation session.

Each participant completed 4 in-person sessions following screening: 1) TMS familiarisation, 2) MRI, for setting up personalised targeting, 3) iTBS (real), 4) iTBS (sham). Sessions 3 and 4 were counter-balanced and identical in structure except for the coil angle (turned sideways for sham). This means that half of the participants received an active stimulation session in session 3 and a sham stimulation in session 4, and vice versa. All participants completed both a real and a sham TMS session. All sessions that included TMS (session 1 (TMS familiarisation), sessions 3 and 4) had to have a minimum of 7 days between them to avoid confounding effects. All participants were asked to come to experimental sessions fully rested, with their sleep noted, and without having consumed caffeine in the last 2 hours, or any psychoactive substances (including nicotine) in the last 24 hours.

TMS familiarisation: The focus of this session was to determine each participant's individual resting motor threshold and confirm the tolerability of iTBS. Single pulses of TMS were applied over the motor cortex to locate the motor hotspot based on the resting motor threshold (RMT), as assessed using electromyography (EMG) measurements. Electromyography signals were captured from the right hand's first dorsal interosseous (FDI) muscle using disposable neonatal ECG electrodes arranged in a belly-tendon configuration. The electrodes were connected to a ground electrode placed at the ulnar styloid process. Signal acquisition was conducted via a D440 Isolated Amplifier (Digitimer, Welwyn Garden City, UK) and a Micro1401 unit (Cambridge Electronic Design, Cambridge, UK), supplemented by a Digitimer HumBug Noise Eliminator, using Signal

version 7.01 software (Cambridge Electronic Design). The system recorded the EMG data with 16-bit resolution, a sampling rate of 10 kHz, an amplifier gain of 1000, and a bandwidth filter ranging from 10 to 1000 Hz. The HumBug Noise Eliminator effectively reduced 50 Hz line noise by subtracting a noise replica from the incoming signal, thus maintaining the integrity of the EMG signals without the need for filtering.

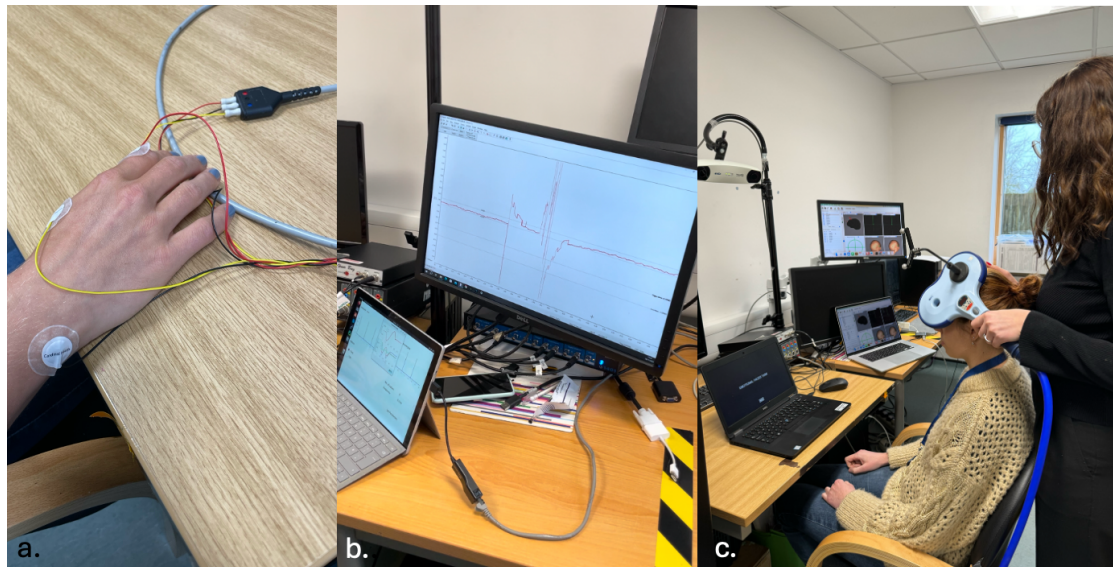


Figure 4.6: **Illustration of the testing setup for the TMS familiarisation and experimental iTBS sessions.** a) shows the setup of EMG on the FDI muscle during the TMS familiarisation session, b) shows the recorded MEP visualised in software during the TMS familiarisation session, and c) shows the setup of neuronavigation, imported MRI scans with pre-set targeting locations, and cognitive tasks ready to be performed by the participant immediately after the stimulation session finishing during the experimental iTBS sessions.

To determine the RMT, key head landmarks were measured (A/P, L/R), and 10 single pulses were applied at each intensity, with the EMG traces visually inspected in real time. The RMT was determined as the lowest intensity, with reference to the maximal output voltage, at which 5 out of 10 consecutive trials evoked an MEP with a peak-to-peak amplitude exceeding $50 \mu\text{V}$. Once the RMT was determined, single TMS pulses at 70% RMT were delivered to the dorsolateral prefrontal cortex (DLPFC), identified using the 5-cm rule, to familiarise participants with the TMS sensation over the brain

region targeted in the main experiment. If the participant was comfortable proceeding, two sample theta burst TMS trains were delivered over the DLPFC. If iTBS over the DLPFC was well tolerated, participants proceeded to the neuroimaging session.

fMRI data acquisition: Prior to the stimulation sessions, each participant completed both structural MRI and resting-state functional MRI scans. The structural scan was used to set up neuronavigation for the experimental iTBS sessions, and the resting-state MRI scan was used to identify the individual DLPFC hotspot for stimulation, as described below. MRI scans were acquired using a 3T Siemens MAGNETOM Prisma MRI scanner (Siemens, Erlangen, Germany) at the Oxford Human Brain Activity (OHBA) centre, with a 32-channel imaging coil. T1-weighted structural images were acquired with a voxel resolution of $1.0 \times 1.0 \times 1.0$ mm on a $232 \times 256 \times 192$ grid, TR / TE / flip angle = 199 ms / 3.96 ms / 8° over 441s. Resting-state fMRI data were acquired with a voxel resolution of $2.4 \times 2.4 \times 2.4$ mm, repetition time (TR) / echo time (TE) / flip angle = 735 ms / 39 ms / 52° over 370s. During both scans, participants were instructed to let their minds wander, avoid repetitive thoughts, keep their eyes open, and keep their attention focused on a central fixation point. The full protocol is provided in **Appendix A**.

fMRI analysis for personalised target generation:

Preprocessing First, each participant’s high-resolution T1-weighted anatomical scan was processed using a standard pipeline, involving reorientation to LR/AP, tissue segmentation, bias field correction, brain extraction, and skull-constrained nonlinear registration to MNI space. The same preprocessing steps were applied to the single-band reference. A MELODIC ICA analysis was then run on the functional resting-state data for each subject individually, which included motion correction (MCFLIRT), fieldmap unwarping, interleaved slice timing correction, brain extraction, high-pass filtering (at 100 Hz), registration to the structural image and to standard MNI space, independent component analysis, prewhitening, and thresholding the image with a Z-threshold of 3.1 and a P-threshold of 0.05. Signal/noise classifications were run using the FMRIB FIX tool

trained on UK BioBank data, and noise components were regressed from the original fMRI dataset to remove the noise contributions from the data. Once completed, 5mm FWHM Gaussian smoothing and registration was applied to the original dataset. Every step of pre-processing was manually validated for registration and signal/noise assignments.

Region-of-interest (ROI) identification: A seed ROI was manually defined in the bilateral subgenual anterior cingulate cortex (sgACC), centred at MNI coordinates [-6, 16, -10] (left) and [6, 16, -10] (right), with a 5mm radius, as described in Cole et al., 2020. For the DLPFC target, ROIs were placed over Brodmann Area 9 and Brodmann Area 46 (often overlapping), using the MNI coordinates [-36, 39, 43] and [-44, 40, 29], respectively, with a 10mm radius. The coordinates were manually verified to correspond to anatomical landmarks on the corresponding structural scan and restricted to brain areas. sgACC was chosen due to its functional relationship with the DLPFC, as explored in the **Introduction**.

Correlation mapping and target identification: Time series data were then extracted from the seed ROI, and whole-brain correlation maps were created using the `fsl_glm` tool between the seed timeseries and the remainder of the brain. The correlation maps were then masked for the DLPFC ROI (BA9 and BA46 areas). A threshold of 75% of the maximum z-score was then set across the masked correlation map, and the peak cluster was identified using the native FSL `cluster` function. The center-of-gravity (COG) coordinates of the DLPFC cluster most anti-correlated with the sgACC seed were then converted back from MNI space to subject native space and noted for use in neuronavigation.

Neuronavigation: To position the TMS coil over the DLPFC region identified using the resting state fMRI analysis pipeline, a Brainsight neuronavigation system (Rogue Research Inc., Montreal, Canada) was used. Neuronavigation, also known as frameless stereotaxy or image-guided TMS, is used to guide interventions to precise locations within the anatomy of the brain of a person. To do so, it uses three reflective spheres

mounted on the subject's head and the stimulating coil that are tracked with an optical camera (Polaris) in real time to scale the location of the spheres in relation to landmarks identified on an individual's structural scan loaded onto the system or onto landmarks set up in standard MNI space. In the familiarisation session, the average head model was used, as the motor cortex, needed for resting motor threshold, is easily identifiable using electromyography and visible finger twitches. In the experimental sessions, the participant's own structural MRI scan was used instead. To do so, the participant's raw T1 scan was loaded onto the Brainsight software's interface, and seven landmarks were manually identified on the structural scan to help register the scan to the participant's physical landmarks. These landmarks included the nasion, theinion, the left preauricular (lpa) and the right preauricular (rpa), the left eyebrow, the right eyebrow, and the tip of the nose. Then, the target DLPFC coordinates in native space were loaded into the interface and saved for targeting. This helped the operator ensure that the position and direction (angle, tilt) of the coil stay on target throughout the stimulation session and reduce coil motion. These digital MRI landmarks were then registered with the participant's physical landmarks in order to map the participant's brain onto their own structural MRI scan, and the DLPFC location could be targeted directly using the coil.

Experimental iTBS active/sham: Both experimental iTBS sessions (sessions 4 and 5) were identical except that either sham or active TMS was delivered in one or the other session, with the order counterbalanced across participants. Firstly, participants completed the STAI and PANAS questionnaires, as well as a brief practice session of the behavioural tasks. STAI and PANAS questionnaires are self-report questionnaires used to assess the emotional state of the participant at the exact time of the intervention. Then, the researcher used neuronavigation to register the participant's head to their structural MRI in order to position the TMS coil over the DLPFC. The participant then received either active or sham TMS (600-pulse monophasic iTBS over the DLPFC, lasting approximately 3 minutes), depending on their counterbalanced order. During sham stimulation, the coil was angled away from the scalp, preserving non-specific aspects of the stimulation experience (e.g., sound artefact) but not stimulating the brain.

Immediately after the stimulation, the participant performed the FERT task, followed by the Information Bias Learning Task (IBLT). At the end of the session, the participant completed the STAI and PANAS questionnaires again. STAI, PANAS and IBLT data analysis was outside of the scope of this study as it was part of other academics' work.

Treatment protocol: The TMS protocol used in the study intervention is known as intermittent theta burst stimulation (iTBS). iTBS was applied at 70% resting motor threshold (RMT) in 2s trains of 10 bursts, each containing 3 pulses at 50 Hz delivered with 200ms intra-burst intervals for a total of 20 cycles, amounting to 600 total pulses over approximately 3 minutes, see Fig. 1.2. The 70% threshold was chosen based on the guidance from CUREC, where appendix 2 of the AP21 procedure (attached in **Appendix A**) indicates that 80% of active MT, equivalent to 70% RMT is to be used for experimental iTBS protocols. Both monophasic and biphasic iTBS and single TMS pulses were applied using the xTMS device, see Fig. 4.2, to the dorsolateral prefrontal cortex, identified using the individualised resting state MRI analysis pipeline. A 70-mm figure-8 coil (Magstim Co., P/N 9925e00) was used to administer all forms of magnetic stimulation.

4.3.4 Facial Expression Recognition Task (FERT)

Task administration: The FERT was administered immediately after every experimental intervention (sham/real monophasic/biphasic iTBS) using a lab-based computer, for a total of four FERT sessions completed by each participant. In the task, participants were required to identify the emotion on the faces shown using a mouse-press. The facial expressions consisted of one of six basic emotions (fear, happy, surprised, sad, disgusted, angry, plus neutral) shown at different intensity levels (e.g. 80% happy mixed with 20% neutral), in increments of 10%. A total of 250 faces were shown over the period of four blocks, with progress shown every 83 faces. Multiple variants of both tasks were used to minimise learning effects.

The analysis of the FERT focused on three key measures: unbiased hit rate, reaction

time, and efficiency score.

Unbiased hit rate (UnHR): The unbiased hit rate has been proposed as a better measure than accuracy, as it corrects for response bias (Bone et al., 2019). It is computed by multiplying mean accuracy for each emotion by the ratio of the total times that the emotion was selected correctly, divided by the total times that emotion was chosen in total (including incorrectly), as follows:

$$UnHR(emotion) = \text{mean correct} * \left(\frac{\text{no of times emotion selected correctly}}{\text{no of times emotion selected in total}} \right)$$

(Wagner, 1993)

This measure accounts for response bias, such as classifying all emotions as 'fear' when unsure, which would (misleadingly) result in a 100 accuracy rate (by contrast with a low unbiased hit rate) for the emotion of 'fear'. Because of this, we think that unbiased hit rate may be a better measure of emotion recognition than raw accuracy, and the **Results** for accuracy are presented with regards to the unbiased hit rate metric.

Reaction time (RT): Reaction time refers to the time between the presentation of a stimulus and the recorded response action of the participant, and is used as a proxy for reaction speed. Given that reaction times of those trials, where the participant's response was incorrect, may not be indicative of emotional processing but of other confounding cognitive events (such as lack of attention), the **Results** section considers reaction times of accurate trials only in the analyses, as is standard practice in tasks assessing reaction time as an outcome variable (Bone et al., 2019).

Efficiency score (ES): The efficiency score is a combined measure of speed and error, which aims to consider the trade-off between the two during emotional processing. ES is computed by dividing the accuracy (measured by the unbiased hit rate) by the reaction time, as follows:

$$EfficiencyScore(ES) = \left(\frac{\text{Unbiased Hit Rate}}{\text{Reaction Time (Acc Trials Only)}} \right)$$

The higher the ES, the more efficient the participant is at accurately recognising an emotion within the same amount of time. This measure aims to characterise whether getting more accurate at recognising emotions comes at the expense of time.

For ease of interpretation, the measure of positive bias, the inverse of negative bias, was used for the analyses. This is because the recognition of positive emotions is generally more accurate than that of negative emotions (Leppanen & Hietanen, 2003), so a positive bias measure is more intuitive to interpret than a negative bias measure for clinical purposes (Xu et al., 2021).

Positive bias: In the FERT, positive bias is typically measured as the ratio of the performance on a particular metric for positive (happy, surprise) versus negative (fear, sadness, anger, disgust) emotions. In order to maintain consistency throughout the Results section, all positive bias measures are computed such that a higher metric indicates higher positive bias. This means that, for each respective metric:

Positive bias (UnHR): Here, a higher positive bias (UnHR) shows that a participant more accurately identified positive rather than negative emotions (regardless of intensity), computed as follows:

$$PositiveBias(UnHR) = \log \left(\frac{\text{mean UnHR for positive emotions}}{\text{mean UnHR for negative emotions}} \right)$$

for every session of every participant;

Positive bias (RT): Here, a higher positive bias (RT) shows that a participant more quickly identified positive rather than negative emotions (regardless of intensity), computed as follows:

$$PositiveBias(RT) = \log \left(\frac{\text{mean RT for negative emotions}}{\text{mean RT for positive emotions}} \right)$$

for every session of every participant;

Positive bias (ES): Here, a higher positive bias (ES) shows that a participant more

efficiently identified positive rather than negative emotions, computed as follows:

$$PositiveBias(ES) = \log \left(\frac{\text{mean ES for positive emotions}}{\text{mean ES for negative emotions}} \right)$$

for every session of every participant.

Quality checks: In order to ensure that raw data pre-processing is consistent with the standards required for appropriate statistical analysis, strict data checks for reaction time and accuracy were performed. Additional checks for data completeness and misclassifications across emotions and intensities were also conducted.

4.3.5 Statistical Analysis

Statistical analyses of the FERT were conducted and visualised in R. Statistical significance was determined at $p < 0.05$ across all analyses, and individual tests that were conducted are described separately in the **Results** section.

4.3.5.1 Sample demographics, clinical and physiological characteristics

Descriptive statistics were computed for demographic and clinical variables. Means and standard deviations (SDs) were reported for continuous variables (e.g., age, RMT levels, BDI scores), and gender distribution was summarised as counts.

4.3.5.2 rsMRI-derived target locations

Individualised stimulation targets in the left dorsolateral prefrontal cortex (DLPFC) were determined using resting-state fMRI scans to identify coordinates most anti-correlated with the subgenual anterior cingulate cortex (sgACC). Coordinates were transformed into both MNI space and participant-specific anatomical space for precision targeting and visual inspection; both are presented in the **Results** section.

4.3.5.3 Single-session changes in emotion recognition bias

Paired-sample *t*-tests were used to assess changes in positive emotion recognition (unbiased hit rate (UnHR), reaction time (RT) and efficiency scores (ES)) between monophasic and biphasic iTBS sessions relative to their corresponding sham sessions. Results were summarised using *t*-statistics, degrees of freedom, and associated *p*-values. Bar plots with error bars representing ± 1 standard deviation were used to visualise group means. For each participant, the effect of stimulation was computed as the within-subject difference between real and sham conditions, separately for the monophasic and biphasic sessions (1 measure per participant per stimulation type) for a total of 11 matched pairs (leading to 10 degrees of freedom).

4.3.5.4 Single-session changes relative to sham stimulation

To determine whether real stimulation induced significant changes relative to sham conditions, paired-sample *t*-tests compared positive bias (UnHR and ES) changes between real and sham sessions separately for monophasic and biphasic stimulation. These comparisons provided a baseline-adjusted evaluation of treatment effects and due to the limited number of planned comparisons (two), no correction for multiple comparisons was applied.

4.3.5.5 Single-session changes in recognition of specific emotions

To assess whether stimulation differentially affected the recognition of specific emotions (happy, sad, fear), two-way repeated measures ANOVAs were conducted. Within-subject factors included stimulation type (monophasic vs biphasic) and emotion category. Main effects and interaction effects were reported alongside generalized effect size (*ges*) measures to interpret magnitude of observed differences.

4.3.5.6 Single-session changes in recognition of ambiguous (50% intensity) emotions

Given the sensitivity of 50% intensity faces in detecting subtle emotional processing shifts, paired-sample *t*-tests were conducted to compare efficiency scores for recognising ambiguous sad, fearful, and happy expressions between monophasic and biphasic stimulation sessions. Bar plots with overlaid individual data points were used to visualise group differences.

4.4 Results

4.4.1 Sample demographics, clinical and physiological characteristics

The final sample consisted of 11 participants (7 female, 4 male) with a mean age of 23.9 years (SD = 3.4), consistent with recruitment from a university student population. Participants presented with moderate to severe depressive symptoms, as indicated by a mean Beck's Depression Inventory (BDI) score of 30.8 (SD = 8.3). Resting motor thresholds (RMT), expressed as a percentage of maximum stimulator output (% MSO), averaged 72.1% (SD = 13.0) for biphasic stimulation and 78.6% (SD = 12.2) for monophasic stimulation.

Variable	Mean	Standard Deviation
Age	23.9	3.4
Gender (F:M)	7:4	
Biphasic RMT (% MSO)	72.1	13.0
Monophasic RMT (% MSO)	78.6	12.2
Beck's Depression Index (BDI)	30.8	8.3

Table 4.1: **Demographics summary of all xTMS study participants.** Includes mean and standard deviation for each variable.

4.4.2 rsMRI-derived target locations

As described in the **Methods**, individual resting state MRI scans were used to generate DLPFC target coordinates most anti-correlated with the sgACC. These coordinates, in both MNI and subject-specific space, are reported in Table 4.2 and the specific pipeline code is also added in the **Appendices**.

Participant number	MNI Coords			Subject Space Coords		
	x	y	z	x	y	z
1	-38.4	37.5	32.2	-33.9414	35.1125	50.2489
2	-37.7	37.8	30.4	-40.1313	38.2395	20.8079
3	-32.9	35.3	38.4	-32.6812	48.4551	37.1631
4	-47	38	30.7	-39.3859	38.6344	27.0172
5	-38.2	37	30.7	-35.1782	52.8751	48.1432
6	-38	46	27	-37.1345	59.0483	33.5884
7	-36.8	35.7	30.8	-39.7034	47.6495	37.3302
8	-40.1	37.7	27.8	-37.8941	37.761	25.1152
10	-38	37.6	31.7	-36.682	49.2227	45.3911
11	-37.6	36.6	30.9	-39.3209	45.3445	47.8675
12	-38.5	37.2	31.9	-43.2835	49.5932	32.6016
18	-36.8	37.1	30	-32.5188	37.1133	46.0706

Table 4.2: Individualised functional connectivity MRI-guided DLPFC target coordinates in MNI and Subject Space across participants.

For all participants, the coordinates were also visually confirmed to fall within the anatomical area of the DLPFC to ensure data integrity.

4.4.3 Single-session changes in negative bias after monophasic vs biphasic iTBS

Given the small sample size in this pilot study ($n = 11$), it is not surprising that paired-sample t -tests on these difference scores did not detect any significant differences in positive emotion recognition under monophasic vs biphasic stimulation relative to sham.

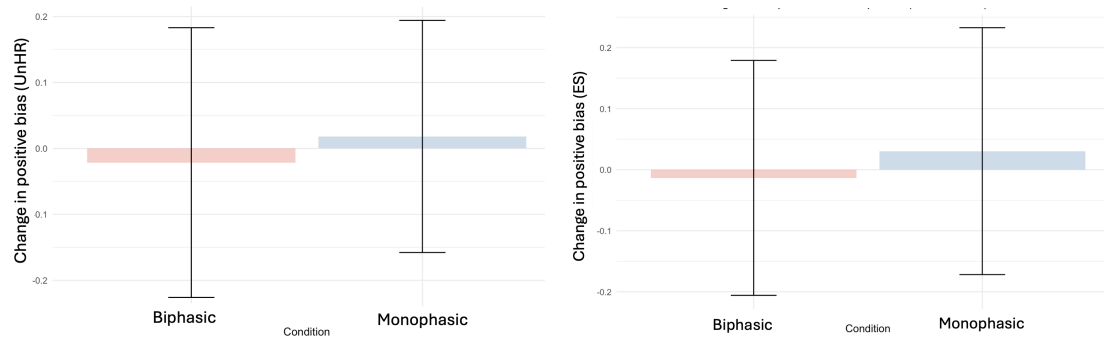


Figure 4.7: **Change in positive bias after a single iTBS stimulation session does not differ between monophasic and biphasic stimulation.** Standard bar graphs show the change in positive bias for accuracy (left) and efficiency (right) of recognising positive compared to negative emotions after biphasic and monophasic stimulation, with error bars representing ± 1 standard deviation. Paired t-tests indicate no significant differences in neither accuracy (UnHR) ($(t(10) = 0.612, p = 0.554)$, Cohen's $d = 0.184$) and efficiency (ES) ($(t(10) = 0.611, p = 0.555)$, Cohen's $d = 0.184$).

4.4.4 Single-session changes relative to sham stimulation

To further investigate, we tested the difference between biphasic sham and real biphasic, as well as monophasic sham and real monophasic stimulation sessions as shown in Fig. 4.8 as a way to approximate single-session emotional recognition differences from 'baseline'. No statistically significant differences were found. It is worth noting that the sham stimulation sessions are not a classic 'baseline' measure, as they still involve a patient in an engaged, placebo-like state, but they are the closest measure to relevant change we had access to in the context of this study.

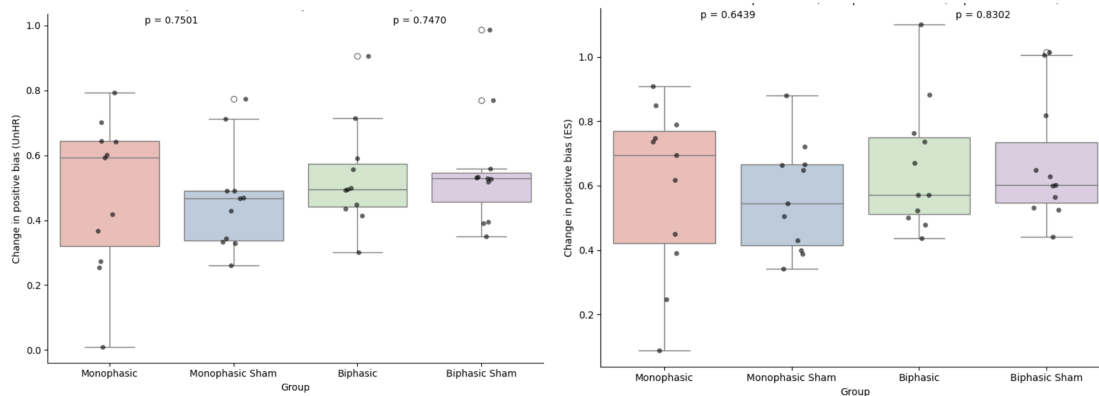
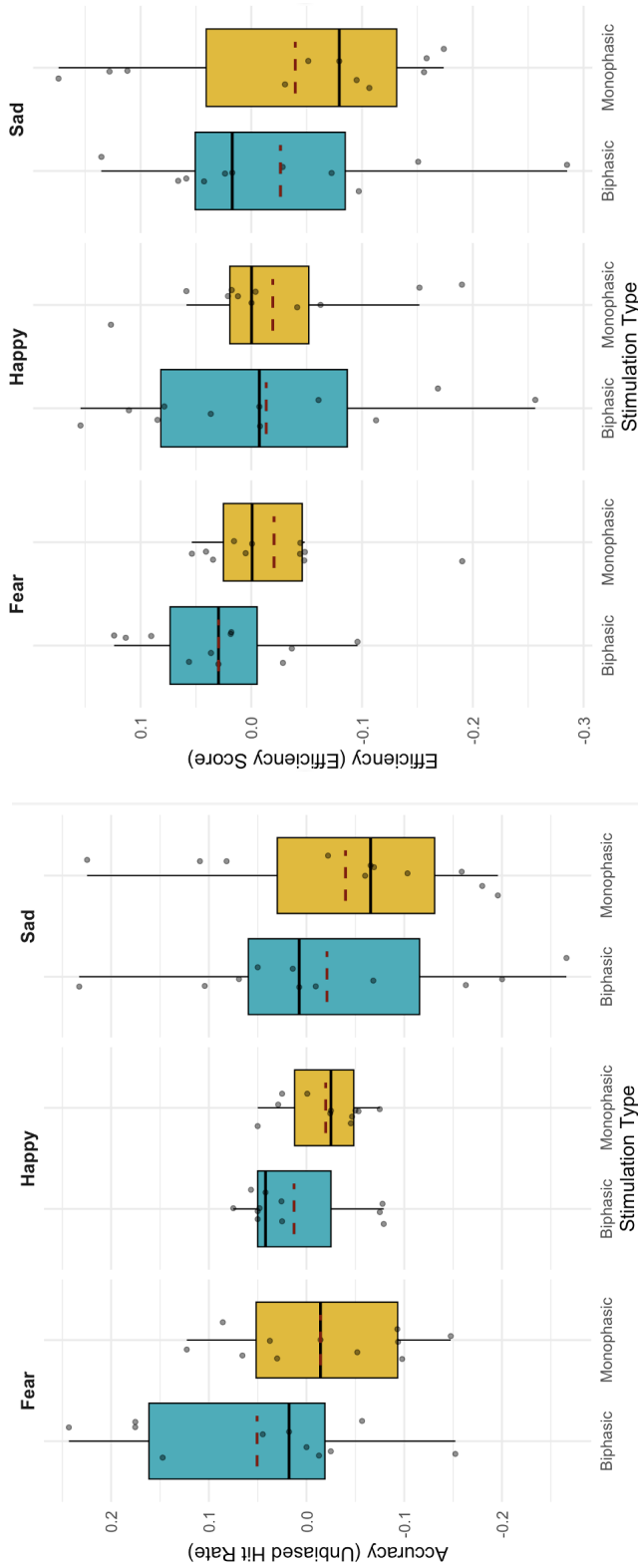


Figure 4.8: **No significant differences in change in positive bias between real and sham stimulation across monophasic and biphasic conditions.** Boxplots display the change in positive bias for accuracy (UnHR; left) and efficiency (ES; right) in recognising positive over negative emotions following monophasic and biphasic iTBS stimulation, compared with their respective sham conditions. Paired t-tests revealed no statistically significant differences between real and sham conditions for either waveform: Monophasic ($p = 0.7501$ for UnHR, $p = 0.6439$ for ES) and Biphasic ($p = 0.7470$ for UnHR, $p = 0.8302$ for ES).

4.4.5 Single-session changes in individual emotion recognition after monophasic vs biphasic iTBS

Further, we investigated whether despite the fact that there were no overarching differences in positive bias recognition, there were any significant differences in the recognition of specific emotions (fear, happy, sad) between monophasic and biphasic stimulation. As shown in Fig. ??, no differences were found. These three emotions in particular were tested given their implication in other studies focusing on low mood and depressive symptoms in clinical populations. A two-way repeated measures ANOVA showed no significant main effects for emotion or stimulation type on either accuracy, speed or efficiency scores.



(a) Accuracy for recognising emotions

(b) Efficiency for recognising emotions

Table 4.3: No difference in recognising key emotions between biphasic and monophasic stimulation. Standard box plots show the accuracy (left) and efficiency (right) for recognising fear, happy, and sad emotions after biphasic and monophasic stimulation. Each box represents the interquartile range (IQR), with the median shown by the solid black line and the mean shown by the dashed red line. Whiskers extend to 1.5 times the IQR, and individual data points are shown overlaid. A two-way repeated measures ANOVA was conducted to assess differences in emotion recognition across stimulation types. For accuracy, there were no significant main effects for emotion ($F(2, 20) = 0.823, p = 0.453, \text{ges} = 0.038$) or stimulation type ($F(1, 10) = 2.279, p = 0.162, \text{ges} = 0.037$), and no interaction effects ($F(2, 20) = 1.117, p = 0.347, \text{ges} = 0.009$). Similarly for efficiency, there were no significant main effects for emotion ($F(2, 20) = 0.714, p = 0.502, \text{ges} = 0.024$) or stimulation type ($F(1, 10) = 0.651, p = 0.438, \text{ges} = 0.014$), and no significant interaction effects ($F(2, 20) = 1.694, p = 0.209, \text{ges} = 0.010$).

4.4.6 Single-session changes in the recognition of ambiguous (50% intensity) emotions in monophasic vs biphasic iTBS

We then hypothesised that the changes may be much more subtle and need to be probed with more sensitive analytic approaches. Specifically, we hypothesised that if monophasic iTBS led to a shift in the psychometric curve of emotion recognition over increasing intensities, then there may be significant differences between emotion recognition at the most ambiguous, 50% intensity faces. However, the paired t-tests showed no significant differences in the efficiency for recognising ambiguous sad ($t(10) = -0.49, p = 0.64$), fearful ($t(10) = -1.79, p = 0.10$), or happy faces ($t(10) = -1.52, p = 0.16$) as shown in Fig. 4.9. These findings suggest that a single session of monophasic and biphasic iTBS does not appear to differentially impact the processing of subtle emotional cue recognition.

4.5 Discussion

4.5.1 Summary of findings

The pilot study presented in this chapter investigated the effects of a single session of monophasic and biphasic intermittent theta burst stimulation (iTBS) on emotion recognition in individuals with symptoms of major depressive disorder (MDD). Resting-state MRI scans were used to identify dorsolateral prefrontal cortex (DLPFC) targets that were maximally anti-correlated with the subgenual anterior cingulate cortex (sgACC), allowing for personalised stimulation targeting. Following a single session of stimulation, there were no statistically significant improvements in positive emotional bias between monophasic and biphasic iTBS. When comparing biphasic iTBS and monophasic iTBS to their respective sham conditions, no difference in single-session response was found. No significant effects were found for recognition of specific emotions or for recognition of

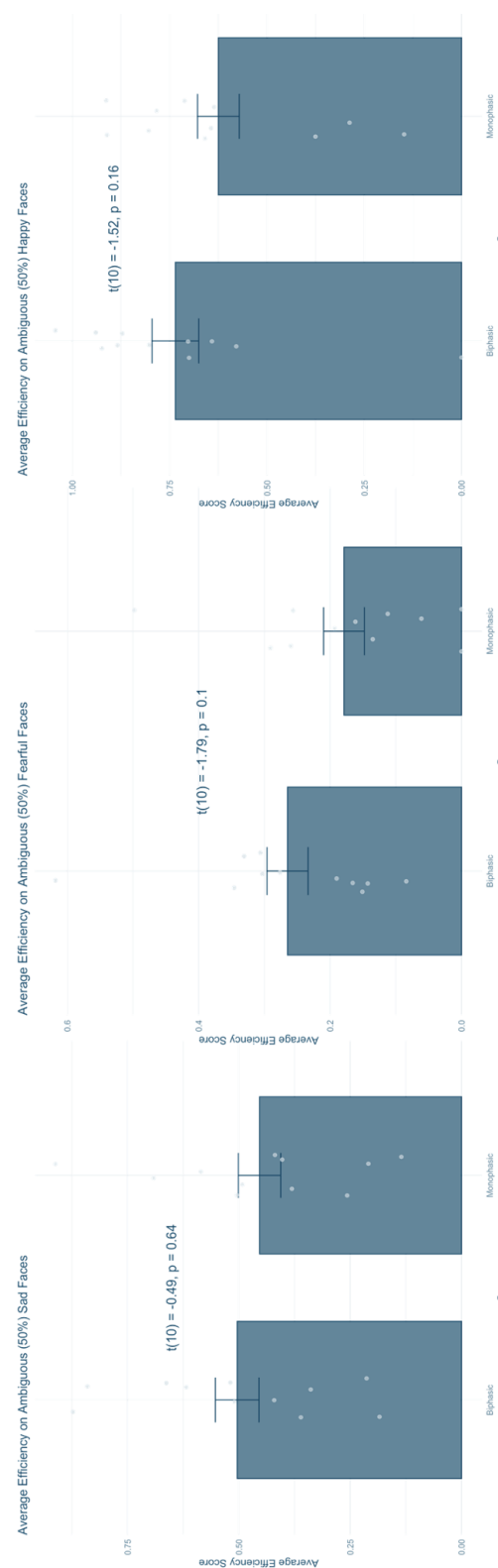


Figure 4.9: **No statistically significant shifts in ambiguous emotion recognition.** Standard bar plots show the average efficiency scores for recognising ambiguous (50%) sad, fearful, and happy faces after biphasic and monophasic stimulation. Each bar represents the mean efficiency score, with error bars showing ± 1 standard error of the mean. Individual data points are overlaid. Paired t-tests show no significant differences between biphasic and monophasic stimulation for ambiguous sad ($t(10) = -0.49, p = 0.64$), fearful ($t(10) = -1.79, p = 0.10$), or happy faces ($t(10) = -1.52, p = 0.16$).

ambiguous (50% intensity) emotional stimuli across either stimulation type. Given the limited sample size and wide range of responses, very brief intervention period, confounds relating to the use of sham stimulation as baseline, and the absence of significant findings highlight the need for larger studies to more robustly assess the effects of monophasic iTBS and determine their clinical relevance.

4.5.2 Interpretation of findings

The study's findings highlight the promise of optimising TMS protocols when administering clinical treatment. Specifically, the study focused on optimising multiple TMS parameters to best capture the effects, if any, of a single stimulation session, including personalised targeting using rsMRI scans, an iTBS rather than rTMS protocol, and individual pulses, with monophasic pulse shapes, hypothesised to be more efficient, and shown to be so in studies of the motor cortex. The differences in the DLPFC target coordinates across participants suggest that individual brain anatomy and connectivity need to be considered for optimising stimulation efficacy. The fact that no effects were found, and given the very small sample (n=11), points to the importance of running larger studies with potentially more sensitive study designs to further test the promise of monophasic iTBS as a potential treatment improvement for MDD patients, especially focusing on the mechanisms by which iTBS influences emotional processing, and whether longer or more targeted interventions are required to address subtle emotional cue processing.

4.5.3 Clinical relevance

As mentioned above, further larger (non-pilot) studies are needed to better understand the impact of monophasic vs biphasic pulse efficiency on clinically relevant cognitive measures. This pilot study provides early methodology and pilot data about the immediate cognitive responses to monophasic vs biphasic pulses, very early during the course of treatment of people with MDD symptomatology. To our knowledge, it is the first study

to investigate monophasic iTBS in the context of clinically relevant measures, such as negative bias in people with low mood. However, before broader clinical implications can be drawn, larger studies, cost-efficiency and feasibility will need to be evaluated to better inform the clinical direction of TMS treatment for MDD.

Specifically, shifting to using personalised targeting of the DLPFC based on rsMRI would require a significant upskilling of clinicians administering the vast majority of TMS treatment sessions, who are not usually trained in MRI data processing or analysis, as well as the development and accessibility (or commercialisation) of pipelines to ensure consistency across patients and clinical sites. This would be a significant change in state-of-the-art practice and would need to be carefully weighed against, and significantly more effective than, stimulation of standard DLPFC coordinates based on individual structural MRI scans, or the 5-cm rule, the challenges of which in real-world clinical practice have been discussed in **Chapter 3**.

If larger studies with clinical populations show that monophasic pulses are more efficient than biphasic pulses and lead to more effective treatment, or more rapid response to treatment, many TMS clinics would need to update their hardware to a new generation of TMS devices able to administer monophasic iTBS. Similarly to above, this would need to be carefully considered in the context of increased efficacy of treatment.

Chapter 3 highlighted the substantial inter-individual variability in treatment response to NIBS interventions. Within this chapter, we saw no effects following a single session of stimulation in a pilot sample with monophasic compared to biphasic stimulation, and there are still many unresolved questions when it comes to understanding the potential of optimising stimulation protocols and device parameters to enhance TMS efficacy for MDD. Given the exploratory nature and limited sample size of this study, these findings should be interpreted cautiously, and further research is necessary to determine whether such approaches can reliably improve treatment outcomes and broaden the accessibility of monophasic iTBS as a clinical tool in the future.

4.5.4 Limitations

4.5.4.1 Sources of error

Given that this is the first experimental study with monophasic iTBS pulses administered via the xTMS machine in clinical populations, we believe it is important to note the various sources of error that could be contributing to the observed -or missed- results.

Motor threshold measures

A common limitation in TMS research, particularly when establishing individualised stimulation intensities, arises from variability in motor threshold (RMT) measurements. The resting motor threshold (RMT), commonly used to calibrate stimulation intensity, is subject to several sources of error that can introduce inconsistencies both within and between participants. This variability can stem from several factors, including the precision of coil positioning, individual differences in cortical excitability, and muscle activation state. While not replicated in this thesis and prior work from our lab (Wendt et al., 2023), it has been long believed that factors such as time of day, participant fatigue, caffeine or other stimulant intake or other transient psychological states could alter the baseline excitability of motor cortex neurons, leading to changes in the MEP response to the same stimulation intensity. In order to account for some of that potential variability, all participants were asked to come to experimental sessions fully rested, with their sleep noted, and without having consumed caffeine in the last 2 hours, or any psychoactive substances (including nicotine) in the last 24 hours. However, fluctuations discussed here and beyond which are harder to account for, such as the participant's psychological state, continue to complicate the ability to reliably determine the true RMT.

In addition to inter-individual variability, shifts in coil positioning over the motor cortex may affect the reproducibility of RMT measurements. Small deviations in the angle or position of the coil, even by a few millimeters, can lead to significant changes in the induced electric field, resulting in differences in the observed MEPs. In order to minimise

this type of variability in this pilot study, we used neuronavigation systems (Brainsight), as well as two researchers observing the stimulation interface to note any deviations, but we recognise that intrinsic individual differences in head shape and coil angling, which cannot be fully captured by neuronavigation software could have left some variability unaccounted for.

Finally, individual differences in muscle activity and baseline tension in the target muscle (FDI) can also influence RMT measurements, which are based on MEP measures. Variability in resting muscle tone could either amplify or dampen the motor response, contributing to noise in the threshold measurement. In our study, we aimed to mitigate this by positioning participants comfortably and supporting their resting hands with a pillow, while ensuring that they could get used to a few pulses before starting MEP measurements but these factors were difficult to eliminate entirely.

Sham stimulation as a baseline

Another important consideration relates to the use of sham stimulation sessions as a baseline comparison. Although sham conditions are typically employed to control for placebo-like effects, it is critical to note that they do not represent a true 'resting' baseline. Participants remained engaged in the experimental environment during sham sessions and, despite the lack of active stimulation, may have experienced heightened agitation, expectancy effects, or cognitive fatigue from prior real stimulation sessions. Although a 1-hour rest period was included between stimulation sessions to minimise carry-over effects, it cannot be fully excluded that residual physiological or cognitive changes persisted, particularly given the novelty and intensity of TMS procedures in this clinical sample and some recent work showing that cognitive effects can be detected 60-70 minutes after active stimulation (Harrington et al., 2023), so this remains an important source of potential noise and could have contributed to variability in outcomes. Consequently, comparisons between real and sham conditions in this study should be interpreted cautiously, recognising that sham stimulation does not fully reset participants

to a pre-stimulation baseline state.

Stimulation location

Another limitation in TMS, discussed in more detail in the Introduction, is the precise identification and targeting of the stimulation site. Although in this pilot study we aimed to use the most advanced DLPFC targeting method, individually-derived DLPFC targets mapped onto the participant's own structural MRI scan, and stimulated with the use of neuronavigation systems, sources of error could have arisen at a couple of critical points.

The resting state MRI analysis pipeline, while as standardised as possible between participants, is still applied individually, which could lead to inter-individual variation. For example, smoothing, segmentation and registration steps, applied as part of the pipeline, could lead to different clustering of brain regions, which could impact the size and location of the final DLPFC target cluster. Additionally, we know that resting state MRIs are state-dependent, which could mean that the anti-correlation measures between the sgACC and the DLPFC on the day of the MRI scan may not be the most representative of the functional relationship on the days of experimental session. While we aimed to reduce this variability by scheduling MRI sessions at most a week prior to experimental sessions in order to reduce the time in between the rsMRI scan and iTBS, and applied the analysis pipeline consistently across participants, we recognise that this remains a potential source of error that could be mitigated in future studies by using standardised pipelines or integrated analysis tools.

It is also important to note that once subject-dependent target DLPFC coordinates are noted and used for neuronavigation on the participant in the real world, there is still actual registration of the participants anatomical landmarks to the structural MRI-based 3D model of their brain in the neuronavigation system. Given that the DLPFC coordinates are highly precise, even small errors when taking a single anatomical landmark (of which there are seven total) could lead to the neuronavigation system indicating perfect coil positioning, when in fact it may be up to 1 cm off-target due to cross-registration

errors. Again, this is an integral limitation and source of error when using neuronavigation systems with landmark sampling by [human] researchers, such as Brainsight. We attempted to account for this by having two researchers in all experimental sessions verify anatomical sampling, and not allowing larger than 0.1cm deviations between the 3D model and the participant (when impossible to get perfectly due to factors such as hair), but acknowledge that some variation here may remain.

Experimental task sensitivity

When choosing a cognitive measure to assess the impact of a single session of monophasic vs biphasic iTBS on participants with MDD symptomatology, we prioritised measures that we knew had implications on clinical outcomes in MDD, could be administered promptly after stimulation, and multiple times, and would be sensitive enough to pick up even slight changes in emotional cognition. This reasoning led to the choice of the FERT which, as discussed in the introduction, has been shown to sensitively capture changes after a single administration of antidepressant medication, appears to predict clinical outcomes in MDD, takes only 12-15 minutes to complete, and has been administered in pre-post studies in the past. Given that we did not have good models of similar studies being conducted with TMS and FERT, the FERT was also an appealing measure due to its multi-level structure, i.e. the ability to ask questions at the general emotional processing level, such as negative or positive bias, at the individual emotional processing level, such as the recognition of specific emotions, and at the subtle emotional processing level, such as the recognition of ambiguous emotions. Studies with the FERT, however, don't have a large literature basis in the field of TMS, and even less so in the context of MDD patients, which makes the results harder to interpret in the context of the broader literature. There is also a high likelihood that the signal we are trying to capture, that of cognitive changes after a single iTBS stimulation session, are incredibly small, and that the FERT may not be the most sensitive tool to capture that change, if any, potentially due to its ceiling effects with higher-intensity faces (Ramli et al., 2024), and alternative cognitive and emotional measures should be considered when designing

larger-scale studies.

4.5.5 Recommendations for future research

The findings of this pilot study propose several important considerations for future research in the application of monophasic and biphasic iTBS for individuals with MDD symptomatology.

4.5.5.1 Larger sample sizes

This pilot study was conducted with a very small sample size, composed primarily of young people with MDD symptoms, which limits the generalisability of the findings. Future studies should aim to recruit larger, clinically and demographically diverse samples to increase the statistical power and representativeness of the results. Larger studies would provide better insight into the effects of both monophasic and biphasic stimulation on mood-related cognitive biases, especially in patients with varying levels of symptom severity and length, and potentially allowing for explorations of differentiated effects, if any, in different subtypes of MDD. This would also allow for the investigation of potential moderators, such as age, gender, and treatment history, on TMS outcomes.

4.5.5.2 Different sub-populations

We explored the impact of novel iTBS on a low mood participant population, but as per our findings in **Chapter 2**, it may be worth investigating further the impact of monophasic vs biphasic iTBS in treatment free and/or drug-naive patients, and patients on antidepressant medication but with no response to treatment, as the usual population for whom TMS is prescribed is that of treatment-resistant MDD not responding to pharmacological treatment. This would help elucidate the single-session changes in the most representative clinical population.

4.5.5.3 Longitudinal designs

While this pilot study focused on the effects of a single stimulation session, future research should explore the clinical, as well as long-term effects of monophasic vs biphasic iTBS. A longitudinal design would help determine whether the improvements in emotional processing observed with monophasic stimulation are sustained over time, especially as standard TMS treatment for MDD lasts 6 weeks, and whether they correspond to clinical improvements in particular depressive symptoms, such as mood and anhedonia, and overall functioning, which are key outcomes in the treatment of MDD, and on what timescales, when compared to standard iTBS treatment.

4.5.5.4 Further investigation of stimulation parameters

This pilot study's results suggest that monophasic stimulation may be more effective than biphasic stimulation in improving emotional processing, but the mechanisms behind this remain unclear. Future studies should investigate and compare a broader range of iTBS parameters, such as pulse shape, stimulation frequency, intensity, and duration, to identify the optimal conditions for enhancing emotional processing in MDD.

4.5.5.5 Neural mechanisms of emotional processing changes

Similarly, although significant changes in emotional processing were observed with monophasic iTBS, the precise neural mechanisms driving these changes are not well understood. Future studies should incorporate neuroimaging techniques, such as fMRI or EEG, to monitor the neural correlates of emotion recognition and cognitive bias following stimulation. This would help understand the specific brain regions and networks modulated by monophasic iTBS and clarify whether changes in sgACC-DLPFC connectivity truly underlie the observed behavioural improvements.

4.5.5.6 Clinical applicability of personalised targeting

The use of individualised rsMRI-derived DLPFC targeting in this study represents a novel and promising approach, but it also poses practical challenges for routine clinical use. Future research should evaluate the clinical feasibility and usefulness of implementing personalised targeting in broader, real-world clinical settings. This would involve assessing the costs, time, and expertise required for rsMRI data collection and analysis, as well as comparing its effectiveness to traditional structural MRI-based targeting or other methods such as the 5-cm rule.

4.5.5.7 Alternative cognitive and emotional measures

While the FERT provided a useful measure for assessing emotion recognition in this pilot, future research should consider using alternative, or a wider range of cognitive and emotional assessments to capture different aspects of emotional processing. Tasks that measure implicit bias, attention to emotional stimuli, or emotion regulation abilities may offer additional insights into how iTBS affects mood-related cognition, though the magnitude and nature of the expected change remains to be understood. Considering cognitive tasks with greater sensitivity to subtle changes in a more diverse set of features underlying emotion recognition, particularly for single-session iTBS interventions, could help detect early cognitive shifts following stimulation that we were not able to detect, if they were present, in this study.

4.6 Conclusions and contributions

This pilot study aims to make several important contributions to the field of TMS research, particularly regarding the potential of monophasic and biphasic iTBS to impact emotional processing in individuals with MDD symptomatology.

One of the key findings of this study was that there was no significant improvement in positive bias observed after a single session of monophasic, but not biphasic, iTBS in

the pilot sample. The data from this sample and further analyses suggest that the interpretability of this finding for future use cases is limited, and further work is encouraged to test whether monophasic iTBS could enable better clinical outcomes with NIBS clinical interventions in the future.

Another contribution is that this pilot study is among the first wave of studies using a novel, personalised targeting approach with rsMRI-derived DLPFC coordinates to stimulate the brain more effectively based on individual brain connectivity patterns. This approach highlights the potential of personalised neuromodulation protocols to improve clinical outcomes, particularly those related to mood-related cognitive biases.

Finally, the study also noted important findings about the limitations and potential challenges of using a single-session iTBS intervention for altering emotional processing. While monophasic stimulation improved overall positive bias, neither monophasic nor biphasic iTBS led to significant changes in the recognition of individual emotions (e.g., fear, happy, sad) or ambiguous emotional cues. This suggests that a single session may not be sufficient to produce nuanced changes in emotion recognition, and highlights the need for more comprehensive, multi-session, clinical interventions with larger samples in future studies.

In conclusion, this pilot study provides some early investigations of the potential benefits of monophasic iTBS for improving positive emotional bias in individuals with MDD, emphasising the need for larger, more robust studies to build on these initial insights. By introducing personalised targeting using rsMRI and comparing monophasic to biphasic stimulation, this study aims to lay the groundwork for future investigations into more effective and tailored TMS protocols with innovative tools, such as the xTMS, as well as study protocol paradigms.

5.1 Summary

In this thesis, we set out to enhance the understanding of the mechanisms, clinical applications, and innovations in transcranial magnetic stimulation (TMS) for major depressive disorder (MDD), focused on three primary objectives: understanding how underlying brain activity differs across MDD patients, which may impact studies of TMS treatment efficacy and mechanisms of action, evaluating real-world application of TMS in clinical practice, and investigating potential improvements to TMS therapy through emerging technology and novel treatment protocols. We aim to provide actionable insights for advancing TMS as a treatment modality based on our understanding of different levels - both theoretical and practical - of bringing NIBS as a more accessible care modality for patients with MDD.

In **Chapter 2**, we established significant differences in resting-state functional connectivity (rsFC) between drug-naïve and drug-experienced MDD patients, specifically enhanced connectivity between the left mediodorsal thalamus and the default mode network (DMN) in drug-naïve individuals. These findings are in line with previous reports of the thalamus's central role in mediating the effects of antidepressant medication on brain networks, and align with theories of thalamocortical dysrhythmia, which propose altered thalamic connectivity as a hallmark of MDD. The lack of differences in rsFC between currently medicated and unmedicated patients highlights the nuanced and potentially long-lasting impact of medication exposure rather than acute pharmacological effects, which are worth considering as well.

The most important implication of this chapter is that it demonstrates the necessity of accounting for medication history in research and clinical practice. Failing to do so, especially for treatments that are rarely administered to drug-naïve individuals, such as NIBS, risks confounding results and potentially misguiding the development of person-

alised TMS protocols.

In **Chapter 3**, we focused on the real-world clinical application of TMS, showing the lack of significant relationships between RMTs, treatment timing and patient age on influencing clinical outcomes. Consistently with previous findings (Wendt et al., 2023), our work found high inter-clinic variability when it came to both standard physiological measurements (RMT) and data collection (fewer than 20% of clinics reported basic demographic and medical history data), which highlights inconsistencies in clinical practice that may undermine TMS efficacy shown in research settings if such data are not only not collected, but also not considered in clinical treatment plans.

The absence of significant effects based on treatment timing supports flexibility in treatment scheduling, potentially improving patient access without compromising outcomes. However, the observed demographic variability across clinics suggests that population-specific factors might influence results, warranting further exploration. Our early predictive analyses showed that early treatment responses had some but limited predictive power for ultimate outcomes, emphasising once more the complexity of MDD and the multifactorial nature of treatment response which needs to be accounted for. These findings show the critical need for standardised protocols, clinician training, and robust data collection in clinical settings. Furthermore, given that this study benefitted significantly from networked data collection across Horizon 3.0 machines deployed across the US, it further highlights the opportunity for the use of networked devices that allow for population-level quality control and protocol execution, to be considered in future, large-scale studies.

In **Chapter 4**, we showed the experimental results of a pilot study where we implemented all the best practices around TMS use - from personalised rsMRI-based DLPFC targeting to monophasic iTBS protocols. While we were not able to show significant effects after a single session within a small sample, the study contributes some early data that stimulation protocols based in scientifically-informed methodology and technical innovation (such as the xTMS) should be further investigated to even further improvements in TMS

efficacy and speed of action.

The use of personalised targeting based on rsMRI-derived DLPFC coordinates represents a significant methodological advancement. This approach ensures stimulation accuracy by accounting for individual variability in brain anatomy and connectivity, offering a promising direction for improving TMS outcomes. Nonetheless, its clinical implementation would require significant investment in infrastructure, training, and standardisation.

5.2 Clinical implications and future directions

This thesis advances understanding of TMS by considering mechanistic neuroimaging insights, real-world challenges, and innovative protocols. Key clinical implications include:

- The importance of accounting for medication history in designing and interpreting rsFC analyses.
- The need for standardised practices in RMT measurement and outcome reporting to enhance the reliability and generalisability of TMS research, as well as the opportunity to use networked devices to deploy standardised protocols at scale.
- The potential of monophasic iTBS as a more effective treatment modality, pending further validation in larger, longitudinal studies.

Future research should prioritise:

- Longitudinal studies investigating the sustained effects of monophasic vs. biphasic iTBS on clinical and cognitive outcomes. Such studies would allow researchers to determine whether there are any short-term effects of monophasic iTBS, which could not be detected, if present, in our small sample, and whether they translate into long-term benefits for MDD remission and functional recovery. This is crucial for understanding whether monophasic stimulation offers a meaningful advantage over standard protocols in real-world treatment settings.

- Incorporation of advanced predictive modelling techniques to identify robust markers and predictors of treatment response. These models could help tailor TMS protocols to individual patients, ideally without much expert support, which is often not available in standard clinical settings. This would advance the field toward precision psychiatry, reducing trial-and-error in clinical practice that costs MDD patients years of ill health when seeking effective treatment.
- Exploration of alternative stimulation parameters, such as frequency and intensity, to optimise iTBS efficacy. This line of research could help discover new ways to fine-tune stimulation protocols for specific patient populations, potentially improving outcomes for patients who do not respond to current standard protocols or who exhibit unique brain network dysfunctions.
- Evaluation of the feasibility and cost-effectiveness of implementing personalised targeting in clinical practice. Understanding the practical, educational and economic implications of advanced techniques, such as rsMRI-guided DLPFC targeting, is essential for translating these innovations into scalable, accessible treatments. If well understood, this could make personalised TMS a viable option for a broader patient population.

5.3 Concluding remarks

Our findings highlight some critical factors influencing TMS efficacy, such as the enduring effects of antidepressant medication on brain networks, the need for standardised clinical practices, and the eventual promise of monophasic iTBS for modulating mood-related cognitive processes.

The results of our work also emphasise the need for a continued focus on innovation, particularly in adopting emerging technologies and personalised targeting methods when addressing the challenge of the increasing burden of MDD on society. While challenges such as scalability, cost, and clinical training remain, the potential benefits of more precise

and effective TMS interventions for MDD patients are significant, especially as adoption of NIBS increases over the coming years.

Concluding, we hope this thesis serves as a foundation for future research and clinical advancements in TMS, with the ultimate goal of making this treatment modality not only more effective but also more accessible to the diverse populations who stand to benefit from it. By bridging the gaps between mechanistic insights, clinical practice, and emerging innovations, we aimed to contribute to the evolving landscape of MDD treatment and reinforce the value of TMS as a powerful tool in modern neuropsychiatry.

6 | Literature

1. Abdallah, C. G., De Feyter, H. M., Averill, L. A., Jiang, L., Averill, C. L., Chowdhury, G. M. I., Purohit, P., de Graaf, R. A., Esterlis, I., Juchem, C., Pittman, B. P., Krystal, J. H., Rothman, D. L., Sanacora, G., & Mason, G. F. (2018). The effects of ketamine on prefrontal glutamate neurotransmission in healthy and depressed subjects. *Neuropsychopharmacology: Official Publication of the American College of Neuropsychopharmacology*, 43(10), 2154-2160. <https://doi.org/10.1038/s41386-018-0136-3>
2. Abdallah, C. G., Dutta, A., Averill, C. L., McKie, S., Akiki, T. J., Averill, L. A., & Deakin, J. F. W. (2018). Ketamine, but Not the NMDAR Antagonist Lanicemine, Increases Prefrontal Global Connectivity in Depressed Patients. *Chronic Stress (Thousand Oaks, Calif.)*, 2, 2470547018796102. <https://doi.org/10.1177/2470547018796102>
3. Aberra, A. S., Wang, B., Grill, W. M., & Peterchev, A. V. (2020). Simulation of transcranial magnetic stimulation in head model with morphologically-realistic cortical neurons. *Brain Stimulation*, 13(1), 175-189. <https://doi.org/10.1016/j.brs.2019.10.002>
4. Alemi, F., Min, H., Yousefi, M., Becker, L. K., Hane, C. A., Nori, V. S., & Wojtusiak, J. (2021). Effectiveness of common antidepressants: A post market release study. *eClinicalMedicine*, 41. <https://doi.org/10.1016/j.eclinm.2021.101171>
5. Ali, K., Wendt, K., Sorkhabi, M. M., Benjaber, M., Denison, T., & Rogers, D. J. (2023). xTMS: A Pulse Generator for Exploring Transcranial Magnetic Stimulation Therapies. *Conference Proceedings. IEEE Applied Power Electronics Conference and Exposition, 2023*, 1875-1880. <https://doi.org/10.1109/APEC43580.2023.10131554>
6. Allaert, J., Sanchez-Lopez, A., Raedt, R. D., Baeken, C., & Vanderhasselt, M.-

- A. (2019). Inverse effects of tDCS over the left versus right DLPC on emotional processing: A pupillometry study. *PLOS ONE*, 14(6), e0218327. <https://doi.org/10.1371/journal.pone.0218327>
7. Ancelin, M.-L., Carrière, I., Artero, S., Maller, J., Meslin, C., Ritchie, K., Ryan, J., & Chaudieu, I. (2019). Lifetime major depression and grey-matter volume. *Journal of Psychiatry & Neuroscience: JPN*, 44(1), 45-53. <https://doi.org/10.1503/jpn.180026>
8. Anderson, I. M., Shippen, C., Juhasz, G., Chase, D., Thomas, E., Downey, D., Toth, Z. G., Lloyd-Williams, K., Elliott, R., & Deakin, J. F. W. (2011). State-dependent alteration in face emotion recognition in depression. *The British Journal of Psychiatry: The Journal of Mental Science*, 198(4), 302-308. <https://doi.org/10.1192/bjp.bp.110.078139>
9. Arai, N., Okabe, S., Furubayashi, T., Mochizuki, H., Iwata, N. K., Hanajima, R., Terao, Y., & Ugawa, Y. (2007). Differences in after-effect between monophasic and biphasic high-frequency rTMS of the human motor cortex. *Clinical Neurophysiology: Official Journal of the International Federation of Clinical Neurophysiology*, 118(10), 2227-2233. <https://doi.org/10.1016/j.clinph.2007.07.006>
10. Avari, J. N., Kanellopoulos, D., Solomonov, N., Oberlin, L., & Alexopoulos, G. S. (2020). Minocycline augmentation in older adults with persistent depression: An open label proof of concept study. *International Psychogeriatrics*, 32(7), 881-884.
11. Baghaei, N., Chitale, V., Hlasnik, A., Stemmet, L., Liang, H.-N., & Porter, R. (2021). Virtual Reality for Supporting the Treatment of Depression and Anxiety: Scoping Review. *JMIR Mental Health*, 8(9), e29681. <https://doi.org/10.2196/29681>
12. Basiru, T., Onyeaka, H., Oladunjoye, A. F., Acholonu, C., Egbeocha, S., Ogala, F., Enemuo, S., Okoronkwo, O. U., Annor, E., Holmes, K., Oloniyo, T., & Kritzer, M. D. (2024). Trend and geo-availability of somatic therapies for treatment resistant

- depression in the US. *Psychiatry Research Communications*, 4(1), 100157. <https://doi.org/10.1016/j.psycom.2024.100157>
13. Beam, W., Borckardt, J. J., Reeves, S. T., & George, M. S. (2009). An efficient and accurate new method for locating the F3 position for prefrontal TMS applications. *Brain Stimulation*, 2(1), 50â54. <https://doi.org/10.1016/j.brs.2008.09.006>
 14. Beard, C., Hsu, K. J., Rifkin, L. S., Busch, A. B., & BjÃ¶rgvinsson, T. (2016). Validation of the PHQ-9 in a psychiatric sample. *Journal of Affective Disorders*, 193, 267-273. <https://doi.org/10.1016/j.jad.2015.12.075>
 15. Beck, A. T. (2008). The evolution of the cognitive model of depression and its neurobiological correlates. *The American Journal of Psychiatry*, 165(8), 969-977. <https://doi.org/10.1176/appi.ajp.2008.08050721>
 16. Beck, A. T., & Alford, B. A. (2009). *Depression: Causes and Treatment* (2nd ed.). University of Pennsylvania Press. <https://www.jstor.org/stable/j.ctt6wr94x>
 17. Beckmann, C. F., Jenkinson, M., Woolrich, M. W., Behrens, T. E. J., Flitney, D. E., Devlin, J. T., & Smith, S. M. (2006). Applying FSL to the FIAC data: Model-based and model-free analysis of voice and sentence repetition priming. *Human Brain Mapping*, 27(5), 380-391. <https://doi.org/10.1002/hbm.20246>
 18. Benschop, L., Vanhollebeke, G., Li, J., Leahy, R. M., Vanderhasselt, M.-A., & Baeken, C. (2022a). Reduced subgenual cingulate-dorsolateral prefrontal connectivity as an electrophysiological marker for depression. *Scientific Reports*, 12(1), Article 1. <https://doi.org/10.1038/s41598-022-20274-9>
 19. Berboth, S., & Morawetz, C. (2021). Amygdala-prefrontal connectivity during emotion regulation: A meta-analysis of psychophysiological interactions. *Neuropsychologia*, 153, 107767. <https://doi.org/10.1016/j.neuropsychologia.2021.107767>

20. Berna, C., Lang, T. J., Goodwin, G. M., & Holmes, E. A. (2011). Developing a measure of interpretation bias for depressed mood: An ambiguous scenarios test. *Personality and Individual Differences*, 51(3), 349-354. <https://doi.org/10.1016/j.paid.2011.04.005>
21. Biswal, B., Yetkin, F. Z., Haughton, V. M., & Hyde, J. S. (1995). Functional connectivity in the motor cortex of resting human brain using echo-planar MRI. *Magnetic Resonance in Medicine*, 34(4), 537-541. <https://doi.org/10.1002/mrm.1910340409>
22. Bludau, S., Bzdok, D., Gruber, O., Kohn, N., Riedl, V., Sorg, C., Palomero-Gallagher, N., MÃ¼ller, V. I., Hoffstaedter, F., Amunts, K., & Eickhoff, S. B. (2016). Medial prefrontal aberrations in major depressive disorder revealed by cytoarchitecturally informed voxel-based morphometry. *The American Journal of Psychiatry*, 173(3), 291-298. <https://doi.org/10.1176/appi.ajp.2015.15030349>
23. Blumberger, D. M., Vila-Rodriguez, F., Thorpe, K. E., Feffer, K., Noda, Y., Giacobbe, P., Knyahnytska, Y., Kennedy, S. H., Lam, R. W., Daskalakis, Z. J., & Downar, J. (2018). Effectiveness of theta burst versus high-frequency repetitive transcranial magnetic stimulation in patients with depression (THREE-D): A randomised non-inferiority trial. *Lancet (London, England)*, 391(10131), 1683-1692. [https://doi.org/10.1016/S0140-6736\(18\)30295-2](https://doi.org/10.1016/S0140-6736(18)30295-2)
24. Bone, J. K., Lewis, G., Button, K. S., Duffy, L., Harmer, C. J., Munafo, M. R., Penton-Voak, I. S., Wiles, N. J., & Lewis, G. (2019). Variation in recognition of happy and sad facial expressions and self-reported depressive symptom severity: A prospective cohort study. *Journal of Affective Disorders*, 257, 461-469. <https://doi.org/10.1016/j.jad.2019.06.025>
25. Brennan, S., McLoughlin, D. M., OâConnell, R., Bogue, J., OâConnor, S., McHugh, C., & Glennon, M. (2017). Anodal transcranial direct current stimulation of the

- left dorsolateral prefrontal cortex enhances emotion recognition in depressed patients and controls. *Journal of Clinical and Experimental Neuropsychology*, 39(4), 384-395. <https://doi.org/10.1080/13803395.2016.1230595>
26. Brunoni, A. R., Chaimani, A., Moffa, A. H., Razza, L. B., Gattaz, W. F., Daskalakis, Z. J., & Carvalho, A. F. (2017). Repetitive Transcranial Magnetic Stimulation for the Acute Treatment of Major Depressive Episodes: A Systematic Review With Network Meta-analysis. *JAMA Psychiatry*, 74(2), 143-152. <https://doi.org/10.1001/jamapsychiatry.2016.3644>
27. Brunoni, A. R., Sampaio-Junior, B., Moffa, A. H., Aparício, L. V., Gordon, P., Klein, I., Rios, R. M., Razza, L. B., Loo, C., Padberg, F., & Valiengo, L. (2018). Noninvasive brain stimulation in psychiatric disorders: A primer. *Revista Brasileira de Psiquiatria*, 41(1), 70-81. <https://doi.org/10.1590/1516-4446-2017-0018>
28. Buckman, J. E. J., Underwood, A., Clarke, K., Saunders, R., Hollon, S. D., Fearon, P., & Pilling, S. (2018). Risk factors for relapse and recurrence of depression in adults and how they operate: A four-phase systematic review and meta-synthesis. *Clinical Psychology Review*, 64, 13-38. <https://doi.org/10.1016/j.cpr.2018.07.005>
29. Bueno-Notivol, J., Gracia-García, P., Olaya, B., Lasheras, I., Lopez-Anton, R., & Santabarbara, J. (2021). Prevalence of depression during the COVID-19 outbreak: A meta-analysis of community-based studies. *International Journal of Clinical and Health Psychology*, 21(1), 100196. <https://doi.org/10.1016/j.ijchp.2020.07.007>
30. Capitaó, L. P., Chapman, R., Filippini, N., Wright, L., Murphy, S. E., James, A., Cowen, P. J., & Harmer, C. J. (2020). Neural effects of a single dose of fluoxetine on resting-state functional connectivity in adolescent depression. *Journal of Psychopharmacology (Oxford, England)*, 34(12), 1461-1465. <https://doi.org/10.1177/0269881120959608>

31. Cappon, D., den Boer, T., Jordan, C., Yu, W., Metzger, E., & Pascual-Leone, A. (2022). Transcranial magnetic stimulation (TMS) for geriatric depression. *Ageing Research Reviews*, 74, 101531. <https://doi.org/10.1016/j.arr.2021.101531>
32. Chakrabarty, T., Hadjipavlou, G., & Lam, R. W. (2016). Cognitive Dysfunction in Major Depressive Disorder: Assessment, Impact, and Management. *Focus: Journal of Life Long Learning in Psychiatry*, 14(2), 194-206. <https://doi.org/10.1176/appi.focus.20150043>
33. Chang, C.-C., Yu, S.-C., McQuoid, D. R., Messer, D. F., Taylor, W. D., Singh, K., Boyd, B. D., Krishnan, K. R. R., MacFall, J. R., Steffens, D. C., & Payne, M. E. (2011). Reduction of dorsolateral prefrontal cortex gray matter in late-life depression. *Psychiatry Research*, 193(1), 1-6. <https://doi.org/10.1016/j.psychresns.2011.01.003>
34. Chen, Z., Xu, T., Li, Q., Shu, Y., Zhou, X., Guo, T., & Liang, F. (2024). Grey matter abnormalities in major depressive disorder patients with suicide attempts: A systematic review of age-specific differences. *Heliyon*, 10(3), e24894. <https://doi.org/10.1016/j.heliyon.2024.e24894>
35. Chibaatar, E., Watanabe, K., Okamoto, N., Orkhonselenge, N., Natsuyama, T., Hayakawa, G., Ikenouchi, A., Kakeda, S., & Yoshimura, R. (2023). Volumetric assessment of individual thalamic nuclei in patients with drug-naïve, first-episode major depressive disorder. *Frontiers in Psychiatry*, 14, 1151551. <https://doi.org/10.3389/fpsy.2023.1151551>
36. Cho, S.-E., Kim, N., Na, K.-S., Kang, C.-K., & Kang, S.-G. (2021). Thalamo-Habenular Connection Differences Between Patients With Major Depressive Disorder and Normal Controls. *Frontiers in Psychiatry*, 12. <https://doi.org/10.3389/fpsy.2021.699416>
37. Choi, K. W., Han, K.-M., Kim, H., Kim, A., Kang, W., Kang, Y., Tae, W.-S., & Ham, B.-J. (2020). Comparison of shape alterations of the thalamus and caudate

- nucleus between drug-naïve major depressive disorder patients and healthy controls. *Journal of Affective Disorders*, 264, 279-285. <https://doi.org/10.1016/j.jad.2020.01.011>
38. Chu, A., & Wadhwa, R. (2023). Selective Serotonin Reuptake Inhibitors. In *StatPearls*. StatPearls Publishing. <http://www.ncbi.nlm.nih.gov/books/NBK554406/>
39. Cole, E. J., Phillips, A. L., Bentzley, B. S., Stimpson, K. H., Nejad, R., Barmak, F., Veerapal, C., Khan, N., Cherian, K., Felber, E., Brown, R., Choi, E., King, S., Pankow, H., Bishop, J. H., Azeez, A., Coetzee, J., Rapier, R., Odenwald, N., & Williams, N. R. (2022). Stanford Neuromodulation Therapy (SNT): A Double-Blind Randomized Controlled Trial. *The American Journal of Psychiatry*, 179(2), 132-141. <https://doi.org/10.1176/appi.ajp.2021.20101429>
40. Connolly, C. G., Wu, J., Ho, T. C., Hoeft, F., Wolkowitz, O., Eisendrath, S., Frank, G., Hendren, R., Max, J. E., Paulus, M. P., Tapert, S. F., Banerjee, D., Simmons, A. N., & Yang, T. T. (2013). Resting-state functional connectivity of subgenual anterior cingulate cortex in depressed adolescents. *Biological Psychiatry*, 74(12), 898-907. <https://doi.org/10.1016/j.biopsych.2013.05.036>
41. Cotovio, G., Oliveira-Maia, A. J., Paul, C., Faro Viana, F., Rodrigues da Silva, D., Seybert, C., Stern, A. P., Pascual-Leone, A., & Press, D. Z. (2021). Day-to-day variability in motor threshold during rTMS treatment for depression: Clinical implications. *Brain Stimulation*, 14(5), 1118-1125. <https://doi.org/10.1016/j.brs.2021.07.013>
42. Croarkin, P. E., & MacMaster, F. P. (2019). Transcranial Magnetic Stimulation for Adolescent Depression. *Child and Adolescent Psychiatric Clinics of North America*, 28(1), 33-43. <https://doi.org/10.1016/j.chc.2018.07.003>
43. Cui, J., Wang, Y., Liu, R., Chen, X., Zhang, Z., Feng, Y., Zhou, J., Zhou, Y., & Wang, G. (2021). Effects of escitalopram therapy on resting-state functional connectivity of subsystems of the default mode network in unmedicated patients

- with major depressive disorder. *Translational Psychiatry*, 11, 634. <https://doi.org/10.1038/s41398-021-01754-4>
44. Dalili, M. N., Penton-Voak, I. S., Harmer, C. J., & Munafo, M. R. (2015). Meta-analysis of emotion recognition deficits in major depressive disorder. *Psychological Medicine*, 45(6), 1135-1144. <https://doi.org/10.1017/S0033291714002591>
45. Dannhauer, M., Gomez, L. J., Robins, P. L., Wang, D., Hasan, N. I., Thielscher, A., Siebner, H. R., Fan, Y., & Deng, Z.-D. (2023). Electric field modeling in personalizing TMS interventions. *Biological Psychiatry*. <https://doi.org/10.1016/j.biopsych.2023.11.022>
46. Dhuna, A., Gates, J., & Pascual-Leone, A. (1991). Transcranial magnetic stimulation in patients with epilepsy. *Neurology*, 41(7), 1067-1071. <https://doi.org/10.1212/wnl.41.7.1067>
47. Diagnostic and Statistical Manual of Mental Disorders. (2015). *American Psychiatric Association*. <https://dsm.psychiatryonline.org/doi/book/10.1176/appi.books.9780890425596>
48. Diamond, D. M., Dunwiddie, T. V., & Rose, G. M. (1988). Characteristics of hippocampal primed burst potentiation in vitro and in the awake rat. *Journal of Neuroscience*, 8(11), 4079-4088. <https://doi.org/10.1523/JNEUROSCI.08-11-04079.1988>
49. Dichter, G. S., Gibbs, D., & Smoski, M. J. (2015). A Systematic Review of Relations between Resting-State functional-MRI and Treatment Response in Major Depressive Disorder. *Journal of Affective Disorders*, 172, 8-17. <https://doi.org/10.1016/j.jad.2014.09.028>
50. Disner, S. G., Beevers, C. G., Haigh, E. A. P., & Beck, A. T. (2011). Neural mechanisms of the cognitive model of depression. *Nature Reviews Neuroscience*, 12(8), Article 8. <https://doi.org/10.1038/nrn3027>

51. Drysdale, A. T., Grosenick, L., Downar, J., Dunlop, K., Mansouri, F., Meng, Y., Fetcho, R. N., Zebley, B., Oathes, D. J., Etkin, A., Schatzberg, A. F., Sudheimer, K., Keller, J., Mayberg, H. S., Gunning, F. M., Alexopoulos, G. S., Fox, M. D., Pascual-Leone, A., Voss, H. U., & Liston, C. (2017). Resting-state connectivity biomarkers define neurophysiological subtypes of depression. *Nature Medicine*, 23(1), 28-38. <https://doi.org/10.1038/nm.4246>
52. Dumitru, A., Rocchi, L., Saini, F., Rothwell, J. C., Roiser, J. P., David, A. S., Richieri, R. M., Lewis, G., & Lewis, G. (2020). Influence of theta-burst transcranial magnetic stimulation over the dorsolateral prefrontal cortex on emotion processing in healthy volunteers. *Cognitive, Affective, & Behavioral Neuroscience*, 20(6), 1278-1293. <https://doi.org/10.3758/s13415-020-00834-0>
53. Dunlop, B. W., Cha, J., Choi, K. S., Rajendra, J. K., Nemeroff, C. B., Craighead, W. E., & Mayberg, H. S. (2023). Shared and Unique Changes in Brain Connectivity Among Depressed Patients After Remission With Pharmacotherapy Versus Psychotherapy. *The American Journal of Psychiatry*, 180(3), 218-229. <https://doi.org/10.1176/appi.ajp.21070727>
54. Ekstrom, A. (2009). How and when the fMRI BOLD signal relates to underlying neural activity: The danger in dissociation. *Brain Research Reviews*, 62(2), 233. <https://doi.org/10.1016/j.brainresrev.2009.12.004>
55. Everaert, J., Podina, I. R., & Koster, E. H. W. (2017). A comprehensive meta-analysis of interpretation biases in depression. *Clinical Psychology Review*, 58, 33-48. <https://doi.org/10.1016/j.cpr.2017.09.005>
56. Ferguson, B. R., & Gao, W.-J. (2015). Development of thalamocortical connections between the mediodorsal thalamus and the prefrontal cortex and its implication in cognition. *Frontiers in Human Neuroscience*, 8, 1027. <https://doi.org/10.3389/fnhum.2014.01027>

57. Fitzgerald, P. B. (2021). Targeting repetitive transcranial magnetic stimulation in depression: Do we really know what we are stimulating and how best to do it? *Brain Stimulation*, 14(3), 730-736. <https://doi.org/10.1016/j.brs.2021.04.018>
58. Fitzgerald, P. B., Hoy, K., McQueen, S., Maller, J. J., Herring, S., Segrave, R., Bailey, M., Been, G., Kulkarni, J., & Daskalakis, Z. J. (2009). A randomized trial of rTMS targeted with MRI based neuro-navigation in treatment-resistant depression. *Neuropsychopharmacology: Official Publication of the American College of Neuropsychopharmacology*, 34(5), 1255-1262. <https://doi.org/10.1038/npp.2008.233>
59. Fox, M. D., & Raichle, M. E. (2007). Spontaneous fluctuations in brain activity observed with functional magnetic resonance imaging. *Nature Reviews Neuroscience*, 8(9), 700-711. <https://doi.org/10.1038/nrn2201>
60. Gaffrey, M. S., Luby, J. L., Repovš, G., Belden, A. C., Botteron, K. N., Luking, K. R., & Barch, D. M. (2010). Subgenual cingulate connectivity in children with a history of preschool-depression. *Neuroreport*, 21(18), 1182-1188. <https://doi.org/10.1097/WNR.0b013e32834127eb>
61. Gautam, M., Tripathi, A., Deshmukh, D., & Gaur, M. (2020). Cognitive Behavioral Therapy for Depression. *Indian Journal of Psychiatry*, 62(Suppl 2), S223-S229. https://doi.org/10.4103/psychiatry.IndianJPsychiatry_772_19
62. Gaynes, B. N., Lux, L., Gartlehner, G., Asher, G., Forman-Hoffman, V., Green, J., Boland, E., Weber, R. P., Randolph, C., Bann, C., Coker-Schwimmer, E., Viswanathan, M., & Lohr, K. N. (2020). Defining treatment-resistant depression. *Depression and Anxiety*, 37(2), 134-145. <https://doi.org/10.1002/da.22968>
63. Gerlach, A. R., Karim, H. T., Pecina, M., Ajilore, O., Taylor, W. D., Butters, M. A., & Andreescu, C. (2022). MRI predictors of pharmacotherapy response in

- major depressive disorder. *NeuroImage: Clinical*, 36, 103157. <https://doi.org/10.1016/j.nicl.2022.103157>
64. Godlewska, B. R., Browning, M., Norbury, R., Cowen, P. J., & Harmer, C. J. (2016). Early changes in emotional processing as a marker of clinical response to SSRI treatment in depression. *Translational Psychiatry*, 6(11), e957. <https://doi.org/10.1038/tp.2016.130>
65. Godlewska, B. R., & Harmer, C. J. (2021). Cognitive neuropsychological theory of antidepressant action: A modern-day approach to depression and its treatment. *Psychopharmacology*, 238(5), 1265-1278. <https://doi.org/10.1007/s00213-019-05448-0>
66. Golyszny, M., & Obuchowicz, E. (2019). Are neuropeptides relevant for the mechanism of action of SSRIs? *Neuropeptides*, 75, 1-17. <https://doi.org/10.1016/j.npep.2019.02.002>
67. Goodwin, G. M., Aaronson, S. T., Alvarez, O., Arden, P. C., Baker, A., Bennett, J. C., Bird, C., Blom, R. E., Brennan, C., Bruschi, D., Burke, L., Campbell-Coker, K., Carhart-Harris, R., Cattell, J., Daniel, A., DeBattista, C., Dunlop, B. W., Eisen, K., Feifel, D., & Malievskaia, E. (2022). Single-Dose Psilocybin for a Treatment-Resistant Episode of Major Depression. *New England Journal of Medicine*, 387(18), 1637-1648. <https://doi.org/10.1056/NEJMoa2206443>
68. Greenberg, P., Chitnis, A., Louie, D., Suthoff, E., Chen, S.-Y., Maitland, J., Gagnon-Sanschagrin, P., Fournier, A.-A., & Kessler, R. C. (2023). The Economic Burden of Adults with Major Depressive Disorder in the United States (2019). *Advances in Therapy*, 40(10), 4460-4479. <https://doi.org/10.1007/s12325-023-02622-x>
69. Greicius, M. D., Krasnow, B., Reiss, A. L., & Menon, V. (2003). Functional connectivity in the resting brain: A network analysis of the default mode hypothesis. *Proceedings of the National Academy of Sciences of the United States of America*, 100(1), 253-258. <https://doi.org/10.1073/pnas.0135058100>

70. Grieve, S. M., Korgaonkar, M. S., Koslow, S. H., Gordon, E., & Williams, L. M. (2013). Widespread reductions in gray matter volume in depression. *NeuroImage: Clinical*, 3, 332-339. <https://doi.org/10.1016/j.nicl.2013.08.016>
71. Gudayol-Ferre, E., Pero-Cebollero, M., Gonzalez-Garrido, A. A., & Guardia-Olmos, J. (2015). Changes in brain connectivity related to the treatment of depression measured through fMRI: A systematic review. *Frontiers in Human Neuroscience*, 9, 582. <https://doi.org/10.3389/fnhum.2015.00582>
72. Gury, C., Cousin, F. (1999). [Pharmacokinetics of SSRI antidepressants: Half-life and clinical applicability]. *L'Encephale*, 25(5), 470-476.
73. Hack, L. M., Tozzi, L., Zenteno, S., Olmsted, A. M., Hilton, R., Jubeir, J., Korgaonkar, M. S., Schatzberg, A. F., Yesavage, J. A., O'Hara, R., & Williams, L. M. (2023). A Cognitive Biotype of Depression and Symptoms, Behavior Measures, Neural Circuits, and Differential Treatment Outcomes. *JAMA Network Open*, 6(6), e2318411. <https://doi.org/10.1001/jamanetworkopen.2023.18411>
74. Hallett, M. (2007). Transcranial magnetic stimulation: A primer. *Neuron*, 55(2), 187-199. <https://doi.org/10.1016/j.neuron.2007.06.026>
75. Hamilton, J. P., Farmer, M., Fogelman, P., & Gotlib, I. H. (2015). Depressive Rumination, the Default-Mode Network, and the Dark Matter of Clinical Neuroscience. *Biological Psychiatry*, 78(4), 224-230. <https://doi.org/10.1016/j.biopsych.2015.02.020>
76. Harmer, C. J., Bhagwagar, Z., Perrett, D. I., Völlm, B. A., Cowen, P. J., & Goodwin, G. M. (2003). Acute SSRI Administration Affects the Processing of Social Cues in Healthy Volunteers. *Neuropsychopharmacology*, 28(1), Article 1. <https://doi.org/10.1038/sj.npp.1300004>
77. Harmer, C. J., & Browning, M. (2022). Emotional cognition in depression: Is it relevant for Clinical practice? *European Neuropsychopharmacology*, 56, 1-3. <https://doi.org/10.1016/j.euroneuro.2021.11.004>

78. Harmer, C. J., Duman, R. S., & Cowen, P. J. (2017). How do antidepressants work? New perspectives for refining future treatment approaches. *The Lancet. Psychiatry*, 4(5), 409-418. [https://doi.org/10.1016/S2215-0366\(17\)30015-9](https://doi.org/10.1016/S2215-0366(17)30015-9)
79. Harmer, C. J., Hill, S. A., Taylor, M. J., Cowen, P. J., & Goodwin, G. M. (2003). Toward a Neuropsychological Theory of Antidepressant Drug Action: Increase in Positive Emotional Bias After Potentiation of Norepinephrine Activity. *American Journal of Psychiatry*, 160(5), 990-992. <https://doi.org/10.1176/appi.ajp.160.5.990>
80. Harmer, C. J., O'Sullivan, U., Favaron, E., Massey-Chase, R., Ayres, R., Reinecke, A., Goodwin, G. M., & Cowen, P. J. (2009). Effect of Acute Antidepressant Administration on Negative Affective Bias in Depressed Patients. *American Journal of Psychiatry*, 166(10), 1178-1184. <https://doi.org/10.1176/appi.ajp.2009.09020149>
81. Harmer, C. J., Shelley, N. C., Cowen, P. J., & Goodwin, G. M. (2004). Increased positive versus negative affective perception and memory in healthy volunteers following selective serotonin and norepinephrine reuptake inhibition. *The American Journal of Psychiatry*, 161(7), 1256-1263. <https://doi.org/10.1176/appi.ajp.161.7.1256>
82. Harrington, R. M., Krishnamurthy, L. C., Ossowski, A., Jeter, M., Davis, A., Bledniak, E., Ware, A. L., Morris, R., & Arrington, C. N. (2023). Preliminary evidence of prolonged timing effects of theta-burst stimulation in the reading system. *Frontiers in Human Neuroscience*, 17, 1227194. <https://doi.org/10.3389/fnhum.2023.1227194>
83. Hernandez, R. V., Navarro, M. M., Rodriguez, W. A., Martinez, J. L., & LeBaron, R. G. (2005). Differences in the magnitude of long-term potentiation produced by theta burst and high frequency stimulation protocols matched in stimulus number. *Brain Research. Brain Research Protocols*, 15(1), 6-13. <https://doi.org/10.1016/j.brainresprot.2005.01.001>

[1016/j.brainresprot.2005.02.003](https://doi.org/10.1016/j.brainresprot.2005.02.003)

84. Hsu, C.-W., Chou, P.-H., Brunoni, A. R., Hung, K.-C., Tseng, P.-T., Liang, C.-S., Carvalho, A. F., Vieta, E., Tu, Y.-K., Lin, P.-Y., Chu, C.-S., Hsu, T.-W., Chen, Y.-C. B., & Li, C.-T. (2024). Comparing different non-invasive brain stimulation interventions for bipolar depression treatment: A network meta-analysis of randomized controlled trials. *Neuroscience & Biobehavioral Reviews*, 156, 105483. <https://doi.org/10.1016/j.neubiorev.2023.105483>
85. Ilmoniemi, R. J., Deng, Z.-D., Gomez, L., Koponen, L. M., Nieminen, J. O., Peterchev, A. V., & Epstein, C. M. (2024). Transcranial magnetic stimulation coils. In E. M. Wassermann, A. V. Peterchev, U. Ziemann, S. H. Lisanby, H. R. Siebner, & V. Walsh (Eds.), *The Oxford Handbook of Transcranial Stimulation: Second Edition* (p. 0). Oxford University Press. <https://doi.org/10.1093/oxfordhb/9780198832256.013.4>
86. Imbert, L., Moirand, R., Bediou, B., Koenig, O., Chesnoy, G., Fakra, E., & Brunelin, J. (2022). A Single Session of Bifrontal tDCS Can Improve Facial Emotion Recognition in Major Depressive Disorder: An Exploratory Pilot Study. *Biomedicines*, 10(10), 2397. <https://doi.org/10.3390/biomedicines10102397>
87. Ionescu, D. F., Rosenbaum, J. F., & Alpert, J. E. (2015). Pharmacological approaches to the challenge of treatment-resistant depression. *Dialogues in Clinical Neuroscience*, 17(2), 111-126. <https://doi.org/10.31887/DCNS.2015.17.2/dionescu>
88. Jain, F. A., Chernyak, S. V., Nickerson, L. D., Morgan, S., Schafer, R., Mischoulon, D., Bernard-Negron, R., Nyer, M., Cusin, C., Ramirez Gomez, L., & Yeung, A. (2022). Four-Week Mentalizing Imagery Therapy for Family Dementia Caregivers: A Randomized Controlled Trial with Neural Circuit Changes. *Psychotherapy and Psychosomatics*, 91(3), 180-189. <https://doi.org/10.1159/000521950>

89. Jenkinson, M., Beckmann, C. F., Behrens, T. E. J., Woolrich, M. W., & Smith, S. M. (2012). FSL. *NeuroImage*, 62(2), 782-790. <https://doi.org/10.1016/j.neuroimage.2011.09.015>
90. Kaminski, J. A., Korb, F. M., Villringer, A., & Ott, D. V. M. (2011). Transcranial Magnetic Stimulation Intensities in Cognitive Paradigms. *PLoS ONE*, 6(9), e24836. <https://doi.org/10.1371/journal.pone.0024836>
91. Karabanov, A. N., Raffin, E., & Siebner, H. R. (2015). The Resting Motor Threshold - Restless or Resting? A Repeated Threshold Hunting Technique to Track Dynamic Changes in Resting Motor Threshold. *Brain Stimulation*, 8(6), 1191-1194. <https://doi.org/10.1016/j.brs.2015.07.001>
92. Ketter, T. A., George, M. S., Kimbrell, T. A., Benson, B. E., & Post, R. M. (1996). Functional Brain Imaging, Limbic Function, and Affective Disorders. *The Neuroscientist*, 2(1), 55-65. <https://doi.org/10.1177/107385849600200113>
93. Kim, H.-Y., Lee, H.-J., Jhon, M., Kim, J.-W., Kang, H.-J., Lee, J.-Y., Kim, S.-W., Shin, I.-S., & Kim, J.-M. (2021). Predictors of Remission in Acute and Continuation Treatment of Depressive Disorders. *Clinical Psychopharmacology and Neuroscience*, 19(3), 490-497. <https://doi.org/10.9758/cpn.2021.19.3.490>
94. Kim, M., Lee, T. H., Park, H., Moon, S.-Y., Lho, S. K., & Kwon, J. S. (2022). Thalamocortical dysrhythmia in patients with schizophrenia spectrum disorder and individuals at clinical high risk for psychosis. *Neuropsychopharmacology*, 47(3), 673-680. <https://doi.org/10.1038/s41386-021-01180-6>
95. Koponen, L. M., & Peterchev, A. V. (2022). Preventing misestimation of transcranial magnetic stimulation motor threshold with MTAT 2.0. *Brain Stimulation*, 15(5), 1073-1076. <https://doi.org/10.1016/j.brs.2022.07.057>
96. Krause, F. C., Linardatos, E., Fresco, D. M., & Moore, M. T. (2021). Facial emotion recognition in major depressive disorder: A meta-analytic review. *Journal*

- of *Affective Disorders*, 293, 320-328. <https://doi.org/10.1016/j.jad.2021.06.053>
97. Lai, C. H., & Wu, Y. T. (2014). Alterations in white matter micro-integrity of the superior longitudinal fasciculus and anterior thalamic radiation of young adult patients with depression. *Psychological Medicine*, 44(13), 2825-2832. <https://doi.org/10.1017/S0033291714000440>
98. Lecler, A., Duron, L., Charlson, E., Kolseth, C., Kossler, A. L., Wintermark, M., Moulin, K., & Rutt, B. (2022). Comparison between 7 Tesla and 3 Tesla MRI for characterizing orbital lesions. *Diagnostic and Interventional Imaging*, 103(9), 433-439. <https://doi.org/10.1016/j.diii.2022.03.007>
99. Lee, K. H., Shin, J., Lee, J., Yoo, J. H., Kim, J.-W., & Brent, D. A. (2023). Measures of Connectivity and Dorsolateral Prefrontal Cortex Volumes and Depressive Symptoms Following Treatment With Selective Serotonin Reuptake Inhibitors in Adolescents. *JAMA Network Open*, 6(8), e2327331. <https://doi.org/10.1001/jamanetworkopen.2023.27331>
100. Lee, S., Pyun, S.-B., Choi, K. W., & Tae, W.-S. (2020). Shape and Volumetric Differences in the Corpus Callosum between Patients with Major Depressive Disorder and Healthy Controls. *Psychiatry Investigation*, 17(9), 941-950. <https://doi.org/10.30773/pi.2020.0157>
101. Leppänen, J. M., & Hietanen, J. K. (2004). Positive facial expressions are recognized faster than negative facial expressions, but why? *Psychological Research*, 69(1), 22-29. <https://doi.org/10.1007/s00426-003-0157-2>
102. Li, C.-S. R., Zhang, S., Hung, C.-C., Chen, C.-M., Duann, J.-R., Lin, C.-P., & Lee, T. S.-H. (2017). Depression in chronic ketamine users: Sex differences and neural bases. *Psychiatry Research. Neuroimaging*, 269, 1-8. <https://doi.org/10.1016/j.psychresns.2017.09.001>

103. Li, F., Zheng, X., Wang, H., Meng, L., Chen, M., Hui, Y., Liu, D., Li, Y., Xie, K., Zhang, J., & Guo, G. (2024). Mediodorsal thalamus projection to medial prefrontal cortex mediates social defeat stress-induced depression-like behaviors. *Neuropsychopharmacology*, 49(8), 1318-1329. <https://doi.org/10.1038/s41386-024-01829-y>
104. Li, G., Liu, Y., Zheng, Y., Wu, Y., Li, D., Liang, X., Chen, Y., Cui, Y., Yap, P.-T., Qiu, S., Zhang, H., & Shen, D. (2021). Multiscale neural modeling of resting-state fMRI reveals executive-limbic malfunction as a core mechanism in major depressive disorder. *NeuroImage: Clinical*, 31, 102758. <https://doi.org/10.1016/j.nicl.2021.102758>
105. Li, K., Fan, L., Cui, Y., Wei, X., He, Y., Yang, J., Lu, Y., Li, W., Shi, W., Cao, L., Cheng, L., Li, A., You, B., & Jiang, T. (2022). The human mediodorsal thalamus: Organization, connectivity, and function. *NeuroImage*, 249, 118876. <https://doi.org/10.1016/j.neuroimage.2022.118876>
106. Liang, J., Yu, Q., Liu, Y., Qiu, Y., Tang, R., Yan, L., & Zhou, P. (2023). Gray matter abnormalities in patients with major depressive disorder and social anxiety disorder: A voxel-based meta-analysis. *Brain Imaging and Behavior*, 17(6), 749-763. <https://doi.org/10.1007/s11682-023-00797-z>
107. Lindner, P., Hamilton, W., Miloff, A., & Carlbring, P. (2019). How to Treat Depression With Low-Intensity Virtual Reality Interventions: Perspectives on Translating Cognitive Behavioral Techniques Into the Virtual Reality Modality and How to Make Anti-Depressive Use of Virtual Reality-Unique Experiences. *Frontiers in Psychiatry*, 10. <https://www.frontiersin.org/articles/10.3389/fpsy.2019.00792>
108. Liston, C., Chen, A. C., Zebly, B. D., Drysdale, A. T., Gordon, R., Leuchter, B., Voss, H. U., Casey, B. J., Etkin, A., & Dubin, M. J. (2014). Default Mode Network

- Mechanisms of Transcranial Magnetic Stimulation in Depression. *Biological Psychiatry*, 76(7), 517-526. <https://doi.org/10.1016/j.biopsych.2014.01.023>
109. Liu, C., Li, L., Pan, W., Zhu, D., Lian, S., Liu, Y., Ren, L., Mao, P., Ren, Y., & Ma, X. (2023). Altered topological properties of functional brain networks in patients with first episode, late-life depression before and after antidepressant treatment. *Frontiers in Aging Neuroscience*, 15. <https://doi.org/10.3389/fnagi.2023.1107320>
110. Llinás, R. R., Ribary, U., Jeanmonod, D., Kronberg, E., & Mitra, P. P. (1999a). Thalamocortical dysrhythmia: A neurological and neuropsychiatric syndrome characterized by magnetoencephalography. *Proceedings of the National Academy of Sciences of the United States of America*, 96(26), 15222-15227. <https://doi.org/10.1073/pnas.96.26.15222>
111. Luking, K. R., Repovs, G., Belden, A. C., Gaffrey, M. S., Botteron, K. N., Luby, J. L., & Barch, D. M. (2011). Functional connectivity of the amygdala in early-childhood-onset depression. *Journal of the American Academy of Child and Adolescent Psychiatry*, 50(10), 1027-1041.e3. <https://doi.org/10.1016/j.jaac.2011.07.019>
112. Ma, H., Cai, M., & Wang, H. (2021). Emotional Blunting in Patients With Major Depressive Disorder: A Brief Non-systematic Review of Current Research. *Frontiers in Psychiatry*, 12, 792960. <https://doi.org/10.3389/fpsy.2021.792960>
113. Ma, K., Hamada, M., Lazzaro, V. D., Hand, B., Guerra, A., Opie, G. M., & Goetz, S. M. (2023). Correlating active and resting motor thresholds for transcranial magnetic stimulation through a matching model. *Brain Stimulation: Basic, Translational, and Clinical Research in Neuromodulation*, 16(6), 1686-1688. <https://doi.org/10.1016/j.brs.2023.11.009>
114. Machado-Vieira, R., Baumann, J., Wheeler-Castillo, C., Latov, D., Henter, I. D., Salvadore, G., & Zarate, C. A. (2010). The Timing of Antidepressant Effects: A

- Comparison of Diverse Pharmacological and Somatic Treatments. *Pharmaceuticals (Basel, Switzerland)*, 3(1), 19-41. <https://doi.org/10.3390/ph3010019>
115. Malhi, G. S., & Mann, J. J. (2018). Depression. *Lancet (London, England)*, 392(10161), 2299-2312. [https://doi.org/10.1016/S0140-6736\(18\)31948-2](https://doi.org/10.1016/S0140-6736(18)31948-2)
116. Malik, A., Ayuso-Mateos, J. L., Baranyi, G., Barbui, C., Thornicroft, G., van Ommeren, M., & Akhtar, A. (2023). Mental health at work: WHO guidelines. *World Psychiatry*, 22(2), 331-332. <https://doi.org/10.1002/wps.21094>
117. Martens, M. A. G., Filippini, N., Harmer, C. J., & Godlewska, B. R. (2022a). Resting state functional connectivity patterns as biomarkers of treatment response to escitalopram in patients with major depressive disorder. *Psychopharmacology*, 239(11), 3447-3460. <https://doi.org/10.1007/s00213-021-05915-7>
118. Martens, M. A. G., Filippini, N., Harmer, C. J., & Godlewska, B. R. (2022b). Resting state functional connectivity patterns as biomarkers of treatment response to escitalopram in patients with major depressive disorder. *Psychopharmacology*, 239(11), 3447-3460. <https://doi.org/10.1007/s00213-021-05915-7>
119. Martins, D., Lockwood, P., Cutler, J., Moran, R., & Paloyelis, Y. (2021). Oxytocin modulates neurocomputational mechanisms underlying prosocial reinforcement learning (p. 2021.05.26.445739). *bioRxiv*. <https://doi.org/10.1101/2021.05.26.445739>
120. Maruyama, S., Fukunaga, M., Fautz, H.-P., Heidemann, R., & Sadato, N. (2019). Comparison of 3T and 7T MRI for the visualization of globus pallidus sub-segments. *Scientific Reports*, 9(1), 18357. <https://doi.org/10.1038/s41598-019-54880-x>
121. Matsuo, K., Glahn, D. C., Peluso, M. A. M., Hatch, J. P., Monkul, E. S., Najt, P., Sanches, M., Zamarripa, F., Li, J., Lancaster, J. L., Fox, P. T., Gao, J.-H., & Soares, J. C. (2007). Prefrontal hyperactivation during working memory task in untreated individuals with major depressive disorder. *Molecular Psychiatry*, 12(2), Article 2. <https://doi.org/10.1038/sj.mp.4001894>

122. McClintock, S. M., Reti, I. M., Carpenter, L. L., McDonald, W. M., Dubin, M., Taylor, S. F., Cook, I. A., OâReardon, J., Husain, M. M., Wall, C., Krystal, A. D., Sampson, S. M., Morales, O., Nelson, B. G., Latoussakis, V., George, M. S., & Lisanby, S. H. (2018). Consensus Recommendations for the Clinical Application of Repetitive Transcranial Magnetic Stimulation (rTMS) in the Treatment of Depression. *The Journal of Clinical Psychiatry*, 79(1), 16cs10905. <https://doi.org/10.4088/JCP.16cs10905>
123. Memarian Sorkhabi, M., Wendt, K., OâShea, J., & Denison, T. (2022). Pulse width modulation-based TMS: Primary motor cortex responses compared to conventional monophasic stimuli. *Brain Stimulation*, 15(4), 980-983. <https://doi.org/10.1016/j.brs.2022.06.013>
124. Miron, J.-P., Jodoin, V. D., LespÃ©rance, P., & Blumberger, D. M. (2021). Repetitive transcranial magnetic stimulation for major depressive disorder: Basic principles and future directions. *Therapeutic Advances in Psychopharmacology*, 11, 20451253211042696. <https://doi.org/10.1177/20451253211042696>
125. Mueller, F., Musso, F., London, M., de Boer, P., Zacharias, N., & Winterer, G. (2018). Pharmacological fMRI: Effects of subanesthetic ketamine on resting-state functional connectivity in the default mode network, salience network, dorsal attention network and executive control network. *NeuroImage. Clinical*, 19, 745-757. <https://doi.org/10.1016/j.nicl.2018.05.037>
126. Nam, B., Bae, S., Kim, S. M., Hong, J. S., & Han, D. H. (2017). Comparing the Effects of Bupropion and Escitalopram on Excessive Internet Game Play in Patients with Major Depressive Disorder. *Clinical Psychopharmacology and Neuroscience*, 15(4), 361-368. <https://doi.org/10.9758/cpn.2017.15.4.361>
127. Nejati, V., Majdi, R., Salehinejad, M. A., & Nitsche, M. A. (2021). The role of dorsolateral and ventromedial prefrontal cortex in the processing of emotional dimensions. *Scientific Reports*, 11(1), 1971. <https://doi.org/10.1038/s41598-021-81454-7>

128. Nugent, A. C., Farmer, C., Evans, J. W., Snider, S. L., Banerjee, D., & Zarate, C. A. (2019). Multimodal imaging reveals a complex pattern of dysfunction in corticolimbic pathways in major depressive disorder. *Human Brain Mapping*, 40(13), 3940-3950. <https://doi.org/10.1002/hbm.24679>
129. Oakes, T. R., Fox, A. S., Johnstone, T., Chung, M. K., Kalin, N., & Davidson, R. J. (2007). Integrating VBM into the General Linear Model with Voxelwise Anatomical Covariates. *NeuroImage*, 34(2), 500-508. <https://doi.org/10.1016/j.neuroimage.2006.10.007>
130. Organization, W. H. (2022). World mental health report: Transforming mental health for all [Report]. *World Health Organization*. <https://archive.hshsl.umaryland.edu/handle/10713/20295>
131. Ouhaz, Z., Fleming, H., & Mitchell, A. S. (2018). Cognitive Functions and Neurodevelopmental Disorders Involving the Prefrontal Cortex and Mediodorsal Thalamus. *Frontiers in Neuroscience*, 12. <https://doi.org/10.3389/fnins.2018.00033>
132. Overview | Repetitive transcranial magnetic stimulation for depression | Guidance | NICE. (2015, December 16). *NICE*. <https://www.nice.org.uk/guidance/ipg542>
133. Palmiero, M., & Piccardi, L. (2017). Frontal EEG Asymmetry of Mood: A Mini-Review. *Frontiers in Behavioral Neuroscience*, 11. <https://doi.org/10.3389/fnbeh.2017.00224>
134. Parnaudeau, S., Bolkan, S. S., & Kellendonk, C. (2018). The Mediodorsal Thalamus: An Essential Partner of the Prefrontal Cortex for Cognition. *Biological Psychiatry*, 83(8), 648-656. <https://doi.org/10.1016/j.biopsych.2017.11.008>
135. Patel, K., Allen, S., Haque, M. N., Angelescu, I., Baumeister, D., & Tracy, D. K. (2016). Bupropion: A systematic review and meta-analysis of effectiveness as

- an antidepressant. *Therapeutic Advances in Psychopharmacology*, 6(2), 99-144.
<https://doi.org/10.1177/2045125316629071>
136. Pedersen, C. B., Mors, O., Bertelsen, A., Waltoft, B. L., Agerbo, E., McGrath, J. J., Mortensen, P. B., & Eaton, W. W. (2014). A comprehensive nationwide study of the incidence rate and lifetime risk for treated mental disorders. *JAMA Psychiatry*, 71(5), 573-581. <https://doi.org/10.1001/jamapsychiatry.2014.16>
137. Perera, T., George, M. S., Grammer, G., Janicak, P. G., Pascual-Leone, A., & Wirecki, T. S. (2016). The Clinical TMS Society Consensus Review and Treatment Recommendations for TMS Therapy for Major Depressive Disorder. *Brain Stimulation*, 9(3), 336-346. <https://doi.org/10.1016/j.brs.2016.03.010>
138. Peterchev, A. V., Murphy, D. L., & Lisanby, S. H. (2011). Repetitive transcranial magnetic stimulator with controllable pulse parameters. *Journal of Neural Engineering*, 8(3), 036016. <https://doi.org/10.1088/1741-2560/8/3/036016>
139. Pilmeyer, J., Huijbers, W., Lamerichs, R., Jansen, J. F. A., Breeuwer, M., & Zinger, S. (2022). Functional MRI in major depressive disorder: A review of findings, limitations, and future prospects. *Journal of Neuroimaging*, 32(4), 582. <https://doi.org/10.1111/jon.13011>
140. Posner, J., Cha, J., Wang, Z., Talati, A., Warner, V., Gerber, A., Peterson, B. S., & Weissman, M. (2016). Increased Default Mode Network Connectivity in Individuals at High Familial Risk for Depression. *Neuropsychopharmacology*, 41(7), 1759-1767. <https://doi.org/10.1038/npp.2015.342>
141. Quinn, B. P. (1999). Diagnostic and Statistical Manual of Mental Disorders, Fourth Edition, Primary Care Version. *Primary Care Companion to The Journal of Clinical Psychiatry*, 1(2), 54-55.
142. Radyte, E., Wendt, K., Sorkhabi, M. M., OâShea, J., & Denison, T. (2022). Relative Comparison of Non-Invasive Brain Stimulation Methods for Modulating

- Deep Brain Targets. *Annual International Conference of the IEEE Engineering in Medicine and Biology Society. IEEE Engineering in Medicine and Biology Society. Annual International Conference*, 2022, 1715-1718. <https://doi.org/10.1109/EMBC48229.2022.9871476>
143. Raichle, M. E. (2015). The Brain's Default Mode Network. *Annual Review of Neuroscience*, 38, 433-447. <https://doi.org/10.1146/annurev-neuro-071013-014030>
144. Ramli, F. F., Singh, N., Emir, U. E., Villa, L. M., Waters, S., Harmer, C. J., Cowen, P. J., & Godlewska, B. R. (2024). Effects of ebselen addition on emotional processing and brain neurochemistry in depressed patients unresponsive to antidepressant medication. *Translational Psychiatry*, 14(1), 200. <https://doi.org/10.1038/s41398-024-02899-8>
145. Razza, L. B., da Silva, P. H. R., Busatto, G. F., Duran, F. L. de S., Pereira, J., De Smet, S., Klein, I., Zanillo, T. A., Luethi, M. S., Baeken, C., Vanderhasselt, M.-A., Buchpiguel, C. A., & Brunoni, A. R. (2022). Brain Perfusion Alterations Induced by Standalone and Combined Non-Invasive Brain Stimulation over the Dorsolateral Prefrontal Cortex. *Biomedicines*, 10(10), Article 10. <https://doi.org/10.3390/biomedicines10102410>
146. Renner, F., Cuijpers, P., & Huibers, M. J. H. (2014). The effect of psychotherapy for depression on improvements in social functioning: A meta-analysis. *Psychological Medicine*, 44(14), 2913-2926. <https://doi.org/10.1017/S0033291713003152>
147. Roddy, D., & O'Keane, V. (2019). Cornu Ammonis Changes Are at the Core of Hippocampal Pathology in Depression. *Chronic Stress (Thousand Oaks, Calif.)*, 3, 2470547019849376. <https://doi.org/10.1177/2470547019849376>
148. Roiser, J. P., Elliott, R., & Sahakian, B. J. (2012). Cognitive Mechanisms of Treatment in Depression. *Neuropsychopharmacology*, 37(1), Article 1. <https://doi.org/10.1038/npp.2011.183>

149. Rossi, S., Hallett, M., Rossini, P. M., & Pascual-Leone, A. (2009). Safety, ethical considerations, and application guidelines for the use of transcranial magnetic stimulation in clinical practice and research. *Clinical Neurophysiology*, 120(12), 2008-2039. <https://doi.org/10.1016/j.clinph.2009.08.016>
150. Rottenberg, J., Gross, J. J., & Gotlib, I. H. (2005). Emotion Context Insensitivity in Major Depressive Disorder. *Journal of Abnormal Psychology*, 114(4), 627-639. <https://doi.org/10.1037/0021-843X.114.4.627>
151. Ruhe, H. G., Mocking, R. J. T., Figueroa, C. A., Seeverens, P. W. J., Ikani, N., Tyborowska, A., Browning, M., Vrijzen, J. N., Harmer, C. J., & Schene, A. H. (2019). Emotional Biases and Recurrence in Major Depressive Disorder. Results of 2.5 Years Follow-Up of Drug-Free Cohort Vulnerable for Recurrence. *Frontiers in Psychiatry*, 10. <https://doi.org/10.3389/fpsy.2019.00145>
152. Rush, A. J., Trivedi, M. H., Wisniewski, S. R., Nierenberg, A. A., Stewart, J. W., Warden, D., Niederehe, G., Thase, M. E., Lavori, P. W., Lebowitz, B. D., McGrath, P. J., Rosenbaum, J. F., Sackeim, H. A., Kupfer, D. J., Luther, J., & Fava, M. (2008). Acute and Longer-Term Outcomes in Depressed Outpatients Requiring One or Several Treatment Steps: A STAR*D Report. *FOCUS*, 6(1), 128-142. <https://doi.org/10.1176/foc.6.1.foc128>
153. Rzepa, E., Dean, Z., & McCabe, C. (2017). Bupropion Administration Increases Resting-State Functional Connectivity in Dorso-Medial Prefrontal Cortex. *The International Journal of Neuropsychopharmacology*, 20(6), 455-462. <https://doi.org/10.1093/ijnp/pyx016>
154. Sackeim, H. A., Aaronson, S. T., Carpenter, L. L., Hutton, T. M., Pages, K., Lucas, L., & Chen, B. (2024). When to hold and when to fold: Early prediction of nonresponse to transcranial magnetic stimulation in major depressive disorder. *Brain Stimulation: Basic, Translational, and Clinical Research in Neuromodulation*, 17(2), 272-282. <https://doi.org/10.1016/j.brs.2024.02.019>

155. Salkovskis, P. M., Sighvatsson, M. B., & Sigurdsson, J. F. (2023). How effective psychological treatments work: Mechanisms of change in cognitive behavioural therapy and beyond. *Behavioural and Cognitive Psychotherapy*, 51(6), 595-615. <https://doi.org/10.1017/S1352465823000590>
156. Sansone, R. A., & Sansone, L. A. (2014). Serotonin Norepinephrine Reuptake Inhibitors: A Pharmacological Comparison. *Innovations in Clinical Neuroscience*, 11(3-4), 37-42.
157. Sarpal, D. K., Tarcijonas, G., Calabro, F. J., Foran, W., Haas, G. L., Luna, B., & Murty, V. P. (2022). Context-specific abnormalities of the central executive network in first-episode psychosis: Relationship with cognition. *Psychological Medicine*, 52(12), 2299-2308. <https://doi.org/10.1017/S0033291720004201>
158. Saul, H. (2020, July 3). Combined drug and psychological therapies may be most effective for depression. *NIHR Evidence*. https://doi.org/10.3310/alert_40468
159. Schick Tanz, N., Schwegler, K., Fastenrath, M., Spalek, K., Milnik, A., Pappasotiropoulos, A., Nyffeler, T., & de Quervain, D. J.-F. (2014). Motor threshold predicts working memory performance in healthy humans. *Annals of Clinical and Translational Neurology*, 1(1), 69-73. <https://doi.org/10.1002/acn3.22>
160. Schmaal, L., Hibar, D. P., Sämann, P. G., Hall, G. B., Baune, B. T., Jahanshad, N., Cheung, J. W., van Erp, T. G. M., Bos, D., Ikram, M. A., Vernooij, M. W., Niessen, W. J., Tiemeier, H., Hofman, A., Wittfeld, K., Grabe, H. J., Janowitz, D., Bäcklund, R., Selton, M., & Veltman, D. J. (2017). Cortical abnormalities in adults and adolescents with major depression based on brain scans from 20 cohorts worldwide in the ENIGMA Major Depressive Disorder Working Group. *Molecular Psychiatry*, 22(6), Article 6. <https://doi.org/10.1038/mp.2016.60>
161. Schulman, J. J., Cancro, R., Lowe, S., Lu, F., Walton, K. D., & Llinás, R. R. (2011). Imaging of Thalamocortical Dysrhythmia in Neuropsychiatry. *Frontiers*

- in Human Neuroscience*, 5. <https://doi.org/10.3389/fnhum.2011.00069>
162. Seeley, W. W. (2019). The Salience Network: A Neural System for Perceiving and Responding to Homeostatic Demands. *The Journal of Neuroscience: The Official Journal of the Society for Neuroscience*, 39(50), 9878-9882. <https://doi.org/10.1523/JNEUROSCI.1138-17.2019>
163. Shad, M. U., Muddasani, S., & Rao, U. (2012). Gray Matter Differences Between Healthy and Depressed Adolescents: A Voxel-Based Morphometry Study. *Journal of Child and Adolescent Psychopharmacology*, 22(3), 190-197. <https://doi.org/10.1089/cap.2011.0005>
164. Shao, Z., Guo, Y., Yue, L., Liu, X., Liu, J., Zhao, X., Sheng, X., Yu, D., Zhu, Y., & Yuan, K. (2024). Comparisons of transcranial alternating current stimulation and repetitive transcranial magnetic stimulation treatment therapy for insomnia: A pilot study. *General Psychiatry*, 37(1), e101184. <https://doi.org/10.1136/gpsych-2023-101184>
165. Sheline, Y. I., Price, J. L., Yan, Z., & Mintun, M. A. (2010). Resting-state functional MRI in depression unmasks increased connectivity between networks via the dorsal nexus. *Proceedings of the National Academy of Sciences*, 107(24), 11020-11025. <https://doi.org/10.1073/pnas.1000446107>
166. Smith, S. M., Jenkinson, M., Woolrich, M. W., Beckmann, C. F., Behrens, T. E. J., Johansen-Berg, H., Bannister, P. R., De Luca, M., Drobnjak, I., Flitney, D. E., Niazy, R. K., Saunders, J., Vickers, J., Zhang, Y., De Stefano, N., Brady, J. M., & Matthews, P. M. (2004). Advances in functional and structural MR image analysis and implementation as FSL. *NeuroImage*, 23 Suppl 1, S208-219. <https://doi.org/10.1016/j.neuroimage.2004.07.051>
167. Sommer, M., Alfaro, A., Rummel, M., Speck, S., Lang, N., Tings, T., & Paulus, W. (2006). Half sine, monophasic and biphasic transcranial magnetic stimulation

- of the human motor cortex. *Clinical Neurophysiology*, 117(4), 838-844. <https://doi.org/10.1016/j.clinph.2005.10.029>
168. Sommer, M., Ciocca, M., Chieffo, R., Hammond, P., Neef, A., Paulus, W., Rothwell, J. C., & Hannah, R. (2018). TMS of primary motor cortex with a biphasic pulse activates two independent sets of excitable neurones. *Brain Stimulation*, 11(3), 558-565. <https://doi.org/10.1016/j.brs.2018.01.001>
169. Sorkhabi, M. M., Wendt, K., O'Shea, J., & Denison, T. (2021). A digital transcranial magnetic stimulator for generating arbitrary pulse-shapes and patterns. *Brain Stimulation: Basic, Translational, and Clinical Research in Neuromodulation*, 14(6), 1613-1614. <https://doi.org/10.1016/j.brs.2021.10.083>
170. Southam-Gerow, M. A., McLeod, B. D., Brown, R. C., Quinoy, A. M., & Avny, S. B. (2011). Cognitive-Behavioral Therapy for Adolescents. In B. B. Brown & M. J. Prinstein (Eds.), *Encyclopedia of Adolescence* (pp. 100-108). Academic Press. <https://doi.org/10.1016/B978-0-12-373951-3.00106-X>
171. Stahl, S. M. (1998). Mechanism of action of serotonin selective reuptake inhibitors. Serotonin receptors and pathways mediate therapeutic effects and side effects. *Journal of Affective Disorders*, 51(3), 215-235. [https://doi.org/10.1016/S0165-0327\(98\)00221-3](https://doi.org/10.1016/S0165-0327(98)00221-3)
172. Suppa, A., Huang, Y.-Z., Funke, K., Ridding, M. C., Cheeran, B., Di Lazzaro, V., Ziemann, U., & Rothwell, J. C. (2016). Ten Years of Theta Burst Stimulation in Humans: Established Knowledge, Unknowns and Prospects. *Brain Stimulation*, 9(3), 323-335. <https://doi.org/10.1016/j.brs.2016.01.006>
173. Tahmasian, M., Knight, D., Manoliu, A., Schwerthöffer, D., Scherr, M., Meng, C., Shao, J., Peters, H., Doll, A., Khazaie, H., Drzezga, A., Bäuml, J., Zimmer, C., Förlstl, H., Wohlschläger, A., Riedl, Valentin, & Sorg, C. (2013). Aberrant Intrinsic Connectivity of Hippocampus and Amygdala Overlap in the Fronto-Insular and Dorsomedial-Prefrontal Cortex in Major Depressive Disorder.

Frontiers in Human Neuroscience, 7. <https://www.frontiersin.org/articles/10.3389/fnhum.2013.00639>

174. Temesi, J., Gruet, M., Rupp, T., Verges, S., & Millet, G. Y. (2014). Resting and active motor thresholds versus stimulus-response curves to determine transcranial magnetic stimulation intensity in quadriceps femoris. *Journal of NeuroEngineering and Rehabilitation*, 11(1), 40. <https://doi.org/10.1186/1743-0003-11-40>
175. Tian, Y., Du, J., Spagna, A., Mackie, M.-A., Gu, X., Dong, Y., Fan, J., & Wang, K. (2016). Venlafaxine treatment reduces the deficit of executive control of attention in patients with major depressive disorder. *Scientific Reports*, 6, 28028. <https://doi.org/10.1038/srep28028>
176. Tik, M., Woletz, M., Schuler, A.-L., Vasileiadi, M., Cash, R. F. H., Zalesky, A., Lamm, C., & Windischberger, C. (2023). Acute TMS/fMRI response explains offline TMS network effects - An interleaved TMS-fMRI study. *NeuroImage*, 267, 119833. <https://doi.org/10.1016/j.neuroimage.2022.119833>
177. Tozzi, L., Zhang, X., Chesnut, M., Holt-Gosselin, B., Ramirez, C. A., & Williams, L. M. (2021). Reduced functional connectivity of default mode network subsystems in depression: Meta-analytic evidence and relationship with trait rumination. *NeuroImage: Clinical*, 30, 102570. <https://doi.org/10.1016/j.nicl.2021.102570>
178. Tranter, R., Bell, D., Gutting, P., Harmer, C., Healy, D., & Anderson, I. M. (2009). The effect of serotonergic and noradrenergic antidepressants on face emotion processing in depressed patients. *Journal of Affective Disorders*, 118(1), 87-93. <https://doi.org/10.1016/j.jad.2009.01.028>
179. Trapp, N. T., Pace, B. D., Neisewander, B., Eyck, P. T., & Boes, A. D. (2023). A randomized trial comparing beam F3 and 5.5 cm targeting in rTMS treatment of depression demonstrates similar effectiveness. *Brain Stimulation*, 16(5), 1392-1400. <https://doi.org/10.1016/j.brs.2023.09.006>

180. Triantafyllou, C., Hoge, R. D., Krueger, G., Wiggins, C. J., Potthast, A., Wiggins, G. C., & Wald, L. L. (2005). Comparison of physiological noise at 1.5 T, 3 T and 7 T and optimization of fMRI acquisition parameters. *NeuroImage*, 26(1), 243-250. <https://doi.org/10.1016/j.neuroimage.2005.01.007>
181. Tura, A., & Goya-Maldonado, R. (2023). Brain connectivity in major depressive disorder: A precision component of treatment modalities? *Translational Psychiatry*, 13, 196. <https://doi.org/10.1038/s41398-023-02499-y>
182. van Velzen, L. S., Kelly, S., Isaev, D., Aleman, A., Aftanas, L. I., Bauer, J., Baune, B. T., Brak, I. V., Carballedo, A., Connolly, C. G., Couvy-Duchesne, B., Cullen, K. R., Danilenko, K. V., Dannlowski, U., Enneking, V., Filimonova, E., Förster, K., Frodl, T., Gotlib, I. H., & Schmaal, L. (2020). White matter disturbances in major depressive disorder: A coordinated analysis across 20 international cohorts in the ENIGMA MDD working group. *Molecular Psychiatry*, 25(7), 1511-1525. <https://doi.org/10.1038/s41380-019-0477-2>
183. Vanneste, S., Song, J.-J., & De Ridder, D. (2018). Thalamocortical dysrhythmia detected by machine learning. *Nature Communications*, 9(1), Article 1. <https://doi.org/10.1038/s41467-018-02820-0>
184. Vasic, N., Walter, H., Sambataro, F., & Wolf, R. C. (2009). Aberrant functional connectivity of dorsolateral prefrontal and cingulate networks in patients with major depression during working memory processing. *Psychological Medicine*, 39(6), 977-987. <https://doi.org/10.1017/S0033291708004443>
185. Vasiliu, O. (2023). Esketamine for treatment-resistant depression: A review of clinical evidence (Review). *Experimental and Therapeutic Medicine*, 25(3), 111. <https://doi.org/10.3892/etm.2023.11810>
186. Vidal-Pineiro, D., Valls-Pedret, C., Fernandez-Cabello, S., Arenaza-Urquijo, E. M., Sala-Llloch, R., Solana, E., Bargallo, N., Junque, C., Ros, E., & Bartràs-Faz, D. (2014). Decreased Default Mode Network connectivity correlates with

- age-associated structural and cognitive changes. *Frontiers in Aging Neuroscience*, 6, 256. <https://doi.org/10.3389/fnagi.2014.00256>
187. Wagner, H. L. (1993). On measuring performance in category judgment studies of nonverbal behavior. *Journal of Nonverbal Behavior*, 17(1), 3-28. <https://doi.org/10.1007/BF00987006>
188. Wang, B., Zhang, J., Li, Z., Grill, W. M., Peterchev, A. V., & Goetz, S. M. (2023). Optimized Monophasic Pulses with Equivalent Electric Field for Rapid-Rate Transcranial Magnetic Stimulation. *Journal of Neural Engineering*, 20(3), 10.1088/1741-2552/acd081. <https://doi.org/10.1088/1741-2552/acd081>
189. Wassermann, E. M. (1998). Risk and safety of repetitive transcranial magnetic stimulation: Report and suggested guidelines from the International Workshop on the Safety of Repetitive Transcranial Magnetic Stimulation, June 5-7, 1996. *Electroencephalography and Clinical Neurophysiology*, 108(1), 1-16. [https://doi.org/10.1016/s0168-5597\(97\)00096-8](https://doi.org/10.1016/s0168-5597(97)00096-8)
190. Wendt, K., Sorkhabi, M. M., OâShea, J., Cagnan, H., & Denison, T. (2021). Comparison between the modelled response of primary motor cortex neurons to pulse-width modulated and conventional TMS stimuli. *Annual International Conference of the IEEE Engineering in Medicine and Biology Society. IEEE Engineering in Medicine and Biology Society. Annual International Conference*, 2021, 6058-6061. <https://doi.org/10.1109/EMBC46164.2021.9629605>
191. Wendt, K., Sorkhabi, M. M., OâShea, J., & Denison, T. (2023). Emerging non-invasive technologies to stimulate the brain more effectively. *Brain Stimulation: Basic, Translational, and Clinical Research in Neuromodulation*, 16(1), 175. <https://doi.org/10.1016/j.brs.2023.01.181>
192. Wendt, K., Sorkhabi, M. M., OâShea, J., Denison, T., & van Rheede, J. (2023). Influence of time of day on resting motor threshold in clinical TMS practice. *Clin-*

- ical Neurophysiology: Official Journal of the International Federation of Clinical Neurophysiology*, 155, 65-67. <https://doi.org/10.1016/j.clinph.2023.08.017>
193. Wendt, K., Sorkhabi, M. M., Stagg, C. J., Fleming, M. K., Denison, T., & O'Shea, J. (2023). The effect of pulse shape in theta-burst stimulation: Monophasic vs biphasic TMS. *Brain Stimulation*, 16(4), 1178-1185. <https://doi.org/10.1016/j.brs.2023.08.001>
194. Williams, L. M. (2016). Precision psychiatry: A neural circuit taxonomy for depression and anxiety. *The Lancet. Psychiatry*, 3(5), 472-480. [https://doi.org/10.1016/S2215-0366\(15\)00579-9](https://doi.org/10.1016/S2215-0366(15)00579-9)
195. Wise, T., Radua, J., Via, E., Cardoner, N., Abe, O., Adams, T. M., Amico, F., Cheng, Y., Cole, J. H., de Azevedo Marques PÃ©rico, C., Dickstein, D. P., Farrow, T. F. D., Frodl, T., Wagner, G., Gotlib, I. H., Gruber, O., Ham, B. J., Job, D. E., Kempton, M. J., & Arnone, D. (2017). Common and distinct patterns of grey-matter volume alteration in major depression and bipolar disorder: Evidence from voxel-based meta-analysis. *Molecular Psychiatry*, 22(10), 1455-1463. <https://doi.org/10.1038/mp.2016.72>
196. Woolrich, M. W., Jbabdi, S., Patenaude, B., Chappell, M., Makni, S., Behrens, T., Beckmann, C., Jenkinson, M., & Smith, S. M. (2009). Bayesian analysis of neuroimaging data in FSL. *NeuroImage*, 45(1 Suppl), S173-186. <https://doi.org/10.1016/j.neuroimage.2008.10.055>
197. Xiong, G., Dong, D., Cheng, C., Jiang, Y., Sun, X., He, J., Li, C., Gao, Y., Zhong, X., Zhao, H., Wang, X., & Yao, S. (2021). Potential structural trait markers of depression in the form of alterations in the structures of subcortical nuclei and structural covariance network properties. *NeuroImage: Clinical*, 32, 102871. <https://doi.org/10.1016/j.nicl.2021.102871>
198. Xiong, G., Wu, S., Dong, Z., Li, Y., & Guo, Y. (2023). Modulating the activity in the dorsolateral prefrontal cortex changes gain-loss framing effect of intertem-

- poral choice: A transcranial direct current stimulation study. *Journal of Neuroscience, Psychology, and Economics*, 16(4), 216-228. <https://doi.org/10.1037/npe0000179>
199. Xu, Q., Ye, C., Gu, S., Hu, Z., Lei, Y., Li, X., Huang, L., & Liu, Q. (2021). Negative and Positive Bias for Emotional Faces: Evidence from the Attention and Working Memory Paradigms. *Neural Plasticity*, 2021, 8851066. <https://doi.org/10.1155/2021/8851066>
200. Yan, C.-G., Chen, X., Li, L., Castellanos, F. X., Bai, T.-J., Bo, Q.-J., Cao, J., Chen, G.-M., Chen, N.-X., Chen, W., Cheng, C., Cheng, Y.-Q., Cui, X.-L., Duan, J., Fang, Y.-R., Gong, Q.-Y., Guo, W.-B., Hou, Z.-H., Hu, L., & Zang, Y.-F. (2019). Reduced default mode network functional connectivity in patients with recurrent major depressive disorder. *Proceedings of the National Academy of Sciences*, 116(18), 9078-9083. <https://doi.org/10.1073/pnas.1900390116>
201. Yan, J. (2008). FDA Approves New Option to Treat Major Depression. *Psychiatric News*. <https://doi.org/10.1176/pn.43.22.0002>
202. Yang, C., Xiao, K., Ao, Y., Cui, Q., Jing, X., & Wang, Y. (2023). The thalamus is the causal hub of intervention in patients with major depressive disorder: Evidence from the Granger causality analysis. *NeuroImage: Clinical*, 37, 103295. <https://doi.org/10.1016/j.nicl.2022.103295>
203. Zhang, X., Pan, W.-J., & Keilholz, S. D. (2020). The relationship between BOLD and neural activity arises from temporally sparse events. *NeuroImage*, 207, 116390. <https://doi.org/10.1016/j.neuroimage.2019.116390>
204. Zheng, E. Z., Wong, N. M. L., Yang, A. S. Y., & Lee, T. M. C. (2024). Evaluating the effects of tDCS on depressive and anxiety symptoms from a transdiagnostic perspective: A systematic review and meta-analysis of randomized controlled trials. *Translational Psychiatry*, 14(1), 1-15. <https://doi.org/10.1038/s41398-024-03003-w>

205. Zheng, J., Anderson, K. L., Leal, S. L., Shestyuk, A., Gulsen, G., Mnatsakanyan, L., Vadera, S., Hsu, F. P. K., Yassa, M. A., Knight, R. T., & Lin, J. J. (2017). Amygdala-hippocampal dynamics during salient information processing. *Nature Communications*, 8(1), 14413. <https://doi.org/10.1038/ncomms14413>
206. Zheng, R., Zhang, Y., Yang, Z., Han, S., & Cheng, J. (2021). Reduced Brain Gray Matter Volume in Patients With First-Episode Major Depressive Disorder: A Quantitative Meta-Analysis. *Frontiers in Psychiatry*, 12, 671348. <https://doi.org/10.3389/fpsy.2021.671348>

A | xTMS Study Documents

Table of Contents

A.1 Step-by-step study procedures	171
A.2 MRI Safety Screening Form	182
A.3 TMS Safety Screening Form	185
A.4 SCID Scoresheet	188
A.5 Beck Depression Inventory (BDI)	198
A.6 CUREC 2 Approval	202
A.7 MRI Scanning Protocol	204
A.8 Participant Information Sheet (PIS)	209
A.9 Follow-up Letter for participants not included in the study	216
A.10 AP21 CUREC procedure appendix for TMS parameters	218
A.11 sgACC Localisation Raw Code	221

A.1 Step-by-step study procedures

Step-by-Step Procedures

Prior to session 1:

1. Participant expresses interest in the study
2. Em sends the participant the PIS and the online integrated form with online consent to screening, pre-screening questions, including the BDI + contra-indications for MRI and TMS + question about age and handedness.
3. Em evaluates if they have a BDI score ≥ 10 and confirms they don't have contraindications for TMS and MRI, are right-handed and within the age range.
 - a. If some answers indicate potential contraindications to participation, Em emails the participants with a follow up.
4. If the participant is eligible, Em schedules an MS Teams eligibility call (asks for their general availabilities, mornings/afternoons, days of the week).
 - a. If the participant is ineligible, Em sends the ineligibility email with a letter with resources and deletes the participant's data.

Session 1 (Psychiatric screening):

1. Em welcomes the participant, takes verbal consent, conducts the SCID and takes notes.
2. If the participant is eligible, a TMS practice session and an MRI session are scheduled.
 - a. If the participant is found to have a likely BPD diagnosis, or is found out to have contraindications for the MRI/TMS, Em sends them the ineligibility email with a letter with resources and deletes the participant's data. The SCID scoresheet is destroyed and no record is kept.
 - b. If it is unclear from the SCID whether the participant is eligible/Em needs to consult with Verena/Mike, the participant is told that they will be informed of their eligibility and next steps over email.
 - c. If it is unclear based on additional data if the participant is safe to undergo MRI scanning, a safety ticket is created, following procedures.
3. The SCID scoresheet is filed with the participant's number (anonymised) in their folder.

Session 2 (TMS familiarisation):

Consent, Safety and Eligibility

1. Discussion of the study with the participant + informed consent + inform participant that they can discontinue the session at any time.
2. Em takes the signed consent form and files it safely.
3. Participant fills in the safety form for TMS and MRI (to double-check online answers)
4. Em confirms the participant is safe to receive TMS that day.
5. The participant completes the Edinburgh Handedness Inventory.
6. Em confirms the participant is right handed.
7. Payment details are taken and noted down.
8. TMS, MRI and EHI forms are filed in the participant's folder with their SCID scoresheet.

Neuronavigation:

9. Key head measurements are taken to identify the 5-cm location and marked with a marker
10. Key landmarks are taken to align the participant's head with the MNI template

Finding RMT:

11. Single pulses of TMS are applied to the motor cortex (5 cm to the left of the midline) to locate the motor hotspot.
12. Find the resting motor threshold assessed by a visible twitch (5/10).
13. The RMT is noted and kept in the participant's folder.

Familiarisation with DLPFC stimulation:

14. 70% of the participant's RMT is calculated and the pTMS variac is adjusted accordingly to the conversion.
15. Using 70% RMT, single TMS pulses are given to the dorsolateral prefrontal cortex (DLPFC) identified using the 5-cm rule, to familiarize participants with the TMS sensation over the brain region that will be targeted in the main experiment. If the RMT is high, might start with a couple of pulses as low as 30% RMT in the DLPFC.
16. If the participant is comfortable proceeding further, a sample of theta burst TMS trains will be delivered over the DLPFC. The coil position and angle will be adjusted to minimize discomfort for participants.
17. Participant is asked to confirm whether or not they wish to continue their participation to the main TMS experimental sessions.

Session 3 (MRI):

Safety:

1. Em welcomes the participant and walks them through the instructions of what's about to happen, indicating that there will be two scans.
2. Em walks through the MRI safety checklist one more time to ensure the participant is safe to be scanned that day.
3. Em asks the participant to change into MRI-safe clothing for the testing session.
4. Em brings the safety checklist to the radiographers.
5. The radiographers review the safety checklist and then bring the participant in for scanning.

Scanning:

6. The participant lies on the MRI table until structural and resting state scans are completed.
7. Em escorts the participant to change back into their clothing, and the session is concluded for the day.

Session 3: TMS familiarisation session

Lab Setup	Turn on PC: Neuronav Mac computer – password: tdcсандtms	
Set up Neuronavigation	Connect Polaris camera (USB) and the second monitor (HDMI) to Mac	
	Plug in the USB cord for the Polaris + monitor cord	
	Calibrate + name the coil (Window → Coil Calibration) - Tighten the screws of the coil calibrator - Measure 4.7cm from the tip to the middle of the coil - Align the middle (marked in black) of the coil with the coil calibrator holder	
	Open Brainsight new project	
	Take a pillow from the metal cabinet and cover with a reusable cover sheet for the participant's comfort	
Set up EMG	Start software – Signal 7.0 PC (password: tmstms)– D440 monitoring software	
	Load configuration from the Emile folder	
Set up xTMS	<ol style="list-style-type: none"> 1. Turn on auxiliary 2. Turn on primary 3. Turn on tablet (connected to ethernet, password: password) 4. Terminal → ssh, then ./loader 5. PyCharm GUI emile_2.9 6. Log into Multiple (not single) 7. Set up pulse type + strength 	
Set up Patient Materials	Ensure you have: <ul style="list-style-type: none"> • TMS safety form, • MRI safety form • Edinburgh Handedness Inventory, • Consent form. 	
Prepare Equipment	Ensure you have: <ul style="list-style-type: none"> • Coil with a triple eye coil tracker, • Head tracker with attached electrodes, • Coil calibrator, • Pointer, • Neonatal electrodes, 	

	<ul style="list-style-type: none"> • Abrasive tape, • Alcohol wipes. 	
Meet Participant	Informed consent, questions + signature	
	TMS safety form and answer any outstanding questions	
	MRI safety form and answer any outstanding questions	
	Payment details	
	Edinburgh Handedness Inventory	
	OFFER PARTICIPANTS BATHROOM BREAK	
Measure Head	<p>Measure the head:</p> <ul style="list-style-type: none"> - Inion to nasion, divide by 2 - Lpa to rpa, divide by 2 - The intersection of the two lines → cross 	
	Mark the M1 5 cm to the left of the cross	
EMG setup	Clean right hand with abrasive tape + alcohol wipes	
	<p>Attach surface EMG electrodes:</p> <ul style="list-style-type: none"> • Ground – styloid process of the ulna -> black • Tendon – medial aspect of index finger-> red • Muscle belly – bulk of FDI-> yellow 	
Neuronavigation	Clean the participant's forehead with a wipe	
	Attach the subject tracker with two electrodes to the participant's forehead, leaning more towards the right side to allow for left DLPFC stim	
	Registration of landmarks	
	Validation of landmarks	
	Set the coil as the 'Driver' in the bottom pane of 'Perform'	
Motor threshold	Start with the 5cm MC location and send a single pulse starting around 30%	
Finding the right location/angle	Go up in 10% increments until you see a visible twitch in the FDI.	
	Mark this location as the hotspot in Brainsight.	
	Then, sample multiple spots in 1 cm steps around this MC location until you find the "best" twitch.	
	Then, sample 2 pulses in each of the target "quadrants" to determine the best twitch location.	

	If any of the quadrants performs better than the middle, set it as a target and repeat the quadrant procedure. Repeat until you find the best location.	
	Set the best location as the “target” in Brainsight.	
Finding the right biphasic MT	In that same location, apply 10 biphasic pulses in a row, count how many twitches are observed, if higher than 5, reduce the intensity and do the same. Repeat until you cannot get 5/10 twitches, one step above was the right intensity. Then note it as the biphasic MT (in xTMS measurements).	
Finding the right monophasic MT	In that location, apply 10 monophasic pulses in a row, count how many twitches are observed, if higher than 5, reduce the intensity by 2% and do the same. Repeat until you cannot get 5/10 twitches, one step above was the right intensity. Then note it as the monophasic MT (in xTMS measurements).	
Explain DLPFC stimulation and iTBS protocol	Explain to the participant that now we will stimulate a different location on their brain which may lead to some muscles twitching. The type of stimulation will be using sounds like this (show in the air). And this goes on for about 3 minutes. Initially we’ll demonstrate it with the same pulses we’ve just done.	
iTBS Familiarisation	Position the coil over the 6-cm DLPFC coordinates	
	Send a couple of single pulses at 70% to the DLPFC	
	Send a practice mono/biphasic iTBS train (60 pulses)	
Clean participant	Remove marker spots from the participant’s head	
Confirm participation	Confirm the participant is comfortable proceeding with the study/adjust the angle of that coil if that makes a difference to be comfortable	
Schedule	Schedule the MRI session (if not yet scheduled) and the experimental sessions.	
Turning off xTMS	<ol style="list-style-type: none"> 1. Close all software 2. ./shutdown 3. Auxiliary then primary 	
Cleaning		

Before Session 4 (Brainsight set up):

1. Em downloads the participant's structural scan from Calpendo → Projects → My Scans
2. Em completes the resting state scans analysis pipeline to localise the DLPFC spot most anti-correlated with the sgACC
3. Em sets up Brainsight
4. Em prepares the session for neuronavigation.

Session 4 (Experimental iTBS active/sham):

Detailed step-by-step instructions at the bottom.

Safety:

1. Participant fills in the safety form for TMS
2. Em confirms the participant is safe to receive TMS that day.
3. Em files the TMS and MRI forms in the participant's individual folder.

State questionnaires:

4. Participant completes the STAI and PANAS questionnaires
5. Em files the STAI and PANAS questionnaires in the participant's individual folder.

FERT practice:

6. Participant completes a brief practice session of the FERT

Neuronavigation:

7. Em uses Brainsight to register the participant's head to their MRI, where the DLPFC is already marked
8. A couple of single pulses are delivered to the target location to ensure that stimulation is comfortable for the participant.

iTBS session 1:

9. Active/sham biphasic/monophasic iTBS is delivered (lasting ~3 minutes).
10. Immediately after iTBS is completed, the participant performs the full FERT/IBLT task.
11. After the first task is completed, the participant performs the full IBLT/FERT (counter-balanced) task.

"Washout" period

12. Wait 45-60 minutes

iTBS session 2:

13. Active/sham biphasic/monophasic iTBS is delivered (lasting ~3 minutes).
14. Immediately after iTBS is completed, the participant performs the full FERT/IBLT task.
15. After the first task is completed, the participant performs the full IBLT/FERT (counter-balanced) task.

State questionnaires:

16. Participant completes the STAI and PANAS questionnaires
17. Em files the STAI and PANAS questionnaires in the participant's individual folder.

Blinding:

18. Participant is asked which of the two sessions they believe was active or sham.

Session 5 (Experimental iTBS active/sham)

Detailed step-by-step instructions at the bottom.

Safety:

1. Participant fills in the safety form for TMS and MRI
2. Em confirms the participant is safe to receive TMS that day.
3. Em files the TMS and MRI forms in the participant's individual folder.

State questionnaires:

4. Participant completes the STAI and PANAS questionnaires
5. Em files the STAI and PANAS questionnaires in the participant's individual folder.

FERT practice:

6. Participant completes a brief practice session of the FERT

Neuronavigation:

7. Em usesBrainsight to register the participant's head to their MRI, where the DLPFC is already marked
8. A couple of single pulses are delivered to the target location to ensure that stimulation is comfortable for the participant.

iTBS session 1:

1. Active/sham biphasic/monophasic iTBS is delivered (lasting ~3 minutes).
2. Immediately after iTBS is completed, the participant performs the full FERT/IBLT task.
3. After the first task is completed, the participant performs the full IBLT/FERT (counter-balanced) task.

"Washout" period

4. Wait 45-60 minutes

iTBS session 2:

5. Active/sham biphasic/monophasic iTBS is delivered (lasting ~3 minutes).
6. Immediately after iTBS is completed, the participant performs the full FERT/IBLT task.
7. After the first task is completed, the participant performs the full IBLT/FERT (counter-balanced) task.

State questionnaires:

8. Participant completes the STAI and PANAS questionnaires
9. Em files the STAI and PANAS questionnaires in the participant's individual folder.

State questionnaires:

10. Participant completes the STAI and PANAS questionnaires

11. Em files the STAI and PANAS questionnaires in the participant's individual folder

Blinding:

12. Participant is asked which of the two sessions they believe was active or sham.

Session 4/5: iTBS session 1 and 2 detailed setup

Lab Setup	Turn on PC: Neuronav Mac computer – password: tdcsandtms	
	Connect Polaris camera (USB) and the second monitor (HDMI) to Mac	
	Open Brainsight new project	
	Ensure you have: <ul style="list-style-type: none"> • TMS safety form, • STAI/PANAS/BDI forms, • Coil with a triple eye coil tracker, • Head tracker with attached electrodes, • Coil calibrator, • Pointer 	
Set up xTMS	8. Turn on auxiliary 9. Turn on primary 10. Turn on tablet (connected to ethernet, password: password) 11. Terminal → ssh, then ./loader 12. PyCharm GUI emile_2.9	
Set up Neuronavigation	Plug in the USB cord for the Polaris + monitor cord	
	Calibrate + name the coil (Window → Coil Calibration)	
Set up behavioural testing	Set up PsychoPy (FERT & IBLT) practice sessions on the Windows computer.	
Meet Participant	Verbally confirm consent	
	Go through the TMS safety form and answer any outstanding questions	
State assessment	Have the participant complete the STAI-trait, BDI (session 1 only) and PANAS questionnaires	
Practice FERT	Read instructions and walk the participant through a FERT demo session.	
Practice IBLT	Read instructions and walk the participant through an IBLT demo session, followed by the practice block.	
	OFFER PARTICIPANTS BATHROOM BREAK	
Neuronavigation	Clean the participant's forehead with a wipe	

	Attach the subject tracker with two electrodes to the participant's forehead, leaning more towards the right side to allow for left DLPFC stim	
	Registration of landmarks	
	Validation of landmarks	
	Set the coil as the 'Driver' in the bottom pane of 'Perform'	
Mono/bi iTBS	Position the coil over the DLPFC coordinates	
	Send a couple of single pulses to ensure participant is comfortable	
	Send a full mono/biphasic iTBS train + note the time of start	
Behavioural testing	Note the time when iTBS stopped and behavioural tasks were started	
	Run FERT, then the IBLT	
Debrief	Confirm the patient is ok, any notes/feedback.	
Washout	Wait 60 minutes since end of iTBS train	
Mono/bi iTBS	Position the coil over the DLPFC coordinates	
	Send a couple of single pulses to ensure participant is comfortable	
	Send a full mono/biphasic iTBS train	
Behavioural testing	Run FERT, then the IBLT	
State assessment	Have the participant complete the PANAS questionnaire	
Blinding (session 2 only)	Ask the participant which (if any) of the sessions they think were active/sham.	
Turning off xTMS	<ol style="list-style-type: none"> 1. Confirm all the behavioural data is appropriately saved and stored. 2. Close all software. 3. Auxiliary then primary and sudo ./shutdown of the xTMS system. 	
Cleaning		

A.2 MRI Safety Screening Form

3T VOLUNTEER MRI SCREENING FORM



Please carefully check the following. Some items can interfere with MR examinations and may be hazardous to your safety. Clearly mark your answer with a circle and add any relevant information. To ensure your safety we must ask for your biological sex, weight and height. Your answers will be kept strictly confidential.

Volunteer name _____ Sex _____

Date of birth _____ Weight _____ kg Height _____ cm

IF YOU HAVE ANY QUESTIONS THEN PLEASE ASK US BEFORE YOUR SCAN

Do you have a heart pacemaker or pacing wires?	YES	NO
Have you had any heart surgery (e.g. coronary stent, PFO closure)?	YES	NO
Have you had any surgery to your head including eyes / ears / brain?	YES	NO
Have you had any surgery to your neck or spine?	YES	NO
Do you have any implanted devices (e.g. aneurysm clip, hydrocephalus shunt, nerve stimulator, cochlear implant, mesh)?	YES	NO
Have you had any operations involving metallic pins / plates / screws / wires?	YES	NO
Have you had any surgical procedures or endoscopy in the last 6 weeks? (Please write below)	YES	NO
Have you ever had any other surgical procedures of any kind? (Please write below)	YES	NO
Have you ever sustained any injuries involving metal to the eyes or other part of the body (e.g. from drilling, grinding or welding)?	YES	NO
Have you ever had a serious accident or injury (e.g. road traffic accident, industrial accident, explosion injury, shooting injury or shrapnel injury)?	YES	NO
Have you ever had a fit or blackout, or do you suffer from epilepsy or diabetes?	YES	NO
Do you have any of the following (if yes please circle):		
Body piercing, eye makeup, coloured contact lenses	Hearing aid, wearable medical device (e.g. drug pump, glucose monitor)	Tattoos (including cosmetic)
Dentures, dental braces, dental implant, dental bridge	Medicated skin patch (e.g. pain, HRT, nicotine, contraceptive)	Artificial limb, prosthesis, splint, brace or support
FOR WOMEN OF CHILDBEARING AGE:	Do you have an IUD (coil)?	YES NO
	Could you be pregnant?	YES NO
Are you wearing any clothing, including underwear, that contains metallic threads or has been silver impregnated (e.g. anti-microbial)?	YES	NO
Do you understand that this is a research scan and is not useful for diagnosis?	YES	NO
Have you removed your jewellery, hairgrips, hearing aids, watch, spectacles, keys and coins?	YES	NO

Volunteer / Guardian signature _____ Date of study _____

Screened by _____ Signature _____ Consent sighted _____

IMPORTANT: NO METAL OBJECTS TO BE TAKEN INTO THE MAGNET ROOM

Notes

For scans using contrast agent only: *(please ask a member of staff if you don't know whether your scan will involve contrast agent)*

Have you had MR contrast agent before? (please leave blank if unknown)	YES	NO
Are you aware of any problems with your kidneys?	YES	NO
Do you have any allergies to medications? If yes please give details	YES	NO
Are you currently breast-feeding?	YES	NO

A.3 TMS Safety Screening Form



Brain Stimulation Safety Screening Form (Confidential)

If you agree to take part in this study, please answer the following questions. The information you provide is for screening purposes only and will be kept completely confidential

1. Do you have epilepsy, or have you ever had a convulsion or a seizure (fit)? YES NO

2. Has anyone in your wider family suffered from seizures? YES NO

If YES please state your relationship to the affected family member _____

3. Have you ever had a fainting spell or syncope? YES NO

If YES please describe on which occasion(s) _____

4. Have you ever had a head trauma that was diagnosed as a concussion or was associated with loss of consciousness? YES NO

5. Do you have any hearing problems or ringing in your ears? YES NO

6. Do you have cochlear implants? YES NO

7. Are you pregnant, or is there any chance that you might be? YES NO

8. Do you have metal in the brain, skull or elsewhere in your body (e.g., splinters, fragments, clips, etc.)? YES NO

If YES, specify the type of metal and where it is located _____

9. Do you have an implanted neurostimulator (e.g. DBS, epidural/subdural, VNS)? YES NO

10. Do you have a cardiac pacemaker or intracardiac lines? YES NO

11. Do you have a medication infusion device? YES NO

12. Are you taking any prescribed or unprescribed medications (or herbal remedies)? YES NO

If YES, please list _____

13. Did you ever undergo TCS or TMS in the past? YES NO

If YES, please state if there were any problems and describe them _____

When was your last TMS/TCS session? _____

How many TMS/TCS sessions have you had in the past month? _____

How many TMS/TCS sessions have you had in the past 12 months? _____

14. Did you ever undergo MRI in the past? YES NO



**Department of Psychiatry
Warneford Hospital Oxford OX3 7JX
Telephone: +44 (0) 1865 618200
Fax: +44 (0) 1865 618200**

If YES, please state if there were any problems and describe them _____

- | | | |
|---|-----|----|
| 15. Have you ever undergone a neurosurgical procedure (including eye surgery)? | YES | NO |
| If YES, please give details _____ | | |
| 16. Are you currently undergoing anti-malarial treatment? | YES | NO |
| 17. Have you drunk more than 3 units of alcohol in the last 24 hours? | YES | NO |
| 18. Have you drunk alcohol already today? | YES | NO |
| 19. Have you had more than one cup of coffee, or other sources of caffeine, in the last hour? | YES | NO |
| 20. How much liquid in total have you drunk already today? _____ ml | | |
| 21. When was your last meal? _____ hours ago | | |
| 22. Have you used recreational drugs in the last 24 hours? | YES | NO |
| 23. How many hours sleep did you have last night? _____ | | |

I (please give full name in CAPITALS) _____ confirm that I have personally completed the above questionnaire.

Signature _____ Date _____

Please note: All data arising from this study will be held and used in accordance with the Data Protection Act (2018). The results of the study will not be made available in a way that could reveal the identity of individuals.

A.4 SCID Scoresheet

SCID 5 - Scoresheet

Low mood study

Participant number: _____

Visit date: ____/____/____

I'M GOING TO ASK YOU SOME QUESTIONS ABOUT YOUR MENTAL HEALTH. THIS IS A LONG PROTOCOL OF QUESTIONS. SOME QUESTIONS MIGHT NOT APPLY TO YOU AT ALL, BUT WE NEED TO MAKE SURE TO ASK THE SAME QUESTIONS TO ALL PARTICIPANTS. IF THERE IS ANYTHING YOU DON'T WANT TO TALK ABOUT THAT'S OKAY. I WILL DISCUSS YOUR ANSWERS WITH MY SUPERVISOR. OTHERWISE, EVERYTHING YOU SAY WILL BE STRICTLY CONFIDENTIAL, UNLESS THERE IS AN IMMEDIATE RISK TO YOURSELF OR OTHER PEOPLE. I AM NOT ALLOWED TO GIVE YOU A DIAGNOSIS, WE CONDUCT THIS INTERVIEW ONLY FOR RESEARCH PURPOSES. AFTER THE INTERVIEW, I CAN TELL YOU IF YOU ARE ELIGIBLE FOR THE STUDY (OR WILL GET BACK TO YOU LATER).

ASK ONLY ONE QUESTION AT A TIME. BRACKETS ARE FOR CLARIFYING.

MAJOR DEPRESSIVE EPISODE

		C	P
1	Depressed mood most of the day, nearly every day, for 2 weeks , subjective or objective report		
2	Markedly diminished interest or pleasure in all, or almost all, activities, most of day nearly every day for 2 weeks (subjective or objective)		
	Significant weight loss when not dieting or weight gain (5% weight change) or decrease in appetite nearly every day		
	Insomnia or hypersomnia nearly every day		
	Psychomotor agitation or retardation nearly every day OBSERVED BY OTHERS		
	Fatigue or loss of energy nearly every day		
	Feelings of worthlessness or excessive or inappropriate guilt nearly every day		
	Diminished ability to think or concentrate, or indecisiveness, nearly every day (objective or observed by others)		
	Recurrent thoughts of death, recurrent suicidal ideation w/o plan, suicide attempt or specific plan		

At least five of these are positive, and at least one is 1 or 2.

	Clinically significant distress or impairment in social, occupational, or other important areas of functioning		
	Not due to direct physiological effects of a substance or general medical condition		
	Total number of major depressive episodes, including current		

THIS BOX IS NECESSARY FOR DIAGNOSIS

MANIC EPISODE

	C	P
A distinct period of abnormally and persistently elevated or expansive mood Lasting at least 1 week OR hospitalisation was necessary		
Abnormally irritable mood (ask separately about duration of elevated vs irritable) Lasting at least 1 week OR hospitalisation was necessary		
Abnormally and persistently increased activity or energy		
During this period, when were you the most high/irritable/own words ? Ask A31-A37 about the most severe period of the episode		
A31: Inflated self-esteem or grandiosity		
Decreased need for sleep		
More talkative than usual or pressure to keep talking		
Flight of ideas or subjective experience that thoughts are racing		
Distractibility		
Increase in goal-directed activity (socially, at work or school, or sexually) or psychomotor agitation		
A37: Excessive involvement in pleasurable activities that have a high potential for painful consequences (e.g. shopping, sexual indiscretions, foolish investments)		
At least 3 of A31-A37 are + (4 if mood only irritable)		
Marked impairment in occupational functioning or usual social activities or relationships with others, or to necessitate hospitalisation, or there are psychotic features IF NO SIGNIFICANT IMPAIRMENT -> HYPOMANIC EPISODE		
Not due to the direct physiological effects of a substance or a general medical condition		

HYPOMANIC EPISODE

	C	P
A distinct period of abnormally and persistently elevated or expansive mood Lasting at least 4 days most of the day nearly every day		
Abnormally irritable mood (ask separately about duration of elevated vs irritable) Lasting at least 4 days most of the day nearly every day		
Abnormally and persistently increased activity or energy		
A31: Inflated self-esteem or grandiosity		
Decreased need for sleep		
More talkative than usual or pressure to keep talking		
Flight of ideas or subjective experience that thoughts are racing		
Distractibility		
Increase in goal-directed activity (socially, at work or school, or sexually) or psychomotor agitation		
A37: Excessive involvement in pleasurable activities that have a high potential for painful consequences (e.g. shopping, sexual indiscretions, foolish investments)		
At least 3 of A31-A37 are + (4 if mood only irritable) → IF NOT, GO TO PAST MANIC EPISODE		
<i>Was it very different from the way you usually are?</i>		
<i>Did other people notice the change in you?</i> → IF NOT, GO TO PAST MANIC EPISODE		
Marked impairment in occupational functioning or usual social activities or relationships with others, or to necessitate hospitalisation, or there are psychotic features		
Not due to the direct physiological effects of a substance or a general medical condition		

SCID 5 - Scoresheet

Low mood study

Participant number: _____

Visit date: ____/____/____

PERSISTENT DEPRESSIVE DISORDER

1	Depressed mood for most of the day, for more days than not, as indicated either by subjective account or observation by others , for at least 2 years	
	Poor appetite or overeating	
	Insomnia or hypersomnia	
	Low energy or fatigue	
	Low self-esteem	
	Poor concentration or difficulty making decisions	
	Feelings of hopelessness	
	<i>At least two of these are positive, + number 1 must be positive</i>	
	During the 2 year period, the person has never been without the above for over 2 months	
	Never been a manic episode, mixed, or hypomanic episode, and never met criteria for cyclothymic disorder	
	Does not occur exclusively during the course of a chronic Psychotic disorder	
	Symptoms not due to the direct physiological effects of a substance or general medical condition	
	Symptoms cause clinically significant distress or impairment in social, occupational, or other important areas of functioning	

SCID 5 - Scoresheet

Low mood study

Participant number: _____

Visit date: ____/____/____

ANXIETY AND OTHER DISORDERS**Panic disorder**

	Had a panic attack that came on suddenly	
	F2 Palpitations, pounding heart, or accelerated heart rate	
	Sweating	
	Trembling or shaking	
	Sensations of shortness of breath or smothering	
	Feeling of choking	
	Chest pain or discomfort	
	Nausea or abdominal distress	
	Feeling dizzy, unsteady, lightheaded, or faint	
	Chills or hot flushes	
	Paresthesias (numbness or tingling sensations)	
	Derealization (unreality) or depersonalization (detached from oneself)	
	Fear of losing control or going crazy	
	Fear of dying	
	At least four of these (from F2) are positive → IF NOT, GO TO AGORAPHOBIA	
	F16 Attacks come out of the blue	
	F17 Persistent concern or worry about additional panic attacks or consequences	
	F18 Significant maladaptive change in behaviour	
	F17 or F18 are positive → IF NO, AGORAPHOBIA	
	Not due to the direct physiological effects of a substance or to a general medical condition	
	Not better accounted for by another mental disorder such as specific phobia, OCD, PTSD, separation anxiety, or social phobia (panic attacks don't exclusively occur in those situations)	

Agoraphobia

	Marked fear or anxiety about TWO OR MORE of the following: 1) Using public transportation, 2) being in open spaces, 3) being in enclosed places, 4) standing in line or crowd, 5) being outside of home alone	
	Thoughts that escape might be difficult or help may not be available in case of panic like-symptoms or other embarrassing symptoms	
	Almost always feels anxious in these situations	
	Situations actively avoided, require companion or are endured with intense anxiety	
	Fear out of proportion to actual danger	
	Present for most of past 6 months	
	Significant distress or impairment	
	If due to another medical condition (e.g. IBS), fear is out of proportion	
	Not better explained by another disorder (eg not solely due to OCD or phobia worries)	

Social anxiety disorder

	Marked fear or anxiety about one or more social situations in which the individual is exposed to possible scrutiny by others. Eg. Social interactions (conversations; meeting unfamiliar people), being observed (eg eating/drinking) and performing in front of others (eg giving a speech).	
	Fears negative evaluation	
	Social situations almost always provoke fear	
	Social situations avoided or endure with intense fear and anxiety	
	Fear out of proportion to actual threat	
	Fear, anxiety or avoidance persistent for at least 6 months	
	Significant distress or impairment	
	Not due to drugs/caffeine etc	

SCID 5 - Scoresheet

Low mood study

Participant number: _____

Visit date: ____/____/____

Generalized anxiety disorder

	Excessive worry and anxiety more days than not for at least 6 months , about a number of events or activities (such as work or school performance) At least 3 from F45-F50	
	Significant distress or impairment	
	Not due to drugs/caffeine etc	
	Not better explained by another disorder	

Obsessive-compulsive disorder

	1. <u>Obsessions</u> : Recurrent and persistent thoughts, impulses, or images that are experienced at some time during the disturbance, as intrusive and inappropriate and that cause marked anxiety or distress	
	2. The person attempts to ignore or suppress such thoughts, impulses, or images, or to neutralize them with some other thought or emotion	
	<i>All the above are positive (obsessions)</i>	
	1. <u>Compulsions</u> : Repetitive behaviours (e.g. hand washing, ordering, checking) or mental acts (praying, counting, repeating words) that the person feels driven to perform in response to an obsession, or according to certain rules that must be applied rigidly	
	2. The behaviours or mental acts are aimed at preventing or reducing distress or preventing some dreaded event or situation; however, these behaviours or mental acts are either not realistically connected to what they are designed to prevent or are clearly excessive	
	<i>Either obsessions or compulsions are present in the past month</i>	
	The obsessions or compulsions cause marked distress, are time-consuming (take over an hour a day), or significantly interfere with the person's normal routine, occupational functioning, or usual social activities or relationships	
	Not due to the direct physiological effects of a substance or a general medical condition	

Post-traumatic stress disorder – STRESS THEY CAN OPT OUT OF TRAUMA QUESTIONS

<p>The person has been exposed to a traumatic event in which both of the following were present: the person experienced, witnessed, or was confronted with an event or events that involved actual or threatened death or serious injury, or a threat to the physical integrity of self or others</p> <p>EVENT(S):</p> <p>→ IF THE ONLY TRAUMATIC EVENT WAS WITHIN PAST MONTH, DON'T ASSESS PTSD</p> <p>→</p>	
G14. Reexperienced in one of these ways: recurrent and intrusive distressing recollection of the event, including images, thoughts or perceptions	
Recurrent distressing dreams of the event	
Dissociative reactions: acting or feeling as if the traumatic event were recurring (includes a sense of reliving the experience, illusions, hallucinations, and dissociative flashback episodes, including those that occur on awakening or when intoxicated)	
Intense psychological distress at exposure to external or internal cues that symbolise or resemble an aspect of the traumatic event	
18. Physiological reactivity on exposure to internal or external cues that symbolize or resemble an aspect of the traumatic event	
<i>At least one of 14-18 is + for past month</i>	

If yes, criterion B is met, go on to test for criteria C, D, E, G

G20	Avoidance of distressing memories	
G21	Avoidance of external reminders	
	At least one of G20/21 is positive	

G23	Inability to remember important aspects	
G24	Persistent and exaggerated negative beliefs	
G25	Persistent distorted cognitions about cause of the event	
G26	Persistent negative emotional state	
G27	Markedly diminished interest or participation in significant activities	

SCID 5 - Scoresheet

Low mood study

Participant number: _____

Visit date: ___/___/___

G28	Feelings of detachment or estrangement from others	
G29	Persistent inability to experience positive emotions	
	At least 3 of G23-29 are positive	

G31	Irritable behaviour and angry outbursts	
G32	Reckless or self-destructive behaviour	
G33	Hypervigilance	
G34	Exaggerated startle response	
G35	Problems with concentration	
G36	Sleep disturbance	
	<i>At least two of G31-G36 are positive.</i>	
	<i>Duration of symptoms is more than 1 month.</i>	
	<i>Significant impairment in functioning.</i>	
	<i>Not due to substance/illness.</i>	

A.5 Beck Depression Inventory (BDI)

Beck's Depression Inventory

This depression inventory can be self-scored. The scoring scale is at the end of the questionnaire.

1.
 - 0 I do not feel sad.
 - 1 I feel sad
 - 2 I am sad all the time and I can't snap out of it.
 - 3 I am so sad and unhappy that I can't stand it.
2.
 - 0 I am not particularly discouraged about the future.
 - 1 I feel discouraged about the future.
 - 2 I feel I have nothing to look forward to.
 - 3 I feel the future is hopeless and that things cannot improve.
3.
 - 0 I do not feel like a failure.
 - 1 I feel I have failed more than the average person.
 - 2 As I look back on my life, all I can see is a lot of failures.
 - 3 I feel I am a complete failure as a person.
4.
 - 0 I get as much satisfaction out of things as I used to.
 - 1 I don't enjoy things the way I used to.
 - 2 I don't get real satisfaction out of anything anymore.
 - 3 I am dissatisfied or bored with everything.
5.
 - 0 I don't feel particularly guilty
 - 1 I feel guilty a good part of the time.
 - 2 I feel quite guilty most of the time.
 - 3 I feel guilty all of the time.
6.
 - 0 I don't feel I am being punished.
 - 1 I feel I may be punished.
 - 2 I expect to be punished.
 - 3 I feel I am being punished.
7.
 - 0 I don't feel disappointed in myself.
 - 1 I am disappointed in myself.
 - 2 I am disgusted with myself.
 - 3 I hate myself.
8.
 - 0 I don't feel I am any worse than anybody else.
 - 1 I am critical of myself for my weaknesses or mistakes.
 - 2 I blame myself all the time for my faults.
 - 3 I blame myself for everything bad that happens.
9.
 - 0 I don't have any thoughts of killing myself.
 - 1 I have thoughts of killing myself, but I would not carry them out.
 - 2 I would like to kill myself.
 - 3 I would kill myself if I had the chance.
10.
 - 0 I don't cry any more than usual.
 - 1 I cry more now than I used to.
 - 2 I cry all the time now.
 - 3 I used to be able to cry, but now I can't cry even though I want to.

- 11.
- 0 I am no more irritated by things than I ever was.
 - 1 I am slightly more irritated now than usual.
 - 2 I am quite annoyed or irritated a good deal of the time.
 - 3 I feel irritated all the time.
- 12.
- 0 I have not lost interest in other people.
 - 1 I am less interested in other people than I used to be.
 - 2 I have lost most of my interest in other people.
 - 3 I have lost all of my interest in other people.
- 13.
- 0 I make decisions about as well as I ever could.
 - 1 I put off making decisions more than I used to.
 - 2 I have greater difficulty in making decisions more than I used to.
 - 3 I can't make decisions at all anymore.
- 14.
- 0 I don't feel that I look any worse than I used to.
 - 1 I am worried that I am looking old or unattractive.
 - 2 I feel there are permanent changes in my appearance that make me look unattractive
 - 3 I believe that I look ugly.
- 15.
- 0 I can work about as well as before.
 - 1 It takes an extra effort to get started at doing something.
 - 2 I have to push myself very hard to do anything.
 - 3 I can't do any work at all.
- 16.
- 0 I can sleep as well as usual.
 - 1 I don't sleep as well as I used to.
 - 2 I wake up 1-2 hours earlier than usual and find it hard to get back to sleep.
 - 3 I wake up several hours earlier than I used to and cannot get back to sleep.
- 17.
- 0 I don't get more tired than usual.
 - 1 I get tired more easily than I used to.
 - 2 I get tired from doing almost anything.
 - 3 I am too tired to do anything.
- 18.
- 0 My appetite is no worse than usual.
 - 1 My appetite is not as good as it used to be.
 - 2 My appetite is much worse now.
 - 3 I have no appetite at all anymore.
- 19.
- 0 I haven't lost much weight, if any, lately.
 - 1 I have lost more than five pounds.
 - 2 I have lost more than ten pounds.
 - 3 I have lost more than fifteen pounds.

- 20.
- 0 I am no more worried about my health than usual.
 - 1 I am worried about physical problems like aches, pains, upset stomach, or constipation.
 - 2 I am very worried about physical problems and it's hard to think of much else.
 - 3 I am so worried about my physical problems that I cannot think of anything else.
- 21.
- 0 I have not noticed any recent change in my interest in sex.
 - 1 I am less interested in sex than I used to be.
 - 2 I have almost no interest in sex.
 - 3 I have lost interest in sex completely.

INTERPRETING THE BECK DEPRESSION INVENTORY

Now that you have completed the questionnaire, add up the score for each of the twenty-one questions by counting the number to the right of each question you marked. The highest possible total for the whole test would be sixty-three. This would mean you circled number three on all twenty-one questions. Since the lowest possible score for each question is zero, the lowest possible score for the test would be zero. This would mean you circles zero on each question. You can evaluate your depression according to the Table below.

Total Score _____ Levels of Depression

1-10 _____	These ups and downs are considered normal
11-16 _____	Mild mood disturbance
17-20 _____	Borderline clinical depression
21-30 _____	Moderate depression
31-40 _____	Severe depression
over 40 _____	Extreme depression

A.6 CUREC 2 Approval

MEDICAL SCIENCES INTERDIVISIONAL RESEARCH ETHICS COMMITTEE

Research Services, Boundary Brook House, Churchill Drive, Headington, Oxford, OX3 7GB

Tel: +44(0)1865 616575

ethics@medsci.ox.ac.uk



CONFIDENTIAL

Dr Jacinta O'Shea & Emilè Radytè
Department of Psychiatry
University of Oxford
Warneford Hospital
Oxford

2 August 2023

Dear Dr O'Shea and Emilè,

Research Ethics Approval - CUREC 2

Ethics Approval Reference: R87506/RE001

Study title: Short-term effects of a monophasic iTBS protocol on emotional processing in participants with low mood

Short title: Effect of iTBS on emotional processing

The above application has been considered on behalf of the Medical Sciences Interdivisional Research Ethics Committee (MS IDREC) in accordance with the University's procedures for ethical approval of all research involving human participants.

I am pleased to inform you that, on the basis of the information provided to the IDREC, the proposed research has been judged as meeting appropriate ethical standards, and approval has been granted from **2nd August 2023** until **1st August 2025**.

Insurance-provided indemnity arrangements are in place for the duration of the approval stated above. It is your responsibility to ensure that you request an extension to the end date for indemnity to remain in place should you continue the research beyond the dates covered.

You will be required to submit an annual progress report on each anniversary of study approval, until the study is completed, and your study may be selected for review during an annual audit.

Amendments

Should there be any subsequent changes to the study, you should submit details to the MS IDREC for consideration and approval. Details of changes must be listed on an [amendment form](#).

Yours Sincerely

DocuSigned by:

9F14889D2BC549A...

Mrs Leah Butts

Research Ethics Administrator

for

Dr Helen Barnby-Porritt
Research Ethics Manager

A.7 MRI Scanning Protocol



Author: **Name** Juliet Semple
 Position Lead Research Radiographer

Sign *Juliet Semple* 24/10/23

Checked: **Name** Emile Radyte
 Position 2023_120 Lead Study Researcher

Sign *Emile Radyte* xx/xx/xx

Name
Position

Sign xx/xx/xx

Document History

Version	Initials	Date	Comment
1	JS	24/10/23	

Related Documents and Location

- 2023_120 CUREC Application (electronic, study docs folder)
- 2023_120 CUREC Approval Letter (electronic, study docs folder)
- 2023_120 PIS and Consent Form (electronic, study docs folder)

Study Information

Study Title: Short-term effects of a monophasic iTBS protocol on emotional processing in participants with low mood

Study Group: Neurology and Psychiatry

PI: Jacinta O'Shea

Calpendo ID: 2023_120 – iTBS

Ethics Number: R87506/RE001

Introduction: This study investigates the potential of a novel TMS protocol, monophasic theta burst, in reducing negative bias associated with depression, when compared to standard biphasic iTBS and sham. Building on prior research that demonstrated its enhanced neurophysiological plasticity effects on the motor cortex, this study aims to stimulate the left dorsolateral prefrontal cortex (DLPFC) to determine its impact on mood. Participants, healthy volunteers exhibiting low mood symptoms, will undergo a four-session protocol with one MRI scan, one practice TMS session, and two experimental TMS sessions. Each participant will experience both sham and real TMS sessions, with brain scans guiding the TMS targeting. Screening for suitability will include checks for TMS/MRI contraindications, psychiatric evaluations, and pre-post session mood assessments.

General Info: 1 study visit, 40 healthy volunteers, 18-45 years old

Scanner: 3T

Category: Category 1a - Healthy Subjects

Staffing levels: 1x scanner operator and 1x researcher

Session Time: 45mins

Incidental Findings Procedure:

Joint SOP Dealing with Research Neuroimaging Incidental Findings
(OHBA_014_V1, FMRIB_002_V5, Neuro_002_V5)

Researchers and their contact details

PI

Prof Jacinta O'Shea
Associate Professor
Department of Psychiatry
07855622790
Jacinta.oshea@psych.ox.ac.uk

Main researcher conducting the experiment

Emilé Radyté
DPhil Student
Department of Psychiatry
07908033202
Emile.radyte@chch.ox.ac.uk

Other Team Members

Verena Sarrazin
Post-Doctoral Fellow
Department of Psychiatry
07759903366
Verena.sarrazin@balliol.ox.ac.uk

Equipment Required

Standard

32 Channel Head Coil
Regular mirror
Ear plugs
Immobilization sponges
Buzzer

Lighting and stimulus

Bore lights on
Room lights on
LCD on if you want to show pretty pictures

Ancillary

None

Protocol Sequences

USER >> OHBA Projects VE11C >> 2023_120 iTBS >> Protocol v1

1. **localiser_3plane_32ch** **14s**
2. **t1_mpr_ax_1mm_iso_withNose_32ch_v2** **7m21s**
 - True axial orientation, do not angle or straighten
 - Cover whole head including nose, ears, vertex and occiput
3. **– 3 x Manual Shim --** **3m0s**
4. **MB8_FMRI_fov210_2.4mm_resting** **6m10s**
 - Axial orientation, angle to ACPC, straighten on coronal if required
 - Cover whole brain
 - Open adjustments, click the 3D Shim tab and do 3x manual shims (ie Measure, Apply (top), Calculate, Apply (bottom))

Resting state instructions: “Please look at the cross on the screen. You are allowed to blink normally. Try not to close your eyes or fall asleep”

5. **fieldmap_210FoV_2.4mm** **1m47s**
 - Auto-copies COSG&SR from 4. MB8_FMRI_fov210_2.4mm_resting
 - **Need to manually copy adj vol from** 4. MB8_FMRI_fov210_2.4mm_resting
 - Click “OK” on the Copy Reference Parameter Conflict prompt

Post Scan

Researcher to return stimulus equipment to default state

A.8 Participant Information Sheet (PIS)

Principal investigator: Dr Jacinta O'Shea
E-mail: jacinta.oshea@psych.ox.ac.uk
Primary researcher: Emilé Radytè, DPhil student
Oxford University email address: emile.radyte@chch.ox.ac.uk

Effect of iTBS on emotional processing

A transcranial magnetic stimulation (TMS) and magnetic resonance imaging (MRI) study

PARTICIPANT INFORMATION SHEET

Version 4, October 31st 2023

Central University Research Ethics Committee Approval Reference: R87506/RE003

We would like to invite you to take part in a research project. This sheet provides some information to help you decide whether to do so. Please take time to read this carefully and discuss it with friends, family or your GP if you wish. If there is anything that you do not understand, or if you would like more information, please ask us. Please take time to consider whether you wish to take part.

What is the purpose of the research?

We are interested in understanding the effects of a brain stimulation protocol on emotion recognition. The stimulation we use is called Transcranial Magnetic Stimulation (TMS), which can stimulate the brain by placing a stimulation coil over the head which generates a magnetic field that passes painlessly through the skull to change activity in the brain underneath. TMS (when applied daily for several weeks) is an approved treatment for depression and has the potential to treat a range of other illnesses. Here we are testing the effect of a single session of different protocols of TMS on people's ability to recognise different emotional facial expressions and perform on learning tasks. We hope that this study will provide us with new information that will ultimately help improve TMS treatment for depression in future.

Why have I been invited to take part?

You have been invited to take part in this research because you are healthy, aged 18 to 45 years of age, right-handed and speak fluent English. For safety reasons we can only include volunteers without a family history of epilepsy and who are not currently taking any medication (other than oral contraceptives). We will be recruiting up to 100 participants in this research.

Do I have to take part?

No. It is up to you to decide if you want to take part in this research. We will describe the research, go through this information sheet with you, and answer any questions you may have. If you agree to take part, we will ask you to sign a consent form and will give you a copy for you to keep. However, you would still be free to withdraw at any time, without needing to give a reason. This would not affect legal rights you would receive. If you withdraw from the study, we will retain any data collected from you up to that point, unless you tell us otherwise. If you are a student, there would be no academic penalty if you do not want to take part, or if you decide to withdraw at any point.

What will happen to me if I take part in the research?

Pre-screening

A researcher will email you to share more information about the study and explain the procedures. Then, you will be asked to give your consent for screening procedures and complete an online pre-screening questionnaire. If your answers indicate that it is safe for you to take part in the research, and that you qualify for the study's requirements, the researcher will then invite you to a 1-hour screening interview to further determine your eligibility for the study.

Screening (30 mins – 1 hr)

The screening interview will be conducted over Microsoft Teams, lasting about 30 minutes and up to 1 hour, for which you will be compensated. This interview will involve questions about your mental health, and resources to support you will be provided if needed. If the researcher determines that you are eligible for the study, you will be invited to participate in the full study, involving 4 visits to the Oxford Centre for Human Brain Activity at the Department of Psychiatry in Oxford (1 of those visits may be to the FMRIB Building at the WIN Centre). If you are not invited to take part in the study following the screening, your screening information will be deleted.

TMS familiarisation (1-1.5 hrs)

During this session, you will be provided with ample time to review the study information once again and have the opportunity to discuss it in detail with the researcher. Following this discussion, if you're comfortable proceeding with the study, you will go through the process of giving informed consent by signing and dating the consent form. Then, you will complete the safety screening form to ensure that it is safe for you to receive stimulation on that day.

During your first visit we will use TMS to stimulate your brain by rapid switching of a magnetic field in a coil placed over the head. You will hear a 'click' sound and may feel a tap on your scalp. You may also feel a brief twitch in your thumb and other right hand muscles. It should NOT be painful.

We will first measure the effects of this stimulation by recording the activity of muscles (electromyography; EMG). EMG activity of the muscle is measured at the surface of the skin by attaching an electrode (small silver disc). Several electrodes will be taped on the skin over muscles on your hands. In the first block, the intensity of stimulation is varied until the EMG recording consistently shows activity in the muscle in response to the stimulation. Once we have determined the minimum intensity at which this muscle activity is observed, we proceed with the research.

We will use an intensity lower than this level for the two test sessions. To give you a better understanding of what the stimulation will feel like, we will deliver a short sample of theta-burst stimulation (which involves bursts of high-frequency (50 Hz) triplets applied every 200ms for 2 s periods, separated by 8 s of rest) over the left front part of your head. We will adjust the stimulation for your comfort. You will have the opportunity to confirm after the stimulation sample whether you wish to continue participating in the study. If so, you will be invited to a neuroimaging session.

MRI (1-1.5 hrs total, 20 mins scanning time)

During this session, the aim is to take an image of your brain (using magnetic resonance imaging, or MRI) that will be used to target a specific brain region with TMS. In the beginning, the researcher will ask some safety questions to confirm that it is safe for you to be scanned that day. Then, you will be provided with some magnet-safe clothing to change into, and complete 15-20 minutes of scanning. During that time, you will not need to do anything specific other than laying at rest in a scanner, after which you will be escorted to change back into your clothing, and the session will be completed.

iTBS session (up to 3 hrs)

During this session, you will first complete a safety and two brief mood questionnaires. Next, you will be given a brief practice of the emotion recognition task. Then, the researcher will use your brain scan to locate the stimulating coil on your head by measuring some sample points on your head. Then, you will receive the theta-burst stimulation described above. The total stimulation time will be 190 seconds (just over 3 minutes, a total of 600 pulses). The stimulation could be in active or sham (i.e. fake) mode. Right after the stimulation, you will complete two tasks, which take about 30 minutes total. Then, you will be given 30 minutes of rest time, during which you are welcome to walk around, read, or work (remotely). After this break, you will receive another stimulation of the same length (just over 3 minutes, a total of 600 pulses). The stimulation could be in active or sham (i.e. fake) mode. Right after the stimulation, you will complete the tasks, which

take about 30 minutes total. Finally, you will complete the brief mood questionnaires again. At the end of the session, we will ask you which of the sessions (real or sham) came first.

Your second iTBS session will be the same as the first, except that a different form of stimulation (biphasic or monophasic) will be used in the two different sessions.

The TMS device used for this study has been developed in our research lab and is not CE marked, however it has been developed and undergone electrical safety testing according to the relevant standards for electrical medical devices, and previous research with humans and modelling has shown it to have the same effect on the brain as conventional, CE-marked TMS devices.

You may experience some discomfort during TMS. This can usually be relieved by adjusting the angle of the stimulating coil. In susceptible individuals, TMS may cause headache, which usually responds well to over-the-counter painkillers (e.g. paracetamol) but remember you can always ask the researcher to stop or adjust the stimulation at any point if you become uncomfortable. The session can be terminated at any point in time, for any reason, including if discomfort cannot be eliminated by adjusting the coil position.

What else do I have to do?

Before you take part in our research, we ask that you get a good night's sleep the night before, so that you are alert. In addition, we ask you not to drink much alcohol (more than 3 units) the day before the visit and none on the day. We also ask that you do not use recreational drugs before the visit. You may drink coffee or tea as normal but please do not drink coffee within one hour of the visit. If you are unsure about any of the above, please talk to the researcher before taking part. We will also remind you of the above prior to your scheduled research visits.

Are there any disadvantages or risks in taking part?

MRI is safe and does not involve any ionising radiation (x-rays). However, because it uses a large magnet to work, MRI scans are not suitable for everybody. You would be asked to answer some safety questions to determine if you can take part. Normally, we would need more information before you take part in the research MRI scan if you have a heart pacemaker or stent, mechanical heart valve, mechanical implants such as an aneurysm clip, joint replacement (e.g. hip/knee), or if you carry other pieces of metal that have accidentally entered your body.

While there is no evidence that MRI is harmful to unborn babies, as a precaution, the Department of Health advises against scanning pregnant women unless there is a clinical benefit. We do not test for pregnancy as routine so if you think you may be pregnant you should not take part in this research.

While very rare, tattoos can occasionally warm up in the scanner. Please inform the person operating the scanner immediately if you feel any heating. If you have a new tattoo, you should not take part in a scan until 48 hours after receiving the tattoo.

If you think you might be claustrophobic, please talk to the researcher in advance, or let the person operating the scanner know before you start.

Some of the scans are noisy, so we will give you earplugs to make this quieter for you. It is important that these are fitted correctly, as they are designed to protect your hearing.

In preparation for your scan and for your comfort and safety we may ask you to change into scrubs ("pyjama-style" top and trousers), available in a range of sizes. You may keep your underwear and socks on, but you will need to remove underwired bras. If you have a suitable non-wired bra, you may wear this instead. Do not wear any fabrics that contain metallic threads or are silver impregnated (often marketed as anti-microbial/bacterial or anti-odour/stink). Metal jewellery, including body piercing, must also be removed. If you wish to wear eye makeup to your scan, we will give you makeup removal wipes because you should not wear eye shadow or mascara in the scanner. Please bring your own makeup to reapply. Lockers are provided to secure your personal belongings and clothing.

You will be introduced carefully to the scanner and allowed to leave at any stage. Whilst in the scanner you will have a call button, which you can press if you need to stop the scan or speak with the person operating the scanner.

It is important to note that we do not carry out scans for diagnostic purposes, only for research. Our scans are not routinely looked at by a doctor and are therefore not a substitute for a doctor's appointment. Occasionally, however, a possible abnormality may be detected. In this case, we would have the scan checked by a doctor. If the doctor felt that the abnormality was medically important, you would be contacted directly and recommended to have a hospital (NHS) diagnostic scan arranged. You would not be informed unless the doctor considers the finding has clear implications for your current or future health. All information about you is kept strictly confidential.

TMS carries a small risk of causing seizures (fits) in susceptible individuals, such as people with a family history of epilepsy, with certain neurological (brain) disease or taking certain medications. The risk of a seizure occurring in healthy individuals due to TMS is extremely small. As a precaution, we will go through a screening form with you to make sure that it is safe for you to participate. If you are taking any medication, you should discuss this with the researcher beforehand. If you suffer with migraine headaches, you should not take part in this research.

How often an individual can safely participate in brain stimulation research is unclear. Many studies use brain stimulation to treat disorders (e.g. depression) and administer stimulation daily, as the therapeutic effects are thought to accumulate across periods of stimulation. Sessions separated by 2 days or more do not show cumulative (carry-over) effects. To minimise the possibility of cumulative effects of brain stimulation we recommend that participants receive brain stimulation on a maximum of two consecutive days and not more than four sessions in one month. While no guideline has been provided for "cooling-off" between stimulation periods, some have suggested it to be between 48 hours and one week after stimulation. Therefore, we recommend that you should not take part in another study using brain stimulation for at least one week after completing this study.

It is our policy not to give TMS to someone who is pregnant. If there is a possibility that you are pregnant, you must not take part in this research.

What are the side effects of TMS?

Participants may experience some discomfort during TMS. In susceptible individuals, TMS may cause headache, which usually goes away on its own or responds well to over-the-counter painkillers (e.g. paracetamol).

Are there any benefits in taking part?

No. There will be no direct benefit to you from taking part in this research. It is hoped that the results from this research will help us to identify better treatments for future studies in patients with medical conditions such as depression.

Expenses and payments

Yes. We will compensate you £15 per hour for your time plus reasonable travel costs for every session. You may also be eligible to receive additional compensation for your performance on the tasks during your two last visits.

What information will be collected and why is the collection of this information relevant for achieving the research objectives?

This study involves the collection of contact details, consent forms, bank details, screening forms, questionnaires and health information.

Authorised scanning centre personnel and the research team will have access to the MRI imaging data. MRI imaging data is assigned a unique ID as it is collected and stored in a secure database within the scanning

system. Due to the nature of these images, they remain potentially identifiable, even after we destroy your personal details. Imaging data will be stored on archive tapes indefinitely, even if you withdraw from this research.

Your contact details will be stored in paper format in lockable file cabinets and in digital format on a secure password-protected firewall-protected university server. They will be deleted once all data has been analysed, unless you agree for your contact details to be kept by us in a database for the purpose of contacting you for future studies. We will keep a copy of your consent form with this database, as your consent is our legal basis for re-contacting you under UK data protection law.

Consent and screening forms will be stored on a password-protected firewall-protected university server for 5 years after final publication of the research. Signed paper consent forms will be stored for 5 years. Where possible, research data will be pseudonymised as soon as possible using an ID number. Only members of the research team conducting the study will have access to the code break. The code break will be destroyed after final analysis of the data. MRI Safety screening forms collected on the day of the scan may be kept for up to 5 years in a secure location by the centre. As part of those 5 years, the forms can be scanned and stored digitally on protected university computers and the paper copies shredded. Your bank details will be stored digitally on Nexus365 OneDrive and deleted after 7 years.

The research team will have access to the research data. Responsible members of the University of Oxford may be given access to data for monitoring and/or audit of the research.

Will the research be published? Could I be identified from any publications or other research outputs?

The University of Oxford is committed to the dissemination of its research for the benefit of society and the economy and, in support of this commitment, has established an online archive of research materials. This archive includes digital copies of student theses successfully submitted as part of a University of Oxford postgraduate degree programme. Holding the archive online gives easy access for researchers to the full text of freely available theses, thereby increasing the likely impact and use of that research.

The research will be written up as a thesis. On successful submission of the thesis, it will be deposited both in print and online in the University archives, to facilitate its use in future research. The thesis will be openly accessible.

We hope to publish the results of this study in a scientific journal. We may also present the results at a scientific conference or a seminar in a university. We may also publish results on our website. We would be happy to discuss the results of the study with you and to send you a copy of the published results. It will not be possible to identify you in any report or publication.

Data Protection

The University of Oxford is the data controller with respect to your personal data and, as such, will determine how your personal data is used in the research. The University will process your personal data for the purpose of the research outlined above. Research is a task that we perform in the public interest. Further information about your rights with respect to your personal data is available from <https://compliance.web.ox.ac.uk/individual-rights>.

Who has reviewed this research?

This study has ethics approval from a subcommittee of the Central University Research Ethics Committee. (Ethics reference: R87506/RE001).

Who is organising and funding the research?

This research is led by Dr Jacinta O'Shea at the Department of Psychiatry and Emilè Radytè, a PhD student. The research is funded by the Medical Research Council, the Wellcome Trust, the Department of Psychiatry, and the Pump Priming Award.

Who do I contact if I have a concern about the research or I wish to complain?

If you have a concern about any aspect of this research, please contact Emilè Radytè (emile.radyte@chch.ox.ac.uk) or Dr Jacinta O’Shea (jacinta.oshea@psych.ox.ac.uk), and we will do our best to answer your query. We will acknowledge your concern within 10 working days and give you an indication of how it will be dealt with. If you remain unhappy or wish to make a formal complaint, please contact the Chair of the Medical Sciences Interdivisional Research Ethics Committee, who will seek to resolve the matter as soon as possible - Email: ethics@medsci.ox.ac.uk; Address: Research Services, University of Oxford, Boundary Brook House, Churchill Drive, Headington, Oxford OX3 7GB.

Further Information and Contact Details

If you would like to discuss the research with someone, or if you have any questions, please contact:

Emilè Radytè
Department of Psychiatry
Warneford Hospital, Oxford OX37JX
University tel: 01865 618200
University email: emile.radyte@chch.ox.ac.uk

A.9 Follow-up Letter for participants not included in the study

Department of Psychiatry
Warneford Hospital, Oxford OX3 7JX

Principal investigator: Dr Jacinta O'Shea
E-mail: jacinta.oshea@psych.ox.ac.uk
Primary researcher: Emilé Radytè, DPhil student
E-mail: emile.radyte@chch.ox.ac.uk



Short-term effects of a monophasic iTBS protocol on emotional processing in participants with low mood

Ethics Approval Reference: R87506/RE001

Dear Volunteer,

Thank you for taking part in this research study. This letter is intended for anyone who indicated on their questionnaires that they may be feeling rather worried or in a low mood. Of course, our moods can change from day to day. However, for some people their mood may remain low for some time. If this applies to you, I would like to point out that there are several sources of advice or help which are free and readily available to you and which may prove useful. Specifically, these include:

1. Your General Practitioner
2. Your College nurse (where available)
3. Your University Counselling Service (where available).
[<http://www.brookes.ac.uk/students/wellbeing/counselling/>,
<https://www.ox.ac.uk/students/welfare/counselling?wssl=1/>]
4. NHS 111 and information online: <https://patient.info/mental-health/depression-leaflet>
5. Helplines,
 - a. The Samaritans 116 123
 - b. The Mental Health Crisis Line 01865 251152
 - c. Listening Service (Oxford University Students) 01865 270270

If you would like additional information, or a confidential discussion with a senior member of the research team, please contact Michael Browning on +44 (0)1865 618316 or michael.browning@psych.ox.ac.uk.

Emilé Radytè

A.10 AP21 CUREC procedure appendix for TMS parameters

Appendix 2: Stimulation parameters for TMS studies

Tables from the Rossi et al., Clinical Neurophysiology 120 (2009): 2008-2039.

Consensus has been reached for safe stimulation parameters for the high and low frequency repetitive TMS used at intensities detailed below in Tables 3-5.

Table 3

Summary of the most employed average stimulation parameters in online interaction rTMS protocols and found to be safe. Consensus has been reached for this table.

rTMS frequency	Number of studies	Average train duration	Average inter-train interval	Average number of trials
4-9 Hz	>10	Variable (see Supplemental material, Table S3)		
10 Hz	>50	5-6 pulse-trains for 400-500 ms	3.2 s	250
20-25 Hz	>20	10 pulse-trains for 400-500 ms	17.1 s	80

Table 4

Maximum safe duration (expressed in seconds) of single trains of rTMS. Safety defined as absence of seizure, spread of excitation or afterdischarge of EMG activity. Numbers preceded by > are longest duration tested. Consensus has been reached for this table.

Frequency (Hz)	Intensity (% of MT)				
	90%	100%	110%	120%	130%
1	>1800 ^a	>1800	>1800	>360	>50
5	>10	>10	>10	>10	>10
10	>5	>5	>5	4.2	2.9
20	2.05	2.05	1.6	1.0	0.55
25	1.28	1.28	0.84	0.4	0.24

^a In Japan, up to 5000 pulses have been applied without safety problems (communication of Y. Ugawa).

Table 5

Adapted from Table 4 (Part A) and Table 3 (part B) of Chen et al., 1997, with permission from the authors. Safety recommendations for inter-train intervals for 10 trains at <20 Hz. The maximum duration of pulses for individual rTMS trains at each stimulus intensity should not exceed those listed in the Part B of the table. A consensus has been reached in adopting this table at this point. However, there is a need to extend these investigations and provide more detailed guidelines that may apply also to non-motor areas.

Inter-train interval (ms)	Stimulus intensity (% of MT)							
	100%		105%	110%	120%		130%	
<i>Part A</i>								
5000	Safe		Safe	Safe	Insufficient data			
1000	Unsafe (EMG spread after 3 trains)		Unsafe ^a	Unsafe (EMG spread after 2 trains)	Unsafe (EMG spread after 2 trains)			
250	Unsafe ^a		Unsafe ^a	Unsafe (EMG spread after 2 trains)	Unsafe (EMG spread after 3 trains)			
<i>Part B</i>								
Frequency (Hz)	100%		110%	120%	120%		130%	
	Duration (s)/pulses		Duration (s)/pulses	Duration (s)/pulses	Duration (s)/pulses		Duration (s)/pulses	
1	>270	>270	>270	>270	>180	>180	50	50
5	10	50	10	50	10	50	10	50
10	5	50	5	50	3.2	32	2.2	22
20	1.5	30	1.2	24	0.8	16	0.4	8
25	1.0	25	0.7	17	0.3	7	0.2	5

^a These stimulus parameters are considered unsafe because adverse events occurred with stimulation of lower intensity or longer inter-train interval, but no adverse effects were observed with these parameters.

For patterned rTMS, such as theta-burst stimulation (TBS), the lack of safety studies means that safety guidelines are not currently available. The Rossi et al., (2009) paper summarizes the TBS protocols published up to 2009 in Table 6 below. Based on our previous approvals for TBS from the NRES committees and this table, we propose that protocols involving TBS should follow the standard parameters described by Huang et al., (2005) for continuous (cTBS) and intermittent (iTBS) as detailed below in Table 6. Stimulation intensities for TBS (biphasic stimulation) should be no greater than 60% of maximal stimulator output or 80% of resting motor threshold.

Table 6

Published TBS (biphasic pulses) and QPS (monophasic pulses) protocols on normal subjects. No significant side effects reported, apart vagal reactions after prefrontal cortex stimulation. Consensus reached for this table.

	Pulses in the burst	Total train pulses	Intensity	Stimulation site
"Standard" cTBS (following Huang et al. 2005) Silvanto et al. 2007	3 at 50 Hz, repeated at 5 Hz	600 (40 s)	80% of active MT	Motor cortex, PFC ^c
	8 at 40 Hz, repeated every 1.8 s	200	60% of the maximal stimulator output	Visual cortex
Nyffeler et al. 2006 ^a "Standard" iTBS protocols (following Huang et al. 2005)	3 at 30 Hz, repeated at 10 Hz	200	80% of resting MT	Frontal eye fields
	3 at 50 Hz, repeated at 5 Hz for 2 s	600	80% of active MT	Motor cortex, PFC ^c
QPS ^b (following Hamda et al., 2008)	4 (ISI ranging 1.5 ms–1.25 s), repeated every 5 s	1440	90% of active MT	Motor cortex

^a Also repeated TBS in the same session (at 5, 15, 60, 75 min).

^b 2000 maximal total pulse number per day; highest intensity used resting MT (Y. Ugawa, personal communication).

^c PFC = prefrontal cortex (Grossheinrich et al. 2009).

A.11 sgACC Localisation Raw Code

```

{
  "cells": [
    {
      "cell_type": "markdown",
      "id": "b7fe8ae1",
      "metadata": {},
      "source": [
        "Download files\n",
        "Calpendo -> Projects -> My files\n",
        "\n",
        "eradyte@jalapeno00.cluster.fmrib.ox.ac.uk \n",
        "tVncserver \n",
        "In another terminal:\n",
        "ssh -C -L 5926:localhost:5926
eradyte@jalapeno00.cluster.fmrib.ox.ac.uk\n",
        "\n",
        "cd /vols/Data/MRdata/eradyte/\n",
        "\n",
        "mv W3T_2023_120_002 /home/fs0/eradyte/Desktop/xTMS/raw\n",
        "\n",
        "rename folder to sub-0X\n",
        "\n",
        "run ./clean.sh"
      ]
    },
    {
      "cell_type": "markdown",
      "id": "3ca4b408",
      "metadata": {},
      "source": [
        "# A. Pre-processing other files needed in the analysis\n"
      ]
    },
    {
      "cell_type": "markdown",
      "id": "f290ee3d",
      "metadata": {},
      "source": [
        "## 1. Pre-process T1 scans\n",
        "\n",
        "This step is needed to do basic cleaning and preparation of
structural images. T1 processing (fsl_anat) involves:\n",
        "\n",
        "Reorientation: The anatomical image is reoriented to the standard
orientation for L/R, AP. This ensures consistency across different
datasets.\n",
        "\n",
        "Cropping: The image is cropped to remove unnecessary parts,
focusing on the brain region. This helps in reducing computational
requirements for subsequent steps.\n"
      ]
    }
  ]
}

```

```

    "\n",
    "Segmentation: The brain image is segmented into different tissue
types, typically grey matter, white matter, and cerebrospinal fluid.
This is crucial for various analyses, such as voxel-based morphometry.
This is done using the K-means iterations you'll see in the output.
\n",
    "\n",
    "Bias Field Correction: MRI images can sometimes have intensity
inhomogeneities due to variations in the magnetic field. fsl_anat
corrects for these inhomogeneities, ensuring that the image intensity
is uniform across the entire brain. This is done using the Tanaka
inner loop iterations you'll see in the output.\n",
    "\n",
    "Registration: The anatomical image is registered to a standard
MNI space. This involves two steps:\n",
    "\n",
    "Linear Registration: A linear transformation (e.g., rotation,
translation) is applied to match the image to the standard space.\n",
    "\n",
    "Non-linear Registration: A more complex, non-linear
transformation is applied to ensure a better fit to the standard
template.\n",
    "\n",
    "Non-linear registration is usually more advanced and achieves
better fit.\n",
    "\n",
    "Brain Extraction: This step involves removing non-brain tissues
from the image, resulting in a brain-only image. This is often done
using the BET (Brain Extraction Tool) in FSL.\n",
    "\n",
    "Segmentation of sub-cortical structures: In this case, no sub-
cortical segmentation is performed.\n",
    "\n",
    "Skull-Constrained Registration: This is a specialized
registration that takes into account the presence of the skull,
ensuring a better alignment of the brain with the standard template.
\n",
    "\n",
    "Cleanup: Intermediate files that were generated during the
processing and are no longer needed are cleaned up to save space.\n",
    "\n",
    "### Practical steps (up to 30 mins)\n",
    "\n",
    "1. Make sure folders are in bids format\n",
    "2. Confirm the T1_processing.sh file is set up appropriately\n",
    "2. If you haven't yet enabled the code, allow it to execute and
write with chmod u+x T1_processing.sh \n",
    "3. Run the script to perform the aforementioned steps: ./
T1_processing.sh\n",
    "\n",

```

```

    "### Validation step\n",
    "1. Open the brain-extracted, segmented image (not MNI-registered)
& the original T1 and confirm (visual check) that the segmentation,
brain extraction, cropping, etc is appropriate.\n"
  ]
},
{
  "cell_type": "markdown",
  "id": "b2879dc6",
  "metadata": {},
  "source": [
    "## 2. Pre-process single-band reference for brain extraction and
bias correction \n",
    "\n",
    "This step is needed to prepare the single-band reference image
for processing multi-band scans.\n",
    "\n",
    "Single-band reference pre-processing involves:\n",
    "\n",
    "Reorienting to Standard Orientation: The SBREF image is
reoriented to match a standard orientation (L/R, A/P), ensuring
consistency across datasets.\n",
    "\n",
    "Automatically Cropping the Image: Unnecessary parts of the image,
which might not contain any brain data, are removed.\n",
    "\n",
    "Single Image Segmentation: The SBREF image, which is T2-weighted
in this case, is segmented. The image dimensions and voxel sizes are
provided.\n",
    "\n",
    "Tissue Segmentation: The KMeans clustering algorithm is applied
for tissue classification (grey matter/white matter/CSF) based on
voxel intensities.\n",
    "\n",
    "Bias Field Corrections: Tanaka iterations are applied, each with
inner loops. The method adjusts for intensity inhomogeneities in the
MRI images.\n",
    "\n",
    "Extrapolating Bias Field from Central Region: The bias field,
which represents the intensity inhomogeneities, is extrapolated from
the central region of the image.\n",
    "\n",
    "Registering to Standard Space (Linear): The SBREF image is
registered to a standard space using linear transformations.\n",
    "\n",
    "Cleaning Up Intermediate Files: Temporary files created during
the preprocessing are removed.\n",
    "\n",
    "\n",
    "### Practical steps (up to 10 mins)\n",

```

```

    "1. Make sure folders are in bids format\n",
    "2. Confirm the sbref_processing.sh file is set up appropriately.
\n",
    "2. If you haven't yet enabled the code, allow it to execute and
write with chmod u+x sbref_processing.sh \n",
    "3. Run the script to perform the aforementioned steps: ./
sbref_processing.sh\n",
    "\n",
    "### Validation step\n",
    "1. Confirm the single band reference file was appropriately
created and processed, now available in the derivatives folder."
]
},
{
  "cell_type": "markdown",
  "id": "c45c8563",
  "metadata": {},
  "source": [
    "## 3. Processes the magnitude and phase image from the fieldmaps
into the files needed for feat/melodic analysis\n",
    "\n",
    "This step is needed to prepare the main fieldmap image needed for
Melodic ICA.\n",
    "\n",
    "1. This processing step first takes the phase difference image
that captures the phase differences caused by field inhomogeneities,
as well as the magnitude image that is used to aid in the unwarping
process and brain mask.\n",
    "2. Then, it constrains the phase values within the range of  $[-\pi,$ 
 $\pi]$  for rewrapping.\n",
    "3. Finally, the phase image undergoes unwrapping to remove the
 $2\pi$  jumps and produce a smooth fieldmap and outputs a processed
fieldmap that is ready to use in further processing.\n",
    "\n",
    "*primer on rewrapping and unwrapping of fieldmaps*\n",
    "\n",
    "Phase Rewrapping:\n",
    "\n",
    "Nature of Phase Images: Phase images from MRI scanners typically
provide values in a wrapped range, often between  $0$  and  $2\pi$  or  $-\pi$  to  $\pi$ .
This wrapping occurs because the phase values represent angles in a
circular manner, and once the phase completes a full circle ( $2\pi$ 
radians), it starts over.\n",
    "\n",
    "Problem: The true phase differences due to field inhomogeneities
can exceed the range of  $-\pi$  to  $\pi$ , causing the phase values to wrap
around. This wrapping can introduce artificial jumps in the phase
image, making it challenging to interpret and use for correction.\n",
    "\n",
    "Solution: Phase rewrapping ensures that all phase values are

```

```

constrained within the range of  $-\pi$  to  $\pi$ , providing a consistent
starting point for the unwrapping process.\n",
  "\n",
  "Phase Unwrapping:\n",
  "\n",
  "Nature of Field Inhomogeneities: Field inhomogeneities in the MRI
scanner can cause spatial variations in the magnetic field. These
variations lead to phase accumulations in the acquired MRI data, which
can be captured in the phase images.\n",
  "\n",
  "Problem: The wrapped phase images can have abrupt  $2\pi$  jumps,
making it difficult to discern the true underlying phase differences
caused by field inhomogeneities.\n",
  "\n",
  "Solution: Phase unwrapping aims to remove these  $2\pi$  jumps to
produce a smooth, continuous phase image that accurately represents
the field inhomogeneities. This unwrapped phase image can then be used
to calculate the fieldmap, which quantifies the field deviations in
terms of frequency (e.g., Hz). The fieldmap is crucial for correcting
geometric distortions in EPI (Echo Planar Imaging) sequences, commonly
used in fMRI.\n",
  "\n",
  "### Practical steps (up to 15 mins)\n",
  "1. Make sure folders are in bids format.\n",
  "2. Confirm fieldmap_processing.sh is set up appropriately for the
participant.\n",
  "2. If you haven't yet enabled the code, allow it to execute and
write with chmod u+x fieldmap_processing.sh.\n",
  "3. Run the script to perform the aforementioned steps: ./
fieldmap_processing.sh\n",
  "\n",
  "### Validation step\n",
  "1. Confirm you have the processed files, especially the _rads
file in the derivatives folder. Open to confirm it looks as expected."
]
},
{
  "cell_type": "markdown",
  "id": "590bb637",
  "metadata": {},
  "source": [
    "# B. Running Melodic, denoising, smoothing & registering"
  ]
},
{
  "cell_type": "markdown",
  "id": "7cc49b91",
  "metadata": {},
  "source": [
    "### 4. Run single session melodic (2.5–3 hrs)\n",

```

```

"\n",
"This step is needed to run a first-level Melodic ICA, with the
following features:\n",
"\n",
"Pre-Stats\n",
"1. Single-subject data processing\n",
"2. Motion correction performed using MCFLIRT\n",
"3. Enabled B0 fieldmap unwarping\n",
"4. Interleaved slice timing correction performed\n",
"5. Brain extraction performed\n",
"6. No spatial smoothing applied at this stage\n",
"7. Enabled high-pass filtering (100)\n",
"Registration\n",
"8. Registration to an initial structural image is enabled.\n",
"9. Registration to a main structural image is enabled.\n",
"10. Registration to a standard image (MNI152_T1_2mm_brain) is
enabled, with nonlinear registration also applied.\n",
"11. Single-session ICA performed\n",
"12. Automatic dimensionality estimation is enabled, meaning the
number of components will be determined automatically.\n",
"13. IC maps will be thresholded.\n",
"14. The mixture model threshold is set to 0.5.\n",
"Stats\n",
"15. Main stats are enabled.\n",
"16. Prewhitening is enabled.\n",
"17. The thresholding method is set to cluster-based, with a Z
threshold of 3.1 and a P threshold of 0.05.\n",
" \n",
"Notes on the template:\n",
"- no spatial smoothing\n",
"- use raw sbref as the alternate image\n",
"- use T2_biascorr_brain sbref in the registration. \n",
"- 6DOF for registration between initial_highres and high_res.\n",
"\n",
"### Practical steps (3-6 hrs)\n",
"1. Confirm the design_ss_rest_melodic_2mmstd.sh script is set up
appropriately for the participant.\n",
"2. Run the design_ss_rest_melodic_2mmstd.sh script to create the
melodic template for the actual participant. The script creates a
single-subject melodic .fsf design file for each participant/session.
\n",
"3. Open fsl &, select Melodic ICA, upload the .fsf file for the
participant.\n",
"4. Verify and click \"Go\"\n",
"\n",
"### Validation step\n",
"1. Review the Melodic output and manually inspect the
registration output and the ICA components to ensure appropriate
registration quality.\n"
]

```

```

},
{
  "cell_type": "markdown",
  "id": "ef0260e7",
  "metadata": {},
  "source": [
    "## 5. Run fix to distinguish signal/noise from the Melodic
ICA\n",
    "\n",
    "This step is needed to be able to identify signal from noise in
the Melodic ICA. \n",
    "\n",
    "1. Firstly, for our purposes, the FIX algorithm is trained on UK
BioBank data as a training dataset to be able to identify signal from
noise.\n",
    "2. Then, FIX takes the ICA components identified by Melodic and
for each independent component, FIX extracts a large number of
spatial, temporal, and frequency domain features. These features help
in distinguishing between signal (neuronal activity) and noise (motion
artifacts, physiological noise, etc.).\n",
    "3. Using its pre-trained classifier (here - with UK BioBank) FIX
classifies each component as either \"signal\" or \"noise.\" The
classifier has been trained on labeled components from the training
dataset, allowing it to recognize patterns associated with noise in
new datasets.\n",
    "4. Once the components are classified, FIX regresses out the time
courses of the components labeled as \"noise\" from the original 4D
fMRI dataset. This step effectively removes the noise contributions
from the data.\n",
    "\n",
    "### Practical steps (2-3 hrs)\n",
    "1. Confirm the run_fix.sh script is set up appropriately for your
participant. \n",
    "2. Enable the script.\n",
    "2. Use the run_fix.sh script to run fix using UK BioBank data for
the software + training data there. Don't use the -h or -m flag.\n",
    "\n",
    "### Validation step\n",
    "1. Manually review the FIX classifications and adjust them if
needed. You would do this by opening the edge files and inspecting
each of the components. For example, a component with a score of 95 in
the edge file is very likely to be noise, whereas a component with a
score of 5 is likely to be a signal. \n",
    "2. You can also inspect the timecourses and frequency spectra:
\n",
    "\n",
    "2a) Timecourses: Look at the temporal dynamics of each component.
\n",
    "Signal Components: Should have time courses that look plausible
for neuronal activity, with smooth fluctuations.\n",

```

```

    "Noise Components: Might have sharp spikes (indicative of motion artifacts) or other non-neuronal patterns like high-frequency noise.\n",
    "\n",
    "2b) Frequency spectrum: Examine the power spectrum of each component's time course.\n",
    "Signal Components: Typically have a 1/frequency-like decay.\n",
    "Noise Components: Might have a different spectral pattern, especially if they are related to physiological noise like heartbeat or respiration."
  ]
},
{
  "cell_type": "markdown",
  "id": "6dd5d2d8",
  "metadata": {},
  "source": [
    "## 6. Post-fix smoothing and registering\n",
    "1. Use the post_fix_smooth_and_reg.sh script to smooth and register to MNI space."
  ]
},
{
  "cell_type": "markdown",
  "id": "1e2d2ec6",
  "metadata": {},
  "source": [
    "# C. Creating ROIs"
  ]
},
{
  "cell_type": "markdown",
  "id": "ea7db789",
  "metadata": {},
  "source": [
    "## 7. Creating sgACC seed ROI\n",
    "1. On fsleyes, go to Tools->Edit mode for filtered_func_data_clean_s5_std.nii.gz\n",
    "2. Make a copy\n",
    "3. Select \"select mode\", incremental change, 3D and radius-limited options with a radius size of 5 mm\n",
    "4. Navigate to the [-6, 16, -10] for the left sgACC and [6, 16, -10] for the right sgACC.\n",
    "5. Select and save the mask in the output/ROI folder as seed.nii.gz.\n",
    "\n",
    "### Validation step\n",
    "1. echo \"-6 16 -10\" > MNI_coordinates.txt\n",
    "2. convert_xfm -omat standard2example_func.mat -inverse example_func2standard.mat \n",

```

```

    "3. std2imgcoord -img example_func.nii.gz -std
MNI152_T1_2mm.nii.gz -xfm standard2example_func.mat -vox -mm <
MNI_coordinates.txt\n",
    "4. std2imgcoord -img example_func.nii.gz -std /opt/fmrib/fsl/
data/standard/MNI152_T1_2mm.nii.gz -xfm standard2example_func.mat -vox
-mmm < MNI_coordinates.txt\n"
]
},
{
    "cell_type": "markdown",
    "id": "3da966ae",
    "metadata": {},
    "source": [
        "## 8. Create DLPFC ROI mask\n",
        "1. On fsleyes, go to Edit mode\n",
        "2. Select \"select mode\", incremental change, 3D and radius-
limited options with a radius size of 10 mm\n",
        "3. Navigate to the [-36, 39, 43] for the BA9 area and [-44, 40,
29] for the BA46 area.\n",
        "4. Select and save the mask in the output/ROI folder as
target.nii.gz.\n",
        "\n",
        "### Validation step\n",
        "1. echo \"-6 16 -10\" > MNI_coordinates.txt\n",
        "2. convert_xfm -omat standard2example_func.mat -inverse
example_func2standard.mat \n",
        "3. std2imgcoord -img example_func.nii.gz -std
MNI152_T1_2mm.nii.gz -xfm standard2example_func.mat -vox -mm <
MNI_coordinates.txt\n",
        "4. std2imgcoord -img example_func.nii.gz -std /opt/fmrib/fsl/
data/standard/MNI152_T1_2mm.nii.gz -xfm standard2example_func.mat -vox
-mmm < MNI_coordinates.txt\n"
]
},
{
    "cell_type": "markdown",
    "id": "7a61adca",
    "metadata": {},
    "source": [
        "# D. Creating correlation maps"
]
},
{
    "cell_type": "markdown",
    "id": "0332b872",
    "metadata": {},
    "source": [
        "launching the cluster for fsl_sub ./dlpfc_localisation.sh from
the scripts folder\n",
        "\n",

```

```

        "use qstat -u eradyte to check progress of task\n",
        "\n",
        "std2imgcoord -img rest.ica/reg/example_func.nii.gz -std /opt/
fmrib/fsl/data/standard/MNI152_T1_2mm.nii.gz rest.ica/reg/
example_func2standard.mat -mm target_MNI_coordinates.txt"
    ]
},
{
    "cell_type": "markdown",
    "id": "56046b8e",
    "metadata": {},
    "source": [
        "## 9. Extract seed mean time series data\n",
        "1. fslmeants -i filtered_func_clean_s5_std.nii.gz -o
seed_sub-0X_timecourse.txt -m seed_sub-0X.nii.gz"
    ]
},
{
    "cell_type": "markdown",
    "id": "64c4202b",
    "metadata": {},
    "source": [
        "## 10. Create Whole-brain Correlation Maps (R^2) using
fsl_glm\n",
        "1. fsl_glm -i filtered_func_clean_s5_std.nii.gz -d
seed_sub-0X_timecourse.txt -o corr_map_sub-0X.nii.gz --
out_z=zmap_sub-0X.nii.gz --out_p=pmap_sub-0X.nii.gz\n"
    ]
},
{
    "cell_type": "markdown",
    "id": "71a22465",
    "metadata": {},
    "source": [
        "## 11. Masking the correlation maps\n",
        "fslmaths corr_map_sub-0X.nii.gz -mas DLPFC_target_sub-0X.nii.gz
masked_corr_map_sub-0X.nii.gz"
    ]
},
{
    "cell_type": "markdown",
    "id": "0d647752",
    "metadata": {},
    "source": [
        "# E. Identifying the peak cluster"
    ]
},
{
    "cell_type": "markdown",
    "id": "5d9015b3",

```

```

    "metadata": {},
    "source": [
      "## 12. Setting an image threshold of 75% of the maximum z-
score\n",
      "max_z=$(fslstats zmap_sub-0X.nii.gz -R | awk '{print $2}')\n",
      "threshold_value=$(echo \"\${max_z} * 0.75\" | bc)\n",
      "fslmaths zmap_sub-0X.nii.gz -thr $threshold_value
thresholded_zmap_sub-0X.nii.gz\n",
      "fslmaths masked_corr_map_sub-0X.nii.gz -mas
thresholded_zmap_sub-0X.nii.gz final_masked_corr_map_sub-0X.nii.gz"
    ]
  },
  {
    "cell_type": "markdown",
    "id": "bbcb34ff",
    "metadata": {},
    "source": [
      "## 13. Identifying the peak cluster\n",
      "cluster --in=final_masked_corr_map_sub-0X.nii.gz --thresh=3.1 --
oindex=clustered_image_sub-0X --mm"
    ]
  },
  {
    "cell_type": "markdown",
    "id": "031f584a",
    "metadata": {},
    "source": [
      "## 14. Select DLPFC stimulation target coordinates\n",
      "1. Select the DLPFC parcel/coordinates that are most anti-
correlated with the sgACC seed as the stimulation target.\n",
      "2. To follow Siddiqi et al 2023 protocols, choose the COG
coordinates for stimulation.\n",
      "\n",
      "invwarp -w example_func2standard_warp.nii.gz -o
example_func2standard_invwarp -r example_func.nii.gz\n",
      "\n",
      "cat target_MNI_coordinates.txt | std2img..coord -img /rest.ica/
reg/highres2standard.nii -std /opt/fmrib/fsl/data/standard/
MNI152_T1_2mm.nii.gz -warp example_func2standard_invwarp.nii.gz -mm -
\n",
      "\n",
      "\n",
      "convert_xfm -omat rest.ica/reg/standard2example_func.mat -inverse
rest.ica/reg/example_func2standard.mat\n",
      "std2imgcoord -img rest.ica/reg/example_func.nii.gz -std /opt/
fmrib/fsl/data/standard/MNI152_T1_2mm.nii.gz -xfm \n",
      "rest.ica/reg/standard2example_func.mat -vox -mm <
target_MNI_coordinates.txt"
    ]
  },
  },

```

```

{
  "cell_type": "markdown",
  "id": "5c55d29c",
  "metadata": {},
  "source": [
    "# F. Guiding TMS to target coordinates"
  ]
},
{
  "cell_type": "markdown",
  "id": "ca9d37b9",
  "metadata": {},
  "source": [
    "## 15. Download participant raw T1 onto Brainsight machine\n",
    "1. scp -r eradyte@jalapeno.fmrib.ox.ac.uk:/home/fs0/eradyte/
Desktop/xTMS/derivatives/sub-07/anat/sub-07_T1w.nii ~/Desktop/"
  ]
},
{
  "cell_type": "markdown",
  "id": "437c9cff",
  "metadata": {},
  "source": [
    "## 16. Preprocess T1 to MNI on Brainsight\n",
    "1. Use AC-PC coordinates to register the participant's native
space to MNI coordinates\n",
    "2. Add layers of skin and smoothed brain\n",
    "3. Add reference points (nasion,inion, lpa and rpa) for
neuronavigation"
  ]
},
{
  "cell_type": "markdown",
  "id": "f3563ceb",
  "metadata": {},
  "source": [
    "## 17. Use MNI target coordinates to inversely transform back
into the structural brain scan\n",
    "1. Add in MNI target coordinates\n",
    "2. Use trajectory optimisation to determine optimal coil
positioning\n",
    "3. Save as DLPFC_target"
  ]
},
{
  "cell_type": "markdown",
  "id": "748b7f30",
  "metadata": {},
  "source": [
    "## 18. Start a neuronavigation session with the target

```

```

coordinates\n",
  "1. Save the Brainsight setup as the subject's number\n",
  "2. Start online session\n",
  "3. Select DLPFC_target as the target\n",
  "4. Proceed with neuronavigation steps (registration, calibration,
perform)"
]
},
{
  "cell_type": "code",
  "execution_count": null,
  "id": "96ef44f3",
  "metadata": {},
  "outputs": [],
  "source": []
}
],
"metadata": {
  "kernelspec": {
    "display_name": "Python 3",
    "language": "python",
    "name": "python3"
  },
  "language_info": {
    "codemirror_mode": {
      "name": "ipython",
      "version": 3
    },
    "file_extension": ".py",
    "mimetype": "text/x-python",
    "name": "python",
    "nbconvert_exporter": "python",
    "pygments_lexer": "ipython3",
    "version": "3.8.8"
  }
},
"nbformat": 4,
"nbformat_minor": 5
}

```

B | 7T MRI Study Documents

Table of Contents

B.1 Ethics (NHS) Approval	236
B.2 Participant Information Sheet (PIS)	241
B.3 7T MRI Scanning Protocol	247

B.1 Ethics (NHS) Approval



Health Research Authority

NRES Committee South Central - Oxford B

Bristol Research Ethics Committee Centre
Whitefriars
Level 3, Block B
Lewin's Mead
Bristol
BS1 2NT

Telephone: 0117 342 1333
Facsimile: 0117 342 0445

22 August 2013

Prof Philip Cowen
MRC Clinical Scientist
Medical Research Council
Neurosciences Building
Warneford Hospital
Oxford
OX37JX

Dear Prof Cowen

Study title: Understanding brain neurochemistry in depression
using magnetic resonance spectroscopy at 7T
REC reference: 13/SC/0328
IRAS project ID: 128597

Thank you for your letter of 17 July 2013, responding to the Committee's request for further information on the above research and submitting revised documentation.

The further information has been considered on behalf of the Committee by the Chair.

We plan to publish your research summary wording for the above study on the NRES website, together with your contact details, unless you expressly withhold permission to do so. Publication will be no earlier than three months from the date of this favourable opinion letter. Should you wish to provide a substitute contact point, require further information, or wish to withhold permission to publish, please contact the Co-ordinator Mrs Siobhán Bawn, NRESCommittee.SouthCentral-Oxfordb@nhs.net.

Confirmation of ethical opinion

On behalf of the Committee, I am pleased to confirm a favourable ethical opinion for the above research on the basis described in the application form, protocol and supporting documentation as revised, subject to the conditions specified below.

Ethical review of research sites

NHS sites

The favourable opinion applies to all NHS sites taking part in the study, subject to management permission being obtained from the NHS/HSC R&D office prior to the start of the study (see "Conditions of the favourable opinion" below).

Non-NHS sites

Conditions of the favourable opinion

The favourable opinion is subject to the following conditions being met prior to the start of the study.

Management permission or approval must be obtained from each host organisation prior to the start of the study at the site concerned.

Management permission ("R&D approval") should be sought from all NHS organisations involved in the study in accordance with NHS research governance arrangements.

Guidance on applying for NHS permission for research is available in the Integrated Research Application System or at <http://www.rdforum.nhs.uk>.

Where a NHS organisation's role in the study is limited to identifying and referring potential participants to research sites ("participant identification centre"), guidance should be sought from the R&D office on the information it requires to give permission for this activity.

For non-NHS sites, site management permission should be obtained in accordance with the procedures of the relevant host organisation.

Sponsors are not required to notify the Committee of approvals from host organisations

It is the responsibility of the sponsor to ensure that all the conditions are complied with before the start of the study or its initiation at a particular site (as applicable).

Approved documents

The final list of documents reviewed and approved by the Committee is as follows:

<i>Document</i>	<i>Version</i>	<i>Date</i>
Advertisement	2, Depressed	26 May 2013
Advertisement	2, Healthy	26 May 2013
Covering Letter		29 May 2013
Evidence of insurance or indemnity	GCW Letter	
GP/Consultant Information Sheets	2	26 May 2013
Investigator CV	Prof Cowen	24 April 2013
Letter from Sponsor		04 June 2013
Letter of invitation to participant	1, Email to	28 May 2013

	previous volunteers	
Letter of invitation to participant	1, Invitation Email	29 May 2013
Other: Letter from Funder	MRC Feedback and Peer Review	
Other: CV for Ann Sharpley		13 May 2013
Other: CV for Beata Godlewska		13 April 2013
Other: CV for Clare Williams		08 April 2013
Other: CV for Uzay Emir		07 May 2013
Participant Consent Form: Controls	3	27 May 2013
Participant Consent Form: Patients	4	16 July 2013
Participant Information Sheet: Patients	4	16 July 2013
Participant Information Sheet: Controls	4	16 July 2013
Protocol	2	25 May 2013
Questionnaire: BDI		
Questionnaire: Spielberger state anxiety		
Questionnaire: Chandler Fatigue Scale		
Questionnaire: HAM-D		
Questionnaire: Snaith-Hamilton Anhedonia Scale		
REC application	3.5	07 June 2013
Response to Request for Further Information		17 July 2013

Statement of compliance

The Committee is constituted in accordance with the Governance Arrangements for Research Ethics Committees and complies fully with the Standard Operating Procedures for Research Ethics Committees in the UK.

After ethical review

Reporting requirements

The attached document “*After ethical review – guidance for researchers*” gives detailed guidance on reporting requirements for studies with a favourable opinion, including:

- Notifying substantial amendments
- Adding new sites and investigators
- Notification of serious breaches of the protocol
- Progress and safety reports
- Notifying the end of the study

The NRES website also provides guidance on these topics, which is updated in the light of changes in reporting requirements or procedures.

Feedback

You are invited to give your view of the service that you have received from the National Research Ethics Service and the application procedure. If you wish to make your views known please use the feedback form available on the website.

Further information is available at National Research Ethics Service website > After Review

13/SC/0328

Please quote this number on all correspondence

We are pleased to welcome researchers and R & D staff at our NRES committee members' training days – see details at <http://www.hra.nhs.uk/hra-training/>

With the Committee's best wishes for the success of this project.

Yours sincerely



Mr Chris Foy
Chair

Email: NRESCommittee.SouthCentral-Oxfordb@nhs.net

Enclosures: "After ethical review – guidance for researchers" [Emailed]

Copy to: Ms Heather House

Mrs Sue Jones

B.2 Participant Information Sheet (PIS)

UNIVERSITY OF OXFORD



Neurosciences
Dept of Psychiatry
Warneford Hospital
Oxford
OX3 7JX

Tel. (01865) 226394
Fax. (01865) 251076
E-mail: phil.cowen@psych.ox.ac.uk

Professor P J Cowen
Hon Consultant Psychiatrist

Information Sheet for Patients

Depression and proton MRS at 7T

You are being invited to take part in a research study. Before you decide, it is important for you to understand why the research is being done and what it will involve. Please take time to read the following information carefully and discuss it if you wish with family, friends and your GP. Ask us if there is anything that is not clear or if you would like more information. Take time to decide whether you wish to take part.

Part 1 of this information sheet tells you the purpose of this study and what will happen to you if you take part. Part 2 gives you more detailed information about the conduct of the study).

PART ONE

What is the purpose of the study?

Clinical depression is a common condition. There are effective psychological and drug treatments available to help people with depression but they do not suit everyone and new approaches are needed. In fact, it has proved particularly difficult to develop new drug treatments for depression because not much is known about the chemical changes in the brain that cause depression.

Advances in brain imaging using powerful magnets mean that it is now possible to measure brain chemicals with much greater accuracy than previously and we have access to an advanced brain imaging system at the John Radcliffe Hospital at the Oxford Centre for Functional Imaging of the Brain (fMRIB) (www.fmrib.ox.ac.uk). The aim of this study is to use this new imaging system (magnetic resonance spectroscopy; MRS) to examine brain chemicals in people with depression. In this work we will focus particularly on a natural chemical messenger called glutamate which is thought to be involved in mood regulation. Some people with depression also have changes in the blood which suggest inflammation and also increased production of a stress hormone called cortisol; these bodily changes may also influence brain chemicals. Therefore to improve our understanding of any brain chemical changes that we see, we would also like to carry out some simple measures of inflammation in the blood and cortisol. Finally, if you agree, we would like to continue to see you about every two weeks for about 12 weeks from the start of your treatment to see

whether any of the measures we have made might have a bearing on how well psychological and/or drug treatment suits you on this occasion.

Why have I been chosen?

We are asking you to participate as someone who currently is suffering from clinical depression. Altogether we plan to study 70 depressed patients in this study and 50 people with no history of depression.

Do I have to take part?

This is a research study so it is completely up to you whether or not you take part. If you agree to take part we will give you this information sheet to keep and will ask you to sign a consent form. Even if you agree to take part you can withdraw from the study at any time without giving a reason and without any effect on your current or future treatment.

What will happen to me?

Below we describe the main parts of the research study:

Consent and screening

If you agree to take part in the study we will ask you to sign a consent form saying that you understand the study procedures and agree to take part in the study. You can take at least a week to decide if you want to take part.

For the screening visit we would like you to come to the Neurosciences Building at the Warneford Hospital. Here, we would ask you some questions about your general health and your mood over the last few years. We would also like you to complete some questionnaires about mood, anxiety, energy levels and enjoyment. In addition, The Childhood Trauma Questionnaire asks about some of your experiences growing up as a child and a teenager and are of a personal nature. Altogether this would take about 60-90 minutes. We would also take a single blood sample of a volume of about 20mls which will enable us to measure the level of inflammatory markers. Finally, we would ask you to provide some samples of saliva from which we will be able to measure cortisol. This involves sampling saliva in some special tubes (which we will provide) on a day of your choice, at home. You would take a sample on waking and two further samples while you rest quietly over the next 30 minutes. A fourth sample should be taken at about 10.00pm in the evening of the same day, before you go to bed.

MRS scanning

The MRS scanning will take place at the Oxford Centre for Functional Imaging of the Brain (FMRIB) at the John Radcliffe Hospital and will be within about week of the screening interview. The scan will take about 60 minutes. You will not have to do anything during the scan which will be in two main parts, the first to measure brain chemicals and the second to measure the pattern of how well the different brain regions connect with each other.

The scanner is a large cube shape. Running through the middle of the scanner is a tube, which is open at both ends. You will enter the scanner head-first and your feet will remain outside the tube. During the scan you will hear some tapping and beeping noises. The radiographer and researcher will be able to see you throughout the scan and we will provide you with a call button, which you can press at any time if you want to come out of the scanner. The scanner makes a loud knocking noise when it is running, and therefore participants will be provided with earplugs and protective headphones during the scan. There are no known risks of MRS scanning provided standard safety guidelines are followed carefully.

Follow up

If you agree to be seen during your treatment we will ask you to complete the same rating scales you completed at the assessment every two weeks. This will take about 20 minutes. We will be happy to give you your treatment or it can be carried out by your GP, whichever you prefer. We will be happy to discuss the various treatment options as set out in the current NICE guideline for the treatment of depression (<http://www.nice.org.uk/CG90>).

Expenses and payments

We will reimburse any expenses you incur taking part in the study (for example, travel expenses) and will also offer a payment of £50 to all participants who take part in the scanning as reimbursement for time and inconvenience

What will I have to do?

The main requirement is to take attend for appointments and brain scanning when arranged.

What are the possible disadvantages and risks of taking part?

The use of magnets means that the scan procedure is not suitable for people with pacemakers, mechanical heart valves and hip replacements or with other metal implants in their body. If you are pregnant you should not take part. If there is a possibility of you being pregnant we would wish to carry out a pregnancy test prior to the scan. If you have suffered previously from anxiety in confined spaces it would be better not to take part.

Having a blood test by venipuncture can cause discomfort and there is a risk of bruising.

While the brain scans we will carry out are not designed for diagnosis of any particular medical condition, you should be aware that there is a possibility that they may produce an unexpected result. In the unlikely event of this happening we would have the scan checked by a clinical doctor and hospital radiologist (an imaging specialist), in case the abnormality was simply due to the way the scan was carried, with no relevance for your health. If the radiologist and clinician felt, however, that the abnormality might be medically important, we would discuss this with you and, if necessary, provide any support that you may require, such as contacting your GP or arranging follow-up tests and/or treatment. You would be withdrawn from the study, but all information about you kept strictly confidential. It is important to note that we do not carry out scans for diagnostic purposes, and therefore these scans are not a substitute for a clinical appointment. Rather, our scans are intended for research purposes only. For this reason it is also not possible to have copies of your brain scan.

Sometimes, questions covered in the screening interview or self-report questionnaires can cause distress. Any concerns or issues which may arise as a result of the screening procedures can be discussed in confidence with the research psychiatrist or if you prefer, your GP. Alternatively, contact details of relevant support agencies are outlined below:

Oxford Samaritans: <http://www.samaritans.org/branches/oxford-samaritans> Oxford Sexual Abuse and Rape Crisis Centre: <http://www.oxfordrapecrisis.net/>
The Survivors Trust: <http://www.thesurvivorstrust.org/information-for-survivors/>

What are the benefits of taking part?

The study will not be of direct benefit to you but we hope that the information we obtain will help improve the treatment of depression. Being a participant in a study does result in greater frequency of contact with clinical staff, which some people find helpful and supportive.

Will my taking part in the study be kept confidential?

Yes. We will follow ethical and legal practice and all information about you will be handled in confidence. The details are included in Part 2.

If the information in Part 1 has interested you and you are considering participation please read the additional information in Part 2 before making any decision.

PART TWO

What will happen if I don't want to carry on with the study?

You can leave the study at any time. We will discuss with you what further treatment (if any) you would like to have and who you would like to carry it out. If you have had the MRS scan and blood and saliva tests we would still like to use those for our investigation if you give permission. Any data which could identify you personally will not be kept.

What if there is a problem?

The University has a specialist insurance policy in place which would operate in the event of any participant suffering harm as a result of their involvement in the research (Newline Underwriting Management Ltd, at Lloyd's of London, policy numbered :WD1200463). NHS indemnity operates in all aspects of the clinical treatment with which you are provided. If you wish to complain about any aspect of the way in which you have been approached or treated during the course of this study, you can either contact Dr Beata Godlewska (01865 223609) directly or contact the University of Oxford Clinical Trials and Research Governance (CTRG) office on 01865 857939 or you can email the head of CTRG, ctrig@admin.ox.ac.uk .

Will my taking part in the study be kept confidential?

Your data will be collected by clinical researchers and anonymised which means that it will be coded and only the study investigators will have access to the code. All the investigators have a duty of confidentiality towards you exactly as in usual medical practice. Responsible members of the University of Oxford or the Oxford University Hospitals NHS Trust may be given access to data for monitoring and/or audit of the study to ensure we are complying with regulations. We also should inform you that very occasionally responses to questionnaires about childhood treatment can reveal information indicating that you and/or others may currently be at risk from criminal activity. In this situation we have a statutory duty to inform the relevant authorities of this information.

Anonymised study data will be stored for ten years and then disposed of securely unless we obtain further ethical committee approval to use it in a subsequent study. Your anonymised scan data might be shared with other bona fide researchers so that the maximum value of

your contribution can be realised. However, no researchers outside the immediate research team will have access to any personal information about you and it will not be possible to link the scans to any particular individual.

Involvement of your general practitioner

For this study we would contact your GP explaining that you have agreed to take part in the study and inform them about your treatment choice.

What will happen to the results of the research study?

We hope to publish the results of the study in the scientific literature. You will not be identified in the publication. The results of the study will also be made available on our Departmental Web-site (<http://www.psych.ox.ac.uk/research/psychopharmacology>).

Who is funding the research?

The Medical Research Council is funding the study, the research is being sponsored by the University of Oxford and organized by the University Department of Psychiatry. No payment is made to either the doctors conducting the research or the hospitals where this research is carried out if you were to decide to help with the study.

Who has reviewed the study?

All research in the NHS is looked at by independent group of people, called a Research Ethics Committee to protect your safety, rights, wellbeing and dignity. This study has been reviewed and given a favourable opinion by the Oxford B Research Ethics Committee.

If you have any questions please get in touch with Dr Beata Godlewska (tel: 01865-223609) or beata.godlewska@psych.ox.ac.uk

Professor PJ Cowen (phil.cowen@psych.ox.ac.uk)
Dr Beata Godlewska (beata.godlewska@psych.ox.ac.uk)
Dr Ann Sharpley (ann.sharpley@psych.ox.ac.uk)
Ms Clare Williams (clare.williams@psych.ox.ac.uk)

B.3 7T MRI Scanning Protocol

SIEMENS MAGNETOM Investigational_Device_7T syngo MR B17

\\USER\FMRIB Developer\uzay\interferon\localizer_250V

TA: 8.1 s PAT: Off Voxel size: 1.2x1.2x5.0 mm Rel. SNR: 1.00 SIEMENS: gre

Properties

Prio Recon	On
Before measurement	
After measurement	
Load to viewer	On
Inline movie	Off
Auto store images	On
Load to stamp segments	On
Load images to graphic segments	On
Auto open inline display	Off
Start measurement without further preparation	On
Wait for user to start	Off
Start measurements	single

Routine

Slice group 1	
Slices	1
Dist. factor	20 %
Position	Isocenter
Orientation	Sagittal
Phase enc. dir.	A >> P
Rotation	0.00 deg
Slice group 2	
Slices	1
Dist. factor	20 %
Position	Isocenter
Orientation	Transversal
Phase enc. dir.	A >> P
Rotation	0.00 deg
Slice group 3	
Slices	1
Dist. factor	20 %
Position	Isocenter
Orientation	Coronal
Phase enc. dir.	R >> L
Rotation	0.00 deg
Phase oversampling	0 %
FoV read	300 mm
FoV phase	100.0 %
Slice thickness	5.0 mm
TR	8.6 ms
TE	4.00 ms
Averages	1
Concatenations	3
Filter	Elliptical filter
Coil elements	V32

Contrast

TD	0 ms
MTC	Off
Magn. preparation	None
Flip angle	20 deg
Fat suppr.	None
Water suppr.	None
SWI	Off

Averaging mode	Short term
Reconstruction	Magnitude
Measurements	1
Multiple series	Each measurement

Resolution

Base resolution	256
Phase resolution	100 %

Phase partial Fourier	Off
Interpolation	On

PAT mode	None

Image Filter	Off
Distortion Corr.	Off
Prescan Normalize	Off
Normalize	Off
B1 filter	Off
Raw filter	Off
Elliptical filter	On
Mode	Inplane

Geometry

Multi-slice mode	Sequential
Series	Interleaved

Saturation mode	Standard
Special sat.	None

Table position	H
Table position	0 mm
Inline Composing	Off

Tim CT mode	Off

System

V32	On
A32	Off

Positioning mode	REF
MSMA	S - C - T
Sagittal	R >> L
Coronal	A >> P
Transversal	F >> H
Save uncombined	Off
Coil Combine Mode	Adaptive Combine
AutoAlign	---
Auto Coil Select	Off

Shim mode	Tune up
Adjust with body coil	Off
Confirm freq. adjustment	Off
Assume Silicone	Off
! Ref. amplitude 1H	250.000 V
Adjustment Tolerance	Auto
Adjust volume	
Position	Isocenter
Orientation	Transversal
Rotation	0.00 deg
R >> L	350 mm
A >> P	263 mm
F >> H	350 mm

Physio

1st Signal/Mode	None
Segments	1

Tagging	None
Dark blood	Off

Resp. control	Off

Inline

Subtract	Off
Liver registration	Off
Std-Dev-Sag	Off
Std-Dev-Cor	Off

Std-Dev-Tra	Off
Std-Dev-Time	Off
MIP-Sag	Off
MIP-Cor	Off
MIP-Tra	Off
MIP-Time	Off
Save original images	On

Wash - In	Off
Wash - Out	Off
TTP	Off
PEI	Off
MIP - time	Off

MapIt	None
Contrasts	1

Sequence

Introduction	On
Dimension	2D
Phase stabilisation	Off
Asymmetric echo	Allowed
Bandwidth	320 Hz/Px
Flow comp.	No

RF pulse type	Normal
Gradient mode	Normal
Excitation	Slice-sel.
RF spoiling	On

SIEMENS MAGNETOM Investigational_Device_7T syngo MR B17

\\USER\FMRIB Developer\uzay\interferon\quick_Tx_calib_200V

TA: 0:11 Voxel size: 3.9x3.9x5.0 mm Rel. SNR: 1.00 USER: b1map_658

Properties

Prio Recon	Off
Before measurement	
After measurement	
Load to viewer	On
Inline movie	Off
Auto store images	On
Load to stamp segments	Off
Load images to graphic segments	Off
Auto open inline display	Off
Start measurement without further preparation	On
Wait for user to start	Off
Start measurements	single

Routine

Slice group 1	
Slices	1
Dist. factor	150 %
Position	L0.0 A12.2 H10.9
Orientation	Transversal
Phase enc. dir.	A >> P
Rotation	0.00 deg
FoV read	250 mm
FoV phase	100.0 %
Slice thickness	5 mm
TR	100 ms
TE 1	14 ms
TE 2	14 ms
Averages	1
Filter	None
Coil elements	A32

Contrast

Flip angle 1	90 deg
Flip angle 2	120 deg
Flip angle 3	60 deg
Flip angle 4	135 deg
Flip angle 5	45 deg
Measurements	1

Resolution

Base resolution	64
Phase resolution	100 %
Raw filter	Off

Geometry

Series	Interleaved
Navigator 1	
Position	L0.0 A11.5 H11.6
Orientation	Transversal
Rotation	0.00 deg
Base size phase	50 mm
Base size read	50 mm
Thickness	50 mm
Table position	H
Table position	0 mm
Inline Composing	Off

System

V32	Off
A32	On

Positioning mode	FIX
MSMA	S - C - T
Sagittal	R >> L
Coronal	A >> P
Transversal	F >> H
Save uncombined	Off
Coil Combine Mode	Adaptive Combine
AutoAlign	---
Auto Coil Select	Default

Shim mode	Tune up
Adjust with body coil	Off
Confirm freq. adjustment	Off
Assume Silicone	Off
! Ref. amplitude 1H	200.000 V
Adjustment Tolerance	Auto
Adjust volume	
Position	Isocenter
Orientation	Transversal
Rotation	0.00 deg
R >> L	350 mm
A >> P	263 mm
F >> H	350 mm

Composing

Sequence

Contrasts	2
Bandwidth	260.416667 Hz/Px
T1 Compensation	Mean T1
Mean T1	500.0 ms
Angles	1
Amplitude Weighting	Linear
Scale Bar	Enabled
Raw Data	Disabled

SIEMENS MAGNETOM Investigational_Device_7T syngo MR B17

\\USER\FMRIB Developer\uzay\interferon\t1_mprage_1.0iso_sag_PAT4_nonsel

TA: 2:51 PAT: 4 Voxel size: 1.0x1.0x1.0 mm Rel. SNR: 1.00 SIEMENS: tfl

Properties

Prio Recon	Off
Before measurement	
After measurement	
Load to viewer	On
Inline movie	Off
Auto store images	On
Load to stamp segments	Off
Load images to graphic segments	Off
Auto open inline display	Off
Start measurement without further preparation	On
Wait for user to start	Off
Start measurements	single

Routine

Slab group 1	
Slabs	1
Dist. factor	50 %
Position	R2.9 A19.9 F16.6
Orientation	Sagittal
Phase enc. dir.	A >> P
Rotation	0.00 deg
Phase oversampling	0 %
Slice oversampling	0.0 %
Slices per slab	176
FoV read	192 mm
FoV phase	100.0 %
Slice thickness	1.00 mm
TR	2200 ms
TE	2.82 ms
Averages	1
Concatenations	1
Filter	None
Coil elements	A32

Contrast

Magn. preparation	Non-sel. IR
TI	1050 ms
Flip angle	7 deg
Fat suppr.	Water excit. fast
Water suppr.	None
Averaging mode	Long term
Reconstruction	Magnitude
Measurements	1
Multiple series	Each measurement

Resolution

Base resolution	192
Phase resolution	100 %
Slice resolution	100 %
Phase partial Fourier	Off
Slice partial Fourier	Off
Interpolation	Off
PAT mode	GRAPPA
Accel. factor PE	4
Ref. lines PE	40
Accel. factor 3D	1
Reference scan mode	Integrated
Image Filter	Off
Distortion Corr.	Off
Prescan Normalize	Off

Normalize	Off
B1 filter	Off
Raw filter	Off
Elliptical filter	Off

Geometry

Multi-slice mode	Single shot
Series	Ascending
Table position	H
Table position	0 mm
Inline Composing	Off

System

V32	Off
A32	On
Positioning mode	FIX
MSMA	S - C - T
Sagittal	R >> L
Coronal	A >> P
Transversal	F >> H
Save uncombined	Off
Coil Combine Mode	Adaptive Combine
AutoAlign	Head > Brain
Auto Coil Select	Default
Shim mode	Standard
Adjust with body coil	Off
Confirm freq. adjustment	On
Assume Silicone	Off
? Ref. amplitude 1H	0.000 V
Adjustment Tolerance	Auto
Adjust volume	
Position	R2.9 A19.9 F16.6
Orientation	Sagittal
Rotation	0.00 deg
F >> H	192 mm
A >> P	192 mm
R >> L	176 mm

Physio

1st Signal/Mode	None
Dark blood	Off
Resp. control	Off

Inline

Subtract	Off
Std-Dev-Sag	Off
Std-Dev-Cor	Off
Std-Dev-Tra	Off
Std-Dev-Time	Off
MIP-Sag	Off
MIP-Cor	Off
MIP-Tra	Off
MIP-Time	Off
Save original images	On

Sequence

Introduction	On
Dimension	3D
Elliptical scanning	Off
Asymmetric echo	Off
Bandwidth	240 Hz/Px
Flow comp.	No

SIEMENS MAGNETOM Investigational_Device_7T syngo MR B17

Echo spacing	6.9 ms
RF pulse type	Normal
Gradient mode	Fast
Excitation	Non-sel.
RF spoiling	On

SIEMENS MAGNETOM Investigational_Device_7T syngo MR B17

\\USER\FMRIB Developer\uzay\interferon\Head_shim_3D

TA: 0:44 PAT: Off Voxel size: 4.0x4.0x4.0 mm Rel. SNR: 1.00 USER: CV_shim_452B

Properties

Prio Recon	Off
Before measurement	
After measurement	
Load to viewer	On
Inline movie	Off
Auto store images	On
Load to stamp segments	Off
Load images to graphic segments	Off
Auto open inline display	Off
Start measurement without further preparation	On
Wait for user to start	Off
Start measurements	single

Routine

Slab group 1	
Slabs	1
Dist. factor	20 %
Position	Isocenter
Orientation	Transversal
Phase enc. dir.	A >> P
Rotation	0.00 deg
Auto	Off
Phase oversampling	0 %
Slice oversampling	12.5 %
Slices per slab	64
FoV read	384 mm
FoV phase	100.0 %
Slice thickness	4.00 mm
TR	600.00 ms
TE 1	2.04 ms
TE 2	4.08 ms
Averages	1
Concatenations	1
Filter	None
Coil elements	A32

Contrast

Magn. preparation	None
Flip angle	15 deg
Fat suppr.	None
Restore magn.	Off
Averaging mode	Long term
Reconstruction	Magnitude
Measurements	1
Multiple series	Off

Resolution

Base resolution	96
Phase resolution	100 %
Slice resolution	100 %
Phase partial Fourier	Off
Slice partial Fourier	Off
Trajectory	Cartesian
Interpolation	Off
PAT mode	None
Image Filter	Off
Distortion Corr.	Off
Prescan Normalize	Off
Normalize	Off
B1 filter	Off

Raw filter	Off
Elliptical filter	Off
POCS	Off

Geometry

Multi-slice mode	Sequential
Series	Ascending
Special sat.	None
Table position	H
Table position	0 mm
Inline Composing	Off

System

V32	Off
A32	On
Positioning mode	REF
MSMA	S - C - T
Sagittal	R >> L
Coronal	A >> P
Transversal	F >> H
Save uncombined	Off
Coil Combine Mode	Adaptive Combine
AutoAlign	---
Auto Coil Select	Default
Shim mode	Tune up
Adjust with body coil	Off
Confirm freq. adjustment	Off
Assume Silicone	Off
? Ref. amplitude 1H	0.000 V
Adjustment Tolerance	Auto
Adjust volume	
Position	Isocenter
Orientation	Transversal
Rotation	0.00 deg
R >> L	350 mm
A >> P	263 mm
F >> H	350 mm

Physio

1st Signal/Mode	None
Segments	96
Tagging	None
Dark blood	Off
Cine	Off
Inline ventricular function	Off
Resp. control	Off

Inline

Subtract	Off
Std-Dev-Sag	Off
Std-Dev-Cor	Off
Std-Dev-Tra	Off
Std-Dev-Time	Off
MIP-Sag	Off
MIP-Cor	Off
MIP-Tra	Off
MIP-Time	Off
Save original images	On

Sequence

Introduction	Off
Dimension	3D

SIEMENS MAGNETOM Investigational_Device_7T syngo MR B17

Elliptical scanning	Off
Reordering	Linear
Asymmetric echo	Weak
Contrasts	2
Bandwidth 1	651 Hz/Px
Bandwidth 2	651 Hz/Px
Flow comp. 1	No
Flow comp. 2	No
Readout mode	Monopolar
Optimization	None
Allowed delay	0 s
Echo spacing	6.3 ms
Sequence type	Gre

Define	Shots
Shots per slice	1
RF pulse type	Fast
Gradient mode	Fast
Excitation	Slab-sel.
Flip angle mode	Constant
RF spoiling	On
Phase Enc. Rewinder	On

SIEMENS MAGNETOM Investigational_Device_7T syngo MR B17

\\USER\FMRIB Developer\uzay\interferon\fastestmap_cmrr_parameter

TA: 0:40 Vol: 20 x20 x20 mm Rel. SNR: 1.00 USER: fastestmap_577

Properties

Prio Recon	Off
Before measurement	
After measurement	
Load to viewer	On
Inline movie	Off
Auto store images	On
Load to stamp segments	Off
Load images to graphic segments	Off
Auto open inline display	Off
Start measurement without further preparation	On
Wait for user to start	Off
Start measurements	single

Routine

Position	L13.2 P40.7 F15.9
Orientation	Coronal
Rotation	0.00 deg
Vol R >> L	20 mm
Vol F >> H	20 mm
Vol A >> P	20 mm
TR	3357 ms
TE	46.00 ms
Averages	1
Filter	None
Coil elements	A32

Contrast

Tau	10.00 ms
Excite flip angle	90 deg
Refocus flip angle	180 deg
Measurements	1

Resolution

Vector size	256
-------------	-----

Geometry

Table position	H
Table position	0 mm
Inline Composing	Off

System

V32	Off
A32	On
Positioning mode	FIX
MSMA	S - C - T
Sagittal	R >> L
Coronal	A >> P
Transversal	F >> H
Save uncombined	Off
AutoAlign	---
Auto Coil Select	Default
Shim mode	Tune up
Adj. water suppr.	Off
Adjust with body coil	Off
Confirm freq. adjustment	Off
Assume Silicone	Off
? Ref. amplitude 1H	0.000 V
Adjustment Tolerance	Auto
Adjust volume	
Position	L13.2 P40.7 F15.9
Orientation	Coronal

Rotation	0.00 deg
F >> H	20 mm
R >> L	20 mm
A >> P	20 mm

Physio

1st Signal/Mode	None
-----------------	------

Composing

Sequence

Phase cycling	None
Bandwidth	100000 Hz
Acquisition duration	2 ms
Type of fit	Linear 6-bar
Vol fit factor	100 %
Refocus pulses	Normal
Excitation pulse duration	6400 ms
Refocus pulse duration	5120 ms
Bar FoV	384 mm
Bar thickness	5.0 mm
Multi-echo acquisition	Off
Inversion pulse	Off

\\USER\FMRIB Developer\uzay\interferon\ACC

TA: 0:10

Vol: 20 x20 x20 mm

Rel. SNR: 1.00

USER: sead_uzay_gui

Properties

Prio Recon	Off
Before measurement	
After measurement	
Load to viewer	On
Inline movie	Off
Auto store images	On
Load to stamp segments	Off
Load images to graphic segments	Off
Auto open inline display	Off
Start measurement without further preparation	On
Wait for user to start	Off
Start measurements	single

Routine

Position	L3.9 A77.2 F6.5
Orientation	Coronal
Rotation	0.00 deg
Vol R >> L	20 mm
Vol F >> H	20 mm
Vol A >> P	20 mm
TR	5000 ms
TE	50.00 ms
Averages	1
Filter	None
Coil elements	A32

Contrast

TD	32 ms
Flip angle 1	90 deg
Flip angle 2	180 deg
Spectral suppr.	Water suppr.
Water s. BW	135 ppm
Water s. delta pos.	0.00 ppm
Measurements	1

Resolution

Prescan Normalize	Off
Vector size	2048

Geometry

Table position	H
Table position	0 mm
Inline Composing	Off

System

V32	Off
A32	On
Positioning mode	FIX
MSMA	S - C - T
Sagittal	R >> L
Coronal	A >> P
Transversal	F >> H
Save uncombined	Off
AutoAlign	---
Auto Coil Select	Default
Shim mode	Advanced
Adjust with body coil	Off
Confirm freq. adjustment	Off
Assume Silicone	Off
? Ref. amplitude 1H	0.000 V

Adjustment Tolerance	Auto
Adjust volume	
Position	L3.9 A77.2 F6.5
Orientation	Coronal
Rotation	0.00 deg
F >> H	20 mm
R >> L	20 mm
A >> P	20 mm

Composing

Sequence

Introduction	On
Preparation scans	1
Delta frequency	-2.0 ppm
Phase cycling	Auto
Bandwidth	6000 Hz
Acquisition duration	341 ms
Remove oversampling	On
TX/RX Nucleus	1H
TX/RX delta frequency	0 Hz
TX Nucleus	None
TX delta frequency	0 Hz
Calibration Type	None
VAPOR flip angle	75 deg
90 pulse duration	6000 us
180 pulse duration	6000 us
Increment	0 deg
VAPOR	None
TE1	10000 us
TE2	15000 us
TE3	11000 us
resolve averages	On

\\USER\FMRIB Developer\uzay\interferon\ACC_vapor_cal_50

TA: 0:45 Vol: 20 x20 x20 mm Rel. SNR: 1.00 USER: sead_uzay_gui

Properties

Prio Recon	Off
Before measurement	
After measurement	
Load to viewer	On
Inline movie	Off
Auto store images	On
Load to stamp segments	Off
Load images to graphic segments	Off
Auto open inline display	Off
Start measurement without further preparation	On
Wait for user to start	Off
Start measurements	single

Routine

Position	L3.9 A77.2 F6.5
Orientation	Coronal
Rotation	0.00 deg
Vol R >> L	20 mm
Vol F >> H	20 mm
Vol A >> P	20 mm
TR	5010 ms
TE	50.00 ms
Averages	1
Filter	None
Coil elements	A32

Contrast

TD	32 ms
Flip angle 1	90 deg
Flip angle 2	180 deg
Spectral suppr.	Water suppr.
Water s. BW	135 ppm
Water s. delta pos.	0.00 ppm
Measurements	8

Resolution

Prescan Normalize	Off
Vector size	2048

Geometry

Table position	H
Table position	0 mm
Inline Composing	Off

System

V32	Off
A32	On
Positioning mode	FIX
MSMA	S - C - T
Sagittal	R >> L
Coronal	A >> P
Transversal	F >> H
Save uncombined	Off
AutoAlign	---
Auto Coil Select	Default
Shim mode	Advanced
Adjust with body coil	Off
Confirm freq. adjustment	Off
Assume Silicone	Off
? Ref. amplitude 1H	0.000 V

Adjustment Tolerance	Auto
Adjust volume	
Position	L3.9 A77.2 F6.5
Orientation	Coronal
Rotation	0.00 deg
F >> H	20 mm
R >> L	20 mm
A >> P	20 mm

Composing

Sequence

Introduction	On
Preparation scans	1
Delta frequency	-2.0 ppm
Phase cycling	Auto
Bandwidth	6000 Hz
Acquisition duration	341 ms
Remove oversampling	On
TX/RX Nucleus	1H
TX/RX delta frequency	0 Hz
TX Nucleus	None
TX delta frequency	0 Hz
Calibration Type	VAPOR FA
VAPOR flip angle	70 deg
90 pulse duration	6000 us
180 pulse duration	6000 us
Increment	5 deg
VAPOR	Enabled
TE1	10000 us
TE2	15000 us
TE3	11000 us
resolve averages	On

\\USER\FMRIB Developer\uzay\interferon\ACC_metab

TA: 5:26

Vol: 20 x20 x20 mm

Rel. SNR: 1.00

USER: sead_uzay_gui

Properties

Prio Recon	Off
Before measurement	
After measurement	
Load to viewer	On
Inline movie	Off
Auto store images	On
Load to stamp segments	Off
Load images to graphic segments	Off
Auto open inline display	Off
Start measurement without further preparation	On
Wait for user to start	Off
Start measurements	single

Routine

Position	L3.9 A77.2 F6.5
Orientation	Coronal
Rotation	0.00 deg
Vol R >> L	20 mm
Vol F >> H	20 mm
Vol A >> P	20 mm
TR	5010 ms
TE	50.00 ms
Averages	64
Filter	None
Coil elements	A32

Contrast

TD	32 ms
Flip angle 1	90 deg
Flip angle 2	180 deg
Spectral suppr.	Water suppr.
Water s. BW	135 ppm
Water s. delta pos.	0.00 ppm
Measurements	1

Resolution

Prescan Normalize	Off
Vector size	2048

Geometry

Table position	H
Table position	0 mm
Inline Composing	Off

System

V32	Off
A32	On
Positioning mode	FIX
MSMA	S - C - T
Sagittal	R >> L
Coronal	A >> P
Transversal	F >> H
Save uncombined	Off
AutoAlign	---
Auto Coil Select	Default
Shim mode	Advanced
Adjust with body coil	Off
Confirm freq. adjustment	Off
Assume Silicone	Off
? Ref. amplitude 1H	0.000 V

Adjustment Tolerance	Auto
Adjust volume	
Position	L3.9 A77.2 F6.5
Orientation	Coronal
Rotation	0.00 deg
F >> H	20 mm
R >> L	20 mm
A >> P	20 mm

Composing

Sequence

Introduction	On
Preparation scans	1
Delta frequency	-2.0 ppm
Phase cycling	Auto
Bandwidth	6000 Hz
Acquisition duration	341 ms
Remove oversampling	On
TX/RX Nucleus	1H
TX/RX delta frequency	0 Hz
TX Nucleus	None
TX delta frequency	0 Hz
Calibration Type	None
VAPOR flip angle	80 deg
90 pulse duration	6000 us
180 pulse duration	6000 us
Increment	0 deg
VAPOR	Enabled
TE1	10000 us
TE2	15000 us
TE3	11000 us
resolve averages	On

\\USER\FMRIB Developer\uzay\interferon\ACC_metab_wref1

TA: 0:15

Vol: 20 x20 x20 mm

Rel. SNR: 1.00

USER: sead_uzay_gui

Properties

Prio Recon	Off
Before measurement	
After measurement	
Load to viewer	On
Inline movie	Off
Auto store images	On
Load to stamp segments	Off
Load images to graphic segments	Off
Auto open inline display	Off
Start measurement without further preparation	On
Wait for user to start	Off
Start measurements	single

Routine

Position	L3.9 A77.2 F6.5
Orientation	Coronal
Rotation	0.00 deg
Vol R >> L	20 mm
Vol F >> H	20 mm
Vol A >> P	20 mm
TR	5010 ms
TE	50.00 ms
Averages	1
Filter	None
Coil elements	A32

Contrast

TD	32 ms
Flip angle 1	90 deg
Flip angle 2	180 deg
Spectral suppr.	Water suppr.
Water s. BW	135 ppm
Water s. delta pos.	0.00 ppm
Measurements	2

Resolution

Prescan Normalize	Off
Vector size	2048

Geometry

Table position	H
Table position	0 mm
Inline Composing	Off

System

V32	Off
A32	On
Positioning mode	FIX
MSMA	S - C - T
Sagittal	R >> L
Coronal	A >> P
Transversal	F >> H
Save uncombined	Off
AutoAlign	---
Auto Coil Select	Default
Shim mode	Advanced
Adjust with body coil	Off
Confirm freq. adjustment	Off
Assume Silicone	Off
? Ref. amplitude 1H	0.000 V

Adjustment Tolerance	Auto
Adjust volume	
Position	L3.9 A77.2 F6.5
Orientation	Coronal
Rotation	0.00 deg
F >> H	20 mm
R >> L	20 mm
A >> P	20 mm

Composing

Sequence

Introduction	On
Preparation scans	1
Delta frequency	0.0 ppm
Phase cycling	Auto
Bandwidth	6000 Hz
Acquisition duration	341 ms
Remove oversampling	On
TX/RX Nucleus	1H
TX/RX delta frequency	0 Hz
TX Nucleus	None
TX delta frequency	0 Hz
Calibration Type	None
VAPOR flip angle	80 deg
90 pulse duration	6000 us
180 pulse duration	6000 us
Increment	0 deg
VAPOR	Only RF off
TE1	10000 us
TE2	15000 us
TE3	11000 us
resolve averages	On

\\USER\FMRIB Developer\uzay\interferon\ACC_metab_wref3

TA: 0:15

Vol: 20 x20 x20 mm

Rel. SNR: 1.00

USER: sead_uzay_gui

Properties

Prio Recon	Off
Before measurement	
After measurement	
Load to viewer	On
Inline movie	Off
Auto store images	On
Load to stamp segments	Off
Load images to graphic segments	Off
Auto open inline display	Off
Start measurement without further preparation	On
Wait for user to start	Off
Start measurements	single

Routine

Position	L3.9 A77.2 F6.5
Orientation	Coronal
Rotation	0.00 deg
Vol R >> L	20 mm
Vol F >> H	20 mm
Vol A >> P	20 mm
TR	5010 ms
TE	50.00 ms
Averages	1
Filter	None
Coil elements	A32

Contrast

TD	32 ms
Flip angle 1	90 deg
Flip angle 2	180 deg
Spectral suppr.	Water suppr.
Water s. BW	135 ppm
Water s. delta pos.	0.00 ppm
Measurements	2

Resolution

Prescan Normalize	Off
Vector size	2048

Geometry

Table position	H
Table position	0 mm
Inline Composing	Off

System

V32	Off
A32	On
Positioning mode	FIX
MSMA	S - C - T
Sagittal	R >> L
Coronal	A >> P
Transversal	F >> H
Save uncombined	Off
AutoAlign	---
Auto Coil Select	Default
Shim mode	Advanced
Adjust with body coil	Off
Confirm freq. adjustment	Off
Assume Silicone	Off
? Ref. amplitude 1H	0.000 V

Adjustment Tolerance	Auto
Adjust volume	
Position	L3.9 A77.2 F6.5
Orientation	Coronal
Rotation	0.00 deg
F >> H	20 mm
R >> L	20 mm
A >> P	20 mm

Composing

Sequence

Introduction	On
Preparation scans	1
Delta frequency	0.0 ppm
Phase cycling	Auto
Bandwidth	6000 Hz
Acquisition duration	341 ms
Remove oversampling	On
TX/RX Nucleus	1H
TX/RX delta frequency	0 Hz
TX Nucleus	None
TX delta frequency	0 Hz
Calibration Type	None
VAPOR flip angle	80 deg
90 pulse duration	6000 us
180 pulse duration	6000 us
Increment	0 deg
VAPOR	None
TE1	10000 us
TE2	15000 us
TE3	11000 us
resolve averages	On

SIEMENS MAGNETOM Investigational_Device_7T syngo MR B17

\\USER\FMRIB Developer\uzay\interferon\fastestmap_cmrr_parameter

TA: 0:40 Vol: 10 x16 x20 mm Rel. SNR: 1.00 USER: fastestmap_577

Properties

Prio Recon	Off
Before measurement	
After measurement	
Load to viewer	On
Inline movie	Off
Auto store images	On
Load to stamp segments	Off
Load images to graphic segments	Off
Auto open inline display	Off
Start measurement without further preparation	On
Wait for user to start	Off
Start measurements	single

Routine

Position	R24.2 A37.2 F38.4
Orientation	Coronal
Rotation	-25.00 deg
Vol R >> L	10 mm
Vol F >> H	16 mm
Vol A >> P	20 mm
TR	3357 ms
TE	46.00 ms
Averages	1
Filter	None
Coil elements	A32

Contrast

Tau	10.00 ms
Excite flip angle	90 deg
Refocus flip angle	180 deg
Measurements	1

Resolution

Vector size	256
-------------	-----

Geometry

Table position	H
Table position	0 mm
Inline Composing	Off

System

V32	Off
A32	On
Positioning mode	FIX
MSMA	S - C - T
Sagittal	R >> L
Coronal	A >> P
Transversal	F >> H
Save uncombined	Off
AutoAlign	---
Auto Coil Select	Default
Shim mode	Tune up
Adj. water suppr.	Off
Adjust with body coil	Off
Confirm freq. adjustment	Off
Assume Silicone	Off
? Ref. amplitude 1H	0.000 V
Adjustment Tolerance	Auto
Adjust volume	
Position	R24.2 A37.2 F38.4
Orientation	Coronal

Rotation	-25.00 deg
F >> H	16 mm
R >> L	10 mm
A >> P	20 mm

Physio

1st Signal/Mode	None
-----------------	------

Composing

Sequence

Phase cycling	None
Bandwidth	100000 Hz
Acquisition duration	2 ms
Type of fit	Linear 6-bar
Vol fit factor	100 %
Refocus pulses	Normal
Excitation pulse duration	6400 ms
Refocus pulse duration	5120 ms
Bar FoV	384 mm
Bar thickness	5.0 mm
Multi-echo acquisition	Off
Inversion pulse	Off

\\USER\FMRIB Developer\uzay\interferon\putamen

TA: 0:10

Vol: 10 x16 x20 mm

Rel. SNR: 1.00

USER: sead_uzay_gui

Properties

Prio Recon	Off
Before measurement	
After measurement	
Load to viewer	On
Inline movie	Off
Auto store images	On
Load to stamp segments	Off
Load images to graphic segments	Off
Auto open inline display	Off
Start measurement without further preparation	On
Wait for user to start	Off
Start measurements	single

Routine

Position	R26.7 A32.4 F13.9
Orientation	Coronal
Rotation	-30.00 deg
Vol R >> L	10 mm
Vol F >> H	16 mm
Vol A >> P	20 mm
TR	5000 ms
TE	50.00 ms
Averages	1
Filter	None
Coil elements	A32

Contrast

TD	32 ms
Flip angle 1	90 deg
Flip angle 2	180 deg
Spectral suppr.	Water suppr.
Water s. BW	135 ppm
Water s. delta pos.	0.00 ppm
Measurements	1

Resolution

Prescan Normalize	Off
Vector size	2048

Geometry

Table position	H
Table position	0 mm
Inline Composing	Off

System

V32	Off
A32	On
Positioning mode	FIX
MSMA	S - C - T
Sagittal	R >> L
Coronal	A >> P
Transversal	F >> H
Save uncombined	Off
AutoAlign	---
Auto Coil Select	Default
Shim mode	Advanced
Adjust with body coil	Off
Confirm freq. adjustment	Off
Assume Silicone	Off
? Ref. amplitude 1H	0.000 V

Adjustment Tolerance	Auto
Adjust volume	
Position	R26.7 A32.4 F13.9
Orientation	Coronal
Rotation	-30.00 deg
F >> H	16 mm
R >> L	10 mm
A >> P	20 mm

Composing

Sequence

Introduction	On
Preparation scans	1
Delta frequency	-2.0 ppm
Phase cycling	Auto
Bandwidth	6000 Hz
Acquisition duration	341 ms
Remove oversampling	On
TX/RX Nucleus	1H
TX/RX delta frequency	0 Hz
TX Nucleus	None
TX delta frequency	0 Hz
Calibration Type	None
VAPOR flip angle	75 deg
90 pulse duration	6000 us
180 pulse duration	6000 us
Increment	0 deg
VAPOR	None
TE1	10000 us
TE2	15000 us
TE3	11000 us
resolve averages	On

\\USER\FMRIB Developer\uzay\interferon\putamen_vapor

TA: 0:45 Vol: 10 x16 x20 mm Rel. SNR: 1.00 USER: sead_uzay_gui

Properties

Prio Recon	Off
Before measurement	
After measurement	
Load to viewer	On
Inline movie	Off
Auto store images	On
Load to stamp segments	Off
Load images to graphic segments	Off
Auto open inline display	Off
Start measurement without further preparation	On
Wait for user to start	Off
Start measurements	single

Routine

Position	R26.7 A32.4 F13.9
Orientation	Coronal
Rotation	-30.00 deg
Vol R >> L	10 mm
Vol F >> H	16 mm
Vol A >> P	20 mm
TR	5000 ms
TE	50.00 ms
Averages	1
Filter	None
Coil elements	A32

Contrast

TD	32 ms
Flip angle 1	90 deg
Flip angle 2	180 deg
Spectral suppr.	Water suppr.
Water s. BW	135 ppm
Water s. delta pos.	0.00 ppm
Measurements	8

Resolution

Prescan Normalize	Off
Vector size	2048

Geometry

Table position	H
Table position	0 mm
Inline Composing	Off

System

V32	Off
A32	On
Positioning mode	FIX
MSMA	S - C - T
Sagittal	R >> L
Coronal	A >> P
Transversal	F >> H
Save uncombined	Off
AutoAlign	---
Auto Coil Select	Default
Shim mode	Advanced
Adjust with body coil	Off
Confirm freq. adjustment	Off
Assume Silicone	Off
? Ref. amplitude 1H	0.000 V

Adjustment Tolerance	Auto
Adjust volume	
Position	R26.7 A32.4 F13.9
Orientation	Coronal
Rotation	-30.00 deg
F >> H	16 mm
R >> L	10 mm
A >> P	20 mm

Composing

Sequence

Introduction	On
Preparation scans	1
Delta frequency	-2.0 ppm
Phase cycling	Auto
Bandwidth	6000 Hz
Acquisition duration	341 ms
Remove oversampling	On
TX/RX Nucleus	1H
TX/RX delta frequency	0 Hz
TX Nucleus	None
TX delta frequency	0 Hz
Calibration Type	VAPOR FA
VAPOR flip angle	70 deg
90 pulse duration	6000 us
180 pulse duration	6000 us
Increment	5 deg
VAPOR	Enabled
TE1	10000 us
TE2	15000 us
TE3	11000 us
resolve averages	On

\\USER\FMRIB Developer\uzay\interferon\putamen_metab

TA: 5:25 Vol: 10 x16 x20 mm Rel. SNR: 1.00 USER: sead_uzay_gui

Properties

Prio Recon	Off
Before measurement	
After measurement	
Load to viewer	On
Inline movie	Off
Auto store images	On
Load to stamp segments	Off
Load images to graphic segments	Off
Auto open inline display	Off
Start measurement without further preparation	On
Wait for user to start	Off
Start measurements	single

Routine

Position	R26.7 A32.4 F13.9
Orientation	Coronal
Rotation	-30.00 deg
Vol R >> L	10 mm
Vol F >> H	16 mm
Vol A >> P	20 mm
TR	5000 ms
TE	50.00 ms
Averages	64
Filter	None
Coil elements	A32

Contrast

TD	32 ms
Flip angle 1	90 deg
Flip angle 2	180 deg
Spectral suppr.	Water suppr.
Water s. BW	135 ppm
Water s. delta pos.	0.00 ppm
Measurements	1

Resolution

Prescan Normalize	Off
Vector size	2048

Geometry

Table position	H
Table position	0 mm
Inline Composing	Off

System

V32	Off
A32	On
Positioning mode	FIX
MSMA	S - C - T
Sagittal	R >> L
Coronal	A >> P
Transversal	F >> H
Save uncombined	Off
AutoAlign	---
Auto Coil Select	Default
Shim mode	Advanced
Adjust with body coil	Off
Confirm freq. adjustment	Off
Assume Silicone	Off
? Ref. amplitude 1H	0.000 V

Adjustment Tolerance	Auto
Adjust volume	
Position	R26.7 A32.4 F13.9
Orientation	Coronal
Rotation	-30.00 deg
F >> H	16 mm
R >> L	10 mm
A >> P	20 mm

Composing

Sequence

Introduction	On
Preparation scans	1
Delta frequency	-2.0 ppm
Phase cycling	Auto
Bandwidth	6000 Hz
Acquisition duration	341 ms
Remove oversampling	On
TX/RX Nucleus	1H
TX/RX delta frequency	0 Hz
TX Nucleus	None
TX delta frequency	0 Hz
Calibration Type	None
VAPOR flip angle	75 deg
90 pulse duration	6000 us
180 pulse duration	6000 us
Increment	0 deg
VAPOR	Enabled
TE1	10000 us
TE2	15000 us
TE3	11000 us
resolve averages	On

\\USER\FMRIB Developer\uzay\interferon\putamen_metab_wref1

TA: 0:15

Vol: 10 x16 x20 mm

Rel. SNR: 1.00

USER: sead_uzay_gui

Properties

Prio Recon	Off
Before measurement	
After measurement	
Load to viewer	On
Inline movie	Off
Auto store images	On
Load to stamp segments	Off
Load images to graphic segments	Off
Auto open inline display	Off
Start measurement without further preparation	On
Wait for user to start	Off
Start measurements	single

Routine

Position	R26.7 A32.4 F13.9
Orientation	Coronal
Rotation	-30.00 deg
Vol R >> L	10 mm
Vol F >> H	16 mm
Vol A >> P	20 mm
TR	5000 ms
TE	50.00 ms
Averages	1
Filter	None
Coil elements	A32

Contrast

TD	32 ms
Flip angle 1	90 deg
Flip angle 2	180 deg
Spectral suppr.	Water suppr.
Water s. BW	135 ppm
Water s. delta pos.	0.00 ppm
Measurements	2

Resolution

Prescan Normalize	Off
Vector size	2048

Geometry

Table position	H
Table position	0 mm
Inline Composing	Off

System

V32	Off
A32	On
Positioning mode	FIX
MSMA	S - C - T
Sagittal	R >> L
Coronal	A >> P
Transversal	F >> H
Save uncombined	Off
AutoAlign	---
Auto Coil Select	Default
Shim mode	Advanced
Adjust with body coil	Off
Confirm freq. adjustment	Off
Assume Silicone	Off
? Ref. amplitude 1H	0.000 V

Adjustment Tolerance	Auto
Adjust volume	
Position	R26.7 A32.4 F13.9
Orientation	Coronal
Rotation	-30.00 deg
F >> H	16 mm
R >> L	10 mm
A >> P	20 mm

Composing

Sequence

Introduction	On
Preparation scans	1
Delta frequency	0.0 ppm
Phase cycling	Auto
Bandwidth	6000 Hz
Acquisition duration	341 ms
Remove oversampling	On
TX/RX Nucleus	1H
TX/RX delta frequency	0 Hz
TX Nucleus	None
TX delta frequency	0 Hz
Calibration Type	None
VAPOR flip angle	75 deg
90 pulse duration	6000 us
180 pulse duration	6000 us
Increment	0 deg
VAPOR	Only RF off
TE1	10000 us
TE2	15000 us
TE3	11000 us
resolve averages	On

\\USER\FMRIB Developer\uzay\interferon\putamen_metab_wref3

TA: 0:15

Vol: 10 x16 x20 mm

Rel. SNR: 1.00

USER: sead_uzay_gui

Properties

Prio Recon	Off
Before measurement	
After measurement	
Load to viewer	On
Inline movie	Off
Auto store images	On
Load to stamp segments	Off
Load images to graphic segments	Off
Auto open inline display	Off
Start measurement without further preparation	On
Wait for user to start	Off
Start measurements	single

Routine

Position	R26.7 A32.4 F13.9
Orientation	Coronal
Rotation	-30.00 deg
Vol R >> L	10 mm
Vol F >> H	16 mm
Vol A >> P	20 mm
TR	5000 ms
TE	50.00 ms
Averages	1
Filter	None
Coil elements	A32

Contrast

TD	32 ms
Flip angle 1	90 deg
Flip angle 2	180 deg
Spectral suppr.	Water suppr.
Water s. BW	135 ppm
Water s. delta pos.	0.00 ppm
Measurements	2

Resolution

Prescan Normalize	Off
Vector size	2048

Geometry

Table position	H
Table position	0 mm
Inline Composing	Off

System

V32	Off
A32	On
Positioning mode	FIX
MSMA	S - C - T
Sagittal	R >> L
Coronal	A >> P
Transversal	F >> H
Save uncombined	Off
AutoAlign	---
Auto Coil Select	Default
Shim mode	Advanced
Adjust with body coil	Off
Confirm freq. adjustment	Off
Assume Silicone	Off
? Ref. amplitude 1H	0.000 V

Adjustment Tolerance	Auto
Adjust volume	
Position	R26.7 A32.4 F13.9
Orientation	Coronal
Rotation	-30.00 deg
F >> H	16 mm
R >> L	10 mm
A >> P	20 mm

Composing

Sequence

Introduction	On
Preparation scans	1
Delta frequency	0.0 ppm
Phase cycling	Auto
Bandwidth	6000 Hz
Acquisition duration	341 ms
Remove oversampling	On
TX/RX Nucleus	1H
TX/RX delta frequency	0 Hz
TX Nucleus	None
TX delta frequency	0 Hz
Calibration Type	None
VAPOR flip angle	75 deg
90 pulse duration	6000 us
180 pulse duration	6000 us
Increment	0 deg
VAPOR	None
TE1	10000 us
TE2	15000 us
TE3	11000 us
resolve averages	On

SIEMENS MAGNETOM Investigational_Device_7T syngo MR B17

\\USER\FMRIB Developer\uzay\interferon\fastestmap_cmrr_parameter

TA: 0:40 Vol: 20 x20 x20 mm Rel. SNR: 1.00 USER: fastestmap_577

Properties

Prio Recon	Off
Before measurement	
After measurement	
Load to viewer	On
Inline movie	Off
Auto store images	On
Load to stamp segments	Off
Load images to graphic segments	Off
Auto open inline display	Off
Start measurement without further preparation	On
Wait for user to start	Off
Start measurements	single

Routine

Position	R2.8 P35.8 F38.1
Orientation	Coronal
Rotation	0.00 deg
Vol R >> L	20 mm
Vol F >> H	20 mm
Vol A >> P	20 mm
TR	3357 ms
TE	46.00 ms
Averages	1
Filter	None
Coil elements	A32

Contrast

Tau	10.00 ms
Excite flip angle	90 deg
Refocus flip angle	180 deg
Measurements	1

Resolution

Vector size	256
-------------	-----

Geometry

Table position	H
Table position	0 mm
Inline Composing	Off

System

V32	Off
A32	On
Positioning mode	FIX
MSMA	S - C - T
Sagittal	R >> L
Coronal	A >> P
Transversal	F >> H
Save uncombined	Off
AutoAlign	---
Auto Coil Select	Default
Shim mode	Tune up
Adj. water suppr.	Off
Adjust with body coil	Off
Confirm freq. adjustment	Off
Assume Silicone	Off
? Ref. amplitude 1H	0.000 V
Adjustment Tolerance	Auto
Adjust volume	
Position	R2.8 P35.8 F38.1
Orientation	Coronal

Rotation	0.00 deg
F >> H	20 mm
R >> L	20 mm
A >> P	20 mm

Physio

1st Signal/Mode	None
-----------------	------

Composing

Sequence

Phase cycling	None
Bandwidth	100000 Hz
Acquisition duration	2 ms
Type of fit	Linear 6-bar
Vol fit factor	100 %
Refocus pulses	Normal
Excitation pulse duration	6400 ms
Refocus pulse duration	5120 ms
Bar FoV	384 mm
Bar thickness	5.0 mm
Multi-echo acquisition	Off
Inversion pulse	Off

\\USER\FMRIB Developer\uzay\interferon\occ

TA: 0:10

Vol: 20 x20 x20 mm

Rel. SNR: 1.00

USER: sead_uzay_gui

Properties

Prio Recon	Off
Before measurement	
After measurement	
Load to viewer	On
Inline movie	Off
Auto store images	On
Load to stamp segments	Off
Load images to graphic segments	Off
Auto open inline display	Off
Start measurement without further preparation	On
Wait for user to start	Off
Start measurements	single

Routine

Position	R9.5 P33.6 F10.2
Orientation	Coronal
Rotation	0.00 deg
Vol R >> L	20 mm
Vol F >> H	20 mm
Vol A >> P	20 mm
TR	5000 ms
TE	50.00 ms
Averages	1
Filter	None
Coil elements	A32

Contrast

TD	32 ms
Flip angle 1	90 deg
Flip angle 2	180 deg
Spectral suppr.	Water suppr.
Water s. BW	135 ppm
Water s. delta pos.	0.00 ppm
Measurements	1

Resolution

Prescan Normalize	Off
Vector size	2048

Geometry

Table position	H
Table position	0 mm
Inline Composing	Off

System

V32	Off
A32	On
Positioning mode	FIX
MSMA	S - C - T
Sagittal	R >> L
Coronal	A >> P
Transversal	F >> H
Save uncombined	Off
AutoAlign	---
Auto Coil Select	Default
Shim mode	Advanced
Adjust with body coil	Off
Confirm freq. adjustment	Off
Assume Silicone	Off
? Ref. amplitude 1H	0.000 V

Adjustment Tolerance	Auto
Adjust volume	
Position	R9.5 P33.6 F10.2
Orientation	Coronal
Rotation	0.00 deg
F >> H	20 mm
R >> L	20 mm
A >> P	20 mm

Composing

Sequence

Introduction	On
Preparation scans	1
Delta frequency	-2.0 ppm
Phase cycling	Auto
Bandwidth	6000 Hz
Acquisition duration	341 ms
Remove oversampling	On
TX/RX Nucleus	1H
TX/RX delta frequency	0 Hz
TX Nucleus	None
TX delta frequency	0 Hz
Calibration Type	None
VAPOR flip angle	75 deg
90 pulse duration	6000 us
180 pulse duration	6000 us
Increment	0 deg
VAPOR	None
TE1	10000 us
TE2	15000 us
TE3	11000 us
resolve averages	On

\\USER\FMRIB Developer\uzay\interferon\occ_vapor

TA: 0:45

Vol: 20 x20 x20 mm

Rel. SNR: 1.00

USER: sead_uzay_gui

Properties

Prio Recon	Off
Before measurement	
After measurement	
Load to viewer	On
Inline movie	Off
Auto store images	On
Load to stamp segments	Off
Load images to graphic segments	Off
Auto open inline display	Off
Start measurement without further preparation	On
Wait for user to start	Off
Start measurements	single

Routine

Position	R9.5 P33.6 F10.2
Orientation	Coronal
Rotation	0.00 deg
Vol R >> L	20 mm
Vol F >> H	20 mm
Vol A >> P	20 mm
TR	5000 ms
TE	50.00 ms
Averages	1
Filter	None
Coil elements	A32

Contrast

TD	32 ms
Flip angle 1	90 deg
Flip angle 2	180 deg
Spectral suppr.	Water suppr.
Water s. BW	135 ppm
Water s. delta pos.	0.00 ppm
Measurements	8

Resolution

Prescan Normalize	Off
Vector size	2048

Geometry

Table position	H
Table position	0 mm
Inline Composing	Off

System

V32	Off
A32	On
Positioning mode	FIX
MSMA	S - C - T
Sagittal	R >> L
Coronal	A >> P
Transversal	F >> H
Save uncombined	Off
AutoAlign	---
Auto Coil Select	Default
Shim mode	Advanced
Adjust with body coil	Off
Confirm freq. adjustment	Off
Assume Silicone	Off
? Ref. amplitude 1H	0.000 V

Adjustment Tolerance	Auto
Adjust volume	
Position	R9.5 P33.6 F10.2
Orientation	Coronal
Rotation	0.00 deg
F >> H	20 mm
R >> L	20 mm
A >> P	20 mm

Composing

Sequence

Introduction	On
Preparation scans	1
Delta frequency	-2.0 ppm
Phase cycling	Auto
Bandwidth	6000 Hz
Acquisition duration	341 ms
Remove oversampling	On
TX/RX Nucleus	1H
TX/RX delta frequency	0 Hz
TX Nucleus	None
TX delta frequency	0 Hz
Calibration Type	VAPOR FA
VAPOR flip angle	70 deg
90 pulse duration	6000 us
180 pulse duration	6000 us
Increment	5 deg
VAPOR	Enabled
TE1	10000 us
TE2	15000 us
TE3	11000 us
resolve averages	On

\\USER\FMRIB Developer\uzay\interferon\occ_metab

TA: 5:25 Vol: 20 x20 x20 mm Rel. SNR: 1.00 USER: sead_uzay_gui

Properties

Prio Recon	Off
Before measurement	
After measurement	
Load to viewer	On
Inline movie	Off
Auto store images	On
Load to stamp segments	Off
Load images to graphic segments	Off
Auto open inline display	Off
Start measurement without further preparation	On
Wait for user to start	Off
Start measurements	single

Routine

Position	R9.5 P33.6 F10.2
Orientation	Coronal
Rotation	0.00 deg
Vol R >> L	20 mm
Vol F >> H	20 mm
Vol A >> P	20 mm
TR	5000 ms
TE	50.00 ms
Averages	64
Filter	None
Coil elements	A32

Contrast

TD	32 ms
Flip angle 1	90 deg
Flip angle 2	180 deg
Spectral suppr.	Water suppr.
Water s. BW	135 ppm
Water s. delta pos.	0.00 ppm
Measurements	1

Resolution

Prescan Normalize	Off
Vector size	2048

Geometry

Table position	H
Table position	0 mm
Inline Composing	Off

System

V32	Off
A32	On
Positioning mode	FIX
MSMA	S - C - T
Sagittal	R >> L
Coronal	A >> P
Transversal	F >> H
Save uncombined	Off
AutoAlign	---
Auto Coil Select	Default
Shim mode	Advanced
Adjust with body coil	Off
Confirm freq. adjustment	Off
Assume Silicone	Off
? Ref. amplitude 1H	0.000 V

Adjustment Tolerance	Auto
Adjust volume	
Position	R9.5 P33.6 F10.2
Orientation	Coronal
Rotation	0.00 deg
F >> H	20 mm
R >> L	20 mm
A >> P	20 mm

Composing

Sequence

Introduction	On
Preparation scans	1
Delta frequency	-2.0 ppm
Phase cycling	Auto
Bandwidth	6000 Hz
Acquisition duration	341 ms
Remove oversampling	On
TX/RX Nucleus	1H
TX/RX delta frequency	0 Hz
TX Nucleus	None
TX delta frequency	0 Hz
Calibration Type	None
VAPOR flip angle	75 deg
90 pulse duration	6000 us
180 pulse duration	6000 us
Increment	0 deg
VAPOR	Enabled
TE1	10000 us
TE2	15000 us
TE3	11000 us
resolve averages	On

\\USER\FMRIB Developer\uzay\interferon\occ_metab_wref1

TA: 0:15

Vol: 20 x20 x20 mm

Rel. SNR: 1.00

USER: sead_uzay_gui

Properties

Prio Recon	Off
Before measurement	
After measurement	
Load to viewer	On
Inline movie	Off
Auto store images	On
Load to stamp segments	Off
Load images to graphic segments	Off
Auto open inline display	Off
Start measurement without further preparation	On
Wait for user to start	Off
Start measurements	single

Routine

Position	R9.5 P33.6 F10.2
Orientation	Coronal
Rotation	0.00 deg
Vol R >> L	20 mm
Vol F >> H	20 mm
Vol A >> P	20 mm
TR	5000 ms
TE	50.00 ms
Averages	1
Filter	None
Coil elements	A32

Contrast

TD	32 ms
Flip angle 1	90 deg
Flip angle 2	180 deg
Spectral suppr.	Water suppr.
Water s. BW	135 ppm
Water s. delta pos.	0.00 ppm
Measurements	2

Resolution

Prescan Normalize	Off
Vector size	2048

Geometry

Table position	H
Table position	0 mm
Inline Composing	Off

System

V32	Off
A32	On
Positioning mode	FIX
MSMA	S - C - T
Sagittal	R >> L
Coronal	A >> P
Transversal	F >> H
Save uncombined	Off
AutoAlign	---
Auto Coil Select	Default
Shim mode	Advanced
Adjust with body coil	Off
Confirm freq. adjustment	Off
Assume Silicone	Off
? Ref. amplitude 1H	0.000 V

Adjustment Tolerance	Auto
Adjust volume	
Position	R9.5 P33.6 F10.2
Orientation	Coronal
Rotation	0.00 deg
F >> H	20 mm
R >> L	20 mm
A >> P	20 mm

Composing

Sequence

Introduction	On
Preparation scans	1
Delta frequency	0.0 ppm
Phase cycling	Auto
Bandwidth	6000 Hz
Acquisition duration	341 ms
Remove oversampling	On
TX/RX Nucleus	1H
TX/RX delta frequency	0 Hz
TX Nucleus	None
TX delta frequency	0 Hz
Calibration Type	None
VAPOR flip angle	75 deg
90 pulse duration	6000 us
180 pulse duration	6000 us
Increment	0 deg
VAPOR	Only RF off
TE1	10000 us
TE2	15000 us
TE3	11000 us
resolve averages	On

\\USER\FMRIB Developer\uzay\interferon\occ_metab_wref3

TA: 0:15 Vol: 20 x20 x20 mm Rel. SNR: 1.00 USER: sead_uzay_gui

Properties

Prio Recon	Off
Before measurement	
After measurement	
Load to viewer	On
Inline movie	Off
Auto store images	On
Load to stamp segments	Off
Load images to graphic segments	Off
Auto open inline display	Off
Start measurement without further preparation	On
Wait for user to start	Off
Start measurements	single

Routine

Position	R9.5 P33.6 F10.2
Orientation	Coronal
Rotation	0.00 deg
Vol R >> L	20 mm
Vol F >> H	20 mm
Vol A >> P	20 mm
TR	5000 ms
TE	50.00 ms
Averages	1
Filter	None
Coil elements	A32

Contrast

TD	32 ms
Flip angle 1	90 deg
Flip angle 2	180 deg
Spectral suppr.	Water suppr.
Water s. BW	135 ppm
Water s. delta pos.	0.00 ppm
Measurements	2

Resolution

Prescan Normalize	Off
Vector size	2048

Geometry

Table position	H
Table position	0 mm
Inline Composing	Off

System

V32	Off
A32	On
Positioning mode	FIX
MSMA	S - C - T
Sagittal	R >> L
Coronal	A >> P
Transversal	F >> H
Save uncombined	Off
AutoAlign	---
Auto Coil Select	Default
Shim mode	Advanced
Adjust with body coil	Off
Confirm freq. adjustment	Off
Assume Silicone	Off
? Ref. amplitude 1H	0.000 V

Adjustment Tolerance	Auto
Adjust volume	
Position	R9.5 P33.6 F10.2
Orientation	Coronal
Rotation	0.00 deg
F >> H	20 mm
R >> L	20 mm
A >> P	20 mm

Composing

Sequence

Introduction	On
Preparation scans	1
Delta frequency	0.0 ppm
Phase cycling	Auto
Bandwidth	6000 Hz
Acquisition duration	341 ms
Remove oversampling	On
TX/RX Nucleus	1H
TX/RX delta frequency	0 Hz
TX Nucleus	None
TX delta frequency	0 Hz
Calibration Type	None
VAPOR flip angle	75 deg
90 pulse duration	6000 us
180 pulse duration	6000 us
Increment	0 deg
VAPOR	None
TE1	10000 us
TE2	15000 us
TE3	11000 us
resolve averages	On

SIEMENS MAGNETOM Investigational_Device_7T syngo MR B17

\\USER\FMRIB Developer\uzay\interferon\tryfirst_ep2d_bold_2x2x2_PAT2_200V_5off5on

TA: 5:09 PAT: 2 Voxel size: 2.0x2.0x2.0 mm Rel. SNR: 1.00 USER: ep2d_bold_sine_676a

Properties

Prio Recon	Off
Before measurement	
After measurement	
Load to viewer	On
Inline movie	Off
Auto store images	On
Load to stamp segments	Off
Load images to graphic segments	Off
Auto open inline display	Off
Start measurement without further preparation	On
Wait for user to start	On
Start measurements	single

Routine

Slice group 1	
Slices	52
Dist. factor	0 %
Position	L0.0 A19.7 H0.6
Orientation	Transversal
Phase enc. dir.	A >> P
Rotation	0.00 deg
Phase oversampling	0 %
FoV read	220 mm
FoV phase	100.0 %
Slice thickness	2.0 mm
TR	3000 ms
TE	25 ms
Averages	1
Concatenations	1
Filter	None
Coil elements	A32

Contrast

MTC	Off
Flip angle	90 deg
Fat suppr.	Fat sat.
Averaging mode	Long term
Reconstruction	Magnitude
Measurements	100
Delay in TR	0 ms
Multiple series	Off

Resolution

Base resolution	110
Phase resolution	100 %
Phase partial Fourier	Off
Interpolation	Off
PAT mode	GRAPPA
Accel. factor PE	2
Ref. lines PE	40
Reference scan mode	Separate
Distortion Corr.	Off
Prescan Normalize	Off
Raw filter	On
Elliptical filter	Off
Hamming	Off

Geometry

Multi-slice mode	Interleaved
Series	Descending

Special sat.	None
Table position	H
Table position	0 mm
Inline Composing	Off

System

V32	Off
A32	On
Positioning mode	FIX
MSMA	S - C - T
Sagittal	R >> L
Coronal	A >> P
Transversal	F >> H
Coil Combine Mode	Adaptive Combine
AutoAlign	---
Auto Coil Select	Default

Shim mode	Standard
Adjust with body coil	Off
Confirm freq. adjustment	Off
Assume Silicone	Off
! Ref. amplitude 1H	200.000 V
Adjustment Tolerance	Auto
Adjust volume	
Position	L0.0 A19.7 H0.6
Orientation	Transversal
Rotation	0.00 deg
R >> L	220 mm
A >> P	220 mm
F >> H	104 mm

Physio

1st Signal/Mode	None
-----------------	------

BOLD

GLM Statistics	Off
Dynamic t-maps	On
Starting ignore meas	0
Ignore after transition	0
Model transition states	On
Temp. highpass filter	On
Threshold	4.00
Paradigm size	10
Meas[1]	Baseline
Meas[2]	Baseline
Meas[3]	Baseline
Meas[4]	Baseline
Meas[5]	Baseline
Meas[6]	Active
Meas[7]	Active
Meas[8]	Active
Meas[9]	Active
Meas[10]	Active
Motion correction	On
Interpolation	3D-K-space
Spatial filter	On
Filter setting	1.0

Sequence

Introduction	Off
Bandwidth	1568 Hz/Px
Echo spacing	0.72 ms
EPI factor	110
RF pulse type	Normal
Gradient mode	Fast

Phase Correction	local
FatSat flip angle	110 deg
RF pulse type	Sinc
Excitation length	3072 us
BW-Time product	5.22
FFT factor	1.00

SIEMENS MAGNETOM Investigational_Device_7T syngo MR B17

\\USER\FMRIB Developer\uzay\interferon\resting_state_cmrr_mbep2d_bold_1.2mm_iso_MB1_PAT2_TR1500
 TA: 5:24 PAT: 2 Voxel size: 2.0x2.0x2.0 mm Rel. SNR: 1.00 USER: cmrr_mbep2d_bold

Properties

Prio Recon	Off
Before measurement	
After measurement	
Load to viewer	On
Inline movie	Off
Auto store images	On
Load to stamp segments	Off
Load images to graphic segments	Off
Auto open inline display	Off
Start measurement without further preparation	On
Wait for user to start	On
Start measurements	single

Routine

Slice group 1	
Slices	52
Dist. factor	0 %
Position	R1.3 P17.4 H13.1
Orientation	Transversal
Phase enc. dir.	A >> P
Rotation	0.00 deg
Phase oversampling	0 %
FoV read	220 mm
FoV phase	100.0 %
Slice thickness	2.00 mm
TR	3000 ms
TE	25.0 ms
Multi-band accel. factor	1
Filter	None
Coil elements	A32

Contrast

MTC	Off
Magn. preparation	None
Flip angle	90 deg
Fat suppr.	Fat sat.
Averaging mode	Long term
Reconstruction	Magnitude
Measurements	100
Delay in TR	0 ms
Multiple series	Off

Resolution

Base resolution	110
Phase resolution	100 %
Phase partial Fourier	Off
Interpolation	Off
PAT mode	GRAPPA
Accel. factor PE	2
Ref. lines PE	40
Reference scan mode	GRE
Distortion Corr.	Off
Prescan Normalize	Off
Raw filter	On
Elliptical filter	Off
Hamming	Off

Geometry

Multi-slice mode	Interleaved
Series	Descending

Special sat.	None
Table position	H
Table position	0 mm
Inline Composing	Off

System

V32	Off
A32	On
Positioning mode	FIX
MSMA	S - C - T
Sagittal	R >> L
Coronal	A >> P
Transversal	F >> H
Coil Combine Mode	Sum of Squares
AutoAlign	---
Auto Coil Select	Default

Shim mode	Standard
Adjust with body coil	Off
Confirm freq. adjustment	Off
Assume Silicone	Off
! Ref. amplitude 1H	200.000 V
Adjustment Tolerance	Auto
Adjust volume	
Position	R1.3 P17.4 H13.1
Orientation	Transversal
Rotation	0.00 deg
R >> L	220 mm
A >> P	220 mm
F >> H	104 mm

Physio

1st Signal/Mode	None
-----------------	------

BOLD

GLM Statistics	On
Dynamic t-maps	On
Starting ignore meas	0
Ignore after transition	0
Model transition states	On
Temp. highpass filter	On
Threshold	4.00
Paradigm size	10
Meas[1]	Baseline
Meas[2]	Baseline
Meas[3]	Baseline
Meas[4]	Baseline
Meas[5]	Baseline
Meas[6]	Active
Meas[7]	Active
Meas[8]	Active
Meas[9]	Active
Meas[10]	Active
Motion correction	On
Interpolation	3D-K-space
Spatial filter	On
Filter setting	1.0

Sequence

Introduction	Off
Bandwidth	1748 Hz/Px
Flow comp.	No
Free echo spacing	Off
Echo spacing	0.66 ms
EPI factor	110

Gradient mode	Normal
RF spoiling	Off

Excite pulse duration	5880 us
SENSE1 coil combine	Off
Log physiology to file	Off
Invert RO/PE polarity	Off
FFT scale factor	1.00
GRE iPAT ref. FA	12.0 deg
Triggering scheme	Standard
Starting ignore meas	0
Paradigm size	2
Multiplier	1
Step [1]	1
Step [2]	0

SIEMENS MAGNETOM Investigational_Device_7T syngo MR B17

\\USER\FMRIB Developer\uzay\interferon\gre_field_mapping_2mm

TA: 2:02

Voxel size: 2.0x2.0x2.0 mm

Rel. SNR: 1.00

SIEMENS: gre_field_mapping

Properties

Prio Recon	Off
Before measurement	
After measurement	
Load to viewer	On
Inline movie	Off
Auto store images	On
Load to stamp segments	Off
Load images to graphic segments	Off
Auto open inline display	Off
Start measurement without further preparation	On
Wait for user to start	Off
Start measurements	single

Routine

Slice group 1	
Slices	64
Dist. factor	0 %
Position	Isocenter
Orientation	Transversal
Phase enc. dir.	A >> P
Rotation	0.00 deg
Phase oversampling	0 %
FoV read	192 mm
FoV phase	100.0 %
Slice thickness	2.0 mm
TR	620.0 ms
TE 1	4.08 ms
TE 2	5.1 ms
Averages	1
Concatenations	1
Filter	None
Coil elements	A32

Contrast

MTC	Off
Flip angle	39 deg
Fat suppr.	None

Averaging mode	Long term
Reconstruction	Magn./Phase
Measurements	1
Multiple series	Off

Resolution

Base resolution	96
Phase resolution	100 %
Phase partial Fourier	Off
Interpolation	Off

Image Filter	Off
Distortion Corr.	Off
Prescan Normalize	Off
Normalize	Off
B1 filter	Off
Raw filter	Off
Elliptical filter	Off

Geometry

Multi-slice mode	Interleaved
Series	Interleaved

Special sat.	None

Table position	H

Table position	0 mm
Inline Composing	Off

System

V32	Off
A32	On

Positioning mode	FIX
MSMA	S - C - T
Sagittal	R >> L
Coronal	A >> P
Transversal	F >> H
Save uncombined	Off
Coil Combine Mode	Sum of Squares
AutoAlign	---
Auto Coil Select	Off

Shim mode	Standard
Adjust with body coil	Off
Confirm freq. adjustment	Off
Assume Silicone	Off
? Ref. amplitude 1H	0.000 V
Adjustment Tolerance	Auto
Adjust volume	
Position	Isocenter
Orientation	Transversal
Rotation	0.00 deg
R >> L	192 mm
A >> P	192 mm
F >> H	128 mm

Composing

Sequence

Introduction	On
Dimension	2D
Asymmetric echo	Off
Contrasts	2
Bandwidth	734 Hz/Px
Flow comp.	Yes

RF pulse type	Normal
Gradient mode	Whisper
RF spoiling	On

Table of contents

\\USER

FMRIB Developer

uzay

interferon

localizer_250V
 quick_Tx_calib_200V
 t1_mprage_1.0iso_sag_PAT4_nonsel
 Head_shim_3D
 fastestmap_cmrr_parameter
 ACC
 ACC_vapor_cal_50
 ACC_metab
 ACC_metab_wref1
 ACC_metab_wref3
 fastestmap_cmrr_parameter
 putamen
 putamen_vapor
 putamen_metab
 putamen_metab_wref1
 putamen_metab_wref3
 fastestmap_cmrr_parameter
 occ
 occ_vapor
 occ_metab
 occ_metab_wref1
 occ_metab_wref3
 Run SetShim
 tryfirst_ep2d_bold_2x2x2_PAT2_200V_5off5on
 resting_state_cmrr_mbep2d_bold_1.2mm_iso_MB1_PAT2_TR1500
 Remember to copy adjust volume for fieldmap
 gre_field_mapping_2mm